THE
PHYSICAL REVIEW
A Journal of Experimental and Theoretical Physics Established by E. L. Nichols in 1893
VOL. 57, NO. 5 MARCH 1, 1940 SECOND SERIES

# Radioactive Isotopes of Tellurium

G. T. SEABORG, J. J. LIVINGOOD* AND J. W. KENNEDY
*Radiation Laboratory, Department of Physics, and Department of Chemistry, University of California, Berkeley, California*

(Received December 21, 1939)

Three pairs of radioactive tellurium isomers have been studied with the help of a chemical method for separating the isomers. In the case of each pair of isomers it was found that the longer-lived activity constitutes an isomeric transition from an upper to a lower level in the tellurium nucleus, and that the shorter-lived activity is due to beta-particle decay from the lower level to an iodine isotope. It has been possible to make isotopic assignments for these three pairs of isomers and also for a seventh (single) tellurium activity. The data are collected in the following table:

| ACTIVE ISOTOPE | HALF-LIVES | METHODS OF PRODUCTION |
|---|---|---|
| $Te^{121}$ | 1.2±0.2 days→25±5 min.→$I^{121}$(8 days)→$Xe^{121}$ | Te($d$,$p$); Te($n$,$\gamma$); U($n$,−) |
| $Te^{129}$ | 32±2 days→72±3 min.→$I^{129}$(?) | Te($d$,$p$); Te($n$,$\gamma$); Te($n$,2$n$); Te($\gamma$,$n$); U($n$,−)$Sb^{129}$(4.2 hr.)→$Te^{129}$ |
| $Te^{127}$ | 90±2 days→9.3±0.5 hr.→$I^{127}$ | Te($d$,$p$); Te($n$,$\gamma$); Te($n$,2$n$); I($n$,$p$); Sn($\alpha$,$n$); U($n$,−) $Sb^{127}$(80 hr.)→$Te^{127}$ |
| $Te^{121}$ | 125±5 days→$Sb^{121}$ | Sb($d$,2$n$); Sb($p$,$n$); Sn($\alpha$,$n$). |

THE present paper treats in detail the results of studies on radioactive tellurium isotopes; many of the facts we have already reported briefly.[1-3] Most of the bombardments were made with the 37-inch Berkeley cyclotron, with energies of 4 Mev for protons, 8 Mev for deuterons and 16 Mev for helium ions; a few activations were made with 16 Mev deuterons, with the 60-inch cyclotron of the Crocker Radiation Laboratory. Chemical separations (see the last section) were performed in every case; at least two bombardments (generally many more) were made with each projectile and target, and the full decay curves were followed out to background or to the present date. Most of the activities were measured with a quartz fiber electroscope filled with air at atmospheric pressure; a few were measured with a thin-walled Geiger-Müller counter.

Several pairs of isomers will be discussed in the present paper. It is therefore pertinent to review some of the general features of nuclear isomerism at this point. In cases of observed isomeric pairs

* Now at Harvard University.
[1] J. J. Livingood and G. T. Seaborg, Phys. Rev. **53**, 1015 (1938).
[2] G. T. Seaborg and J. W. Kennedy, Phys. Rev. **55**, 410 (1939).
[3] G. T. Seaborg, J. J. Livingood and J. W. Kennedy, Phys. Rev. **55**, 794 (1939).

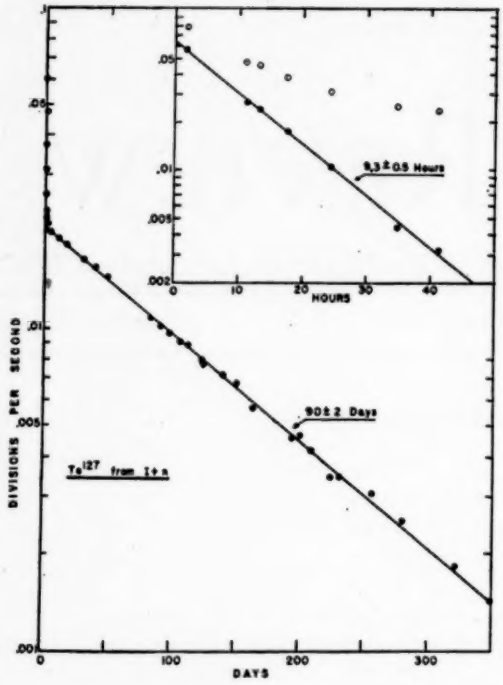


FIG. 1. The isomeric activities of $Te^{127}$ formed from $I+n$. The 9.3-hour activity which is shown here was produced *directly* during the bombardment; this activity corresponds to the lower isomeric state of $Te^{127}$ and can be extracted by means of isomer separation experiments from a sample containing the 90-day activity (see Fig. 3).

the upper state is unstable and may decay to the ground state of that nucleus by the emission of gamma-radiation or conversion electrons (so-called isomeric transitions) or by some other radioactive transformation to one of its stable isobars. In the case of such isomers[4,5] as $Ag^{106}$ and $Mn^{52}$ the upper state and the ground state undergo independent radioactive decay to neighboring elements. On the other hand, in the case of some isomeric pairs the probability of decay of the upper isomeric state by gamma-ray (or conversion electron) emission is greater than the probability of its transformation by beta-ray emission (or $K$-electron capture); such isomers we shall find it convenient to term genetically related (since one is produced by the decay of the other). Examples of this type of isomerism are found in bromine[6-8] ($Br^{80}$), rhodium[9] ($Rh^{104}$), element 43,[10] indium[11,12] ($In^{115}$ and $In^{113}$), cadmium,[13] strontium[14] ($Sr^{87}$), zinc[15] ($Zn^{69}$), selenium,[16] krypton[16] ($Kr^{83}$), scandium[17] ($Sc^{44}$) and, as will be shown here, in tellurium. (It is possible, of course, that isomers may exist in which the probabilities of decay of the upper state in these two ways are comparable; however, the occurrence of such isomers should be statistically improbable.) In the case of all the tellurium isomeric pairs the genetic relationship has been proved by the chemical method.[6]

## CHEMICAL SEPARATION OF THE ISOMERS

We have found a very satisfactory procedure for the application of the chemical method to the separation of the genetically related tellurium isomers. The method depends upon the change of a molecule of telluric acid to one of tellurous acid when the tellurium nucleus in that molecule undergoes an isomeric transition to its ground state. In order to synthesize telluric acid the chemically purified radioactive tellurium was dissolved in nitric acid, and silver tellurite was precipitated from the neutralized solution. The silver tellurite was suspended in water and oxidized with liquid bromine to telluric acid. The excess bromine was boiled off and the product silver bromide filtered out leaving a solution of pure telluric acid.

To the telluric acid solution small amounts of inactive sodium tellurite, iodine and sodium iodate were added as carriers. At suitable intervals aliquots of this sample were taken and the

[4] N. Feather and J. V. Dunworth, Proc. Roy. Soc. **A168**, 566 (1938).
[5] J. J. Livingood and G. T. Seaborg, Phys. Rev. **54**, 391 (1938); A. Hemmendinger, Phys. Rev. **55**, 604 (1939).
[6] E. Segrè, R. S. Halford and G. T. Seaborg, Phys. Rev. **55**, 321 (1939).
[7] D. C. DeVault and W. F. Libby, Phys. Rev. **55**, 322 (1939).
[8] L. I. Roussinow and A. A. Yusephovich, Phys. Rev. **55**, 979 (1939).
[9] B. Pontecorvo, Phys. Rev. **54**, 542 (1938).
[10] G. T. Seaborg and E. Segrè, Phys. Rev. **55**, 808 (1939).
[11] M. Goldhaber, R. D. Hill and L. Szilard, Phys. Rev. **55**, 47 (1939).
[12] S. W. Barnes, Phys. Rev. **56**, 414 (1939).
[13] M. Dodé and B. Pontecorvo, Comptes rendus **207**, 287 (1939).
[14] L. A. Dubridge and J. Marshall, Phys. Rev. **56**, 706 (1939).
[15] J. W. Kennedy, G. T. Seaborg and E. Segrè, Phys. Rev. **56**, 1095 (1939).
[16] A. Langsdorf, Jr., and E. Segrè, Phys. Rev. **56**, 105, (1939).
[17] H. Walke, Phys. Rev. **57**, 163 (1940).

isomer separation performed. The solution was first freed of $I^{131}$ (half-life 8 days), which had grown from the tellurium, by reducing the iodate present with an equivalent amount of iodide and extracting the iodine with chloroform. Sufficient concentrated hydrochloric acid was added to make the solution $3N$, and sulfur dioxide was introduced in order to reduce the tellurous but not the telluric acid to elementary tellurium. (Under these conditions the reaction between telluric acid and sulfur dioxide is extremely slow and may be neglected.) This tellurium precipitate contained the separated daughter isomer (or daughter isomers) with no detectable amount of parent isomer (or isomers) as contaminant.

## Radioactive $Te^{127}$: Genetically Related Isomers with Half-Lives 90±2 Days and 9.3±0.5 Hours

Bombardment of iodine (single stable isotope, $I^{127}$) with the fast neutrons from the reaction of 8-Mev deuterons on lithium produces chemically identified tellurium with two periods, 9.3±0.5 hours and 90±2 days. Fig. 1 shows the decay of such a sample produced by an activation of 725 microampere-hours. (Since this activation was carried out during several days a direct comparison of the yields of the two activities cannot be made from Fig. 1.) This evidence led us to assign the two activities to $Te^{127}$, produced by the reaction $I^{127}$ $(n,p)$ $Te^{127}$, and the results now to be discussed have confirmed that the active bodies are indeed isomers.

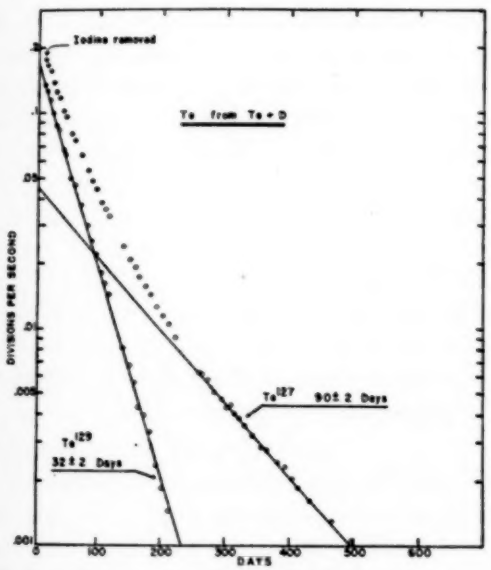


FIG. 2. The 90-day activity of $Te^{127}$ and 32-day activity of $Te^{129}$ obtained from Te+D (35 microampere-hours at 8 Mev). Each of these periods is associated with an upper isomeric state.

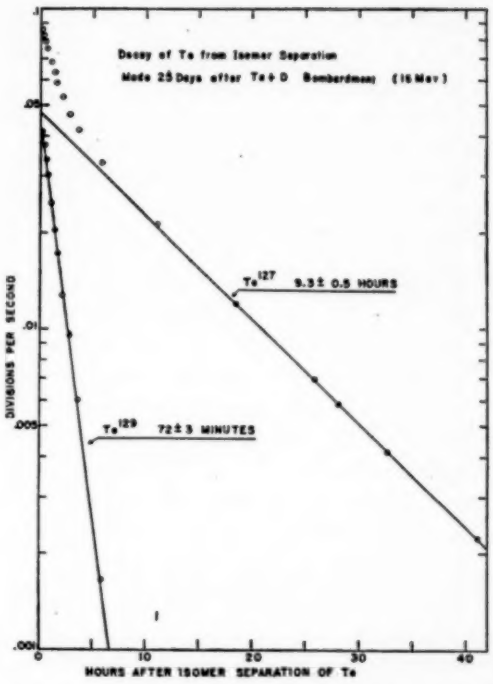
Decay of Te from Isomer Separation
Made 25 Days after Te + D Bombardment (16 Mev)
Te127 9.3 ± 0.5 HOURS
Te129 72 ± 3 MINUTES
DIVISIONS PER SECOND
HOURS AFTER ISOMER SEPARATION OF Te

FIG. 3. A sample decay curve of the 9.3-hour activity of $Te^{127}$ and the 72-minute activity of $Te^{129}$; these activities can be extracted, by means of the isomer separation process, from a sample which contains the activities shown in Fig. 2. (In the present case the tellurium was activated with 16-Mev deuterons in the 60-inch cyclotron.)

Both the 90-day and 9.3-hour activities are produced with much greater intensity by the deuteron bombardment of tellurium, and magnetic deflection experiments show that the sign of the beta-particles is negative. A portion of the decay curve of such a sample, which shows the 90-day period, is exhibited in Fig. 2.

With the chemical method described in the preceding section we have made many extractions of a 9.3-hour tellurium period from radioactive tellurium produced by Te+D. Successive extractions have shown that the parent of this daughter activity decays with a half-life of 90 days. The decay curve of one of these daughter fractions separated 25 days after the deuteron bombardment is shown in Fig. 3. (The 72-minute period shown in the analysis of the decay curve in Fig. 3 is caused by another isomer growing from a

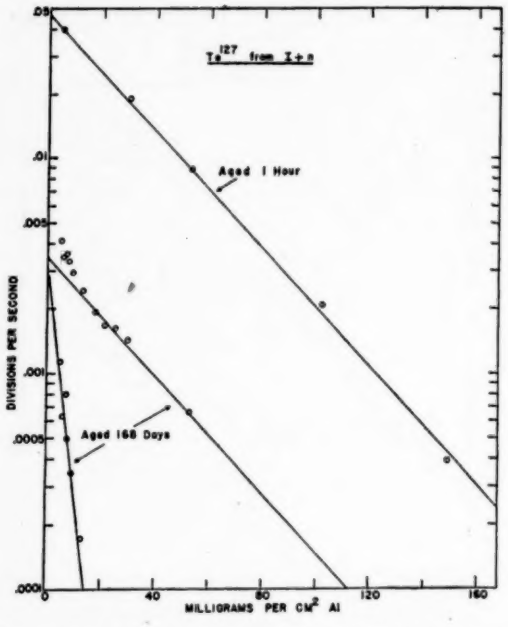


FIG. 4. Absorption curves of the $Te^{127}$ whose decay is shown in Fig. 1. The 9.3-hour activity was predominant at the age of one hour and only the 90-day activity was present at the age of 168 days. The parallel slopes (half-thickness equal to 22 mg per $cm^2$) agree with the interpretation that the beta-particles associated with each period are identical. The soft component present with the 90-day activity probably corresponds to internal conversion electrons associated with the transition to the lower (9.3-hour) isomeric level.

different tellurium parent, as will be explained in a following section.)

These experiments establish that the 90-day activity of $Te^{127}$ decays by gamma-emission to its isomer of 9.3 hours half-life, which in turn transforms to $I^{127}$ by beta-decay. From measurements of the intensities of separated daughter fractions we are able to say that practically all of the 90-day activity decays in this manner (that is, there is no observable alternative mode of decay of the 90-day activity directly to $I^{127}$). It is obvious then that the beta-spectra associated with the two activities should be identical for the apparent beta-spectrum of the 90-day activity is the beta-spectrum of the 9.3-hour activity in equilibrium with it.

The upper curve in Fig. 4 shows the absorption in aluminum of the radiations from radioactive tellurium produced by fast neutrons on iodine, taken soon after the end of the activation. The beta-particles, which belong to the 9.3-hour period, have an end-point of 0.27 $g/cm^2$ according to the method of Feather[18] which corresponds, according to the formula of Feather, to an energy upper limit of about 0.8 Mev. Since no gamma-ray has been observed over an intensity range of about two hundred it appears probable that the 9.3-hour tellurium decays directly to the ground level of $I^{127}$.

The expected identity of the beta-spectra of long and short periods is confirmed by comparison of the upper and middle curves of Fig. 4, which have the same slope. The question is of interest as to whether or not the gamma-ray which corresponds to the transition from the upper to the lower isomeric state is internally converted. A search for low energy particles (which might correspond to internal conversion electrons) was made and the lower curve of Fig. 4 suggests that a soft component is present. Mr. A. C. Helmholz has placed a sample of the 90-day activity in his magnetic spectrograph and his preliminary results indicate the presence of a line of internal conversion electrons (corresponding to a gamma-ray of approximately 125 kev).

We have also found this 9.3-hour period and indications of the 90-day period in tellurium activated with slow neutrons. Abelson[19] has found a 10-hour period which grows from an 80-hour antimony activity produced in the neutron-induced fission of uranium. A 10-hour period has been observed in fast neutron and deuteron activated tellurium by Tape and Cork[20] but was incorrectly assigned by them.

We may summarize these results in the following reactions:

$$_{53}I^{127}+{}_0n^1\rightarrow{}_{52}Te^{127}+{}_1H^1$$
$$_{52}Te^{126}+{}_1D^2\rightarrow{}_{52}Te^{127}+{}_1H^1$$
$$_{52}Te^{126}+{}_0n^1\rightarrow{}_{52}Te^{127}+\gamma$$
$$_{52}Te^{128}+{}_0n^1\rightarrow{}_{52}Te^{127}+2{}_0n^1 \text{ (only 10-hr. observed)}$$
$$_{92}U \text{ (neutron fission)}\rightarrow{}_{51}Sb^{127} \text{ (80-hr.)}$$
$$\rightarrow{}_{52}Te^{127} \text{ (only 10-hr. observed).}$$
$$_{52}Te^{127} \text{ (90-day)}\rightarrow{}_{52}Te^{127} \text{ (9.3-hr.)}+\gamma \text{ (or } e^-)$$
$$_{52}Te^{127} \text{ (9.3-hr.)}\rightarrow{}_{53}I^{127}+\beta^-.$$

[18] N. Feather, Proc. Camb. Phil. Soc. **34**, 599 (1938).
[19] P. Abelson, Phys. Rev. **56**, 1 (1939).
[20] G. F. Tape and J. M. Cork, Phys. Rev. **53**, 676 (1938).

### RADIOACTIVE $Te^{131}$: GENETICALLY RELATED ISOMERS WITH HALF-LIVES 1.2±0.2 DAYS AND 25±5 MINUTES

In a paper concerning radioactive iodine isotopes we have shown[21] that an active iodine, with 8 days half-life, grows from an active tellurium that can be produced by neutron or deuteron bombardment of tellurium; inspection of a table of isotopes shows that two pairs of successive transformations are possible, the parent of the 8-day iodine being either $Te^{129}$ or $Te^{131}$. It was found that the maximum activity of the 8-day iodine was reached 4 days after the bombardment, and by applying the equations for the growth of a daughter substance it was calculated that the parent tellurium must have a half-life of about 1.2 days. However, the initial growth of the iodine was too rapid to be accounted for by the decay of the one parent only and it was suggested that a second tellurium activity, of considerably shorter half-life, might also exist as a second parent of the 8-day iodine. In the interests of economy of space, the details of this work are not repeated here.

The tellurium fraction from deuteron or neutron activated tellurium contains so many activities that it would be extremely difficult to determine the half-lives of these two parents of the 8-day iodine by analysis of the decay curve. However, it is possible to find the short-lived parent of the 8-day iodine by successive extractions of this iodine activity, just as has been done for the 1.2-day parent. Tellurium activated with slow neutrons was used in these experiments in order to avoid the formation of any radioactive iodine by direct transmutation, which would occur in the case of deuteron activation. Successive extractions of iodine from such neutron-activated samples have been made and it has thus been definitely established that the 8-day iodine is growing from a parent of about 25 minutes half-life as well as from the 1.2-day parent.

This demonstration that the 8-day iodine grows from both periods proves that the 1.2-day tellurium is isomeric with the activity of 25 minutes half-life. Both activities are formed by the neutron or deuteron bombardment of tellurium.

We have also proved that these isomers are genetically related by separating chemically the 25-minute tellurium from the 1.2-day tellurium long after the directly formed 25-minute activity was dead. Fig. 5 shows the decay curve of such an extract made from a deuteron-activated sample 30 hours after the bombardment. The 9.3-hour and 72-minute daughter activities also appear in this extract since their parents were also present in this deuteron-activated tellurium. (These activities are discussed in other sections of this paper.) It was possible to make successive extractions containing the 25-minute activity until the 1.2-day period had completely decayed. That these 25-minute samples decayed to 8-day iodine was proved by making successive iodine extractions from one of them, and finding that the iodine fractions did show the 8-day period.

From these experiments we may conclude that the 1.2-day period corresponds to the upper state in this isomeric pair. The lower state is formed by an isomeric transition from the upper state, and decays with a 25-minute half-life by beta-particle emission to radioactive iodine. In turn this iodine decays with a half-life of 8 days to stable xenon.

With a magnetic spectrograph Dr. D. C. Kalbfell and Mr. A. C. Helmholz have observed

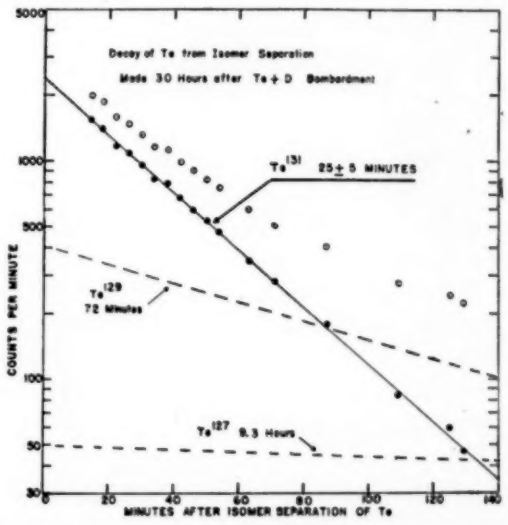
Decay of Te from Isomer Separation
Made 30 Hours after Te + D Bombardment
$Te^{131}$ 25 ± 5 MINUTES
$Te^{129}$ 72 Minutes
$Te^{127}$ 9.3 Hours
COUNTS PER MINUTE
MINUTES AFTER ISOMER SEPARATION OF Te

FIG. 5. A typical decay curve of the 25-minute activity of $Te^{131}$ extracted, by means of the isomer separation process, from a sample whose activity was largely that of the 1.2-day $Te^{131}$ obtained from Te+D. (Some 72-minute $Te^{129}$ and 9.3-hour $Te^{127}$ were also extracted since the 32-day $Te^{129}$ and 90-day $Te^{127}$ were also present.)

[21] J. J. Livingood and G. T. Seaborg, Phys. Rev. **54**, 775 (1938).

a line of conversion electrons which can be attributed to the 1.2-day activity. This line of electrons probably corresponds to the internal conversion electrons accompanying the transition from the upper to the lower state; on this basis the transition gamma-ray has an energy of about 165 kev. There are no data concerning the magnitude of the internal conversion coefficient of this gamma-ray.

Examination of the isotope chart in Fig. 6 shows that this pair of isomers must probably be assigned to $Te^{129}$ or $Te^{131}$. Our choice of $Te^{131}$ rests entirely on the following evidence. Bothe and Gentner[22] did not find a 25-minute activity (but did observe a 60-minute period, which aids us in assigning another pair of isomers to $Te^{129}$) in tellurium which had been exposed to 17-Mev gamma-rays; this activation could produce $Te^{129}$ (by the reaction $Te^{130}$ $(\gamma,n)$ $Te^{129}$) but not $Te^{131}$, so it appears that the 1.2-day and 25-minute isomers must belong to $Te^{131}$.

Abelson[19] has found these tellurium and iodine activities as products of uranium fission; he reports tellurium periods of 1.25 days and 30 minutes which lead to an iodine activity of 7.85 days.

Below we have summarized the reactions involving $Te^{131}$:

$_{52}Te^{130}+{}_{1}D^{2}\rightarrow{}_{52}Te^{131}+{}_{1}H^{1}$

$_{52}Te^{130}+{}_{0}n^{1}\rightarrow{}_{52}Te^{131}+\gamma$

$_{92}U$ (neutron fission)$\rightarrow{}_{52}Te^{131}$

$_{52}Te^{131}$ (1.2-day)$\rightarrow{}_{52}Te^{131}$ (25-min.)$+\gamma$ (or $e^{-}$)

$_{52}Te^{131}$ (25-min.)$\rightarrow{}_{53}I^{131}+\beta^{-}$

$_{53}I^{131}$ (8-day)$\rightarrow{}_{54}Xe^{131}+\beta^{-}$.

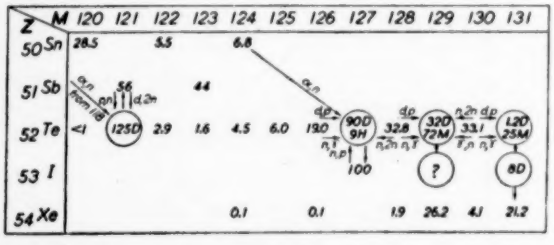


FIG. 6. Percent abundance of stable isotopes in the neighborhood of tellurium. Half-lives of radioactive isotopes are given in circles. In each of the three pairs of isomers the longer half-life corresponds to a transition from an upper to a lower isomeric state in tellurium and the shorter half-life corresponds to negative beta-particle emission to form an iodine isotope.

[22] W. Bothe and W. Gentner, Naturwiss. **25**, 191 (1937).

## $Te^{129}$: Genetically Related Isomers with Half-Lives 32±2 Days and 72±3 Minutes

Figure 2 shows a decay curve of long-lived tellurium which has been freed from the iodine grown from $Te^{131}$; this curve was obtained by allowing the tellurium precipitate from a Te+D bombardment to decay for 12 days and then removing iodine a second time. In addition to the 90-day period of $Te^{127}$ (discussed above) a strong, negative beta-particle-emitting activity of 32±2 days half-life is present. Isomer separation experiments made on tellurium containing this 32-day activity always reveal a 72-minute period in the daughter fraction. (See, for example, Fig. 3.) Moreover, successive isomer separations have proved that the parent of this 72-minute period decays with a 32-day half-life. Clearly these two periods are genetically related isomers, the 32-day period corresponding to the upper state. As in the case of the $Te^{127}$ isomers our measurements enable us to say that practically all of the nuclei in the upper state decay through the lower state rather than directly to iodine. Preliminary results obtained by Mr. A. C. Helmholz indicate that he has observed a line of conversion electrons (corresponding to an energy of about 100 kev for the isomeric transition).

If this beta-particle-emitting 72-minute activity is to be identified with the 60-minute period produced by Bothe and Gentner[22] using gamma-rays, the only reasonable possibility remaining for the assignment of this pair of isomers is $Te^{129}$. ($Te^{121}$ is not a reasonable possibility because the extremely low abundance of stable $Te^{120}$ would prevent the formation of appreciable amounts of $Te^{121}$ in a deuteron bombardment. Also, in the next section we will assign another period to $Te^{121}$.) Heyn[23] has found a 60-minute period after irradiating tellurium with fast neutrons from lithium plus deuterons; presumably his activity is to be identified with our 72-minute $Te^{129}$, the mode of production being $Te^{130}$ $(n,2n)$ $Te^{129}$.

The 72-minute activity, besides being produced by the decay of the 32-day activity, is produced directly by the deuteron and neutron bombardment of tellurium. The production of both the

[23] F. A. Heyn, Nature **139**, 842 (1939).

72-minute $Te^{129}$ and the 25-minute $Te^{121}$ is probably responsible for the unresolved apparent half-life of 45 minutes reported by Amaldi, D'Agostino, Fermi, Pontecorvo, Rasetti and Segrè[24] for the neutron-induced radioactivity of tellurium. We have also observed the production of the 32-day activity after slow neutron activation.

Tape and Cork[20] have reported a 66-minute period produced by deuterons and by fast neutrons on tellurium but their isotopic assignment does not agree with ours.[25]

Abelson,[19] in his work on the identification of the uranium fission products, found a 4.2-hour antimony activity giving rise to a 70-minute tellurium period, which undoubtedly is $Te^{129}$.

Below is given a summary of the $Te^{129}$ reactions:

$_{52}Te^{128}+{}_1D^2\rightarrow{}_{52}Te^{129}+{}_1H^1$

$_{52}Te^{128}+{}_0n^1\rightarrow{}_{52}Te^{129}+\gamma$

$_{52}Te^{130}+{}_0n^1\rightarrow{}_{52}Te^{129}+2{}_0n^1$

$_{52}Te^{130}+\gamma\rightarrow{}_{52}Te^{129}+{}_0n^1$ (only 60-min. observed)

$_{92}U$ (neutron fission)$\rightarrow{}_{51}Sb^{129}$ (4.2-hr.)

$\rightarrow{}_{52}Te^{129}$ (only 70-min. observed)

$_{52}Te^{129}$ (32-day)$\rightarrow{}_{52}Te^{129}$ (72-min.)$+\gamma$ (or $e^-$)

$_{52}Te^{129}$ (72-min.)$\rightarrow{}_{53}I^{129}+\beta^-$.

The iodine isotope $I^{129}$ has not been found in nature; however we have observed no radiations from the decay product of the 72-minute $Te^{129}$.

### Radioactive $Te^{121}$: Half-Life 125±5 Days

The activation of antimony with protons and with deuterons might be expected to yield radioactive $Te^{121}$ in both cases, and the bombardment of tin with helium ions should produce a number of active tellurium isotopes, including $Te^{121}$. These expectations are confirmed, the half-life of the common period of $Te^{121}$ formed in these three ways being close to 125 days, as is shown in the decay curves of Fig. 7. The exposure for the deuteron activated sample is not known accurately as the tellurium was activated by the probe method of Wilson and Kamen[26] for a period of several weeks, using the 37-inch cyclotron adjusted for 8 Mev. The proton bombardment was for 3 hours with 100 microamperes at a little under 4 Mev, while the alpha-particle activation was with 0.75 microampere for 5 hours at 16 Mev.

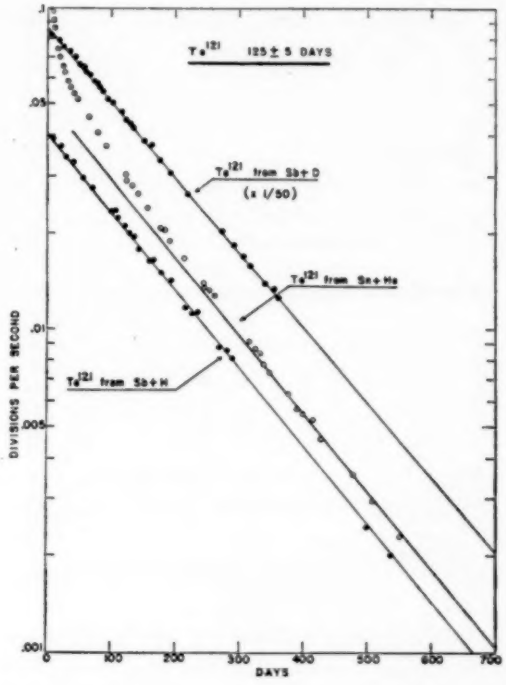


FIG. 7. Decay curves of $Te^{121}$ (125-day half-life). See text for discussion of the additional periods obtained from Sn+He.

Radioactive $Te^{121}$ would be expected to decay to stable $Sb^{121}$ by positron-emission or by $K$-electron capture. Actually the radiations are very complex as shown by the absorption curves in Fig. 8. The predominant sign of the particles, as determined by magnetic deflection experiments, is negative. The negative particles most likely are secondary electrons from the conversion of a gamma-ray. The absorption of the hard component in lead indicates a gamma-ray of about 0.5 Mev energy. This may be annihilation radiation, indicating the presence of positrons in the spectrum, but this cannot be considered certain. A detailed study of these radiations would be necessary in order to establish the decay scheme with certainty. Of course the possibility exists that the electrons come from a converted gamma-ray arising from a transition between two isomeric states in $Te^{121}$ or between an isomer of a stable tellurium isotope and its

[24] E. Amaldi, O. D'Agostino, E. Fermi, B. Pontecorvo, F. Rasetti and E. Segrè, Proc. Roy. Soc. **A149**, 522 (1935).

[25] Tape, in a more recent paper (Phys. Rev. **56**, 965 (1939)), reporting the upper energy limits of several iodine spectra, now favors our isotopic assignments of the tellurium activities.

[26] R. Wilson and M. Kamen, Phys. Rev. **54**, 1031 (1938).

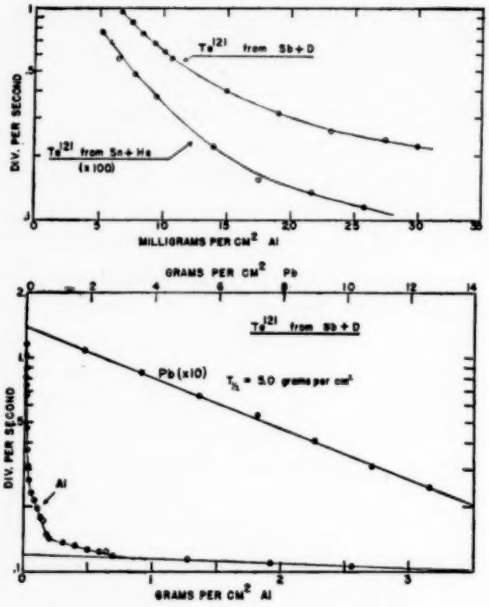


FIG. 8. Absorption curves of 125-day $Te^{121}$.

ground state. The fact that the 125-day period is not observed after deuteron or neutron bombardment of tellurium is consistent with our assignment to $Te^{121}$ because of the extremely low abundance of $Te^{120}$ (<0.1 percent).

Tape and Cork[20] have assigned to $Te^{121}$ a fast neutron-induced activity of 30 days half-life. However we suppose that this is the same activity as that assigned by us to $Te^{129}$.

The reactions involving $Te^{121}$ may be summarized as follows:

$$_{51}Sb^{121}+{}_{1}D^{2}\rightarrow{}_{52}Te^{121}+2{}_{0}n^{1}$$
$$_{51}Sb^{121}+{}_{1}H^{1}\rightarrow{}_{52}Te^{121}+{}_{0}n^{1}$$
$$_{50}Sn^{118}+{}_{2}He^{4}\rightarrow{}_{52}Te^{121}+{}_{0}n^{1}$$
$$_{52}Te^{121}\ (125\text{-day})\rightarrow{}_{51}Sb^{121}+\beta^{+}$$

or

$$_{52}Te^{121}\ (125\text{-day})+e^{-}\rightarrow{}_{51}Sb^{121}.$$

## Other Activities from Tin Plus Helium Ions

In addition to the 125-day period of $Te^{121}$, the bombardment of tin with helium ions should be expected to give a number of other unstable tellurium isotopes. Actually a number of tellurium activities were observed. A period of ten hours is probably to be identified with $Te^{127}$, produced in the reaction $Sn^{124}$ $(\alpha,n)$ $Te^{127}$. The isomeric 90-day $Te^{127}$ is probably also produced in this reaction; it is to be noticed that the $Te^{121}$ produced from tin plus helium ions (see Fig. 7) has a shorter apparent half-life than $Te^{121}$ produced in the other reactions, probably because of the admixture of a small amount of this 90-day $Te^{127}$. We might also include here what information we have concerning the other activities induced in this manner. The half-lives found in the tellurium fraction are about 35 days, 3 to 7 days and less than 3 hours. These activities are probably to be assigned to tellurium isotopes below the stable region or to antimony isotopes growing from them. (The 35-day period cannot be identified with the 32-day $Te^{129}$, for the latter isotope cannot be made from tin plus helium ions.)

## Chemical Identification of the Activities

The proper neighboring elements were added as carrier material in every case. The tellurium from the deuteron or neutron bombardments was dissolved in nitric acid and the iodine activities removed by distillation. The nitric acid was removed by evaporation and the solution adjusted to $3N$ in hydrochloric acid. The tellurium was then precipitated by saturating this solution with sulfur dioxide.[27] The antimony from the deuteron or proton bombardments and the tin from the alpha-particle bombardments were dissolved in hydrochloric acid with the addition of a little potassium chlorate. These solutions were adjusted to $3N$ in hydrochloric acid and the tellurium precipitated as before. In the case of the iodine target the iodine was distilled away before the precipitation of the tellurium. All of the tellurium precipitates obtained as has just been described were further purified by reprecipitation. The absence of selenium impurity in the tellurium was proved by separating carrier selenium from some of the activated samples. Selenium was precipitated before the tellurium by passing sulfur dioxide into the solution while it was $12N$ in hydrochloric acid. Such selenium was inactive.

It is a pleasure to thank Professor Ernest O. Lawrence for his interest in this work. Our thanks are also due to the Research Corporation for financial support.

[27] A. A. Noyes and W. C. Bray, *Qualitative Analysis for the Rare Elements* (Macmillan Company, 1927).

# The Production of Radium E and Radium F (Polonium) from Bismuth

J. M. Cork, J. Halpern and H. Tatel
*University of Michigan, Ann Arbor, Michigan*

(Received December 28, 1939)

It is shown that when bismuth is bombarded with 10-Mev deuterons both radium E and radium F are formed. The former corresponds to a neutron capture and the latter to the capture of a proton. The yield of each product is found as a function of the exciting energy. At 10 Mev the yield of radium F is less than one-fourth of that of radium E. Since the possibility of a neutron and a proton leaving the nucleus should be almost equally probable, this is evidence that the deuteron as a whole has a low probability of entering the nucleus but rather obeys an Oppenheimer-Phillips process. The cross sections for the formation of radium E and radium F at 10 Mev are $4\times10^{-28}$ cm$^2$ and $9\times10^{-29}$ cm$^2$, respectively.

STABLE bismuth consists of a single isotope of mass 109. It was shown by J. Livingood[1] that bismuth bombardment by deuterons of 5.2 Mev resulted in a capture of the neutron giving radium E. At the higher deuteron energies now available it is shown that the bombardment also forms radium F. This process corresponds to the capture of a proton. The arrangement of these isotopes is shown in Fig. 1. Radium E with a half-life of five days disintegrates into radium F by a beta-transition, and radium F with a half-life of 136 days decays to lead (206) by the emission of an alpha-particle.

It is apparent that a knowledge of the intensities of each of these radioactive products as produced by incident deuterons, when the energy of the deuterons is set at various particular values, should be of value. These quantities can be definitely determined. To reduce the energy of the bombarding deuterons the bismuth sample was covered with an aluminum foil of suitable stopping power. Identical exposures in terms of microampere minutes were given to various bismuth samples at energies from ten to six million electron volts, approximately.

The amount of radium F made is obtained directly by placing the specimen immediately after bombardment close to an ionization chamber connected to a linear amplifier. Adjustment could be made to count pulses of any desired magnitude and the bias was usually set such that only alpha-particles originating in a thickness of the bismuth, equivalent to two centimeters of air were counted. Since 10-Mev deuterons penetrated the bismuth to a depth, equivalent to sixty-four centimeters of air, the yield of alpha-particles recorded is that from the thin surface layer and is essentially due to deuterons of the maximum energy.

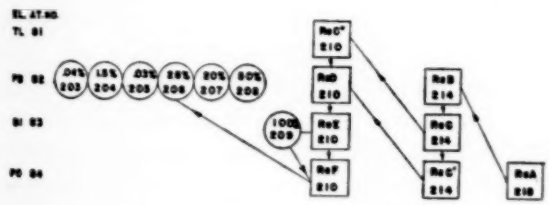


FIG. 1. Arrangement of isotopes.

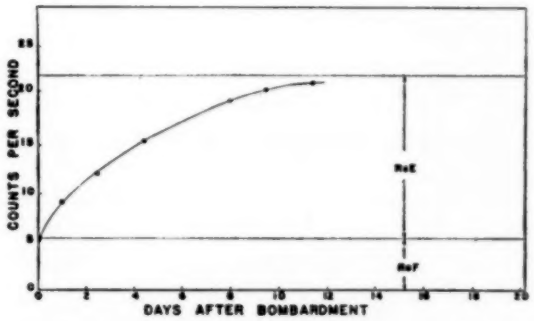


FIG. 2. Counts from sample after bombardment by deuterons.

The atoms of radium E in this same layer will emit beta-rays, thus becoming radium F and consequently be able to give alpha-particles and be counted. Fig. 2 shows the actual counts observed from such a bombarded sample at various times after bombardment. Since the half-lives of each product are known, every observation of the activity ($N$) at a time ($t$) after bombardment is sufficient to allow the calculation of the total

[1] J. Livingood, Phys. Rev. 49, 876 (1936).

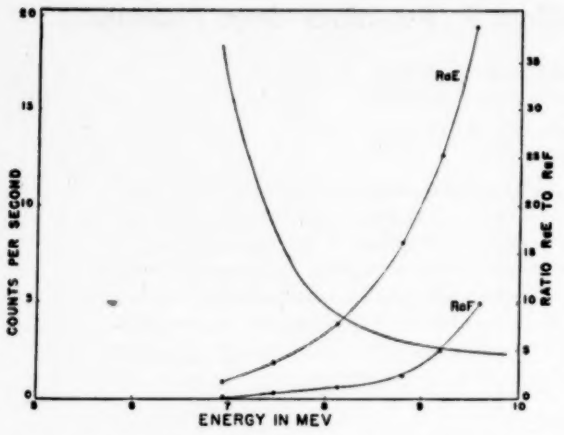


FIG. 3. Activity of targets for various energies of bombarding particles.

number ($N_0$) of radium E atoms formed. Thus

$$N_0 = N \Big/ \frac{\lambda_1}{\lambda_2 - \lambda_1} [e^{-\lambda_1 t} - e^{-\lambda_2 t}],$$

where $\lambda_1$ and $\lambda_2$ are the decay constants for the parent and daughter substances, respectively. The maximum activity is attained twenty-five days after bombardment.

The results obtained from the bismuth targets bombarded by deuterons of various energies are shown collectively in Fig. 3. A practical threshold appears for the formation of radium F at about 6.5 Mev. The ratio of the radium E to radium F is shown by the scale on the right side of the figure. At 10 Mev the yield of radium E is still almost five times that of radium F. If the deuteron in every case entered the nucleus then this ratio should be slightly less than unity since it should be easier for the neutron to leave than for the proton. It thus seems that at these energies the deuteron has a low probability of entering the nucleus as a whole. It must obey an Oppenheimer-Phillips[2] process, in which the deuteron in the external field of the nucleus yields a neutron and a proton and only the neutron enters. The entrance barrier for the deuteron must be considerably above 10 Mev. The cross section ($\sigma$) for each process may be calculated. At 10 Mev these values are $9\times10^{-29}$ cm$^2$ and $4\times10^{-28}$ cm$^2$ for radium F and radium E, respectively.

This investigation is made possible by the support of the Horace H. Rackham Fund.

[2] J. R. Oppenheimer and M. Phillips, Phys. Rev. **48**, 500 (1935).

MARCH 1, 1940 PHYSICAL REVIEW VOLUME 57

# The Distribution in Energy of the Fragments from Uranium Fission

M. H. KANNER AND H. H. BARSCHALL
*Palmer Physical Laboratory, Princeton University, Princeton, New Jersey*

(Received December 12, 1939)

The ionization produced by the fragments from uranium fission was measured. The number-energy curve shows two peaks corresponding to 65 and 98 Mev. The ionization produced by the two fragments simultaneously was measured by using a thin foil coated with U. The number-energy curve has one peak at 159 Mev and a half-width of 30 Mev.

## I. INTRODUCTION

SHORTLY after the discovery of the fission of uranium by Hahn and Strassmann[1] a number of experiments[2–5] were performed in which the kinetic energy liberated in the process was measured. The method used in these experiments was the comparison of the ionization produced by the single fission fragments with that produced by $\alpha$-particles of known energy. The agreement between these experiments was not very good. In each of the above experiments at least two maxima in the number-ionization curve were found, and the sum of the energies corresponding to these maxima was about 125 Mev according to v. Droste, Haxel, and Booth,

[1] O. Hahn and F. Strassmann, Naturwiss. **27**, 11 (1939).
[2] W. Jentschke and F. Prankl, Naturwiss. **27**, 134 (1939).
[3] G. v. Droste, Naturwiss. **27**, 198 (1939).
[4] O. Haxel, Zeits. f. Physik **112**, 681 (1939).
[5] E. T. Booth, J. R. Dunning and F. G. Slack, Phys. Rev. **55**, 981 (1939).

Dunning, and Slack, and 160 Mev according to Jentschke and Prankl.

Recently more direct experiments on the average energy liberated in the fission process have been made by Henderson,[6] who measured the heat evolved in a sample of $U_3O_8$ by a known number of fissions. His preliminary value is 175 Mev. This result is in good agreement with that of Jentschke and Prankl, and also with the theoretical predictions of Bohr and Wheeler.[7]

The experiments here described were undertaken in order to measure directly the total ionization produced in a single fission process and to attempt to reduce the discrepancy among some of the earlier measurements.

## II. Experimental

The measurement of the ionization produced by the fission fragments was made with the ionization chamber shown in Fig. 1. It was filled with air at atmospheric pressure. The chamber consisted of a brass pillbox 12 cm in diameter and 4.5 cm deep, which had in its median plane a brass electrode which supported the U samples. The dimensions were chosen so that the fragments of longest range[8] (2.2 cm) had their entire path in the chamber. The pillbox served as the high voltage electrode and was connected to a rectifier which supplied 5000 volts. The central electrode served as collector and was connected to the linear amplifier. In order to reduce electrical disturbances the collector lead was surrounded by a grounded shield where it passes through the high voltage electrode. The linear amplifier used had six high gain stages and a power stage. Strong negative feedback was used in all stages except the first, with the result that the gain of the amplifier remained constant within 1 percent over times of several days. The pulses were recorded photographically by means of a torsion type mechanical oscillograph of the type described by

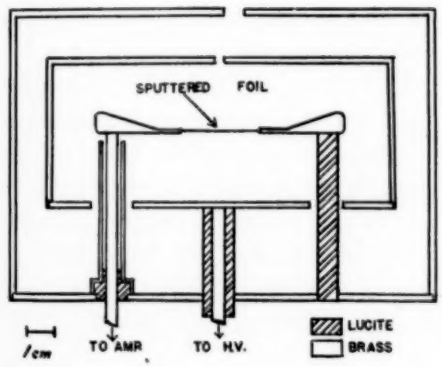


Fig. 1. Schematic diagram of the ionization chamber.

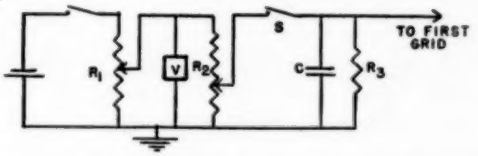


Fig. 2. Circuit of artificial pulse generator. $R_1=1000$-ohm w.w. potentiometer, $R_2=1600$ ohms tapped at 400, 800, 1200 ohms, $R_3=1$ megohm, $C=0.01$ μf, $S=$micro-switch.

Dunning,[9] which has a natural frequency of 1600 cycles/sec. and a sensitivity of 0.7 ma/mm at 1 m.

In order to standardize the amplifier and oscillograph over the large range required for an extrapolation from α-particle to fission energies the artificial pulse generator whose circuit is shown in Fig. 2 was built. The action of the circuit is as follows: $A$ known voltage, which can be varied by means of the voltage divider $R_1$ and the tapped voltage divider $R_2$, is impressed on the condenser $C$ by closing the switch $S$. The voltage across $C$ is transmitted to the grid of the first amplifier tube through a small, lucite-insulated condenser permanently mounted in the amplifier box. The successful action of the generator depends on sharp positive action of $S$. A micro-switch[10] was found to give excellent results. The pulses transmitted through the amplifier had wave forms very similar to those produced by ionizing particles in the chamber. Complete calibrations from this instrument were made at several points on each record.

The energy calibration was made by comparing the artificial pulses with the pulses produced by introducing into the chamber long range α-particles from ThC′. For this purpose the U

[6] M. C. Henderson, Phys. Rev. **56**, 703 (1939).
[7] N. Bohr and J. A. Wheeler, Phys. Rev. **56**, 426 (1939).
[8] E. T. Booth, J. R. Dunning and G. N. Glasoe, Phys. Rev. **55**, 982 (1939).
[9] J. R. Dunning, Rev. Sci. Inst. **5**, 387 (1934).
[10] Manufactured by Micro-Switch Corporation, Freeport, Illinois.

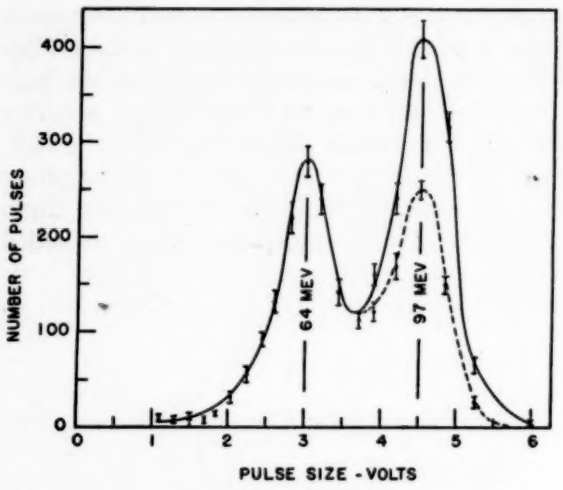


FIG. 3. Number-ionization curve for single fission fragments.

sample and its support were removed from the chamber, and replaced by a solid brass collector having identical dimensions. The $\alpha$-particles were shot into the chamber through a diaphragm and the holes shown in Fig. 1, at an angle of 60° with the plane of the collector. The portion of the range spent in the chamber was defined by the distance between the top of the high voltage electrode and the collector. The calibrations were made from two different portions of the $\alpha$-particle range. The values found were the same within 1 percent and yielded the result that a one-volt standard pulse corresponded to 21.4 Mev. Calibrations made before and after the fission experiments gave the same result. All fission results were measured in terms of standard pulses and converted into energy units by the above correspondence.

In order to check the validity of this method of extrapolation to very high energies the reduction in gain of the amplifier, made in order to reduce the size of the fission pulses, was found by measurement of the ratios of the voltage dividers used as attenuators. The attenuation factor thus found agreed with the ratio of the standard pulses necessary to produce equal oscillograph deflections at each gain setting within 2 percent. We believe, however, that the standard pulse method is more accurate than the attenuation method, since the latter involves some assumptions concerning the linearity of the amplifier.

The U samples used were of two kinds. For the observation of single fission fragments both sides of a sheet of 1 mm Al were covered with thin, quite uniform[11] layers of U metal by cathode sputtering.[12] The Al sheet was then mounted between two recessed brass sheets to form the collector of the ionization chamber. The brass pieces each had a 3.3-cm hole in the center, so that an area of about 8 cm² of U-covered Al was exposed on each side. The surface density of the U was determined by counting the $\alpha$-particles; its value was 0.12 mg/cm², corresponding roughly to a stopping power of 0.3 mm of air.

The simultaneous observation of the ionization due to both fission fragments requires that the U sample be sputtered on a foil of stopping power small compared with the sum of the ranges of the two fragments (about 3.7 cm). This requirement was met by using Al foil of 0.18 mg/cm² (stopping power 1.1 mm) as a support for the U layer. Attempts to use this foil unsupported were unsuccessful because of its extreme fragility. The method of support which proved satisfactory was the following. Sixty No. 33 holes spaced on 0.15-inch centers in a hexagon pattern were punched in a sheet of 2 mil Al with a special die. The 0.18-mg/cm² Al foil was mounted on this with thin shellac, to form a composite foil, which was then sputtered with U. During the sputtering process the composite foil was covered with a 1-mm Al sheet in which was punched a hole pattern identical with the one in the 2-mil sheet. The patterns were made to coincide by means of 3 locating holes in each sheet. In this way U was allowed to fall only on the thin parts of the composite foil, i.e., those not covered by the 2-mil pierced sheet. Foils made in this way were quite strong mechanically and could be easily handled. They were mounted between the brass plates mentioned above to form the collector of the ionization chamber. The surface density of U was

[11] Estimated from the uniformity of the interference color over the surface.

[12] We are indebted to Drs. Rentschler and Marden of the Westinghouse Company for furnishing the uranium rods used in the sputtering process. A description of the sputtering technique by C. C. Van Voorhis has appeared in Rev. Sci. Inst. **11**, 77 (1940).

determined in the same way as before and had the same value, 0.12 mg/cm².

The ionization chamber was put below a $D_2O$ ice target which was bombarded by 50–100 $\mu$a of 350-kv deuteron molecules from th treansformer-rectifier set in this laboratory. On account of the geometry of the target chamber, larger fission yields could be secured by not slowing down the 3-Mev neutrons from the D−D reaction, in spite of the smaller value of the cross section at this energy. Due to the large number of recoil nuclei in the ionization chamber, a considerable statistical ionization background was present during the measurements.

## III. Results

The results of several sets of observations of the single fragments are plotted in Fig. 3. In this plot the abscissae are the standard pulse voltages corresponding to the deflection intervals on the photographic records, and the ordinates are the numbers of pulses ending in these intervals. This method of plotting provides a linear energy scale, but, on account of the fact that the recording oscillograph characteristic

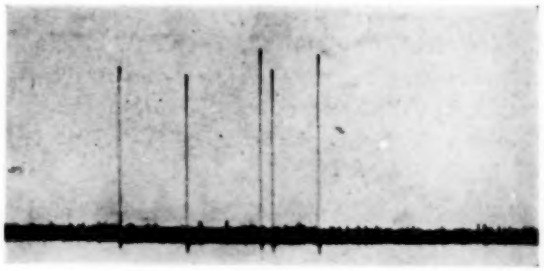

Fig. 5. Record showing 150-Mev pulses from pairs of fission fragments.

becomes somewhat nonlinear for large deflections, it distorts the vertical scale. For large deflections the response of the oscillograph falls off, thus compressing a larger energy interval into the standard deflection interval (1 mm) used in measuring the records. This results in fewer plotted points (with correspondingly larger ordinates) per energy interval. A correction is made for this effect by dividing the ordinates of the points by numbers proportional to the size of the associated energy intervals. The corrected curve is shown as a dashed line in Fig. 3. It is seen from Fig. 3 that there are two peaks, at 3

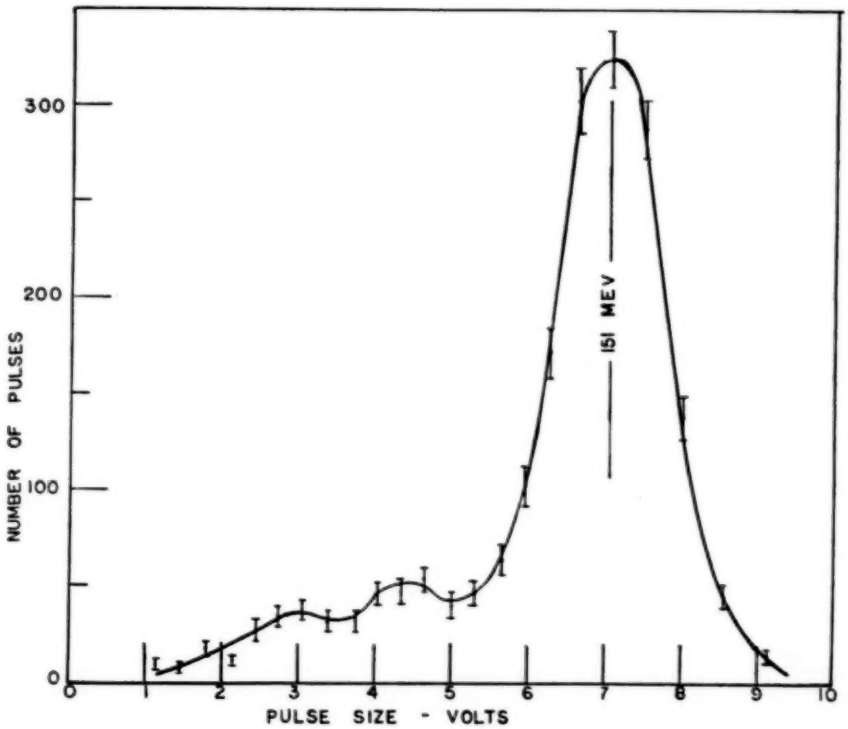


Fig. 4. Distribution of ionization due to both fission fragments.

and 4.5 volts, respectively, corresponding to energies of 64 Mev and 97 Mev. The position of the peaks was unchanged from one run to the next, within the limits of error. The total number of counts plotted is about 2500. Addition of the individual points under each peak shows that the number of counts in each is the same within 3 percent. The half-width of each peak is about 18 Mev. There are some individual pulses corresponding to energies as high as 110 Mev, although their number is small.

The values given are subject to a correction for absorption in the U layer. Under the rough assumption that the energy loss per unit path length is constant over the entire range, its value can be estimated by dividing the measured energies of the peaks in the number-ionization curve by the corresponding ranges.[8] This yields a result of 4.4 Mev per mm of air and therefore about 1 Mev, somewhat less than the accuracy of the experiments, should be added to the energy value of each peak.

The data resulting from a similar set of observations of the total ionization, with the thin Al foil, are plotted in Fig. 4. A total of 1900 pulses was evaluated. There is a fairly sharp maximum at 7.05 volts, corresponding to an energy of 151 Mev. The correction for nonlinearity of the oscillograph would make this peak slightly sharper. As the correction is small no reduced plot is given. Fig. 5 shows a sample record of 150-Mev pulses. Since the Al foil plus the U layer have a combined stopping power of about 1.5 mm, the correction for absorption in this case is somewhat larger, about 8 Mev,[13] which brings the corrected energy to 159 Mev. The half-width of the peak is 32 Mev. The two small peaks in this plot correspond exactly to the single-fragment peaks, and probably arise from small amounts of U which were accidentally deposited on the 2-mil Al support. There are a number of pulses corresponding to 190 Mev and a very few having energies as high as 200 Mev. In order to find out whether the shape of the distribution curve was influenced by a possible uneven deposit of the U layer, some experiments were carried out with a second foil. The distribution curve was the same in each case.

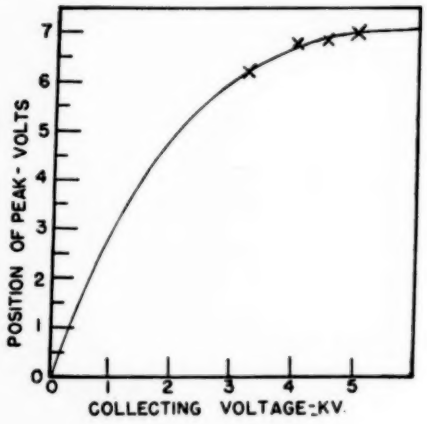


FIG. 6. Saturation curve.

The saturation conditions in the ionization chamber were investigated by making a set of measurements with various collecting voltages, statistically sufficient only to locate the standard pulse voltage corresponding to the maximum of the number-ionization curve. The resulting saturation curve is shown in Fig. 6. The numerical values were roughly as follows. For 3000 volts the value was 6.2 volts, 13 percent below that for 5000 volts. For 4000 volts it was 6.75 volts, only 4 percent below the 5000-volt value. Since this latter is a 20-percent change in voltage, it seems that the chamber was fairly well saturated at 5000 volts.

The reproducibility of the results was such that the value of the 151-Mev peak never shifted by our standard deflection interval (3 percent) from run to run. The presence of the background of statistical ionization mentioned above tends to broaden the peaks, but as it is symmetric about zero deflection, it has no effect on the position of the maximum. This was shown experimentally by the fact that different runs, made with widely different values of ion current in the deuteron beam, gave the same results. Statistical ionization and thickness of the foil influence, however, the width of the peaks somewhat. We estimate that not more than 5 Mev of the half-width is due to these effects. There may be other effects which are responsible for part of the observed widths. It is possible that the values found for the ionization should

[13] An estimation of the distribution in energy loss among the fragments indicates that the mean energy loss in the foil corresponds to about 1.2 times its stopping power.

be slightly increased because of incomplete saturation. It is also possible that the rough assumptions used in our foil corrections may introduce some error into the value of the total ionization peak. Taking these factors into account, we believe that our values, as measures of ionization, are accurate to ±5 percent.

## IV. Discussion

The validity of any quantitative correlation between the ionization produced by fission fragments and their energy is, of course, extremely questionable, since one knows so little about the mechanism of ionization by highly charged particles of high velocity. Some information concerning the mean energy required for the creation of an ion pair by a fission fragment can be got from a comparison of the results of ionization measurements with values obtained by independent methods. The only such result available is that of Henderson,[6] whose preliminary heating experiments give 175 Mev±10 percent, for the energy release per fission. His value includes the heating effect of short-lived $\beta$-emitters, which is of the order of 5 Mev,[14] yielding a value of about 170 Mev for the kinetic energy alone. This agrees within experimental error with our value of 159 Mev, which is found under the assumption that the mean ionization energy is the same for fission fragments as it is for $\alpha$-particles. More precise comparison must await the results of refined heating experiments now being performed by Dr. Henderson.

Our ionization values are in good agreement with those of Jentschke and Prankl,[2] and somewhat above those found by v. Droste,[3] Haxel,[4] and Booth, Dunning and Slack.[5] We were unable to observe the fine structure reported by v. Droste. The ratio of abscissae of the single-fragment peaks, 98 to 65, is in agreement with that found by Jentschke and Prankl and by Booth, Dunning and Slack.

The corrected ionization due to the entire fission (159 Mev) and the sum of the values of the single-fragment peaks (65+98=163 Mev) agree within experimental error. This fact, together with the equality of the numbers of counts in the two energy groups of Fig. 3, suggests the hypothesis that the pairs of fragments corresponding to the two peaks may be associated with single fission processes.

Under this assumption the energy ratio of the two peaks in Fig. 3 (98 : 65) is inversely proportional to the mass ratio of the fission fragments. If the disintegrating nucleus is $U^{239}$ the masses of the most probable fragments are 96 and 143. The latter is in a mass region in which available

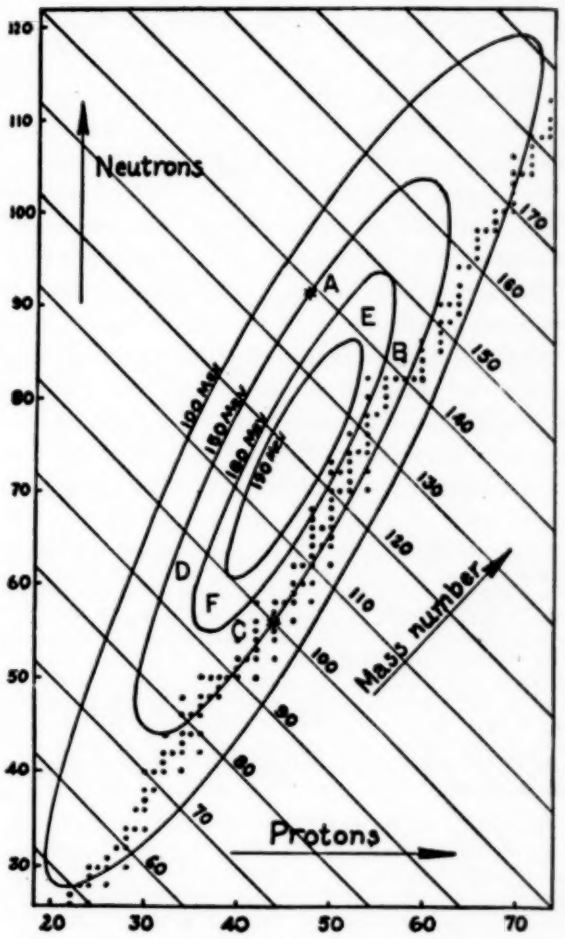


FIG. 7. (After N. Bohr and J. A. Wheeler) The difference in energy between the nucleus $_{92}U^{239}$ in its normal state and the possible fragment nuclei $_{44}Ru^{100}$ and $_{48}Cd^{139}$ (indicated by the crosses in the figure) is estimated to be 150 Mev as shown by the corresponding contour line. In a similar way the estimated energy release for division of $U^{239}$ into other possible fragments can be read from the figure.

[14] H. H. Barschall, W. T. Harris, M. H. Kanner and Louis A. Turner, Phys. Rev. **55**, 989 (1939).

chemical evidence has already placed some of the strongly $\beta$-active fission fragments.*

Figure 7 is a reproduction of Fig. 1 in the paper of Bohr and Wheeler.[7] If one assumes that the energy values found in these experiments represent true absolute values, then it follows that the most probable mode of fission leads to nuclei which lie in a region near the intersection of the line corresponding to mass 143 with the 160-Mev contour ellipse. There are two such intersections ($A$,$B$) on the diagram. The regions $C$ and $D$ represent the lighter fragments corresponding to $A$ and $B$, respectively. To account for the observed radioactivity of both light and heavy fragments, one must assume that nuclei in all four regions are produced, since $B$ and $C$ lie in the region of the stable isotopes. This would indicate that the most probable fragments have neutron-proton ratios very different, both from each other and from that of the original U. This seems rather unlikely, however, as the fragments might be expected, on statistical grounds, to lie along a line corresponding to the U neutron-proton ratio, i.e., the principal axis of the contour ellipses.

Shifts of about 10 percent in the values of the energies reported here could move the position of the most probable fragment nuclei to the regions around points $E$ and $F$, which correspond to radioactive nuclei having the expected neutron-proton ratio. Shifts of this kind could be accounted for if our correlation of ionization and energy were inaccurate. They could also be due to an additional energy release unobservable in these experiments, i.e., emission of $\gamma$-rays or neutrons during the fission process. This possibility is substantiated by the work of Zinn and Szilard[15] who observed that about two neutrons, having energies up to 3.5 Mev, are emitted per fission. It was further found by Gibbs and Thomson[16] that the bulk of the neutrons are emitted less than $10^{-3}$ sec. after the fission. This makes it plausible that the neutrons observed by Zinn and Szilard are associated directly with the fission process.[17] These results indicate that about 15 Mev has to be added to our 160 Mev value for comparison with the theory. In addition, we are informed by Professor Wheeler that the calculated values of Fig. 7 may be in error by as much as 10 Mev.

## V. Acknowledgments

These experiments were performed under the direction of Professor Rudolf Ladenburg, to whom we wish to express our sincere appreciation of his continued interest and encouragement. We wish also to thank Professor J. R. Dunning for his help and advice in the construction of the recording oscillograph, Dr. C. C. Van Voorhis for the sputtering of the foils, and Professors L. A. Turner and J. A. Wheeler for many helpful discussions. The high voltage equipment used in this work was purchased with the aid of a grant from the Rockefeller Institute.

* *Note added in proof.*—In a recent paper O. Hahn (Ann. d. Physik (5) **36**, 368 (1939)) gives two well-established examples for modes of fission: $U^{239} \rightarrow Kr^{88} + Ba^{151}$ and $U^{239} \rightarrow Xe^{139} + Sr^{100}$. Assuming 160 Mev for the total energy liberated in the fission process one obtains from these masses single-fragment energies of 59, 101, 67 and 93 Mev. These values lie almost symmetrically on both sides of the maxima in Fig. 3. As two peaks which are only 8 Mev apart would not have been resolved, particularly if they have any appreciable natural width, the mass-values quoted by Hahn are well compatible with our measurements.

[15] W. H. Zinn and L. Szilard, Phys. Rev. **56**, 619 (1939).
[16] D. F. Gibbs and G. P. Thomson, Nature **144**, 202 (1939).
[17] For a more complete discussion of this point see L. A. Turner, Rev. Mod. Phys. **12**, 1 (1940).

# A Determination of the Masses and Velocities of Three Radium B Beta-Particles

## The Relativistic Mass of the Electron

MARGUERITE M. ROGERS, A. W. MCREYNOLDS* AND F. T. ROGERS, JR.†
*Rice Institute, Houston, Texas*

(Received December 1, 1939)

An accurate determination of the values of $m/e$ and $v$ of three Ra B $\beta$-particles was made by means of an electrostatic spectrograph. It is shown that these particles obey the Lorentz model for electrons rather than the Abraham model, for velocities as high as 0.75 of the velocity of light. The uncertainty in the experiment is less than one-tenth the magnitude of the difference between the two models.

### I. INTRODUCTION

THERE have been many experiments performed[1–9] in order to determine the masses and velocities of $\beta$-rays. All of these experiments were essentially the same. The particles were deflected in a magnetic field, the deflection being a measure of $(mv)$ of the particle, where $m$ is the mass and $v$ is the velocity. They were also deflected in the electric field between two flat plates, the deflection being a measure of $(mv^2)$ of the particles. Thus since $(mv)$ and $(mv^2)$ were known, $m$ and $v$ could be obtained. Usually the magnetic and electric fields were applied simultaneously. In some experiments, such as Kaufman's,[1] the electric and magnetic fields were parallel; other experiments, such as Bucherer's,[2] consisted in balancing the magnetic and electric deflections against each other. But in all of these experiments, a flat parallel plate condenser was used to give the electric field in which the particles were deflected; hence no focusing of the $\beta$-particles was obtained. But in spite of this lack of resolving power these experiments yielded results that indicated that the electronic mass varied in such a way as to conform more nearly to the Lorentz expression[10] than to the Abraham.[10] Since most of the uncertainties in the above experiments were obscured by the large quantity of data taken, the results were accepted as adequate proof of the validity of the Lorentz expression until 1938, when Zahn and Spees[11] reopened the question with a critical survey of all the previous work. They showed that the resolving power of these experiments had been of the same order of magnitude as the effect to be measured, and they suggested that a new and more precise attempt be made to distinguish between the two electronic models. It was this statement that caused the present experiment to be undertaken.

The recent high precision determinations[12–14] of the absolute value of the $H\rho$ of the most intense line of the Ra B $\beta$-particle spectrum (which thus allows the highly precise absolute specification of the $H\rho$ values of the remaining lines in the Ra(B+C) $\beta$-particle spectrum from the precise relative values determined by Ellis and Skinner[15] and by Ellis[16,17]) give us highly accurate data on the $(mv)$ of these $\beta$-particle lines. Hence, in view of the recent advances in the use of radial electric fields for the focusing of

* Now at the University of California, Berkeley, California.
† Now at the Yerkes Observatory, Williams Bay, Wisconsin.
[1] W. Kaufman, Ann. d. Physik **19**, 487 (1906).
[2] A. H. Bucherer, Ann. d. Physik **28**, 513 (1908).
[3] G. Neumann, Ann. d. Physik **45**, 529 (1914).
[4] E. Hupka, Ann. d. Physik **31**, 176 (1910).
[5] Guye, Ratnowski, and Lavanchy, *Handbuch der Physik*, Vol. 22 (1926), p. 76.
[6] R. A. Tricker, Proc. Roy. Soc. **A109**, 384 (1925).
[7] H. Starke, Verh. d. D. Phys. Ges. **5**, 241 (1903).
[8] H. Starke and M. Nacken, Ann. d. Physik **21**, 67 (1934).
[9] H. Lahaye, Ann. d. Physik **34**, 60 (1938).
[10] H. A. Lorentz, *Lectures on Theoretical Physics*, Vol. 3 (1931), p. 266.
[11] C. T. Zahn and A. H. Spees, Phys. Rev. **53**, 511 (1938).
[12] F. A. Scott, Phys. Rev. **46**, 633 (1934).
[13] F. T. Rogers, Jr., Phys. Rev. **50**, 515 (1936).
[14] Norman Roberts, private communication of results just obtained at the University of Sydney.
[15] C. D. Ellis and H. W. B. Skinner, Proc. Roy. Soc. **A105**, 165 (1924).
[16] C. D. Ellis, Proc. Camb. Phil. Soc. **22**, 369 (1924).
[17] Rutherford, Chadwick and Ellis, *Radiations from Radioactive Substances* (Macmillan, 1930), p. 361.

charged particles,[18–20] it was considered that an experiment to determine the variation of mass with velocity of $\beta$-particles could be performed in which the chief source of uncertainty in the previous experiments, i.e., their lack of focusing, could be eliminated. Thus it was hoped that it would be possible to obtain, by a practically new and independent method, precise absolute values for the masses and velocities of three of the discrete spectra $\beta$-particles of Ra(B+C) with sufficient accuracy to allow a conclusive decision as to which model the $\beta$-particles more nearly conform.

## II. Theory

A $\beta$-particle of mass $m$, velocity $v$, and charge $e$, moving in a uniform magnetic field $H$, perpendicularly to $H$, describes a circular path of radius $\rho$, satisfying the equation

$$H\rho = mv/e. \tag{1}$$

$H\rho$ is observable and thus yields the product $mv/e$.

If this particle moves in a radial (in two dimensions), electric field $X$ (see Fig. 1), it can describe a circular path of radius $R$ given by

$$XR = mv^2/e. \tag{2}$$

$XR$ is observable and thus yields the product $mv^2/e$.

Therefore we get $v$ and $m/e$ in terms of $H\rho$ and $XR$ by the equations

$$v = (XR)/(H\rho); \tag{3}$$

$$m/e = (H\rho)^2/(XR). \tag{4}$$

Hence the determination of $XR$ and $H\rho$ for a particle is sufficient to enable us to determine the $v$ and $m/e$ of the particle.

For future reference in the analysis of the data obtained in this experiment, we record the well-known theoretical formulae for the transverse mass of the $\beta$-particle as a function of the velocity of the particle. If the particle follows the Abraham model, its transverse mass, $m_A$, is

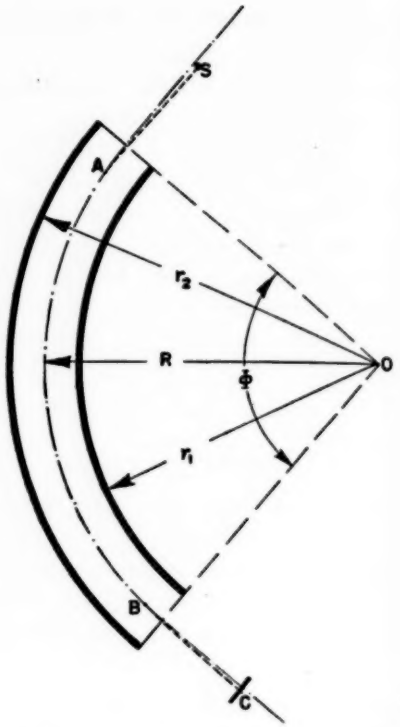


Fig. 1. $S$ and $C$ are source and counter, respectively.

given by

$$\frac{m_A}{e} = \frac{3}{8}\frac{m_0/e}{\beta^3}\left[(1+\beta)^2 \ln\frac{1+\beta}{1-\beta} - 2\beta\right], \tag{5}$$

where $m_0$ is the rest mass of the electron and $\beta = v/c$. If the particle follows the Lorentz model, its transverse mass, $m_L$, is given by

$$m_L/e = (m_0/e)/(1-\beta^2)^{\frac{1}{2}}. \tag{6}$$

## III. Experiment

In order to determine the $XR$ of the three $\beta$-particles, an electrostatic analyzer (Fig. 1) was used. It was constructed of segments of two concentric cylinders so that the mean radius, $R$, was $16.05 \pm 0.007$ cm, the height, 7.16 cm, and the angle subtended, $89° 51' \pm 05'$. If $P$ is the potential difference between the plates of the electrostatic spectrograph and if $r_1$ and $r_2$ are the radii of the inner and outer surfaces of these plates, then

$$X = P/(R \cdot \ln[r_2/r_1]). \tag{7}$$

In this instrument, $r_2 - r_1 = 0.5989 \pm 0.0032$ cm.

[18] A. J. Dempster, Phys. Rev. **51**, 67 (1937).
[19] S. K. Allison, L. S. Skaggs and N. M. Smith, Phys. Rev. **54**, 171 (1938).
[20] F. T. Rogers, Jr., Rev. Sci. Inst. **8**, 22 (1937).

Thus Eq. (7) becomes simply

$$XR=26.79P, \tag{8}$$

which (aside from possible errors which might be present in $P$) is certainly accurate to within 0.5 percent.

The potential difference $P$ was measured by a potentiometer arrangement which measured the potential drop across a 958.3-ohm resistance, caused by the current flowing through a 48.74 $\pm$0.04-megohm resistance (a bank of Taylor self-shielded x-ray resistances, manufactured by Shallcross) across the output of the high potential applied to the plates of the spectrograph. Thus the only current drain was about 0.25 milliampere through this 48.74-megohm resistance. The high potential was obtained thus: The current from a 500-cycle generator was converted to high potential by a 3-kv-amp. transformer rated at 100,000 volts output at 110 volts input. The output voltage of this transformer was controlled by a finely adjustable resistance network in the primary circuit. Two kenotrons rated at 75,000 volts each were used in the rectifying circuit. The filter network was a pair of 0.2-microfarad condensers rated at 60,000 volts d.c. The electrical centers of the transformer secondary, of the filter condensers, and of the voltage measuring resistor were connected to ground.

The spectrograph plates were mounted by fastening them to porcelain beehive insulators about 2½ inches high. These insulators were screwed to a brass base plate. Insulators of this same sort were also put on top of the plates and brass cross-braces were screwed to the top of these insulators. Hence, the path that any leakage current must take is about seven inches across porcelain. Another advantage of this mounting is that the insulators were not in the strong field between the plates. The mounting was quite strong, no difference in the separation being detectable when pressure was exerted in the same manner and of the same magnitude as that existing when a large potential difference is applied to the plates. This type of mounting was found to be superior to Bakelite spacers, because the Bakelite has a tendency to break down in vacuum even in the absence of strong fields.

The spectrograph was enclosed in an iron box, evacuated by a three-inch oil diffusion pump, backed by a Cenco Megavac pump.

The source of $\beta$-particles was a fine platinum wire, 0.75 cm in length, coated with radium active-deposit. It was inserted into the spectrograph container by a device which allowed the wire to be put accurately in place without losing the vacuum in the box. A stopcock was ground to allow a number of turns of fine wire to be wrapped around it. The source was inserted in a groove in a short, thin metal rod. This rod was lowered by means of the wire into an air lock which could be evacuated between two stopcocks. The lower stopcock was then opened and the rod was lowered into the iron box and finally into a hole in a block fastened to the base plate of the spectrograph. This hole held the rod tightly and enabled us to place the source in the same and proper place each time. Two windows in the top of the iron box enabled the source to be observed while it was being put in place.

The particles after being deflected by the plates were incident on a slit one mm wide in front of a Geiger-Müller counter with a glass bubble window 5/10,000 inch thick. The voltage at which the largest number of counts was recorded was taken to be the voltage necessary to deflect the particles along the path of mean radius $R$.

Two slight corrections had to be made to allow for the lack of ideal conditions. One allowed for the stray fields which the particles are in after leaving the plates. This correction was made by calculating how much the source must be moved toward or away from the center in order to cause the particles emitted from it to come into the spectrograph at $A$ along the path of radius $R$ (Fig. 1). Then the detector likewise must be moved this same amount so that particles coming along the $R$ path at $B$ will fall upon it. This correction assumes a perfectly aligned set of plates. Actually we do not have constant spacing of the plates, the maximum deviation from the mean being 0.0040 cm. Hence another correction must be made to allow for this. In order to make this correction, the separation was measured at seven points along the spectrograph, corresponding to $\phi=0°$, 15°,

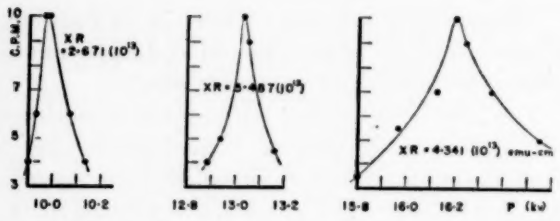


FIG. 2. The ordinates are proportional to the counting rates in particles per minute; the maxima are all normalized to ten.

30°, 45°, 60°, 75°, 90°, by using a Brown and Sharpe dial gauge calibrated in ten-thousandths of an inch. The mean separation was taken and the deviation from the mean plotted as a function of $\phi$. A function was found which closely approximated this, and this function was used in the correction to be added to the field expression in the differential equation of motion of the particle between the plates of the spectrograph. The equation was solved subject to the proper boundary conditions, and the spot at which the detector should be placed in order to detect the particles which have taken the $R$ path was found. Both these corrections turned out to be small, of the order of magnitude of one millimeter.

## IV. Experimental Results

Five independent runs were made for each $\beta$-particle line, and the voltages at which the maximum numbers of counts were found were noted. In practice, very sharp maxima were found. Fig. 2 shows graphs giving for each $\beta$-particle line typical data for counting rate *versus* plate voltage. This voltage was almost identical for a given line for all five runs, the deviations found being far below the estimated error. The data are given in Table I, along with the $v$ and $m/m_0$ values calculated from it by Eqs. (3) and (4), using for $e/m_0$ the value $1.7591(10^7)$ e.m.u./g, given by Dunnington.[21]

[21] F. G. Dunnington, Rev. Mod. Phys. 11, 65 (1939).

The $m/m_0$ values are also calculated from Eqs. (5) and (6) and tabulated as $m_A/m_0$ and $m_L/m_0$. The values of $H\rho$ are those previously measured by one of us.[13]

The results may be summarized by the graph in Fig. 3. It is obvious that the experimental points follow closely the curve given by Eq. (6), i.e., the Lorentz equation. The difference between the experimental values and the values computed on the Abraham theory is about ten times the maximum experimental uncertainty to be expected, as will be shown in the following paragraph.

The maximum error to be expected may be estimated thus. If $\epsilon_3$ and $\epsilon_4$ are the maximum errors which might be present in $H\rho$ and $XR$, respectively, then the maximum relative errors, $\epsilon_1$ and $\epsilon_2$, which can be present in $v$ and $m/e$ are obviously

$$\epsilon_1=\epsilon_3+\epsilon_4$$
$$\epsilon_2=2\epsilon_3+\epsilon_4.$$

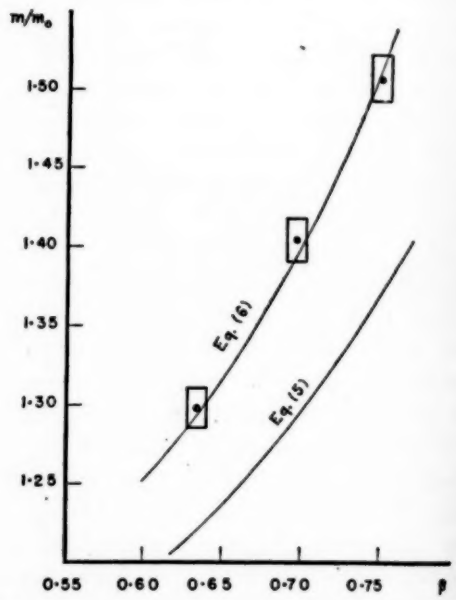


FIG. 3. Curve of $m/m_0$ *vs.* $\beta$ for the Lorentz and Abraham equations. Boxes indicate the maximum error to be expected in the measurements.

TABLE I. *Data on β-particles.*

| LINE | $H\rho$ GAUSS·CM | $P$ VOLTS | $XR$ E.M.U.·CM ($10^{-15}$) | $v$ CM/SEC. ($10^{-10}$) | $\beta$ | $m/m_0$ (OBS.) | $m_L/m_0$ (CALC.) | $m_A/m_0$ (CALC.) |
|---|---|---|---|---|---|---|---|---|
| 1 | 1406.0 | 9970 | 2.671 | 1.8998 | 0.6337 | 1.298 | 1.293 | 1.220 |
| 2 | 1671.1 | 13017 | 3.487 | 2.0868 | 0.6961 | 1.404 | 1.393 | 1.290 |
| 3 | 1931.5 | 16200 | 4.341 | 2.2470 | 0.7496 | 1.507 | 1.511 | 1.369 |

Now the maximum uncertainties present in the $H\rho$'s are no more than 1/3000, or $\epsilon_3=0.03$ percent, and the maximum uncertainty present in $XR$ is no more than 0.8/100, or $\epsilon_4=0.8$ percent. Thus we may say that $v$ is good to less than 0.9 percent and $m/e$ is accurate to well within 1.0 percent. These are the *maximum* relative errors which can be present (aside from any undetected systematic errors) in the values of $v$ and $m/e$ got in this experiment.

Thus the evidence seems to point conclusively to the fact that the RaB $\beta$-particles conform more nearly to the expression derived on the Lorentz theory than to the expression derived on the Abraham theory.

Finally, the writers wish to express their sincere appreciation for the valuable aid given them by Dr. H. A. Wilson throughout the experiment. They wish to thank Mrs. O. S. Moilliet for her help in taking the data.

---

MARCH 1, 1940 PHYSICAL REVIEW VOLUME 57

# Relativistic Magnetic Moment of a Charged Particle

HENRY MARGENAU
*Institute for Advanced Study, Princeton, New Jersey*

(Received December 26, 1939)

Formulas are derived for the magnetic moment of a particle moving rapidly in a central field of force. Possible nuclear applications, particularly to the problem of the deuteron, are discussed. In view of the greatly increased accuracy in the measurement of magnetic moments, the relativity effect appears to be of measurable magnitude.

THE fact that the Zeeman splitting of the hydrogen lines is given correctly by the Landé formula, even when the relativistic wave equation is used in the calculation, was demonstrated by Dirac.[1] Since his interest was confined to the slowly moving electron in the hydrogen atom, he neglected terms of order $v^2/c^2$. Breit[2] has given a formula for the magnetic moment of an electron in a heavy atom. At present there is renewed interest in the Zeeman effect problem because of its intimate relation with nuclear magnetic moments. The precision which has recently been achieved in the measurements of the latter, chiefly by the ingenious magnetic-resonance method of Rabi, makes it appear worth while to inquire how the magnetic moment of a charged particle depends in detail on its velocity. The basis of the computation will be Dirac's equation.

In nonrelativistic theory there are two equivalent ways of calculating the magnetic moment of a particle, both giving the same result. One is to determine the energy change of the particle in a weak field and subsequently to compute $\partial E/\partial H$. The other is to calculate the mean value of the operator $(e/2mc)(L_z+2S_z)$. Relativistically, the two procedures give different answers, and the second is probably not justified. Nevertheless it will be discussed briefly later. We first calculate the magnetic energy of a particle moving in a central field of force.

The magnetic term in the Dirac Hamiltonian is $-e\boldsymbol{\alpha}\cdot\mathbf{A}$, $\boldsymbol{\alpha}$ being the operator for $\mathbf{v}/c$ and $\mathbf{A}$ the vector potential. When the uniform field $H$ is chosen along $z$ this perturbation term takes the form

$$V=\tfrac{1}{2}eH(\alpha_x y-\alpha_y x).$$

Written as a matrix[3] it becomes

$$V=ir\sin\theta\begin{bmatrix}0&0&0&e^{-i\varphi}\\0&0&-e^{i\varphi}&0\\0&e^{-i\varphi}&0&0\\-e^{i\varphi}&0&0&0\end{bmatrix}.$$

We must calculate the diagonal elements of this operator for the two states $j=l+\frac{1}{2}$ and $j=l-\frac{1}{2}$. If the components of a $\psi$-function are $u_1\cdots u_4$,

[1] P. A. M. Dirac, Proc. Roy. Soc. **A118**, 351 (1928).
[2] G. Breit, Nature **122**, 649 (1928).

[3] The representations for $\alpha_x$ and $\alpha_y$ are those in Dirac, *Principles of Quantum Mechanics*.

the diagonal element is

$$\bar{V}=\tfrac{1}{2}ieH\{(1|\rho e^{-i\varphi}|4)-(2|\rho e^{i\varphi}|3)+(3|\rho e^{-i\varphi}|2)-(4|\rho e^{i\varphi}|1)\}, \quad (1)$$

where $\rho=r\sin\theta$ and

$$(1|a|4)=\int u_1^* a u_4 d\tau.$$

The normalized functions $u_1\cdots u_4$ are[4]

$$\left.\begin{aligned}
u_1&=\left(\frac{l-m+\frac{3}{2}}{2l+3}\right)^{\frac{1}{2}} \text{if } (r)Y_{l+1,\,m-\frac{1}{2}}\\
u_2&=\left(\frac{l+m+\frac{3}{2}}{2l+3}\right)^{\frac{1}{2}} \text{if } Y_{l+1,\,m+\frac{1}{2}}\\
u_3&=\left(\frac{l+m+\frac{1}{2}}{2l+1}\right)^{\frac{1}{2}} gY_{l,\,m-\frac{1}{2}}\\
u_4&=-\left(\frac{l-m+\frac{1}{2}}{2l+1}\right)^{\frac{1}{2}} gY_{l,\,m+\frac{1}{2}}
\end{aligned}\right\} \text{if } j=l+\tfrac{1}{2},$$

$$\left.\begin{aligned}
u_1&=\left(\frac{l+m-\frac{1}{2}}{2l-1}\right)^{\frac{1}{2}} \text{if } Y_{l-1,\,m-\frac{1}{2}}\\
u_2&=\left(\frac{l-m-\frac{1}{2}}{2l-1}\right)^{\frac{1}{2}} \text{if } Y_{l-1,\,m+\frac{1}{2}}\\
u_3&=\left(\frac{l-m+\frac{1}{2}}{2l+1}\right)^{\frac{1}{2}} gY_{l,\,m-\frac{1}{2}}\\
u_4&=\left(\frac{l+m+\frac{1}{2}}{2l+1}\right)^{\frac{1}{2}} gY_{l,\,m+\frac{1}{2}}
\end{aligned}\right\} \text{if } j=l-\tfrac{1}{2}.$$

When they are inserted in (1) and the integrals evaluated, the result is

$$\bar{V}=\begin{cases}-4eH\dfrac{(l+1)m}{(2l+3)(2l+1)}\displaystyle\int fgrd\tau \text{ if } j=l+\tfrac{1}{2}\\[2ex] 4eH\dfrac{lm}{(2l-1)(2l+1)}\displaystyle\int fgrd\tau \text{ if } j=l-\tfrac{1}{2}.\end{cases}$$

Both may be combined to

$$\bar{V}=4eH\frac{\kappa m}{(2\kappa-1)(2\kappa+1)}\int fgrd\tau, \quad (2)$$

[4] Cf. H. A. Bethe, *Handbuch der Physik*, Vol. 24/1, p. 311 *et seq.*

if we follow the convention of putting $\kappa=-(l+1)$ for $j=l+\frac{1}{2}$; $\kappa=l$ for $j=l-\frac{1}{2}$. $f$ and $g$ are the two radial functions occurring in $u_1\cdots u_4$.

The integral in (2) can be transformed with the use of the two differential equations defining $f$ and $g$:

$$\begin{aligned}(\hbar c)^{-1}(E-U+Mc^2)f&=g'+(1+\kappa)g/r\\(\hbar c)^{-1}(E-U-Mc^2)g&=-f'+(\kappa-1)f/r.\end{aligned} \quad (3)$$

On multiplying these by $g$ and $f$, respectively, and subtracting, there results

$$rfg=(\hbar/2Mc)\{rg'g+rf'f+(\kappa+1)g^2-(\kappa-1)f^2\}.$$

Now

$$\int rg'gd\tau=\int g'gr^3dr=-\tfrac{3}{2}\int g^2r^2dr,$$

and a similar relation holds for $\int rf'fd\tau$. Hence

$$\int rfgd\tau=\frac{\hbar}{2Mc}\left[(\kappa-\tfrac{1}{2})\int g^2d\tau-(\kappa+\tfrac{1}{2})\int f^2d\tau\right]$$

$$=\frac{\hbar}{2Mc}\left[\kappa-\tfrac{1}{2}-2\kappa\int f^2d\tau\right]$$

because

$$\int g^2d\tau+\int f^2d\tau=1.$$

When this is introduced in Eq. (2), the result is

$$\bar{V}=\frac{e\hbar}{2Mc}Hm\frac{\kappa}{\kappa+\frac{1}{2}}\left[1-\frac{2\kappa}{\kappa-\frac{1}{2}}\int f^2d\tau\right]. \quad (4)$$

The first term of this expression is the ordinary formula for the anomalous Zeeman effect, $\kappa/(\kappa+\frac{1}{2})$ being the Landé $g$ factor (whose value is $2(l+1)/2l+1$ if $j=l+\frac{1}{2}$, $2l/l+1$ if $j=l-\frac{1}{2}$). The second term is the relativistic correction. The magnetic moment is obtained from (4) by putting $m=j$ and dividing $\bar{V}$ by $H$. Thus

$$\mu=\begin{cases}\mu_0(j+\frac{1}{2})\left[1-\dfrac{2j+1}{j+1}\displaystyle\int f^2d\tau\right] \text{ if } j=l+\tfrac{1}{2}\\[2ex] \mu_0\dfrac{j}{j+1}(j+\tfrac{1}{2})\left[1-\dfrac{2j+1}{j}\displaystyle\int f^2d\tau\right] \text{ if } j=l-\tfrac{1}{2}.\end{cases} \quad (5)$$

Here $\mu_0$ is written for $e\hbar/2Mc$. The remaining integral may be evaluated easily for the two limiting cases of high and low energy particles.

If $E-U \gg Mc^2$, then

$$\int f^2 d\tau = \int g^2 d\tau,$$

so that each integral equals $\frac{1}{2}$. This follows at once when Eqs. (3) are multiplied by $f$ and $g$, respectively, and then integrated. Hence, for this case, Eqs. (5) reduce to

$$\mu = \pm \tfrac{1}{2}\mu_0 \frac{j+\frac{1}{2}}{j+1}, \tag{6}$$

the upper sign referring to $j=l+\frac{1}{2}$, the lower to $j=l-\frac{1}{2}$.

To discuss the case where $v/c \ll 1$ we turn to the relation

$$\int (E-U+Mc^2) f^2 d\tau = \int (E-U-Mc^2) g^2 d\tau,$$

which is easily obtainable from (3). If we write $\epsilon$ for the ratio of the kinetic energy $(E-Mc^2-U)$ to $2Mc^2$, we have

$$\int (1+\epsilon) f^2 d\tau = \int \epsilon g^2 d\tau.$$

Neglecting the small quantity $\epsilon$ on the left against 1 we see that $\int f^2 d\tau$ is small against $\int g^2 d\tau$, so that

$$\int f^2 d\tau \doteq \int \epsilon (g^2+f^2) d\tau = \bar{\epsilon}.$$

Thus the correction term in (5) is proportional, in this approximation, to the mean kinetic energy of the particle.

The present results are applicable strictly only to electrons. In attempting to deal with nuclear particles one is confronted with the difficulty that $\mu_0$ is no longer the Bohr (nuclear) magneton. On the other hand, considerable success has been obtained by treating nuclear magnetic moments as composed of two parts, that due to orbital, and that due to spin angular momentum. This corresponds to the assumption that the magnetic moment operator for a single particle is given by

$$\mu_0 \mathbf{L}\delta + 2\gamma \mathbf{S}, \tag{7}$$

where $\delta=1$ if the particle is a proton, 0 if it is a neutron, and $\gamma$ is the intrinsic magnetic moment of the free particle. It is perhaps of some interest to compute the mean value of (7) with Dirac wave functions. The most convenient way is to put at once $m=j$ in the $u$ functions and then to calculate the mean value of the $z$ component of (7). This procedure yields

$$\mu = (j-\tfrac{1}{2})\delta + \gamma + \frac{j+\frac{1}{2}}{j+1}(\delta-2\gamma)\int f^2 d\tau \text{ if } j=l+\tfrac{1}{2}$$

$$= \frac{j(j+\frac{3}{2})}{j+1}\delta - \frac{j}{j+1}\gamma - \frac{j+\frac{1}{2}}{j+1}(\delta-2\gamma)\int f^2 d\tau$$

$$\text{if } j=l-\tfrac{1}{2}.$$

The leading terms of these expressions agree, as they must, with those of (5) when $\delta$ and $\gamma$ are put equal to $\mu_0$. The relativistic terms, however, are quite different, the second even with respect to sign.

The relativity effect here computed seems at present to lie within the accuracy of measurement, and it may be of interest in connection with the magnetic moment of the deuteron. When the question is raised as to the additivity of nuclear moments, the present effect will have to be considered. Thus far experiments[5] indicate that the deuteron moment is the exact sum of proton and neutron magnetic moments. This would not be expected to be the case if the deuteron has a sizeable electric quadrupole moment. For the existence of the latter can only be explained by an admixture of a $D$ state function to the ground state of the deuteron. A $^3D$ state in the relative coordinates of neutron and proton produces a magnetic moment equal to $\frac{3}{4}-\frac{1}{2}(\mu_n+\mu_p)$, while the $S$ state contributes $(\mu_n+\mu_p)$. If we assume, following Bethe,[6] that the relative weights of $S$ and $D$ states in the deuteron wave function are approximately 93 percent and 7 percent, and that[7,8] $\mu_n+\mu_p = (2.789\pm0.003)-(1.935\pm0.030) = 0.854\pm0.033$ nuclear magneton, strict additivity would yield $\mu(H^2) = 0.93(0.854\pm0.033)+0.07(0.323\pm0.016) = 0.817\pm0.032$ n.m. The measured value is $0.856\pm0.002$ n.m. So far, then, there is perhaps

[5] Kellogg, Rabi, Ramsey and Zacharias, Phys. Rev. **56**, 728 (1939).

[6] H. A. Bethe, Phys. Rev. **55**, 1261 (1939). This assumption is of course independent of the meson theory of nuclear forces.

[7] Values and limits of error were kindly communicated by Professor Rabi.

[8] L. W. Alvarez and F. Bloch, Bull. Am. Phys. Soc. **14**, 13 (1939).

no definite evidence against additivity of nuclear moments in the deuteron, although the ranges of error of the computed and measured values barely overlap. It seems, however, that a slight disagreement is produced if the relativity effect is included.

While the exact relativistic treatment of the deuteron problem is ambiguous, it is possible to determine the sign and the order of magnitude of the correction required in the magnetic moment. If we consider the proton alone and apply the first of formulas (5) with $j=\frac{1}{2}$, the correction is $-4\mu_0\bar{\epsilon}/3$. Now $\bar{\epsilon}$ may be computed from any model of the deuteron. It depends of course upon the type of force chosen for the interaction between proton and neutron, and there is a further uncertainty connected with the mass appearing in $Mc^2$. A reasonable estimate for $\bar{\epsilon}$ arrived at by the potential hole model, seems to be 0.006. This would make the correction $-0.022$ n.m. It is difficult to see how to treat the neutron and its negative moment. If its absolute value is also diminished in proportion to its $\mu_0$ the sum of the moments will undergo a correction only about $\frac{1}{3}$ as large as the value stated, but the correction will still be negative. These matters, however, will be of greater interest when the neutron moment is known with greater accuracy.

I express my gratitude to Professor Wigner, whose remarks have stimulated these computations.

---

MARCH 1, 1940 PHYSICAL REVIEW VOLUME 57

# The Gamma-Radiation from Nitrogen Bombarded by Deuterons

E. R. GAERTTNER* AND LOUIS A. PARDUE†
*Kellogg Radiation Laboratory, California Institute of Technology, Pasadena, California*
(Received January 8, 1940)

The energies and the relative intensities of the gamma-rays emitted from nitrogen bombarded by deuterons of 700 kev energy have been measured by the positron-electron pairs and recoil electrons ejected from thin laminae placed inside a cloud chamber. The distribution of pairs ejected from a lead lamina 0.026 cm thick reveals two strong components of quantum energy $7.2\pm0.4$ Mev and $5.3\pm0.4$ Mev, and a number of weaker components which may be attributed to radiation of about 4 and 2 Mev. There are also a number of pairs which extend up to 11 Mev. The distribution of recoil electrons from a carbon lamina 0.12 cm thick indicates two strong groups of quantum energy 4.2 and 2.2 Mev. No attempt was made to extend the recoil measurements to higher energies. The 7.2-Mev radiation is attributed to the reaction

$$N^{14}+H^2\rightarrow C^{12}+He^4,$$

because radiation of this energy has been observed in other reactions producing $C^{12}$. The 5.3-Mev radiation is attributed to an excited state of $N^{15}$ of this energy according to the reaction

$$N^{14}+H^2\rightarrow N^{15}+H^1$$

in good agreement with the value of 5.4 Mev predicted by the range measurements of Cockcroft and Lewis. An attempt is made to correlate the energies and intensities of the gamma-rays produced by excited states in $C^{12}$, $N^{15}$ and $O^{15}$ according to several reactions.

## INTRODUCTION

THE gamma-radiation from nitrogen bombarded by deuterons was first investigated by Crane, Delsasso, Fowler and Lauritsen[1] by measuring the recoil electrons ejected from a thick glass wall of a cloud chamber. They obtained a complex spectrum consisting of a number of components at 1.9, 3.1, 4.0, 5.3 and 7.0 Mev. Employing the method of measuring gamma-ray energies by the positron-electron pairs and recoil electrons ejected from thin laminae placed inside a cloud chamber,[2] we have reinvestigated the radiation, and have obtained results which are not in contradiction with the

* H. H. Rackham, Post-Doctoral Fellow, University of Michigan. Now at Ohio State University.
† On sabbatical leave of absence from the Physics Department of the University of Kentucky.

[1] Crane, Delsasso, Fowler and Lauritsen, Phys. Rev. **48**, 100 (1935).

[2] Delsasso, Fowler and Lauritsen, Phys. Rev. **51**, 391 (1937); Fowler, Gaerttner and Lauritsen, Phys. Rev. **53**, 628 (1938).

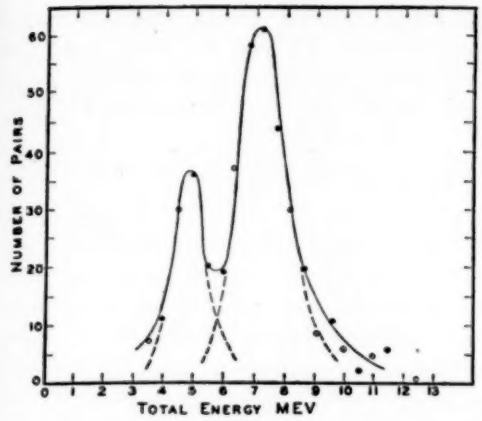


FIG. 1. Positron-electron pairs ejected from lead 0.026 cm thick by the gamma-radiation from nitrogen bombarded by deuterons, plotted in intervals of 0.9 Mev overlapping by one-half their width. $H=1650$ gauss.

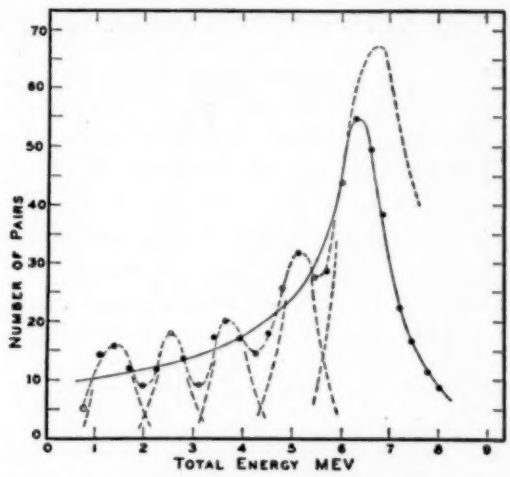


FIG. 2. Positron-electron pairs ejected from lead 0.026 cm thick by the gamma-radiation from nitrogen bombarded by deuterons, plotted in intervals of 0.55 Mev overlapping by one-half their width. $H=1000$ gauss. The solid curve is drawn through the average distribution of the pairs; broken curves are drawn in the regions where the statistical fluctuations are large, and also to indicate expected distributions of gamma-ray lines.

earlier experiments. We have measured the high energy components of the spectrum with pairs and the low energy ones with recoils. The work with recoils has been extended to higher energies by Crane and Halpern, and the results of their work appear in the *Physical Review*.[3]

The experimental arrangement of the cloud chamber was the same as that described in reference 2. The data were obtained with the a.c. accelerating tube operated at about 700 kv peak with a total ion current of about 20 microamperes during the chamber expansion, and with the pressure Van de Graaff generator operated at a voltage of 700 kv and a total ion current of 10 microamperes. The ion beam was not magnetically analyzed in either case, and consequently it consisted of a small amount of protons, estimated to be about 5 percent of the total current in the case of the a.c. tube. That there was little or no contribution from this source up to a voltage of 700 kv was indicated by experiments in which nitrogen (both $N^{14}$ and $N^{15}$)* was bombarded with protons. Targets of C.P. ammonium chloride and sodium nitrite were used, and frequently replaced due to their rapid decomposition in the ion beam. The consistency of the data obtained with the different targets and under different operating conditions supports the conclusion that the observed radiation is due predominantly to $N^{14}$ bombarded with deuterons except for a small contribution from carbon which is always deposited on targets in apparatus employing oil diffusion pumps.

[3] Crane, Halpern and Oleson, Phys. Rev. **57**, 13 (1940).
* $N^{15}$ was generously furnished by Professor H. Urey.

## ENERGY OF THE GAMMA-RADIATION

Figure 1 shows the distribution in total energy (kinetic$+2mc^2$) of (208) positron-electron pairs ejected by the radiation from a lead lamina 0.026 cm thick and measured in a magnetic field of 1650 gauss. The pairs are plotted in overlapping intervals of 0.9 Mev. Fig. 2 shows a similar distribution of (277) pairs measured in a magnetic field of 1000 gauss and plotted in overlapping intervals of 0.55 Mev. Solid curves have been drawn through the average distribution of the pairs, and broken curves in the regions where the statistical fluctuations are large; and also to indicate the theoretical distribution of monochromatic lines broadened roughly to account for the errors in measurement. The broken portion of the curve on the high energy side of the upper group in Fig. 2 is drawn to show the amount which this group must be broadened to agree with the more reliable measurement of this group in the 1650-gauss field. This must be done because there is a tendency in the measuring process to discriminate against the high energy pairs obtained in

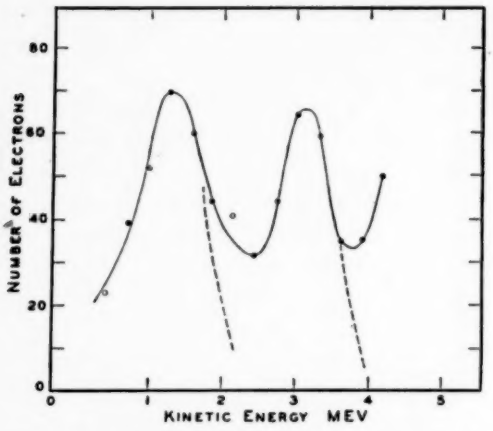


FIG. 3. Recoil electrons ejected from carbon 0.12 cm thick within an angle of 20° with the forward direction of the gamma-radiation from nitrogen bombarded by deuterons, plotted in intervals of 0.64 Mev overlapping by one-half their width. Combined results of measurements in magnetic fields of 1000 and 1500 gauss.

the lower field. The distribution of Fig. 1 reveals two strong groups, whose average energies are 5.3 and 7.4 Mev (after adding 0.3 Mev for the thickness of the scatterer), and a number of pairs extending up to 11 Mev. Similarly in Fig. 2 the average values of the prominent groups are 5.4 Mev for the lower one and 7.0 Mev for the broadened upper group. Consequently, the average values of the quantum energies with their estimated probable errors for the two prominent groups in the spectrum are $5.3\pm0.4$ and $7.2\pm0.4$ Mev. In addition to these two groups, there are a number of pairs forming a "tail" extending to lower energies. This "tail" might be due either to bremsstrahlen produced by the 5.4- and 7.0-Mev radiation, or to a number of gamma-ray lines. The latter conclusion seems more likely since the "tail" contains one-third of the total number of pairs. Furthermore, similar pair distributions from other reactions, notably from the 6.0-Mev line of $F^{19}+H^1$, do not extend to such low energies.[3]

Figure 3 shows the distribution in kinetic energy of (320) electrons ejected from a carbon lamina 0.12 cm thick within an angle of 20° with the forward direction of the quanta, and plotted in overlapping intervals of 0.64 Mev. These electrons were measured in magnetic fields of 1000 gauss and 1500 gauss. The distribution reveals two groups whose extrapolated end points are about 2.0 and 4.0 Mev. Adding 0.25 Mev to the extrapolated recoil energies gives the most probable energies of the two groups as 2.2 and 4.2 Mev. The existence of these two components in the electron distribution affords some justification for drawing the groups corresponding to these quantum energies in the pair distribution of Fig. 2. The fact that the radiation in the neighborhood of 3 Mev is suppressed in the electron distribution and not in the pair distribution may be due in part to the absence of carbon contamination while the recoil data were obtained. This fact was supported by recoil measurements with the new Van de Graaff generator where the carbon contamination was small.

[3] Delsasso, Fowler and Lauritsen, Phys. Rev. **51**, 527 (1937).

## THE RELATIVE INTENSITIES OF THE GAMMA-RAY COMPONENTS

Estimates of the relative intensities of the gamma-rays from both the pair and recoil data are given in Table I. In estimates from the pair curves the relative intensities have been corrected for the variation in the pair formation with energy. In Fig. 1 the relative intensity of the 7.2-Mev component is taken from the corrected curve. Those of the lower energy components are taken from the dotted curves which give roughly the expected distribution of pairs produced by monochromatic lines. The best measure of the relative intensities of the 5.3-Mev group and the 7.2-Mev group can be obtained from Fig. 1. The estimates from the recoil curves have been corrected for the total Klein-Nishina cross section.

TABLE I. *Estimated relative intensities of gamma-rays. $\tau$ is pair-formation cross section and $\sigma$ is Klein-Nishina cross section.*

| GAMMA-RAY ENERGY | RELATIVE INTENSITIES | RELATIVE CROSS SECTIONS | INTENSITY |
|---|---|---|---|
| Pairs | | | |
| 2 | 0.25 | 0.21 | ~1.2 |
| 4 | 0.25 | 0.54 | ~0.45 |
| $5.3\pm0.4$ | 0.5 | 0.74 | 0.7 |
| $7.2\pm0.4$ | 1.0 | 1.00 | 1.0 |
| 11 | 0.1 | 1.3 | ~0.1 |
| Recoils | | | |
| 2.2 | 1.0 | 1.35 | 0.75 |
| 4.2 | 1.0 | 1.0 | 1.0 |

### Origin of the Radiation

To account for the emission of alpha-particles, protons, and neutrons when nitrogen is bombarded by deuterons, the following reactions have been proposed ($Q$ values given by Livingston and Bethe):

$$_7N^{14}+{}_1H^2\rightarrow{}_6C^{12}+{}_2He^4+13.37 \text{ Mev} \quad (1)$$

$$_7N^{14}+{}_1H^2\rightarrow{}_7N^{15}+{}_1H^1+8.57 \text{ Mev} \quad (2)$$

$$_7N^{14}+{}_1H^2\rightarrow{}_8O^{15}+{}_0n^1+5.1 \text{ Mev}. \quad (3)$$

Cockcroft and Lewis[4] observed two discrete groups of alpha-particles of ranges 11.37 and 6.18 cm which they attributed to (1); the longer one forming $C^{12}$ in the ground state and the shorter one forming $C^{12}$ in an excited state 4.32 Mev above ground. In addition to these discrete groups of alpha-particles they observed a continuous distribution or possibly a number of closely spaced groups extending up to 3.2 Mev. They also observed two discrete groups of protons of ranges 85 cm and 18.3 cm which they attributed to (2), forming $N^{15}$ in an excited state 5.4 Mev above ground. The intensity of the short range protons was found to be $\frac{1}{4}$ to $\frac{1}{3}$ that of the short range alpha-particles (6.18 cm) at a bombarding voltage of 0.530 Mev. Stephens, Djanab and Bonner[5] observed two groups of neutrons according to (3), indicating an excited state in $O^{15}$ at 4.0 Mev. All three reactions were observed to have about the same yield at 550 kv.

The group structure of the heavy particles (1), (2) and (3) indicate the existence of 4.32, 5.5 and 4.0-Mev radiation from excited states in $C^{12}$, $N^{15}$ and $O^{15}$, respectively. The observed 4.2-Mev gamma-radiation may be attributed to (1) and (3). From energy considerations the 7.2-Mev radiation may be attributed either to (1) or (2) but it is more reasonable to assign it to (1) because radiation of about this energy has been observed in other reactions in which $C^{12}$ is formed; namely, in the reaction,

$$B^{11}+H^2\rightarrow C^{12}+n^1\,[6]$$

and in the reaction

$$Be^9+He^4\rightarrow C^{12}+n^1.[7]$$

These experiments give strong support for the existence of a level in $C^{12}$ at about 7 Mev. The absence of a group of alpha-particles in (1) which would couple with this gamma-ray to give the total disintegration energy shows that an alpha transition to this level in $C^{12}$ must be very weak if not entirely forbidden. This radiation must then be produced by gamma-ray transitions from levels lying at higher energies which are strongly coupled to the 7.2-Mev level but weakly coupled with the ground state. The presence of such levels is suggested by a number of pairs extending up to about 11 Mev. The corresponding group or groups of alpha-particles would be contained in the continuous distribution of alpha-particles. The 5.3-Mev radiation may from energy considerations be attributed to (1) or (2), but it is tempting to attribute it entirely to (2) because of the good agreement between the observed quantum energy (5.3 Mev) and the value of (5.4 Mev) predicted from (2).

One difficulty arises from the fact that the ratio ($\frac{1}{4}$ to $\frac{1}{3}$) of the number of short range protons from (2) to the short range alpha-particles from (1) is too small to account for the observed ratio ($\sim 2$) for the 5.3- to 4.0-Mev radiation if all the 5.3-Mev radiation is due to $N^{15}$. This difficulty can be removed by assuming that there is another level in $N^{15}$ above 5.4 Mev which is strongly coupled to this level but weakly coupled with the ground state of $N^{15}$.

The assistance and encouragement of Professor C. C. Lauritsen throughout this work is gratefully acknowledged. The authors are indebted to Professor Lauritsen, Dr. W. A. Fowler and Dr. T. Lauritsen for placing the pressure Van de Graaff generator at their disposal for a part of this work. One of us (E.R.G.) is also indebted to the Graduate School of the University of Michigan for an H. H. Rackham Post-Doctoral Fellowship.

[4] J. D. Cockcroft and W. B. Lewis, Proc. Roy. Soc. **A154**, 261 (1936). See also M. G. Holloway and B. L. Moore, Phys. Rev. **56**, 705 (1939).

[5] Stephens, Djanab and Bonner, Phys. Rev. **52**, 1079 (1937).

[6] Gaerttner, Fowler and Lauritsen, Phys. Rev. **55**, 27 (1939).

[7] W. Bothe, Zeits. f. Physik **100**, 273 (1936).

# The Meson Theory of Nuclear Forces

## Part II. Theory of the Deuteron†

H. A. BETHE
*Cornell University, Ithaca, New York*
(Received November 20, 1939)

With the nuclear forces as derived in the first part of this paper the deuteron problem is integrated. In §7, natural units are introduced, *viz.*, the range of the nuclear forces $1/\kappa=\hbar/\mu c$ as the unit of length and the quantity $E_0=\mu^2c^2/M$ as the unit of energy. With the adopted value of the meson mass, $\mu=177$ electron masses, we have $1/\kappa=2.18_6\times10^{-13}$ cm and $E_0=8.68$ Mev. The quantum states to be expected are discussed (§8); each state is characterized by the total angular momentum $J$, the total spin $S=0$ or 1, and the parity. For some states, the orbital momentum $L$ is defined uniquely by these quantum numbers (in this case, $L=J$); for others, we have a linear combination of wave functions with two different values of $L$, *viz.*, $J+1$ and $J-1$. The angular coordinates are eliminated from the Schrödinger equation (§9) and the radial wave equations obtained. The order of the states is discussed qualitatively (§10) and it is made plausible that the ground state is a combination of a $^3S$ and a $^3D_1$ state, both in the neutral and in the symmetrical theory. The next higher triplet state is probably $^3P_1$. Then the wave equation is solved numerically for the $^1S$ state (§11), the position of this state being taken from experiments on the scattering of slow neutrons by protons. The method of the numerical solution is described, and a table constructed giving the interaction constant $a=(2M/\mu)f^2/\hbar c$ as a function of the cut-off distance $x_0=\kappa r_0$; $a$ is found to depend only slightly on $x_0$. The next section (§12) deals with the numerical integration for the triplet (ground) state.

The following sections contain the results. In §13, the results for the neutral theory are given. A cut-off distance of 0.32 to 0.40 of the range of the forces will fit the positions of singlet and triplet state; these figures are very reasonable from general considerations. The calculations are carried out with two alternative ways of cutting off, assuming the potential inside $r_0$ either to be zero, or to retain the value it had at $r_0$. It is found that all physically significant quantities are practically independent of the method of cutting off. The value of $f^2/\hbar c$ is 0.077 or 0.080, according to the method used. The wave function contains about 6.7 percent $^3D_1$ state, the rest being $^3S$. This means that the sum of the magnetic moments of proton and neutron should be about 0.04 nuclear magneton greater than the deuteron moment which is just reconcilable with the present experimental data (§14). In §15, the quadrupole moment of the deuteron is calculated. The values found are 2.70 and $2.61\times10^{-27}$ cm$^2$ using the two methods of cutting off; the sign is positive (cigar-shape). Both sign and magnitude are in good agreement with the experiments of Kellogg, Rabi, Ramsey and Zacharias as evaluated by Nordsieck ($Q=2.7\times10^{-27}$). In §16, the $^3P_1$ state is calculated; it is shown to be unstable and to have no appreciable influence on the scattering of neutrons of moderate energy.

The symmetrical theory is discussed in §17. The calculations for this theory give unacceptable results, particularly for the cut-off distance which must be chosen considerably larger than the range of the nuclear forces ($x_0=1.3$ to 1.7). The quadrupole moment comes out about ten times too large and of the wrong sign. These results are very regrettable since only the symmetrical theory gives a natural explanation of the $\beta$-decay and of the extra magnetic moments of neutron and proton. Therefore an alternative way of cutting off is tried in §18, with even more unfavorable results. The theory of Møller and Rosenfeld is discussed (§19) but it is not considered satisfactory because of its intrinsic complication. The question remains open whether the neutral theory is correct because it gives quantitative agreement for the deuteron, or the symmetrical theory which is qualitatively preferable but in violent quantitative disagreement both with the theory of the deuteron and with the $\beta$-decay.

### §7. The Wave Equation. Abbreviations

THE wave equation of a system consisting of two nuclear particles is

$$\nabla^2\psi+(M/\hbar^2)(E-V)\psi=0, \qquad (36)$$

where $M$ is the mass of the nuclear particle, $E$ the energy of the system and $V$ the potential energy as given by (34). (If both particles are protons, the electrostatic repulsion should be added.) In $V$, the distance between the two particles occurs in the form $\kappa r$; therefore it will be convenient to introduce the abbreviation

$$x=\kappa r, \quad \mathbf{x}=\kappa\mathbf{r}, \qquad (36a)$$

i.e., to measure all distances in units of $1/\kappa$, which is the range of the nuclear forces. According to (8b), $1/\kappa=2.18_5\times10^{-13}$ cm.

† Part I in Phys. Rev. **57**, 260 (1940). The sections, equations and references are consecutively numbered in Parts I and II.

If we now denote by $\nabla'^2$ the Laplacian in the new coordinates $\mathbf{x}$, insert (34) in (36) and remember that $\kappa=\mu c/\hbar$, we obtain for the neutral theory

$$\nabla'^2\psi+\frac{ME}{\mu^2c^2}\psi-2\frac{M}{\mu}\frac{f^2}{\hbar c}\left[\tfrac{1}{3}\boldsymbol{\sigma}_1\cdot\boldsymbol{\sigma}_2\frac{e^{-x}}{x}+\left(-\frac{3}{2}\frac{\boldsymbol{\sigma}_1\cdot\mathbf{x}\,\boldsymbol{\sigma}_2\cdot\mathbf{x}}{x^2}+\tfrac{1}{2}\boldsymbol{\sigma}_1\cdot\boldsymbol{\sigma}_2\right)e^{-x}\left(\frac{1}{x^3}+\frac{1}{x^2}+\frac{1}{3x}\right)\right]\psi=0. \tag{37}$$

Obviously, it will be convenient to measure the energy in units of

$$E_0=\mu^2c^2/M. \tag{38}$$

This quantity appears to be the natural unit of energy[35] in nuclear physics, just as $1/\kappa$ is the natural unit of length. $E_0$ is the rest energy of the meson, multiplied by the ratio of the masses of meson and nuclear particle. With a meson mass of 177 $m$ as assumed here (Eq. (8)), we obtain

$$E_0=8.7 \text{ Mev}. \tag{38a}$$

This is just of the order of nuclear binding energies per particle. It is exactly four times the binding energy $w=2.17$ Mev of the deuteron; actually, the value (8) of the meson mass has been chosen (within the limits allowed by the experimental data) to make $E_0=4w$. We shall be most concerned with the ground state of the deuteron for which $E$ is negative; it is then convenient to put

$$E/E_0=ME/\mu^2c^2=-\epsilon^2. \tag{39}$$

According to the foregoing, we have for the ground state of the deuteron

$$\epsilon=\tfrac{1}{2}. \tag{39a}$$

This simple value makes the numerical work much easier.

Another abbreviation which is called for by the form of (37) is

$$a=2(M/\mu)(f^2/\hbar c). \tag{40}$$

This constant is a convenient expression for the strength of the forces. With our value for $\mu$, we have

$$a=20.8f^2/\hbar c. \tag{40a}$$

Dropping again the prime at the Laplacian, (37) becomes now

$$\nabla^2\psi-\epsilon^2\psi-a\left[\tfrac{1}{3}\boldsymbol{\sigma}_1\cdot\boldsymbol{\sigma}_2\frac{e^{-x}}{x}+\left(-\frac{3}{2}\frac{\boldsymbol{\sigma}_1\cdot\mathbf{x}\,\boldsymbol{\sigma}_2\cdot\mathbf{x}}{x^2}+\tfrac{1}{2}\boldsymbol{\sigma}_1\cdot\boldsymbol{\sigma}_2\right)e^{-x}\left(\frac{1}{x^3}+\frac{1}{x^2}+\frac{1}{3x}\right)\right]\psi=0. \tag{41}$$

At large distances, this equation may be separated in polar coordinates. The spherically symmetrical solution is

$$\psi=e^{-\epsilon x}/x\approx e^{-\frac{1}{2}x}/x, \tag{41a}$$

which means that the probability of finding the particles at a distance between $x$ and $x+dx$, $\psi^2x^2dx$, falls off as $e^{-x}dx$.

## §8. The Quantum States of the Two-Body System

The tensor interaction $V_2$ depends on the direction of $\mathbf{r}$ as well as its magnitude and therefore does not commute with the orbital momentum $\mathbf{L}$ of the system. The orbital momentum $L$ will therefore in general not be a quantum number, i.e., we cannot classify the levels of the two-body system as $S$, $P$, $D$, etc. states. The eigenfunctions will in general be linear combinations of several terms involving spherical harmonics of different orders $L$.

On the other hand, the tensor interaction is, of course, invariant against simultaneous rotation of spin $\boldsymbol{\sigma}$ and spatial coordinates $\mathbf{r}$ because it depends only on the relative orientation of these two vectors. Therefore the Hamiltonian commutes with the *total angular momentum*

$$\mathbf{J}=\mathbf{L}+\mathbf{S}, \tag{42}$$

where $\mathbf{L}$ is the orbital momentum and

$$\mathbf{S}=\tfrac{1}{2}(\boldsymbol{\sigma}_1+\boldsymbol{\sigma}_2) \tag{42a}$$

[35] It has always seemed artificial to me to use the so-called "nuclear units" which are based on $mc^2$ as unit of energy. As far as we know at present, electrons do not play an important part in nuclear forces, and even if they did, their mass would probably be irrelevant. This is already shown by the fact that all mass defects are large numbers in units of $mc^2$, rather than of the order unity.

the total spin. $J$, giving the amount of the total angular momentum, and $M$, giving its component in a given ($z$) direction, are therefore both good quantum numbers.

The Hamiltonian is also invariant against inversion, i.e., against changing the sign of all coordinates. Therefore the eigenfunctions will have a definite *parity*, even or odd, i.e., they will either remain unchanged or change sign when $\mathbf{r}$ is replaced by $-\mathbf{r}$.

Finally, the Hamiltonian commutes with the amount $S^2$ of the total spin although it does not commute with the Cartesian components of $\mathbf{S}$. This fact is not so obvious as the two preceding ones and depends essentially upon the fact that the spin of each nuclear particle is $\frac{1}{2}$. It can be proved by direct evaluation of the commutator $S^2V_2 - V_2S^2$, using relations of the type $\sigma_{1x}\sigma_{1y} = -\sigma_{1y}\sigma_{1x}$. However, the simplest proof is by showing that $V_2$, applied on the wave function of any singlet state, will vanish identically. This means that the tensor interaction can have no matrix elements between a singlet and a triplet state. Therefore the tensor interaction applied to a triplet wave function must again give a triplet function. Consequently the tensor interaction does not mix singlets and triplets, in other words it commutes with the total spin $S$. The rest of the Hamiltonian obviously commutes with $S$, and therefore $S$ is a good quantum number. It can have the values zero (singlet state) or one (triplet).

Thus the quantum numbers of our system are: the total angular momentum $J$, its $z$ component $M$, the total spin $S$, and the parity. Let us now consider the states of given $J$ and $M$. There are four such states, one singlet and three components of the triplet. The singlet state must have $L=J$ because $S=0$ (cf. (42)) so that in this case the orbital momentum is (more or less accidentally) quantized. We have a $^1S$, $^1P$, $^1D$ state, etc.

The triplet states can have $L=J$, $L=J+1$ and $L=J-1$. The parity of a state is determined by $L$, being even for even $L$ and odd for odd $L$ (Part I, reference 27, p. 108). Therefore the states $L=J+1$ and $J-1$ have the same parity while $L=J$ has the opposite parity. Since the parity is quantized, the state $L=J$ will be by itself, i.e., it will not be mixed with any state of a different $L$. Therefore here again $L$ will be "accidentally quantized," we can speak of $^3P_1$, $^3D_2$, $^3F_3$ states, etc.

The two states $L=J+1$ and $L=J-1$ will be mixed, the eigenfunction being a linear combination of two functions involving spherical harmonics of order $J-1$ and $J+1$, respectively. The corresponding radial wave functions satisfy two simultaneous differential equations of the second order (cf. §9). There will, of course, be two such mixed states for a given $J$, the lower in general containing more of $L=J-1$, the higher more of $L=J+1$. For $J=1$, we get thus a mixture of a $^3S$ and a $^3D_1$ state: such a mixture will represent the ground state of the deuteron. For $J=2$, we have a mixture of $^3P_2$ and $^3F_2$, etc. Only $J=0$ is an exception, because $J=0$ in conjunction with $S=1$ implies necessarily $L=1$ so that we get a pure $^3P_0$ state.

Our analysis shows that at most two different values of $L$, and sometimes only one, occur in a given eigenfunction.[36] This makes the two-body problem manageable since it is reduced to the numerical solution of at most two simultaneous differential equations for the radial wave functions. These equations will be derived in the following section.

It need hardly be emphasized that the structure of our spectrum has no relation to that found in Russell-Saunders coupling. In particular, the spectroscopic notation is used only for convenience and does by no means imply that states in the same triplet, e.g., $^3P_0$, $^3P_1$, $^3P_2$, have any relation to each other. They will be as widely separated as states of different $L$ or $S$, and states of the same $J$ will not lie close together either.

## §9. Elimination of the Angular Coordinates

The eigenfunction of a triplet state of given $J$ and $M$, and given parity, may be written:

$$\psi(x, \vartheta, \varphi, M_S) = (1/x)\sum_L u_L(x) F_{J\,LM}(\vartheta, \varphi, M_S). \quad (43)$$

Here the sum contains at most two terms (cf. §8), the $u_L$ are the radial wave functions ($x=\kappa r$) and the $F$ will be called angular functions in the following. They can be expressed in terms of

[36] This was pointed out to me by R. Peierls to whom I am greatly indebted for a stimulating discussion.

ordinary spherical harmonics and of spin functions:

$$F_{JLM}=\sum_{m=M-1}^{M+1} c_{JLMm}\Phi_{LMm}, \tag{44}$$

where

$$\Phi_{LMm}=Y_{Lm}(\vartheta\varphi)\chi_{M-m}. \tag{44a}$$

Here the $Y_{Lm}$ are normalized spherical harmonics,[37] $m$ is the orbital momentum about the $z$ axis (we write $m$ instead of $M_L$ for convenience). The $\chi$ are the usual triplet spin functions, *viz.*

$$\begin{aligned}\chi_1&=\alpha(1)\alpha(2),\\ \chi_0&=2^{-\frac{1}{2}}[\alpha(1)\beta(2)+\beta(1)\alpha(2)],\\ \chi_{-1}&=\beta(1)\beta(2).\end{aligned} \tag{44b}$$

The subscript of the spin function gives the spin in the $z$ direction, $M_S=M-m$. Since $M_S$ goes from $-1$ to $+1$, $m$ will take the values $M-1$, $M$ and $M+1$. The $c$'s are constant coefficients which are given by considerations about angular momenta; they are independent of the potential; a general discussion will be found in Condon and Shortley.[38] We assume the $F$'s normalized, then

$$\sum_{m=M-1}^{M+1}|c_{JLMm}|^2=1. \tag{45}$$

There are several other relations between the $c$'s of different $J$ and $m$ expressing orthogonality and normalization of the $F$'s.

Since the $F$ as well as $\psi$ are normalized, the normalization condition on the radial functions is

$$\sum_L\int u_L{}^2dx=1. \tag{46}$$

TABLE I. *Coefficients $t$ in the tensor interaction (cf. Eq. (50))*

| $L$ | $J=L-1$ | | $J=L$ | | $J=L+1$ | |
|---|---|---|---|---|---|---|
| | TERM | $t_{JL}$ | TERM | $t_{JL}$ | TERM | $t_{JL}$ |
| 0 | | | | | $^3S_1$ | 0 |
| 1 | $^3P_0$ | 2 | $^3P_1$ | $-1$ | $^3P_2$ | 1/5 |
| 2 | $^3D_1$ | 1 | $^3D_2$ | $-1$ | $^3D_3$ | 2/7 |

$t_{J,LL'}$: $J=1$ (coupling $^3S$ and $^3D_1$) $\quad t_{J,LL'}=-\sqrt{2}$
$J=2$ (coupling $^3P_2$ and $^3F_2$) $\quad t_{J,LL'}=-(3/5)\sqrt{6}$.

[37] For the definition of the $Y_{Lm}$ and relations between them see Bethe, *Handbuch der Physik*, Vol. 24, No. 1 (1933), p. 551. The definition is $Y_{Lm}=\left(\frac{2L+1}{4\pi}\right)^{\frac{1}{2}}\frac{1}{2^L L!}\times\left(\frac{(L-m)!}{(L+m)!}\right)^{\frac{1}{2}}\sin^m\vartheta\times\frac{d^{L+m}}{(d\cos\vartheta)^{L+m}}(\cos^2\vartheta-1)^{L+m}e^{im\varphi}$ for any (positive or negative) $m$.

[38] E. U. Condon and G. H. Shortley, *Theory of Atomic Spectra* (Cambridge University Press, 1935).

The $u_L$ obey the differential equations (neutral theory):

$$\begin{aligned}\frac{d^2u_L}{dx^2}-\Big[\epsilon^2+\frac{L(L+1)}{x^2}+\frac{1}{3}\frac{e^{-x}}{a}{x}\\ +t_{JL}\,ae^{-x}\Big(\frac{1}{x^3}+\frac{1}{x^2}+\frac{1}{3x}\Big)\Big]u_L\\ =t_{JLL'}\,ae^{-x}\Big(\frac{1}{x^3}+\frac{1}{x^2}+\frac{1}{3x}\Big)u_{L'}.\end{aligned} \tag{47}$$

Here $-\epsilon^2$ represents the eigenvalue in our units (cf. §7), $L(L+1)/x^2$ the centrifugal force, and $\frac{1}{3}ae^{-x}/x$ the central force $V_1$ in which we have inserted for $\boldsymbol{\sigma}_1\cdot\boldsymbol{\sigma}_2$ its value (unity) for triplet states. The remaining terms arise from the tensor interaction. If $L=J$, the term on the right-hand side will be absent (§8); if $L=J\pm1$, there will be just one term on the right-hand side, with $L'=J\mp1$.

The coefficients $t$ are constants (not depending on $x$) and represent the matrix elements of the characteristic term in the tensor interaction, *viz.*, of

$$T=-\frac{3}{2}\frac{\boldsymbol{\sigma}_1\cdot\mathbf{x}\,\boldsymbol{\sigma}_2\cdot\mathbf{x}}{x^2}+\tfrac{1}{2}\boldsymbol{\sigma}_1\cdot\boldsymbol{\sigma}_2. \tag{48}$$

The definition of the $t$'s is

$$TF_{JLM}=t_{JL}F_{JLM}+t_{JLL'}F_{JL'M}. \tag{48a}$$

Since $T$ commutes with $J$, no terms with different $J$ and $M$ can appear on the right-hand side, and the coefficients $t$ can only depend on $J$ and $L$ but not on $M$. They can easily be calculated using the relations between the spherical harmonics[37] and the method of sums (cf. reference 37, p. 555). The result is

$$t_{J=L+1,\,L}=\frac{L}{2L+3}=\frac{J-1}{2J+1}, \tag{49}$$

$$t_{J=L,\,L}=-1, \tag{49a}$$

$$t_{J=L-1,\,L}=\frac{L+1}{2L-1}=\frac{J+2}{2J+1}, \tag{49b}$$

$$t_{J,\,LL'}=-3J^{\frac{1}{2}}(J+1)^{\frac{1}{2}}/(2J+1). \tag{49c}$$

Table I gives the numerical values for the smallest $J$.

## §10. The Sign of the Interaction and the Order of the Quantum States

Before we proceed to the actual numerical integration of the radial wave equations (47), we shall discuss the sign and relative magnitude of the interactions in the various quantum states.

### A. The neutral theory

In the *singlet states* there is an attraction

$$V_{\text{singl}} = -ae^{-x}/x. \tag{50}$$

This attraction is independent of $L$.

For the *triplet states with* $L=J$, the central force $V_1$ is repulsive, and the tensor interaction $V_2$ is attractive and independent of $L$ since $t_{JL}=-1$. The total interaction is

$$V_{L=J} = V_1+V_2 = \tfrac{1}{3}a\frac{e^{-x}}{x} - ae^{-x}\left(\frac{1}{x^3}+\frac{1}{x^2}+\frac{1}{3x}\right)$$
$$= -ae^{-x}\left(\frac{1}{x^3}+\frac{1}{x^2}\right), \tag{51}$$

i.e., attractive at all distances.

The *other two triplet states*, $L=J\pm1$, are mixed together. This mixing will be unimportant if the coupling interaction

$$V_{\text{coup}} = -3\frac{J^{\frac{1}{2}}(J+1)^{\frac{1}{2}}}{2J+1}ae^{-x}\left(\frac{1}{x^3}+\frac{1}{x^2}+\frac{1}{3x}\right) \tag{52a}$$

is small compared with the difference between the centrifugal potentials,

$$C=\frac{(J+1)(J+2)-(J-1)J}{x^2}=\frac{2(2J+1)}{x^2}. \tag{52b}$$

This will be the case when $J$ is large because then the particles will stay at large distances $x$. Then the two states with different $L$ can be considered separately, and in each of them we shall have two repulsive interactions (central force and tensor interaction). The *repulsion* is *larger for* $L=J+1$ *than for* $L=J-1$ (cf. (49), (49b)). For very high $J$ the two repulsions become equal, we have $t_{JL}=\frac{1}{2}$ for both values of $L$ and

$$\lim_{L\to\infty} V_{L=J+1} = \lim V_{L=J-1}$$
$$= \tfrac{1}{2}ae^{-x}\left(\frac{1}{x^3}+\frac{1}{x^2}+\frac{1}{x}\right). \tag{52c}$$

On the other hand, for the $^3S$ state the tensor interaction does not contribute to the repulsion at all ($t_{JL}=0$) and for $^3P_2$ its contribution is rather small ($t_{JL}=\frac{1}{5}$).

Actually, the coupling between the states $L=J+1$ and $L=J-1$ will tend to lower the lower of the two, and to raise the upper. The centrifugal force is greater for $L=J+1$; and, according to the preceding paragraph, the same is true for the repulsive force arising from the "diagonal term" in the tensor interaction. Therefore the lower state will be mainly $L=J-1$, and the higher state $L=J+1$. In particular, the lower state with $J=1$ will be mainly $^3S$ with some $^3D_1$ mixed in (ground state of the deuteron). For $J=0$, there is only a strongly repulsive state, $^3P_0$.

Since the tensor interaction is attractive (cf. (34b)) when the vector $\mathbf{r}$ from one particle to the other is parallel to the spin $\mathbf{S}$, the "lower" state will tend to have $\mathbf{r}$ and $\mathbf{S}$ parallel while in the "upper" state $\mathbf{r}$ and $\mathbf{S}$ will tend to be at right angles. In particular, in the ground state of the deuteron $\mathbf{r}$ will more often be parallel to $\mathbf{S}$ than this would be the case in a pure $^3S$ state. In such a pure state, there is no preferential direction for $\mathbf{r}$ at all; therefore *the actual ground state of the deuteron will have an oblong shape, with the major axis in the direction of the spin* $\mathbf{S}$. This is equivalent to a *positive quadrupole moment of the deuteron which agrees in sign with the experimental result of Kellogg, Rabi, Ramsey and Zacharias.*[39]

A similar reasoning leads to an understanding of the sign of the diagonal term of the tensor interaction. At least for high orbital momenta, we can apply classical concepts. Then the orbital momentum $\mathbf{L}$ will be perpendicular to the position vector $\mathbf{r}$. Therefore attraction is to be expected when $\mathbf{L}$ is perpendicular to $\mathbf{S}$, and this is the case for $J=L$. When $\mathbf{L}$ is parallel or antiparallel to $\mathbf{S}$ ($J=L\pm1$) repulsion will result.

It is of great interest to decide which of the terms of given $J$ will actually lie lowest, the one with $L=J$ or the lower of the two other terms. The following (nonrigorous) argument decides in favor of the latter. We write the radial equations for $L=J\pm1$ in abbreviated form:

$$d^2u_{J-1}/dr^2-\epsilon^2u_{J-1}=Au_{J-1}-Du_{J+1},$$
$$d^2u_{J+1}/dr^2-\epsilon^2u_{J+1}=-Du_{J-1}+Cu_{J+1}. \tag{53}$$

[39] J. M. B. Kellogg, I. I. Rabi, N. F. Ramsey and J. R. Zacharias, Phys. Rev. **56**, 728 (1939).

Here

$$A=\tfrac{1}{3}ae^{-x}/x+(J-1)J/x^2+(J-1)B/(2J+1),$$
$$B=ae^{-x}\left(\frac{1}{x^3}+\frac{1}{x^2}+\frac{1}{3x}\right),$$
$$C=\tfrac{1}{3}ae^{-x}/x+(J+1)(J+2)/x^2+(J+2)B/(2J+1), \tag{53a}$$
$$D=3J^{\frac{1}{2}}(J+1)^{\frac{1}{2}}B/(2J+1).$$

Then by an argument similar to that used in the derivation of the WKB method it can be shown that the two simultaneous equations (53) are almost equivalent to a single Schrödinger equation with the potential

$$W=\tfrac{1}{2}(A+C)\pm[\tfrac{1}{4}(A-C)^2+D^2]. \tag{53b}$$

The negative sign corresponds to the lower state; inserting (53a), we obtain

$$W_-=\tfrac{1}{3}a\frac{e^{-x}}{x}+\frac{J(J+1)+1}{x^2}+\tfrac{1}{2}B-\left[\left\{\frac{2J+1}{x^2}+\frac{3B}{2(2J+1)}\right\}^2+\left(\frac{3B}{2J+1}\right)^2J(J+1)\right]^{\frac{1}{2}}. \tag{54}$$

This expression must be compared with the potential for the state $L=J$ which is

$$V_{L=J}=\tfrac{1}{3}a\frac{e^{-x}}{x}+\frac{J(J+1)}{x^2}-B. \tag{54a}$$

The difference is

$$V-W=-\frac{1}{x^2}-\tfrac{3}{2}B+\left[\left(\frac{1}{x^2}+\tfrac{3}{2}B\right)^2+\frac{4J(J+1)}{x^4}\right]^{\frac{1}{2}}, \tag{55}$$

which is always positive. Therefore *the mixed state is lower than the state* $L=J$. It may be of interest to give the value of $W_-$ in the limiting cases: For weak coupling ($(2J+1)/x^2\gg 3B/2$) we have

$$W=\tfrac{1}{3}a\frac{e^{-x}}{x}+\frac{(J-1)J}{x^2}+\frac{J-1}{2J+1}B-\frac{9J(J+1)}{2(2J+1)^3}B^2x^2+\cdots, \tag{55a}$$

for strong coupling

$$W=\tfrac{1}{3}a\frac{e^{-x}}{x}-B+\frac{J(J+1)}{x^2}-\frac{4J(J+1)}{3Bx^4}+\cdots. \tag{55b}$$

Therefore the lowest of the triplet states with a given $J$ is that which contains mostly the lowest possible $L$, *viz.*, $L=J-1$, mixed with some $L=J+1$. The next state, which is not much higher if the interaction is large, is the pure state $L=J$, while the highest state, with a strong repulsive potential, is the mixed state which contains mostly $L=J+1$ and a smaller amount of $L=J-1$.

For a given class of states, the potential is higher for higher $J$. Now for $J=0$, there is only one triplet state, *viz.*, $^3P_0$, which has a strongly repulsive potential (cf. Table I). Therefore the lowest triplet state must be found among the states with $J=1$, and according to the preceding paragraph, it must be the state which is composed of $^3S$ and $^3D_1$ with the former predominating. The next state will be $^3P_1$, and after this the lowest state with $J=2$ will follow, *viz.* $^3P_2+{}^3F_2$. That the order of the states is actually as indicated here, in particular that $^3P_1$ lies higher than $^3S+{}^3D_1$, will be shown by numerical calculation in §13 and 16.

Although $L$ is not a true quantum number, it is interesting to investigate the states which have as their predominant part a given $L$. Of these, the state with $J=L$ will in general be the lowest, the state $J=L+1$ somewhat higher and $J=L-1$ by far the highest.

While the sequence of the triplet states and that of the singlet states separately can be thus established, the relative position of triplets and

singlets cannot be derived on qualitative grounds. In particular, it depends on the cut-off distance $x_0$ whether the $^1S$ or the $^3S+^3D_1$ state is the lowest (§11–13).

**B. Symmetrical theory**

As has been mentioned repeatedly, the potential in this theory differs from that in the neutral theory by the factor $\tau_1\cdot\tau_2$ which is 1 for states symmetrical in the charge coordinate, $-3$ for antisymmetrical states. With the discussion of §6 on the symmetry of various states, we find then:

In the *singlet states* the potential is attractive for even $L$, and has then the same value as in the neutral theory, *viz.*,

$$V=-ae^{-x}/x \quad (S=0,\ L \text{ even}). \tag{56}$$

For odd $L$, the potential is repulsive and three times as large:

$$V=3ae^{-x}/x \quad (S=0,\ L \text{ odd}). \tag{56a}$$

For the *triplet states*, the potential is the same as in the neutral theory if $L$ is *odd*, but has the opposite sign and three times the magnitude if $L$ is even. Remembering the sign of the interaction for the various triplet states in the neutral theory, we find: *The "diagonal part" of the interaction is attractive for all triplet states of odd $J$, repulsive for all triplet states of even $J$.*

Since the centrifugal potential increases with $J$, it is thus immediately clear that the lowest triplet states are those with $J=1$. The competition is therefore again between the $^3P_1$ state and the mixed state $^3S+^3D_1$. However, the latter state is much more favored than in the neutral theory, because the potential in the $^3P_1$ state is the same as in the neutral theory (54a), while for the other state all terms involving the interaction constant $a$ are multiplied by $-3$. Denoting by $B$ the same expression as in (53a), we have then instead of (55)

$$V-W=\frac{4}{3}\frac{e^{-x}}{x}+\frac{1}{2}B-\frac{1}{x^2}+\left[\left(\frac{9}{2}B-\frac{1}{x^2}\right)^2+\frac{4J(J+1)}{x^2}\right]^{\frac{1}{2}}, \tag{56b}$$

which is always positive and in general much larger than (55).

In the symmetrical theory, we can also say definitely that $^3S+^3D_1$ must be lower than $^1S$, a statement which was not possible in the neutral theory. The reason is that the central force has the same value for $^1S$ and $^3S$, *viz.*, (50a), and that the diagonal term of the tensor interaction vanishes for $^3S$; the nondiagonal term which couples $^3S$ to $^3D_1$ will then lower $^3S$ below $^1S$. Thus the $^3S+^3D_1$ state is the lowest of all states.

A considerably different situation obtains with respect to the relative orientation of $\mathbf{r}$ and $\mathbf{S}$, and especially to the quadrupole moment of the ground state. For odd $L$, as we know, the symmetrical theory agrees with the neutral theory; for even $L$, on the other hand, the sign of the whole interaction, and particularly the tensor interaction, is reversed; therefore in the low states of even $L$, $\mathbf{r}$ and $\mathbf{S}$ will tend to be perpendicular. The ground state, $^3S+^3D_1$, falls in this class. Therefore, according to the symmetrical theory, the deuteron will have a flat shape, with the short axis in the direction of the spin. It will therefore have a negative quadrupole moment, in contradiction to the experimental result.

## §11. The $^1S$ State

We calculate the radial wave function $u$ of the $^1S$ state for zero energy. $u$ obeys the Schrödinger equation

$$d^2u/dx^2-Vu=0. \tag{57}$$

Outside the cutting-off distance $x_0$, we have

$$V=-ae^{-x}/x \quad (x>x_0). \tag{58}$$

For $x<x_0$, we consider the two alternative ways of cutting off discussed in §6, *viz.*

(a) The "zero cut-off"

$$V=0 \quad \text{for} \quad x<x_0. \tag{58a}$$

(b) The "straight cut-off"

$$V=V_0=-ae^{-x_0}/x_0 \quad \text{for} \quad x<x_0. \tag{58b}$$

The inner boundary condition on $u$ is

$$u(x=0)=0, \tag{59}$$

since $u=x\psi$. The outer boundary condition may be written

$$u(x\to\infty)=c(1+\gamma x), \tag{60}$$

where $c$ is an arbitrary normalization constant and $\gamma$ is determined by the scattering of slow neutrons by protons.

The scattering cross section for slow neutrons is, neglecting the unimportant effect of the finite range of the forces (Part I, reference 27, p. 117)

$$\sigma=\frac{\pi}{\kappa^2}\left(\frac{1}{\gamma^2}+\frac{3}{\epsilon^2}\right), \tag{61}$$

where $\epsilon^2$ is the binding energy of the deuteron in our units (cf. §7) and $\gamma$ the characteristic constant of the singlet state as introduced in (60). With the value of $1/\kappa$ as given in (8b), we have

$$\pi/\kappa^2=1.50\times10^{-25}\text{ cm}^2. \tag{61a}$$

Further, according to (39a), $\epsilon=\frac{1}{2}$. The experimental value of the cross section is not very accurately known because experiments with thermal neutrons involve the effect of chemical binding which has not been calculated accurately, while experiments at higher energies are difficult and involve large experimental errors. The most recent experimental value at thermal energies is that of Carroll and Dunning,[40] *viz.*, $50.7\times10^{-24}$ cm$^2$. The reduction factor for chemical binding was calculated by Arley[41] who found 2.77. This gives $\sigma=18.3\times10^{-24}$ cm$^2$. Direct experiments with Ag and I resonance neutrons above thermal energies) give a lower value,[42] *viz.*, $14.8\times10^{-24}$. Our calculations are not very sensitive to the exact value of the cross section but mainly to the fact that it is large. We have used an average of the two experimental values, *viz.*,

$$\sigma_{\text{exp}}=16.8\times10^{-24}\text{ cm}^2. \tag{61b}$$

With (61) (61a) (61b) and $\epsilon=\frac{1}{2}$, we obtain

$$\gamma=0.1000. \tag{61c}$$

Thus the wave function (60) has almost horizontal tangent outside the range of the force (58). The positive sign of $\gamma$ indicates that the $^1S$ state is virtual rather than real.[43]

[40] H. Carroll and J. R. Dunning, Phys. Rev. **54**, 541 (1938).
[41] N. Arley, Kgl. Dansk. Akad. **16**, 1 (1938).
[42] L. Simon, Phys. Rev. **55**, 792 (1939).
[43] F. G. Brickwedde, J. R. Dunning, H. J. Hoge and J. H. Manley, Phys. Rev. **54**, 266 (1938); J. Halpern, I. Estermann, O. C. Simpson and O. Stern, Phys. Rev. **52**, 142 (1938); L. W. Alvarez and K. S. Pitzer, Phys. Rev. **55**, 596 (1939).

Since $\gamma$ is given experimentally, the solution of the wave equation will give the interaction constant $a$ as a function of the cutting-off distance $x_0$ and of the method of cutting off ("zero" or "straight"). The integration for $x<x_0$ is elementary, we have for zero cut-off

$$u=\alpha x \quad \text{(zero)} \tag{62a}$$

($\alpha$ arbitrary) and for straight cut-off

$$u=\alpha\sin\left[(ae^{-x_0}/x_0)^{\frac{1}{2}}x\right] \quad \text{(straight)}. \tag{62b}$$

For $x>x_0$, we integrate from the outside in. For large $x$ (greater than 2 or 3), an analytical solution is used, for smaller $x$, numerical integration for each value of $a$. The point $x_0$ itself is determined from the condition that the outside and the inside solutions must join smoothly.

In the outside solution, we expand in powers of the potential. Obviously, such an expansion will converge rapidly for large $x$. We shall use it for $x>2$ when $a\leq2$, and only for $x>3$ when $a>2$. We write:

$$u=u_1+\gamma u_2, \tag{63}$$

where both $u_1$ and $u_2$ satisfy the wave equation

$$d^2u/dx^2=-a(e^{-x}/x)u, \tag{63a}$$

while their asymptotic behavior is given by

$$\lim_{x\to\infty}u_1=1, \tag{63b}$$

$$\lim_{x\to\infty}u_2=x. \tag{63c}$$

The integration gives up to terms of order $a^2$:

$$u_1=1-a(xEi(-x)+e^{-x})+a^2(e^{-2x}+e^{-x}Ei(-x)+(2x-1)Ei(-2x))+\cdots, \tag{64a}$$

$$u_2=x-ae^{-x}+a^2(\tfrac{1}{2}e^{-2x}+xEi(-2x))+\cdots, \tag{64b}$$

where $Ei(-x)$ is the exponential integral (cf. Jahnke-Emde, Table of Functions). The terms in $a^3$ can be estimated; they are only noticeable in the derivatives $du/dx$ to which they contribute about one-thousandth of the terms linear in $a$.

For $x$ between $x_0$ and $x_1=2$ or 3, the integration of the wave equation (63a) must be done numerically. To start the numerical integration, $u$ and $du/dx$ are calculated from ((63), (64)) for the joining point $x_1$ (see below), and then the integration carried on to smaller $x$. As shown by

Hartree,[44] the numerical integration is most convenient if

$$y=\log x \tag{65}$$

is used as the independent variable, and

$$F=ux^{-\frac{1}{2}}=x^{\frac{1}{2}}\psi \tag{65a}$$

as the dependent variable.

The numerical integration itself was carried out using Hartree's method, i.e., calculating the wave fundtion $F$ at regular intervals $y$, $y-h$, $y-2h$, etc., and the derivative $F'=dF/dy$ at the midpoints $y-\frac{1}{2}h$, $y-\frac{3}{2}h$, etc. The interval $h$ was chosen equal to 0.2 units of the natural logarithm; four significant figures were carried in $F'$ and $F''$. As a rule, the numerical integration for a given $a$ took about half an hour.

The starting point for the numerical integration was in general $y=0.7$, corresponding to $x=2.014$, while the first point for $F'$ was $y=0.6$ ($x=1.822$). The values $a=1.6$, 1.7, 1.8, 2.0 were used. For larger values of $a$, the analytical formulae would not be accurate enough at $y=0.7$ and 0.6; therefore, the numerical integration was in this case started at $y=1.1$, $x=3.0042$ for $F$ and $y=1.0$, $x=2.7183$ for $F'$. This was done for $a=2.5$, 3, 4 and 5.

The boundary condition at $x_0$ is a smooth join of wave function and derivative to the interior solution (62a) or (62b), respectively This means

for zero cut-off:

$$\left(\frac{1}{F}\frac{dF}{dy}\right)_{x_0}=\frac{x}{F}\frac{dF}{dx}=\frac{x}{u}\frac{du}{dx}-\frac{1}{2}=-\frac{1}{2}, \tag{66a}$$

for straight cut-off:

$$\left(\frac{1}{F}\frac{dF}{dy}\right)_{x_0}=\frac{(ax_0e^{-x_0})^{\frac{1}{2}}}{\tan\,(ax_0e^{-x_0})^{\frac{1}{2}}}-\frac{1}{2}. \tag{66b}$$

In addition to these calculations with a cut-off potential, we calculated $a$ for the case of no cutting off ($x_0=0$). In this case it was obviously not convenient to continue the numerical integration down to $x=0$. An analytical solution of (63a) was therefore obtained, *viz.*,

$$u=z^{\frac{1}{2}}J_1(2z^{\frac{1}{2}})+\tfrac{1}{3}ax^2J_2(2z^{\frac{1}{2}})-0.0417a^2x^4 +(0.0083a^2+0.0229a^3)x^5+\cdots \tag{67}$$

where

$$z=ax, \tag{67a}$$

$J_1$ and $J_2$ are Bessel functions. The value of $a$ was found by trial and error: For a given $a$, $u$ was calculated by numerical integration outwards; then the solution joined to one of the type (63) and $\gamma$ determined. We found $\gamma=0.1496$ for $a=1.4$ and $\gamma=0.0940$ for $a=1.5$. By interpolation we obtained $a=1.489$ for the "experimental value" $\gamma=0.1000$.

In Table II, the resulting relation between $a$ and $x_0$ is given. It is seen that for moderate $x_0$, $a$ changes very slowly with $x_0$. From the general arguments of the field theory given in §6, we expect a cutting-off distance $x_0$ of about $\frac{1}{3}$. According to Table II, this would mean a value of $a$ of about 1.6 to 1.7. Thus we may say that $a$ is almost exactly determined by the position of the singlet level of the deuteron, provided only a reasonable assumption is made about $x_0$. The position of the triplet state can then only be adjusted by varying $x_0$.

Table II has been extended to larger values of $x_0$ because these are needed for the symmetrical theory (§17). Also included in the table are the values of $x_0/(a-a_0)^{\frac{1}{2}}$ where $a_0=1.489$ is the value of $a$ for $x_0=0$. This quantity is seen to vary slowly with $a$ and is therefore most convenient for (graphical) interpolation.

That $x_0$ will, at least as long as it is small, be proportional to $(a-a_0)^{\frac{1}{2}}$ can be seen from a simple calculation. For small $x$, (67) reduces to

$$u=z-\tfrac{1}{2}z^2+\cdots. \tag{68}$$

$u$ is the "regular" solution of the differential equation (63a). Now suppose the potential is zero for $z<z_0$. Then in this region,

$$\psi\sim z \qquad (z<z_0). \tag{68a}$$

(We write $\psi$ for the wave function for arbitrary $z_0$ and reserve $u$ for the case $z_0=0$.) When this "inside function" is joined to a solution of (63a), the latter will be a linear combination of the regular solution (69) and the irregular one, *viz.*,

$$v=1-z\log z+\cdots. \tag{69}$$

We write

$$\psi=u+\alpha v. \tag{69a}$$

Using the boundary condition of smooth join at $z=z_0$, we find (cf. 68a)

$$\alpha=-\tfrac{1}{2}z_0^2. \tag{69b}$$

[44] D. R. Hartree, Phys. Rev. **46**, 738 (1934); Proc. Camb. Phil. Soc. **24**, 89, 111 (1928).

TABLE II. *Relation between cutting-off distance $x_0$ and interaction constant $a$ for the singlet state.*

| $a$ | 1.489 | 1.6 | 1.7 | 1.8 | 2 | 2.5 | 3 | 4 | 5 |
|---|---|---|---|---|---|---|---|---|---|
| $x_0$ Zero Cut-off | 0 | 0.2447 | 0.3554 | 0.4458 | 0.5959 | 0.8933 | 1.121 | 1.486 | 1.732 |
| $x_0$ Straight Cut-off | 0 | 0.4056 | 0.5687 | 0.7012 | 0.9196 | 1.3295 | 1.635 | 2.101 | 2.428 |
| $x_0/(a-a_0)^{\frac{1}{2}}$(Zero) | 0.689 | 0.735 | 0.773 | 0.799 | 0.834 | 0.888 | 0.912 | 0.926 | 0.924 |
| $x_0/(a-a_0)^{\frac{1}{2}}$(Straight) | 1.194 | 1.217 | 1.238 | 1.257 | 1.287 | 1.322 | 1.330 | 1.326 | 1.296 |

The regular function (68) satisfies the boundary condition (60) at large $x$ for $a=a_0$. The new function (69a) will satisfy the same boundary condition if $a$ is changed by an amount proportional to $\alpha$, so that

$$a-a_0=c'z_0^2=cx_0^2. \tag{70}$$

The constants $c'$ and $c$ could only be determined by actually calculating $v$. It is simpler to obtain $c$ from an extrapolation of the data in Table II.

For straight cut-off, we have instead of (68a)

$$\psi\sim\sin(z/z_0^{\frac{1}{2}}) \tag{71}$$

and therefore for the condition of smooth join

$$\left(\frac{z}{\psi}\frac{d\psi}{dz}\right)_{z_0}=\frac{z_0^{\frac{1}{2}}}{\tan z_0^{\frac{1}{2}}}=1-\tfrac{1}{3}z_0+\cdots. \tag{71a}$$

Solving for $\alpha$, we obtain

$$\alpha=-\tfrac{1}{6}z_0^2. \tag{71b}$$

Therefore for straight cut-off (cf. (70))

$$a-a_0=\tfrac{1}{3}cx_0^3, \tag{71c}$$

which shows that the limit, for $x_0\to 0$, of $x_0/(a-a_0)^{\frac{1}{3}}$ is $3^{\frac{1}{3}}$ times greater for straight cut-off than for zero cut-off.—The same results could also be obtained by treating the cutting off as a perturbation of the potential (63a) and applying the Schrödinger-Born theory.

## §12. The Triplet State (Ground State), Calculation

As has been shown in §8–10, the ground state of the deuteron is a mixture of a $^3S$ and a $^3D_1$ state. For convenience, we shall denote the respective radial wave functions of the $S$ and $D$ component by $\chi$ and $\varphi$. Then the complete wave function is

$$\psi=x^{-1}[\chi(x)F_{10M}+\varphi(x)F_{12M}], \tag{72}$$

where the $F_{JLM}$ are the angular functions defined in (44). The radial wave functions satisfy the two simultaneous differential equations

$$\begin{aligned} d^2\chi/dx^2&=A\chi-B\sqrt{2}\varphi,\\ d^2\varphi/dx^2&=(A+B+6/x^2)\varphi-B\sqrt{2}\chi, \end{aligned} \tag{73}$$

where

$$A=ae^{-x}/3x+\epsilon^2, \tag{73a}$$

$$B=ae^{-x}\left(\frac{1}{x^3}+\frac{1}{x^2}+\frac{1}{3x}\right). \tag{73b}$$

The potential will be cut off at small distances, and we consider again the two alternatives

(a) Zero cut-off

$$A=B=0 \quad \text{for} \quad x<x_0. \tag{74a}$$

(b) Straight cut-off

$$A=A_0=e^{-x_0}/3x_0+\epsilon^2, \qquad (x<x_0). \tag{74b}$$

$$B=B_0=e^{-x_0}\left(\frac{1}{x_0^3}+\frac{1}{x_0^2}+\frac{1}{3x_0}\right),$$

Because of the strong divergence of $B$ (73b), the result will be very sensitive to the value of $x_0$. The "experimental" value of $\epsilon$ is $\frac{1}{2}$ (cf. (39a)).

The conditions on the wave functions $\chi\varphi$ are that they vanish for $x\to\infty$ and for $x=0$. Disregarding these conditions, there would be four linearly independent solutions of the two simultaneous equations (73). Two of these solutions may be chosen so as to be finite at $\infty$; they will then behave as $e^{-\epsilon x}$ as can easily be seen from (73) (73a). The two others will become infinite as $e^{+\epsilon x}$. Alternatively, the four solutions may be combined in such a way that two of them vanish at $x=0$, the two others will then not vanish. But for a given value of $x_0$ and $\epsilon$, there will in general not be any solution[45] which vanishes both at $x=0$ and $x=\infty$. For a given $x_0$, there will only be certain eigenvalues of $\epsilon$ for which such a solution exists. Actually, our procedure is the reverse: Since $\epsilon$ is known from experiment, we seek the value of $x_0$ which permits a regular solution for the given $\epsilon$ (and $a$).

The integration is similar to that of the preceding section but complicated by the fact that we have now two pairs of solutions where we had only a single solution before.

### Inside solution

The inside solution is trivial in the case of zero cut-off; we have then the two independent regular solutions

$$\chi_3=c_3x \qquad \varphi_3=0 \tag{75a}$$

and

$$\chi_4=0 \qquad \varphi_4=c_4x^3 \tag{75b}$$

with arbitrary constants $c_3$, $c_4$.

For the straight cut-off, the solutions are

[45] From the two regular solutions at small $x$, we can always form a linear combination such that its continuation to large $x$ does not contain *one* of the functions which become infinite for $x=\infty$. However, the selected linear combination *will* in general contain the other of these functions. The condition for an eigenvalue is then that the coefficient of this other irregular function also vanishes. This is clearly one condition and can be satisfied by the variation of one parameter, e.g., $\epsilon$.

much more complicated. For practical purposes it is convenient to make use of the fact that $B$ (cf. (74b)) is much larger than $A$ if $x_0$ is of the expected magnitude (about 0.4). If $A$ is neglected entirely, the solution of Eq. (73) will be a function of

$$z=B_0^{\frac{1}{3}}x \tag{76}$$

only. The influence of $A$ can then be considered by expanding in powers of

$$b=\frac{A_0}{B_0}=\frac{\frac{1}{3}a+x_0\epsilon^2e^{x_0}}{a(x_0^{-2}+x_0^{-1}+\frac{1}{3})}; \tag{76a}$$

in practice, only terms up to $b^2$ need to be considered. In these variables, the wave equation (73) becomes

$$\begin{aligned} d^2\chi/dz^2&=b\chi-\sqrt{2}\varphi,\\ d^2\varphi/dz^2&=-\sqrt{2}\chi+(1+b+6/z^2)\varphi. \end{aligned} \tag{76b}$$

Both the regular solutions of (76b) contain only odd powers of $z$, one of them contains also a logarithmic term. Similarly as in (75), there is one solution in which $\chi$ is the "leading" wave function and one in which it is $\varphi$. The first pair of solutions is

$$\chi_3=z-0.00900z^5-\cdots+\log z(0.020z^5+\cdots)+b(0.1667z^3-\cdots)+b\log z(\cdots)+\cdots, \tag{77a}$$

$$\varphi_3=0.01298z^5+0.01202z^7+\cdots-\log z(0.2828z^5+\cdots)+b(0.0113z^5+\cdots)+\cdots. \tag{77b}$$

The second pair in which $\varphi$ is the leading function does not contain the $\log z$:

$$-\chi_4=0.07071z^5+0.002405z^7+\cdots+b(0.0041z^7+\cdots), \tag{77c}$$

$$\varphi_4=z^3+0.0714z^5+\cdots+b(0.0714z^5+\cdots)+\cdots. \tag{77d}$$

The values of $\chi$ and $\varphi$ and their derivatives at $x_0$ were computed from these formulae to 4 significant figures. The value of $z$ corresponding to $x_0$ is (cf. (74b), (76))

$$z_0=[ae^{-x_0}(1/x_0+1+x_0/3)]^{\frac{1}{3}}. \tag{78}$$

**Outside solution**

For very large $x$, a solution of (73) was obtained in terms of a power series. Unlike the case of the singlet state, only the terms without $a$ and those linear in $a$ can be expressed in terms of tabulated functions, this difference being due to the energy term $\epsilon^2$ in the wave equation. There is again one pair of functions in which $\chi$ is "leading" while $\varphi$ vanishes for $a=0$, and another pair in which the reverse is true.

The pair in which $\chi$ is the leading function is, up to terms linear in $a$:

$$\chi_1=e^{-\epsilon x}+(a/6\epsilon)G(x), \tag{79a}$$

$$\varphi_1=-\frac{\sqrt{2}a}{8\epsilon^4}\left\{\left[\frac{2\epsilon^3+3\epsilon-3}{x^2}+\frac{(2\epsilon-1)\epsilon^2}{x}\right]e^{-(1+\epsilon)x}+\frac{3-4\epsilon^2}{2\epsilon}F(x)\right\}, \tag{79b}$$

where

$$G(x)=-e^{-\epsilon x}Ei(-x)+e^{\epsilon x}Ei[-x(1+2\epsilon)], \tag{79c}$$

$$F(x)=-e^{-\epsilon x}Ei(-x)\left(\frac{1}{x^2}+\frac{\epsilon}{x}+\frac{\epsilon^2}{3}\right)+e^{\epsilon x}Ei(-x(1+2\epsilon))\left(\frac{1}{x^2}-\frac{\epsilon}{x}+\frac{\epsilon^2}{3}\right). \tag{79d}$$

The second pair of functions in which $\varphi$ is the leading one is:

$$\chi_2=-\frac{\sqrt{2}a}{12}\left\{\left[\frac{1}{x^3}+\frac{1+\epsilon}{x^2}+\frac{2\epsilon-1}{x}\right]e^{-(1+\epsilon)x}+\frac{3-4\epsilon^2}{12\epsilon}G(x)\right\}, \tag{80a}$$

$$\begin{aligned}\varphi_2=e^{-\epsilon x}\left(\frac{1}{x^2}+\frac{\epsilon}{x}+\frac{\epsilon^2}{3}\right)+a\Bigg\{&\left[\frac{1}{6x^3}+\left(-\frac{3}{16\epsilon^4}+\frac{3}{16\epsilon^3}+\frac{3}{8\epsilon^2}-\frac{1}{4\epsilon}+\frac{1}{6}+\frac{1}{12}\epsilon\right)\frac{1}{x^2}+\frac{(2\epsilon^2+3)(2\epsilon-1)}{48\epsilon^2x}\right]e^{-(1+\epsilon)x}\\&+\left[\frac{3}{32\epsilon^5}-\frac{5}{16\epsilon^3}+\frac{1}{12\epsilon}\right]F(x)\Bigg\}.\end{aligned} \tag{80b}$$

TABLE III. *Cut-off distances $x_0$ for the ground state.*

| | ZERO CUT-OFF | STRAIGHT CUT-OFF |
|---|---|---|
| Neutral Theory, $a=1.6$ | 0.3092 | 0.4051 |
| Neutral Theory, $a=2$ | 0.3628 | 0.4989 |
| Symmetrical Theory, $a=2$ | 1.0560 | 1.374 |
| Symmetrical Theory, $a=3.2$ | 1.2975 | 1.733 |

These functions simplify considerably when the value $\frac{1}{2}$ is inserted for $\epsilon$.

The terms in $a^3$ were calculated using an approximate half-analytical procedure. For this purpose, the terms linear in $a$ in the wave functions (79), (80) were approximated as closely as possible by exponentials, and the same was done for the terms proportional to $a$ in the wave equation ((73), (73a,b)). The term $6/x^2$ which is not important for large $x$ was replaced by a suitable average. The resulting wave equation could then be integrated in an elementary way in exponentials. The terms in $a^2$ never contributed more than 1 part in 1000 to the main wave functions $\chi_1$ and $\varphi_2$ and 1 part in 100 to their derivatives, at the point where numerical integration was started.

### Intermediate region

In the region between $x_0$ and $x_1=2$ or 3, the wave equations (73) were integrated numerically. The method used was the same as in §11, i.e., $y=\log x$ was introduced as independent variable, and

$$g=x^{-\frac{1}{2}}\chi \qquad f=x^{-\frac{1}{2}}\varphi \tag{81}$$

as dependent variables. Because of the rapid change of the potentials $A$ and $B$ and of the wave functions, it was necessary to use a smaller interval, *viz.*, $h=0.1$. The numerical integration was started at $y_1=0.7$ for the neutral theory, at $y_1=1.1$ for the symmetrical theory.

The functions $g_1, f_1, g_2, f_2$ increase exponentially towards smaller $x$. The actual wave function, on the other hand, will reach a maximum and then decrease; it must therefore be a small difference between the large functions $g_1, f_1$ and $g_2, f_2$. To improve the accuracy and save labor we calculated, instead of the second pair of functions, a linear combination of the two pairs which was somewhat closer to the actual wave function (but still "on the side of" $g_2, f_2$). We chose for the neutral theory

$$g_{(2)}=0.6g_2+g_1, \qquad f_{(2)}=0.6f_2+f_1. \tag{82a}$$

For the symmetrical theory and $a=2$, we took

$$g_{(2)}=2g_2-g_1, \qquad f_{(2)}=2f_2-f_1, \tag{82b}$$

while for greater $a$ we used $g_2, f_2$ themselves. Even so, it was necessary to carry 5 significant figures in $g_1, f_1, g_2, f_2$ for small $x$ in order to get the fourth figure in the result reasonably correct.

The increased number of wave functions (four instead of one), the smaller interval (0.1 instead of 0.2), the greater accuracy required, and the more complicated differential equation, all together make the integration about 20 to 30 times more laborious than in the case of the singlet state. The integration was therefore carried out only for very few values of $a$. Table II suggests that the correct value of $a$ will be in the neighborhood of 1.6; this value was therefore chosen. Even before the singlet integration was performed, the triplet state had been calculated with $a=2$. These two values, $a=1.6$ and 2, were sufficient to determine the correct $a$ and $x_0$ and the correct wave function by interpolation.

All the foregoing formulae and discussions hold for the neutral theory. In the symmetrical theory, the potential has to be multiplied by $-3$ for the ground state (§4). This can be done formally by replacing $a$ by $-3a$. This makes obviously the convergence of the expansion in powers of $a$ worse; therefore $y_1$ was chosen equal to 1.1 instead of 0.7. The first integration was made with $a=2$ but this was found considerably too small. $a=3.2$ was estimated to be about correct for the straight cut-off, and this estimate was confirmed by actual integration. For the zero cut-off, $a$ was found to be about 3.8 by extrapolation.

### Determination of cut-off distance

$x_0$ is determined by the condition of continuity of the functions and their derivatives, *viz.*,

$$\begin{aligned} c_1g_1+c_2g_2&=c_3g_3+c_4g_4\\ c_1f_1+c_2f_2&=c_3f_3+c_4f_4\\ c_1dg_1/dy+c_2dg_2/dy&=c_3dg_3/dy+c_4dg_4/dy\\ c_1df_1/dy+c_2df_2/dy&=c_3df_3/dy+c_4df_4/dy. \end{aligned} \tag{83}$$

The functions 1, 2 are the outer solutions, obtained by numerical integration, the functions 3, 4 are the inside solutions. Since the functions are all given (for given $a$), the equations (83) represent four linear homogeneous equations for the four coefficients $c_1c_2c_3c_4$. Therefore the determinant must vanish

$$\Delta\equiv\begin{Vmatrix} g_1 & g_2 & g_3 & g_4\\ f_1 & f_2 & f_3 & f_4\\ dg_1/dy & dg_2/dy & dg_3/dy & dg_4/dy\\ df_1/dy & df_2/dy & df_3/dy & df_4/dy \end{Vmatrix}. \tag{84}$$

(84) is the equation for the determination of $x_0$. (Strictly speaking, $x_0$ is the largest root of (84).)

For zero cut-off, the inside functions are very simple (cf. (75a,b)), and (83), (84) reduce to

$$-\frac{c_1}{c_2}=\frac{dg_2/dy-\frac{1}{2}g_2}{dg_1/dy-\frac{1}{2}g_1}=\frac{df_2/dy-(5/2)f_2}{df_1/dy-(5/2)f_1}. \tag{84a}$$

The two fractions in the middle and on the right-hand side were computed from the numerical solution at various points; the point where they are equal was then found by interpolation. For the straight cut-off, the inside functions are

more complicated. In this case, the determinant (84) itself was calculated at various points and then interpolated.

The results obtained are given in Table III. For the neutral theory and straight cut-off, $a=1.6$ gives (accidentally) almost exactly the same value of $x_0$ as was obtained for the same theory and the same $a$ for the $^1S$ state (cf. Table II, 0.4051 and 0.4056). This shows that 1.6 is the correct value of $a$ for this theory. Extrapolation using the result for $a=2$ gives $a=1.5997$, $x_0=0.4050$. For the final wave function, we took the one computed for $a=1.6$.

In the case of *zero cut-off, neutral theory*, $a=1.6$ gives a larger $x_0$ for the triplet state (0.3092) than for the singlet state (0.2447) while for $a=2$ the relation is reversed (0.3628 and 0.5959). That $x_0$ will depend less strongly on $a$ for the ground state is to be expected from the strong divergence of the potential in this state. Since $x_0/a$ (in the triplet state) does not change much from $a=1.6$ to 2 this quantity was used for (linear) interpolation. Then the values of $x_0$ for triplet and singlet state agree for $a=1.664$. Direct linear interpolation of $x_0$ for the triplet state would give $a=1.663_3$. The corresponding value of $x_0$ is 0.318, by both methods of interpolation.

For the symmetrical theory, straight cut-off, $a=3.2$ gives approximate agreement between triplet and singlet state (1.733 and 1.741). If $x_0^2/a$ for the triplet state is linearly interpolated between $a=2$ and 3.2, triplet and singlet will intersect at $a=3.16_5$, $x_0=1.725$. The triplet wave function for $a=3.2$ was taken as final.

The correct value of $a$ for the symmetrical theory, zero cut-off, is obviously greater than 3.2. In view of the generally unsatisfactory results for this theory (too large $x_0$) it was considered sufficient to extrapolate the results for $a=2$ and 3.2. We assumed $x_0^2$ for the triplet state to be a linear function of $a$ and found that $a=3.76$ will make $x_0$ for singlet and triplet agree and will give $x_0=1.396$. The value of $a$ may easily be in error by $\pm 0.05$ unit and $x_0$ by $\pm 0.02$ unit, these estimates being obtained by using different methods of extrapolation. The wave function was also obtained by extrapolation from the results for $a=2$ and 3.2, assuming linearity in $a$. This assumption was checked by the correct behavior of the wave function near $x_0$, *viz.*, $\chi\sim x^{\frac{1}{2}}$ and $\varphi\sim x^{2.5}$.

The wave functions obtained as described were normalized by the condition (46), *viz.*,

$$\int_0^\infty (\chi^2+\varphi^2)dx=1. \tag{85}$$

TABLE IV. *Results.*

| | Neutral Theory | | Symmetrical Theory | |
|---|---|---|---|---|
| | Zero Cut-off | Straight Cut-off | Zero Cut-off | Straight Cut-off |
| $a$ | 1.664 | 1.600 | 3.76 | $3.16_5$ |
| $f^2/\hbar c$ | 0.0800 | 0.0770 | 0.181 | 0.152 |
| $x_0$ | 0.318 | 0.405 | 1.396 | 1.725 |
| Max. of $B\sqrt{2}$ (Mev) | 625 | 288 | 38.4 | 15.1 |
| $c_1$ | 0.323 | 0.322 | 0.286 | $0.267_5$ |
| $c_2$ | $0.122_5$ | 0.119 | −0.446 | −0.390 |
| Percent $D$ | 6.80 | 6.63 | 18.03 | 18.52 |
| $Q$ in $10^{-27}$ cm² | $2.70_5$ | $2.61_5$ | −20.0 | $-17.8_5$ |
| $r'^2_{Av}$ in $10^{-26}$ cm² | 3.31 | 3.28 | 8.31 | 7.51 |
| $\epsilon=Q/r'^2_{Av}$ | $0.081_5$ | 0.080 | 0.241 | 0.238 |

## §13. Results for the Neutral Theory

The calculations in the preceding section gave cut-off distances $x_0=0.405$ for the straight cut-off and 0.318 for the zero cut-off. These values are very reasonable indeed, and are, in fact, just of the order of magnitude which we expected from general considerations of the field theory in §6. It was mentioned in that section that Møller and Rosenfeld found the ratio of second-order to first-order interaction to be about

$$f^2/\hbar c x^2. \tag{86}$$

Our calculations give about 0.08 for $f^2/\hbar c$ (cf. Eq. 87) and therefore 0.5 or 0.8 for the above ratio for straight and zero cut-off, respectively. These figures are quite close to unity.

That $x_0$ must be smaller for the zero cut-off is evident: When the potential is zero inside, instead of having a finite value corresponding to attraction, this must be compensated by a larger potential outside; and the outside potential is increased most effectively by making $x_0$ smaller.

A cut-off at $x_0=0.3$ or 0.4 represents a relatively slight modification of the Yukawa potential $ae^{-x}/x$. This can be seen from the small change of $a$ necessary to compensate the effect of the cutting off for the singlet state: Our $a$ is 1.6 or 1.66 instead of the value 1.489 found without cutting off (§11). In particular, the general behavior of the singlet potential is

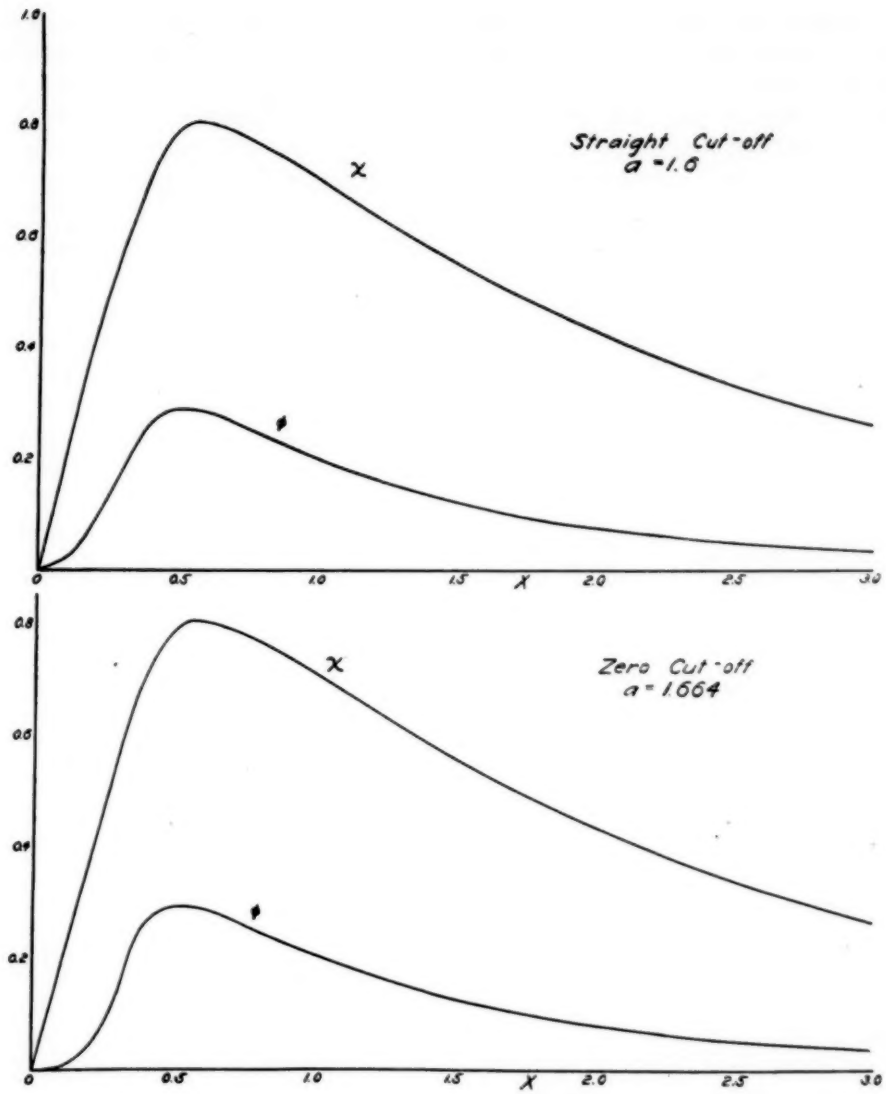


FIG. 1. Radial wave functions of the $S$ and $D$ state of the deuteron. Neutral theory, two ways of cutting off.

preserved, *viz.*, the exponential decrease at large distances and the stronger than exponential increase at small $x$. Especially the latter may be helpful for removing the discrepancies in the older theory of the three- and four-body problems.[46]

The interaction constant $a$ does not depend appreciably on the method of cutting off. This is satisfactory and makes it probable that the actual theory which may be developed in the future will give a similar value for $a$. The most important reason for this insensitivity is that $a$ is principally determined by the singlet state, and that this state is not sensitive to the cutting off (§11). The same fact makes $a$ also insensitive to the mass of the meson. A change of $\mu$ would only change the natural unit of length $1/\kappa$, and therefore also the constant $\gamma$, in the inverse ratio of $\mu$. Because of the small value of $\gamma$, even a change of the meson mass by a factor of two either way would cause only a small absolute change of $\gamma$, and therefore a small change of $a$. We estimate that a doubling of $\mu$ would increase $a$ by about 0.08, i.e., five percent.

[46] W. Rarita and R. D. Present, Phys. Rev. **51**, 788 (1937).

The actual value of $a$ is considerably less than that reported in previous papers. Sachs and Goeppert-Mayer[47] find $a=2.83$ for $\mu=177m$. This difference is due to the fact that these authors assumed that the *triplet state* is determined by a potential of the Yukawa type $ae^{-x}/x$; the lower energy of the triplet state requires of course a larger $a$ than the one found in this paper from the singlet state.

The absolute value of the interaction is most easily appreciated when instead of $a$ we use the quantity $f^2/\hbar c$. From (40), we have

$$f^2/\hbar c=(\mu/2M)a. \tag{87}$$

Therefore, with our value $\mu=177m=0.096_2M$, we find

$$f^2/\hbar c=0.0800 \quad \text{for zero cut-off,} \tag{87a}$$

$$f^2/\hbar c=0.0770 \quad \text{for straight cut-off.} \tag{87b}$$

This means that $f^2$ is about 11 times the square of the electronic charge, $e^2$, or about the geometrical mean between $e^2$ and $\hbar c$.

In Table IV, we have listed the more important results. After the values of $a$ and $x_0$, we have given the maximum value (obtained at $x_0$) of the "coupling potential" between $S$- and $D$-state, $B\sqrt{2}$ (cf. (73), (73b)). It is seen that this quantity does not reach excessive values but remains considerably smaller than the rest energy of the deuteron (1860 Mev). This makes it improbable that the cutting off is due to simple relativistic effects (cf. §6).

The next two rows in Table IV give the coefficients $c_1$ and $c_2$ in the normalized wave function

$$\begin{aligned}\chi&=c_1\chi_1+c_2\chi_2\\ \varphi&=c_1\varphi_1+c_2\varphi_2.\end{aligned} \tag{88}$$

These coefficients are seen to be almost the same for straight and zero cut-off, and what difference there is, is due to the difference in $a$. For the same $a$, the coefficients for the two methods of cutting off agree within the accuracy of the calculation (about 1 in 500). The reason is that a small change in these coefficients would mean a considerable change in the shape of the wave function, owing to the rapid increase of $\chi_1\varphi_1\chi_2\varphi_2$ towards smaller $x$.

[47] R. G. Sachs and M. Goeppert-Mayer, Phys. Rev. **53**, 991 (1938).

The wave functions $\chi$ and $\varphi$ themselves are shown in Fig. 1 for the two ways of cutting off. The two graphs are seen to be very similar. Of the two wave functions, $\chi$ behaves very similar to the usual wave function of the deuteron and has a flat maximum at $x\approx0.6$, i.e., outside the cut-off distance but within the range of the nuclear forces. At large distances, $\chi$ will always behave as $e^{-\alpha x}$ independent of the special form of the nuclear forces as long as the forces have short range.[48] The radial wave function of the $D$ state, $\varphi$, has a steeper maximum at a slightly smaller distance ($x\approx0.5$).

In Table IV, we have also given the percentage of $D$ function contained in the ground state, *viz.*, 100 times the quantity

$$p_D=\int\varphi^2dx. \tag{88a}$$

This percentage is again almost independent of the method of cutting off as is to be expected from the similarity of the wave function. The value of $p_D$ is 6.6 to 6.8 percent, i.e., rather small, in spite of the large effect which the mixing of $S$ and $D$ state has on the energy. The reason for this is the large value of the coupling potential $B\sqrt{2}$.

## §14. The Magnetic Moment

As Schwinger[49] has pointed out, the percentage of $D$ function in the ground state is important for the magnetic moment of the deuteron. For a pure $S$ state, the magnetic moment may be assumed to be equal to the sum of the intrinsic moments of proton and neutron,

$$g_S=\mu_P+\mu_N. \tag{89}$$

In the past the neutron moment has always been calculated from this formula, $g_S$ being identified with the measured magnetic moment of the deuteron. For a pure $^3D_1$ state the moment would be given by the Landé formula

$$g_D=\tfrac{1}{2}(g_S+g_L)+\frac{S(S+1)-L(L+1)}{2J(J+1)}(g_S-g_L) \tag{90}$$

$$=\tfrac{3}{2}g_L-\tfrac{1}{2}g_S, \tag{90a}$$

[48] H. A. Bethe and R. Peierls, Proc. Roy. Soc. **149**, 176 (1934).

[49] J. Schwinger, Phys. Rev. **55**, 235 (1939), Abs. 13; and further unpublished results.

since $L=2$, $S=J=1$. Here $g_L$ is the $g$ value of the orbital momentum, and we have

$$g_L=\tfrac{1}{2}, \tag{90b}$$

since the proton carries one-half of the total orbital momentum of the deuteron. All moments are of course given in nuclear magnetons. If we have a mixture of a ${}^3S_1$ and a ${}^3D_1$ state, the moment will be

$$\begin{aligned} g&=(1-p_D)g_S+p_Dg_D \\ &=g_S-\tfrac{3}{2}p_D(g_S-\tfrac{1}{2}). \end{aligned} \tag{91}$$

The cross terms between the $S$ and $D$ wave function do not contribute to the magnetic moment.

The observations give almost exactly $g=g_S$, i.e., the observed moment of the deuteron is within the experimental error equal to the sum of the moments of neutron and proton. The measurements of Kellogg, Rabi, Ramsey and Zacharias[39] give for the deuteron

$$g=0.855\pm0.006,$$

for the proton

$$\mu_P=2.785\pm0.02,$$

whereas Bloch and Alvarez[50] find for the neutron

$$\mu_N=-1.93_b\pm0.02.$$

Therefore the difference between the deuteron moment and the moment expected for a pure $S$ state is

$$g-g_S=0.005\pm0.03 \tag{91a}$$

nuclear magnetons.

From the theoretical Eq. (107), we should have

$$g-g_S=-0.53p_D. \tag{91b}$$

Therefore a value of $p_D$ of 0.067, as it follows from our theory, would be just outside the limits of the experimental error. However, if it were not known that the deuteron had a quadrupole moment, the result of the experiments would doubtless be taken to indicate exact additivity of the magnetic moments of neutron and proton in the deuteron. Whether a $p_D$ of 6.7 percent is actually permissible, can only be decided after a further increase in the precision of the experimental values of the moments.

Schwinger's theory[49] gives a greater percentage of $D$ function in the deuteron ground state, *viz.*, about 10 percent or more. He introduces a central force and a tensor interaction which are constant inside a certain radius $r_1\approx e^2/mc^2$ and zero outside. The magnitude of the central force is assumed different in triplet and singlet state and is adjusted to give the correct binding energies, and the magnitude of the tensor interaction is adjusted so as to give the observed value of the electrical quadrupole moment. Since our theory also gives the quadrupole moment correctly, the difference between the two theories apparently arises from the different shape of the radial functions. This point requires further consideration. At the moment, Schwinger's result seems somewhat worse than ours.

## §15. The Quadrupole Moment

As has been pointed out repeatedly, the deuteron will, according to the present theory, have a quadrupole moment. We define the quadrupole moment in the same way as Kellogg, Rabi, Ramsey and Zacharias,[39] *viz.*,

$$Q=(3z'^2-r'^2)_{Av}=r'^2(3\cos^2\vartheta-1)_{Av}, \tag{92}$$

where $z'$ and $r'$ are the coordinates of the proton with respect to the center of gravity of the deuteron, i.e., one-half of the coordinates used in this paper which give the position of the proton with respect to the neutron. The average is to be taken for the magnetic state $M=1$; a positive quadrupole moment thus indicates that the deuteron is elongated along the direction of its spin, and vice versa. Putting $r'=\frac{1}{2}r=x/2\kappa$ we have

$$Q=(1/4\kappa^2)\int x^2(3\cos^2\vartheta-1)\psi^2 d\tau. \tag{92a}$$

The wave function $\psi$ of the state $M=1$ is (cf. (72), (44))

$$\begin{aligned} \psi=&x^{-1}\chi(\kappa)Y_{00}(\vartheta,\varphi)\alpha(1)\alpha(2)+x^{-1}\varphi(x)10^{-\frac{1}{2}} \\ &\times[Y_{20}(\vartheta\varphi)\alpha(1)\alpha(2)+3^{\frac{1}{2}}Y_{21}(\vartheta\varphi)\{\alpha(1)\beta(2) \\ &+\beta(1)\alpha(2)\}/\sqrt{2}+6^{\frac{1}{2}}Y_{22}(\vartheta\varphi)\beta(1)\beta(2)]. \end{aligned} \tag{93}$$

[50] L. W. Alvarez and F. Bloch, Phys. Rev. **57**, 111 (1940).

Inserting (93) in (92a) we obtain

$$Q=(1/10\kappa^2)\int x^2dx(\chi\varphi\sqrt{2}-\tfrac{1}{2}\varphi^2). \quad (94)$$

In other words, the $^3D_1$ state *alone* would give a negative contribution to the quadrupole moment $(-\frac{1}{2}\varphi^2)$. The interference term between $S$ and $D$ function, $\chi\varphi\sqrt{2}$, is positive provided $\chi$ and $\varphi$ have the same sign which is the case for our neutral theory. As long as $\varphi$ is not too large which again is fulfilled in our theory the positive term will predominate. Thus *the quadrupole moment will be positive, in agreement with the experiments of Kellogg, Rabi, Ramsey and Zacharias.*[39] This was already deduced from qualitative considerations in §10.

The integral in (94) was calculated from the wave functions for the two types of cut-off. The result is again almost independent of the cut-off and the small existing difference of about three percent is mostly due to the difference in $a$. A correct theory would therefore give a similar value provided the principle of cutting off singlet and triplet potential in the same way is preserved. The final result (cf. Table IV) is

$$Q=2.70_5\times10^{-27}\text{ cm}^2 \quad \text{(zero cut-off)}$$
$$Q=2.61_5\times10^{-27}\text{ cm}^2 \quad \text{(straight cut-off).} \quad (95)$$

This value should be compared with the experimental value

$$Q=2.74\times10^{-27}\text{ cm}^2 \pm 2\text{ percent (experimental),} \quad (95a)$$

which has been derived by Nordsieck[51] from the experiments of Rabi and collaborators.[39] The agreement is excellent.

This is practically[52] the first time that a calculation in the theory of simple nuclear systems gives a quantitative agreement. In all previous instances, any new phenomenon either could not be treated with the theoretical concepts deduced from the phenomena known previously or disagreed with them. E.g., the cross section for the scattering of slow neutrons did not agree with the value deduced previously from the binding energy of the deuteron but required for its explanation the postulation of the singlet state of the deuteron—a postulate which was well confirmed later. The binding energy of the triton cannot be deduced from deuteron data but can be adjusted at will by changing the range of the forces. The binding energy of the $\alpha$-particle disagrees with the forces deduced from the two- and three-body systems. In our theory, there are for the first time more experimental data than there are arbitrary parameters: The data are the positions of triplet and singlet state of the deuteron, the mass of the meson and the quadrupole moment. The parameters are the nuclear unit of length, $1/\kappa$, the interaction constant $a$, and the cut-off distance $x_0$. This makes it possible to calculate one datum from the three others. This has been achieved by using the principle of simplicity in the fundamental theory, particularly by the assumption that the spin-independent interaction is absent (Single Force Hypothesis, §5). The good agreement obtained justifies this hypothesis.

To judge the significance of $Q$ for the shape of the deuteron we compare it with the average value of $r'^2_{Av}$ where $r'$ is the distance of the proton from the center of gravity. We have

$$r_{Av}'^2=(1/4\kappa^2)\int(\chi^2+\varphi^2)x^2dx$$
$$=3.31\times10^{-26}\text{ cm}^2 \quad \text{for zero cut-off}$$
$$=3.28\times10^{-26}\text{ cm}^2 \quad \text{for straight cut-off.} \quad (96)$$

For comparison we note that for infinitely short range of the nuclear forces $r'^2_{Av}=2.39\times10^{-26}\text{ cm}^2$, i.e., the finite range causes a moderate increase in the size of the deuteron as is to be expected. We define the excentricity of the deuteron

$$\epsilon=Q/r'^2_{Av}. \quad (96a)$$

$\epsilon$ would have the value 2 if the proton and neutron were constrained to move on a straight line in the direction of the spin. In our case (cf. (95), (96)) we find $\epsilon=0.081_5$ for the zero

[51] A. Nordsieck, Bull. Am. Phys. Soc., New York Meeting, February, 1940, Abstract No. 9. I am grateful to Dr. Nordsieck for communicating his results to me before publication.

[52] As other instances, the capture cross section of protons for slow neutrons, and the cross section of the photoelectric effect of the deuteron for 2.62-Mev $\gamma$-rays may be quoted; also to some extent the energy dependence of the scattering of neutrons by protons. However, the theory of all these phenomena is almost independent of the range and nature of the nuclear forces so that the agreement proves only the short range of the forces. Our case is quite different in this respect.

and 0.080 for the straight cut-off showing that the deuteron does not differ too much from spherical shape.

## §16. The $^3P_1$ State

As has been shown in §9, the potential in the $^3P_1$ state is strongly attractive. It would therefore be conceivable that this state might be lower than the $^3S+^3D_1$ state. We have made it plausible in §10 by a semi-quantitative argument that this is not the case. However, because of the importance of this question we have made a direct numerical calculation of the $^3P_1$ state. This calculation was also meant to decide whether the $^3P_1$ state is higher than the $^1S$ state which question could not be investigated by the method of §10.

We have calculated the $^3P_1$ wave function for zero energy and zero cut-off. The radial wave function obeys the wave equation (cf. (51))

$$\frac{d^2\psi}{dx^2}=\left(\frac{2}{x^2}-a\frac{e^{-x}}{x^3}(1+x)\right)\psi \quad (x>x_0)$$
$$\frac{d^2\psi}{dx^2}=\frac{2\psi}{x^2} \quad (x<x_0) \tag{97}$$
$$x_0=0.318, \quad a=1.664.$$

The inside solution is simply $\psi\sim x^2$. The asymptotic solution for very large $x$ is

$$\psi=\psi_1+\gamma\psi_2 \tag{98}$$

with

$$\psi_1\sim x^2, \quad \psi_2\sim 1/x. \tag{98a}$$

For values of $x$ which are still large but not infinite we expand in powers of $a$ and find:

$$\psi_1=x^2-ae^{-x}(1+1/x)+\tfrac{1}{4}a^2e^{-2x}/x^2+\cdots, \tag{99}$$

$$\psi_2=\frac{1}{x}-\frac{a}{24}\left[e^{-x}\left(\frac{6}{x^2}-\frac{2}{x}+1-x\right)-x^2Ei(-x)\right]$$
$$+\frac{a^2}{360}\left[e^{-2x}\left(\frac{9}{x^3}-\frac{12}{x^2}-\frac{7}{x}-8+16x\right)\right.$$
$$-15e^{-x}Ei(-x)(1+1/x)$$
$$\left.+32x^2Ei(-2x)\right]+\cdots. \tag{99a}$$

The values of $\psi_1$ and $\psi_2$ were calculated at $y=\log x=0.7$ and the values of their derivatives at $y=0.65$. Then both solutions were integrated numerically towards smaller $x$, using the same method as in §11 and 12 and interval $h=0.1$. Finally, a linear combination of the two solutions was joined at $x_0=0.318$ to the inside solution $\psi\sim x^2$. The result is (cf. (98))

$$\gamma=2.39. \tag{99b}$$

This value of $\gamma$ is positive showing that there is no bound $^3P_1$ state. This confirms the qualitative result of §9 that the $^3S+^3D_1$ state is the ground state. Moreover, the value of $\gamma$ is not excessively large as it would be if a virtual state existed in the neighborhood of zero energy. This shows that the $^3P_1$ state is also "higher" than the $^1S$.

To estimate the scattering of $^3P_1$ neutrons we write down the wave function at a finite energy:

$$\psi=-\cos(kx+\delta)+\sin(kx+\delta)/kx. \tag{100}$$

Here $k^2$ is the relative energy of neutron and proton in nuclear units of 8.7 Mev, $x$ the distance of the two particles and $\delta$ the phase shift. If $kx\ll 1$ but still $x\gg 1$ so that the nuclear forces are negligible, (100) reduces to

$$\psi=\tfrac{1}{3}(kx)^2\cos\delta+\sin\delta/kx. \tag{100a}$$

Comparison with (98) gives

$$\tan\delta\approx\delta=\tfrac{1}{3}k^3\gamma=0.80k^3. \tag{100b}$$

As example let us consider the scattering of D−D neutrons. The kinetic energy is about 3 Mev, therefore the relative kinetic energy $1\frac{1}{2}$ Mev and $k^2=1.5/8.7=0.17$. Eq. (100b) then gives for the phase shift of $^3P_1$ the value $\delta=0.056=3.2°$ which is small but not negligible. In spite of the strong attraction, the $^3P_1$ state is therefore only of slight importance for the scattering of neutrons of moderate energy. The angular distribution of the scattered neutrons will be almost spherically symmetrical as in the older theory and in experiment.[53]

## §17. Results of the Symmetrical Theory

The main results of the calculations have already been given in Table IV, §13. The most

[53] The angular distribution of the scattered neutrons as a function of the phase shifts of the $^1S$, $^1P$, $^3S$, $^3P_{0,1,2}$ waves has been given by Hoisington, Share and Breit, Phys. Rev. **56**, 884 (1939).

conspicuous feature is the enormous value of the cut-off distance, $x_0=1.396$ and 1.725 for zero and straight cut-off. It can be said that the potential must be cut off before it has really begun to act. This is also shown by the smallness of the maximum value of the coupling potential $B\sqrt{2}$ which is 38.4 and 15 Mev, respectively.

It is evident that these results are entirely unacceptable from the standpoint of general nuclear theory. A potential which exists only at distances *greater* than $3\times10^{-13}$ cm (zero cut-off) is obviously in violent contradiction with the known short range character of nuclear forces. Such a potential could never explain that the binding energies of the triton and the $\alpha$-particle are large compared with that of the deuteron; it would lead to nuclear radii at least three times as large as the observed ones, and it would mean a very considerable influence of the $P$ waves in the scattering of 2-Mev protons by protons for which no such influence has been observed.[54] The potential obtained with straight cut-off which is constant up to $4\times10^{-13}$ cm and then falls off rather slowly is equally out of the question.

Moreover, it seems inconceivable that the theory of the meson field should break down at such enormous distances. The relativistic corrections are minute, the potentials being only 38 and 15 Mev. Likewise, the second-order interaction (cf. (86)) should give only 0.09 or 0.05 times the first order. That the field theory would be worthless in the case of such an early breakdown goes without saying.

In view of this situation, it seems hardly necessary to give additional evidence against the symmetrical theory. However, it should be mentioned that the *quadrupole moment has the wrong sign*, negative instead of positive (cf. Table IV, and reference 50). This was already realized by Heitler[55] and it seems very difficult to devise a mechanism to change this result. The enormous size of the quadrupole moment, 7 to 8 times the observed value, is only in keeping with the long range of the nuclear forces.

The reason for these results can be appreciated most easily by a comparison with the neutral theory. The central force $V_1$ (cf. (34)) has the same value for singlet and triplet state in the symmetrical theory so that the tensor interaction is only responsible for the difference between these two states. In the neutral theory, the central force is repulsive in the triplet state, therefore the tensor interaction must overcome this repulsion, must provide an attraction equal to that in the singlet state, and in addition make the triplet state lower than the singlet. This means that the tensor interaction must have a much smaller effect in the symmetrical than in the neutral theory. But the analytical expression for the tensor interaction, in terms of $a$ and $x$, is three times larger in the symmetrical theory. Therefore its effect can only be reduced by cutting the interaction off at a very much larger distance $x_0$.

This effect is further enhanced by the fact that an increase of $x_0$ means a reduction of the effective potential in the singlet state which must be compensated by an increase of $a$ (cf. Table II). In fact, the final value of $a$ is twice as large or more in the symmetrical than in the neutral theory. An increase of $a$ increases the tensor interaction still further and thus necessitates an even larger cut-off radius $x_0$, etc.

Our result that the symmetrical theory disagrees violently with experiment is very regrettable indeed. For all *qualitative* arguments are in favor of the symmetrical and speak against the neutral theory. In this connection we do not think primarily of the fact that charged mesons have been observed in cosmic rays while there is up to the present no experimental evidence for neutral ones: The existence of neutral mesons is indispensable for *any* theory of nuclear forces, symmetrical as well as neutral. But the symmetrical theory is capable of explaining at least in principle the *$\beta$-disintegration* and the *magnetic moments* of neutron and proton.

There is as yet no actual theory of the extra magnetic moments, and it is already clear that such moments could not be expected in the approximation of the field theory which has been considered in this paper. However, it seems at least possible qualitatively to interpret the moments as due to charged mesons which are present part of the time. With neutral mesons no such possibility seems to exist; moreover, we

[54] G. Breit, H. M. Thaxton and L. Eisenbud, Phys. Rev. 55, 1018 (1939).
[55] W. Heitler, Report to the Solvay Conference 1939.

have assumed in our theory that neutrons and protons have exactly the same meson fields around them so that it would be impossible for them to have different signs of the extra magnetic moment if that moment is due to the mesons.

Another strong qualitative argument for the symmetrical theory is the $\beta$-disintegration. In the symmetrical theory this process will proceed according to Yukawa's scheme, *viz.*,

$$\begin{aligned} &N\rightarrow P+M^-, \quad M^-\rightarrow\epsilon^-+n \\ &P\rightarrow N+M^+, \quad M^+\rightarrow\epsilon^++n \end{aligned} \tag{101}$$

($N$=neutron, $P$=proton, $M^+$ and $M^-$=positive and negative meson, $\epsilon$=electron, $n$=neutrino). Obviously no such scheme for the $\beta$-disintegration is available when only neutral mesons interact with the nuclear particle. In the neutral theory it would therefore be necessary to fall back on the original Fermi theory in which a direct interaction was postulated between nuclear particle and electron-neutrino field. There are many points in favor of an indirect interaction via the meson field as in (101): The direct splitting of a nuclear particle into three particles seems to lead to much more serious divergences at high energies than the splitting into two particles postulated in (101). No other instance is known in nature where the fundamental process is a simultaneous emission of two particles whereas the emission of light or of gravitational waves is quite analogous to (101) in that a Bose particle is emitted or absorbed by a Fermi particle. Moreover, the assumption that mesons are an intermediate stage in $\beta$-emission obviously provides a much more unified picture of nuclear phenomena; and finally, it seems rather unlikely that the charged meson which, after all, is known to exist should play no role at all in nuclear phenomena.

On the other hand, it is well known that there is a serious quantitative discrepancy in the meson theory of $\beta$-decay. As Nordheim[56] has pointed out the observed lifetimes of $\beta$-active nuclei require an extremely short life for the meson itself. With the latest data on $\beta$-decay, and the most favorable theoretical assumptions, the half-life of the meson comes out[57] to be $9\times10^{-9}$ sec. which should be regarded as an upper limit. With such a short life, the meson could not be observed in cosmic rays whereas actual cosmic-ray data set a *lower* limit of about $2\times10^{-6}$ sec. to the lifetime. The discrepancy of a factor 200 cannot be removed by a reasonable change of the mass $\mu$ of the meson; since the theoretical life is inversely proportional to $\mu^4$, the mass would have to be reduced by a factor of 4 to about 45 electron masses which is entirely irreconcilable with direct experimental determinations and also would lead to an impossible range of the nuclear forces, of about $10^{-12}$ cm.

This quantitative discrepancy in the $\beta$ theory must be regarded as a serious argument against the symmetrical theory in its present form.

## §18. An Alternative Method of Cutting Off

Since the qualitative arguments for the symmetrical theory are certainly very strong we attempted to improve the quantitative agreement by using different ways of cutting off. In a recent discussion in which he emphasized the arguments for the symmetrical theory, Heisenberg suggested to cut off the potential *before* the differentiations implied in Eq. (18). Such a procedure would correspond to a cut-off in momentum space which seems to be the only reasonable way to achieve a relativistically invariant cut-off.[58] Moreover, it would seem promising for a solution of our difficulties because it might be expected that the tensor interaction being a second derivative would be more strongly reduced than the central force, which would indeed bring about better agreement with the experimental positions of triplet and singlet states (cf. §17).

Unfortunately, this is not the case but the results are even less favorable than in our earlier calculations, §12 and 17. Let $\frac{1}{2}v$ be the potential before the differentiation so that the spin-dependent interaction is

$$V=-\tfrac{1}{2}\boldsymbol{\sigma}_1\cdot\text{curl curl}\,(\boldsymbol{\sigma}_2 v)\boldsymbol{\tau}_1\cdot\boldsymbol{\tau}_2. \tag{102}$$

In the Yukawa theory, $v=(2f^2/\kappa^2)(e^{-\kappa r}/r)$. For

[56] L. W. Nordheim and G. Nordheim, Phys. Rev. **54**, 254 (1938); L. W. Nordheim, *ibid.* **55**, 506 (1939); H. Yukawa, V. and S. Sakata, Nature **143**, 761 (1939).

[57] H. A. Bethe and L. W. Nordheim, to be published shortly in *The Physical Review*.

[58] G. Wataghin, Zeits. f. Physik **88**, 92 (1934); W. Heisenberg, *ibid.* **110**, 251 (1938).

our present investigation, we shall assume that $v$ is a certain unknown function of $r$ which is already "cut off," i.e., which does not diverge strongly at small $r$. The central force is then

$$V_1=\tfrac{1}{3}\boldsymbol{\sigma}_1\cdot\boldsymbol{\sigma}_2\,\boldsymbol{\tau}_1\cdot\boldsymbol{\tau}_2\,\nabla^2 v \tag{102a}$$

and the tensor force

$$V_2=\tfrac{1}{2}\boldsymbol{\tau}_1\cdot\boldsymbol{\tau}_2\left(-\frac{\boldsymbol{\sigma}_1\cdot\mathbf{r}\,\boldsymbol{\sigma}_2\cdot\mathbf{r}}{r^2}+\tfrac{1}{3}\boldsymbol{\sigma}_1\cdot\boldsymbol{\sigma}_2\right)r\frac{d}{dr}\left(\frac{1}{r}\frac{dv}{dr}\right). \tag{102b}$$

We see therefore that both $V_1$ and $V_2$ are second derivatives of $v$ so that there is no reason to suppose that $V_2$ is more strongly reduced by the cutting off than $V_1$.

In order to investigate the general potential $v$ further, we note that the radial factor in $V_1$ plays the role of the charge density associated with $v$. It is therefore easy to calculate, for a given $V_1$, the corresponding $v$ and $V_2$. Let us introduce the abbreviations

$$\rho=\nabla^2 v=\frac{1}{r}\frac{d^2}{dr^2}(rv), \tag{103}$$

$$w=r\frac{d}{dr}\left(\frac{1}{r}\frac{dv}{dr}\right), \tag{103a}$$

so that $\rho$ is proportional to the central force $V_1$, $w$ to the tensor interaction $V_2$. Then we have

$$v(r)=-\int_0^r(1/r)\rho(r')r'^2dr'-\int_r^\infty(1/r')\rho(r')r'^2dr'+A/r+B. \tag{104}$$

It seems reasonable to require that the potential $v$ at large distances should approach zero and should do so faster than $1/r$. This means

$$B=0,\qquad A=\int_0^\infty\rho(r')r'^2dr', \tag{104a}$$

i.e., $A$ is the "total charge." Then

$$v=\int_r^\infty(1/r-1/r')\rho(r')r'^2dr'. \tag{104b}$$

In order to give attraction in the singlet state, $\rho$ must be in the main positive, and therefore $v$ also positive, just as in the original Yukawa theory. For small $r$, $v$ will behave as

$$v=A/r+c_0+c_1r+c_2r^2, \tag{104c}$$

where $A$ is the total charge (104a) and $c_1=0$ if $\rho$ is finite at $r=0$. Inserting into (103a), we obtain

$$w=3A/r^3-c_1/r+3c_3r+\cdots. \tag{105}$$

Thus we see that $w$ diverges as $1/r^3$ unless $A$ is zero. Since any such divergence would lead to infinite binding energy, we have to require

$$A=\int_0^\infty\rho(r)r^2dr=0. \tag{105a}$$

This means that $\rho$, and therefore $V_1$, must change sign somewhere in order to avoid divergences of $w$. In other words, $V_1$ is more effectively cut off than $V_2$, in contrast to the expectation mentioned above. The singlet potential, if attractive at large $r$, must be repulsive at small $r$, whereas the tensor interaction may have the same sign for all $r$.

As a simple example we assume for $\rho$ the following "rectangular" function:

$$\begin{aligned}&\rho=-a \quad \text{for} \quad r<r_1\\ &\rho=b \quad \text{for} \quad r<r<r_2\\ &\rho=0 \quad \text{for} \quad r_2<r.\end{aligned} \tag{106}$$

The neutrality condition (105a) requires then

$$a=b(r_2^3/r_1^3-1) \tag{106a}$$

and we have

$$\begin{aligned}&w=br_2^3/r^3 \quad (r_1<r<r_2)\\ &w=0 \quad (r<r_1 \text{ and } r>r_2).\end{aligned} \tag{106b}$$

This shows that $w$ is relatively smallest if $r_1$ is very close to $r_2$. Since smallness of $w$ is desirable we assume

$$r_2-r_1=\delta\ll r_2. \tag{107}$$

Then (129a) gives

$$a\approx 3b\delta/r_1. \tag{107a}$$

The potential for the singlet state is (cf. (102a)) simply $-\rho$. After a simple calculation, and with the abbreviations

$$\begin{aligned}&x=(3b\delta r_1)^{\frac{1}{4}},\quad \eta=\gamma r_1,\\ &\gamma=0.100\kappa=4.58\times10^{11}\ \text{cm}^{-1},\end{aligned} \tag{107b}$$

we obtain

$$\frac{x}{\tanh x}-\tfrac{1}{3}x^2=\frac{\eta}{1+\eta}. \tag{108}$$

Because of the smallness of $\gamma$ (cf. (107b)), $\eta$ will be quite small provided $r_1$ is of the order of magnitude of the range of the nuclear forces, i.e., a few times $10^{-13}$ cm. For $\eta=0$, the solution of (108) is

$$x(\eta=0)=3.015. \tag{108a}$$

For the triplet state in the symmetrical theory we find

$$\left(\frac{z+y}{x^2}-\frac{1}{3}\right)\left(\frac{f(z)+g(y)}{x^2}-\frac{4}{3}\right)=2, \tag{109}$$

where $y=\epsilon r_1, \quad \epsilon=0.500\kappa=5\gamma,$ (109a)

$$z=(x^2+y^2)^{\frac{1}{2}}, \tag{109b}$$

$$f(z)=z+\frac{z-2}{z^2/3-z+1}, \tag{109c}$$

$$g(y)=y+(y+2)/(y^2/3+y+1). \tag{109d}$$

Terms of order $e^{-2z}$ have been neglected since $z$ is about 6.5. If we assume a moderate range of the nuclear forces, $x$ will be about 3 (cf. (108a)), $y$ will be small and $z\approx 3$ (cf. (109b)). This will make the first factor of (109) vanish, while the second factor has the value $-\frac{2}{3}$. This shows that there can be no solution with a moderate range of the forces. The reason is obviously that the right-hand side, as well as the subtracted term 4/3, is too large. It can be shown easily that the right-hand side of (109) arises from the coupling of $S$ and $D$ state, and the 4/3 from the attractive potential in the $D$ state itself. These quantities are therefore too large to allow a moderate range of the forces, as we know already from the calculations in §12, 17.

The actual solution of the Eqs. (108), (109), with $y=5\eta$, was found by trial and error. It is

$$x=2.3595, \quad y=5.963, \quad z=6.414$$
$$r_1=y/\epsilon=2.61\times 10^{-12} \text{ cm}. \tag{110}$$

This result is obviously out of the question, the range of the forces being more than ten times too large. The result is very much worse than the previous result, in §17, where a cutting-off distance of $3.7\times 10^{-13}$ cm was required. This shows that the cutting off before differentiation makes matters considerably more unfavorable for the symmetrical theory.

For the neutral theory, we get again a perfectly reasonable result. We have to replace $x^2$ by $-\frac{1}{3}x^2$ in all formulae referring to the triplet state, i.e., Eq. (109) to (109d). The result is, instead of (110)

$$x=2.8840, \quad y=0.744, \quad z=1.490$$
$$r_1=3.25\times 10^{-13} \text{ cm}. \tag{110a}$$

This range of the forces is only slightly too large and, correspondingly, the quadrupole moment will also come out somewhat too large, *viz.*, about $5\times 10^{-27}$ cm$^2$. It is evident that a minor modification will make this theory agree with experiment—e.g., going back to the original theory discussed in §§1 to 17.

For the sake of completeness, we finally investigated a potential which is repulsive in the narrow region from $r_1$ to $r_2$ and attractive inside $r_1$. Such a potential is not very plausible and quite contrary to all usual assumptions about nuclear forces. It gave a slightly better result, *viz.* $y\approx 1.8$, $r_1\approx 8\times 10^{-13}$ cm for the symmetrical theory. Its main advantage is to give the correct sign of the quadrupole moment, but the range of the forces is still much too large.

The results of this section can therefore be described as wholly negative.

## §19. Other Possibilities. Conclusion

Møller and Rosenfeld[58, 59] have proposed to introduce two entirely separated meson fields, one of which is described by a vector wave function just as our field, while the other has a pseudoscalar wave function. The interaction between two nuclear particles consists then of two parts: The part due to the vector field which we have considered in this paper may be written

$$V=(f^2/\kappa^2)[\boldsymbol{\sigma}_1\cdot\boldsymbol{\sigma}_2\nabla^2(e^{-\kappa r}/r) - \boldsymbol{\sigma}_1\cdot\text{grad}\,(\boldsymbol{\sigma}_2\cdot\text{grad}\,(e^{-\kappa r}/r))]. \tag{111}$$

The interaction due to the pseudoscalar field has the form

$$V'=(f'^2/\kappa^2)\boldsymbol{\sigma}_1\cdot\text{grad}\,(\boldsymbol{\sigma}_2\cdot\text{grad}\,(e^{-\kappa r}/r)).$$

Choosing, e.g., $f'=f$, the grad grad terms will cancel and thus the tensor interaction will vanish. There remains then only the central force $\boldsymbol{\sigma}_1\cdot\boldsymbol{\sigma}_2\nabla^2$. If we choose $f'$ slightly larger than $f$, we shall retain a small tensor interaction whose sign is opposite to that in the vector theory.

It is evident that this will solve our difficulties, at least qualitatively: The smallness of the tensor interaction will enable us to get the correct position of singlet and triplet state with a small, and therefore reasonable, cutting-off radius. The change of sign will give the correct (positive) sign of the quadrupole moment.

Møller and Rosenfeld have pointed out[59] that their assumption will also solve the discrepancies

[59] C. Møller and L. Rosenfeld, Nature **144**, 476 (1939). I am indebted to Drs. Møller and Rosenfeld for sending me the manuscript before publication.

in the theory of the $\beta$-decay. They assume that one of the two kinds (vectorial and pseudoscalar) of mesons disintegrates rapidly into electron plus neutrino while the other kind disintegrates only slowly. The second kind would then be the one found in cosmic rays while the first kind is responsible for the $\beta$-decay of nuclei.

While it must be admitted that the Møller-Rosenfeld theory solves the difficulties of the symmetrical meson theory, I do not think that a solution should be sought on these lines. I believe that the solution of the problem of nuclear forces ought to be fundamentally simple, and this cannot be said of the Møller-Rosenfeld proposition. It seems that one type of mesons, either represented by a vector or by a pseudoscalar field, is entirely sufficient to account qualitatively for all properties of nuclei, i.e., the forces between the nuclear particles as well as the $\beta$-transformation, and it seems rather superfluous to have a second type. Moreover, the theory would bring us back to the previous stage of nuclear physics in that it contains as many (or more) adjustable constants as there are experimental data to fit. It can even be said that the situation is worse than before because there has been added to nuclear theory a very complicated field theory, without achieving any greater definiteness in the results.

If the symmetrical meson theory is fundamentally correct, I believe it is much more likely that its quantitative aspects will be corrected by a better understanding of the cut-off process. It is true that our alternative method of cutting off in §18 only made matters worse, but we do not know the correct method yet.

A possibility of preserving at least one essential feature of the symmetrical theory, plus the single force hypothesis (§5), is suggested by Schwinger's calculations.[49] The feature in question is the equality of the central forces for triplet and singlet state. We may try to keep this feature but disregard all the information of the meson theory on the shape and relative magnitude of the potentials. Then we would simply assume "old-fashioned" square wells or Gaussian potentials, etc., for both the central and tensor force and adjust the constants so as to give the correct binding energies for the singlet and triplet state of the deuteron. (Since the range of the forces is then also unknown, the binding energy of the triton, or the analysis of the proton-proton scattering,[15] is required for its determination.) Schwinger's calculations show that with such assumptions a value for the quadrupole moment of the deuteron can be obtained which agrees well with the observed value (§15). This agreement is made possible by assuming the tensor interaction much smaller than the symmetrical field theory would predict.

The single force hypothesis itself seems to be well substantiated by our results. The introduction of a spin-independent force $U$ (cf. (19a)) into the symmetrical theory would lower the triplet and raise the singlet state (cf. §4*D*). Actually, we have found that the tensor interaction already lowers the triplet state too much (§17), therefore the force $U$ would make the disagreement even worse.

In the neutral theory, $U$ would be felt mostly in the singlet state in which it is subtracted from $V_1$. To make up for this, the interaction constant $a$ would have to be raised; to compensate for the effect of the raise in $a$ on the triplet state, $x_0$ must be increased as well, and therefore the quadrupole moment would come out somewhat larger. Since the neutral theory in its present form seems to agree well with experiment, there is no reason to introduce the force $U$.

In the present situation, there seem to be two alternative assumptions on nuclear forces which are distinguished by inherent simplicity and seem to us to merit further investigation. One is the symmetrical theory with the single force hypothesis but arbitrary choice of shape, range and depth of the force (see the discussion of Schwinger's theory above). It is superior to older nuclear theory in that the dependence of the forces on charge and spin follows from general principles being simply given by $\sigma_1 \cdot \sigma_2 \; \tau_1 \cdot \tau_2$, but it shares with the older theory the arbitrariness of the constants in the force. Obviously, in such a theory we could not say anything about the interaction of mesons with nuclear particles because we would consider the nuclear forces following from the meson theory as incorrect. This would invalidate all calculations about the production of mesons in nuclear collisions, about the meson theory of $\beta$-disintegrations, etc.

The second alternative is to consider, for the

time being, the neutral meson theory as correct. Although it may not be the final solution it may be a promising working hypothesis for the problem of nuclear forces as such, i.e., disregarding the problems of $\beta$-disintegration and the magnetic moment. In view of the good result for the quadrupole moment it seems worth while to investigate the consequences of the neutral theory for other problems, particularly the three- and four-body problem. The steep increase of the potential at small distances seems rather promising of a solution of the well-known discrepancies[46] in that it may increase considerably the binding energy of the triton. It should be realized that a treatment of systems containing more than two particles is quite difficult with a force as complicated as that following from the meson theory but it may be possible to find some simplification which preserves the most important features—such as the potential discussed in §18.

---

MARCH 1, 1940 PHYSICAL REVIEW VOLUME 57

# Electromagnetic Self-Energy of Mesotrons

R. D. RICHTMYER
*Stanford University, Palo Alto, California*
(Received November 28, 1939)

We have calculated the electromagnetic self-energy of a mesotron of unit spin according to the Proca-Yukawa-Kemmer theory by an approximate method equivalent to the second order of perturbation theory. The method enables the result to be separated into various parts whose physical significance can be seen more clearly than that of the total result, but is of course open to the same objection as perturbation theory for such calculations. The various parts of the self-energy are due to the longitudinal electric field (Coulomb part), the transverse electric field (arising from the spin), the magnetic field (also from spin) and a part due to the influence of the zero point fluctuations of the radiation field on the motion and therefore on the proper field of the particle. In terms of a "cut-off radius" $a$, introduced to make the various contributions finite, but which will later be set equal to zero, the first and last parts diverge as $1/a^3$. The second and third parts diverge as $1/a^4$, but are of opposite sign and cancel to this order. The whole self-energy diverges as $1/a^3$ in our approximation. These results are compared with similar ones for spins 0 and $\frac{1}{2}$ recently obtained by Weisskopf.

## I. INTRODUCTION—SOME EQUATIONS OF MESOTRON THEORY

WITH a notation similar to those of Yukawa,[1] Proca,[2] and Kemmer,[3] the system mesotrons+electromagnetic field is characterized by the four vectors $A_\mu U_\mu U_\mu^*$, whose space-components are treated as "generalized coordinates" depending parametrically on $x$, $y$, $z$, as well as $\mu$, and by the canonical conjugates of these "coordinates," $A_k^\dagger U_k^\dagger U_k^{*\dagger}$ $(k=1,2,3)$.

The Hamiltonian function is (it is understood that we sum our repeated suffixes, including those occurring in the square of a quantity having a suffix—Latin suffixes go from 1 to 3 and Greek ones from 1 to 4)

$$H=\int[(1/8\pi)|G_{kj}|^2+4\pi\kappa^2c^2|U_j^\dagger|^2$$
$$+(1/4\pi)|U_j|^2+(1/8\pi)\{(F_{kj})^2+(4\pi cA_j^\dagger)^2\}$$
$$+4\pi c^2|\{\partial/\partial x^j+(ie/\hbar c)A_j\}U_j^\dagger|^2]dV, \quad (1)$$

where $\kappa=(c/h)\times$mass of mesotron and we have used the abbreviations

$$G_{\mu\nu}=\frac{1}{\kappa}[\{\partial/\partial x^\mu-(ie/\hbar c)A_\mu\}U_\nu$$
$$-\{\partial/\partial x^\nu-(ie/\hbar c)A_\nu\}U_\mu], \quad (2)$$

$$F_{\mu\nu}=\partial A_\nu/\partial x^\mu-\partial A_\mu/\partial x^\nu$$
$$=(\boldsymbol{B},\boldsymbol{E}) \text{ (electromagnetic field)}. \quad (3)$$

[1] H. Yukawa, Proc. Phys. Math. Soc. Japan **20**, 1 (1938).
[2] A. Proca, J. de phys. et rad. **7**, 347, 532 (1936).
[3] N. Kemmer, Proc. Roy. Soc. **A166**, 127 (1938).

The canonical commutation relations are

$$(i/\hbar)[U_\mu^\dagger(x,t),\ U_\nu(x',t)]=\delta_{\mu\nu}\delta(x-x') \quad (4)$$

and similar equations for $U_\mu^*$, $A_\mu$, while other commutators of these quantities vanish. From this and the rule

$$\partial f/\partial t=(i/\hbar)[H,f],$$

where $f$ is any one of the generalized coordinates or momenta, we get the equations of motion

$$4\pi cA_k^\dagger=\partial A_k/c\partial t \text{ (electric field)}, \quad (5)$$

$$\partial F_{ik}/\partial x^k+4\pi\partial A_i^\dagger/\partial t=4\pi S_i \text{ (Maxwell)}, \quad (6)$$

$$4\pi\kappa^2c^2U_k^{*\dagger}-4\pi c^2\left(\frac{\partial}{\partial x^k}-\frac{ie}{\hbar c}A_k\right)\times\left(\frac{\partial}{\partial x^j}-\frac{ie}{\hbar c}A_j\right)U_j^{*\dagger}=\frac{\partial U_k}{\partial t}, \quad (7)$$

$$-\frac{1}{4\pi\kappa}\left(\frac{\partial}{\partial x^k}+\frac{ie}{\hbar c}A_k\right)G_{kj}^*+\frac{1}{4\pi}U_j^*=-\frac{\partial U_j^\dagger}{\partial t}, \quad (8)$$

in which $S_i$ is the current density. $S_i$ and the charge density $\rho$ are given by Eq. (11) below. The fourth Maxwell equation of classical electrodynamics would require that the quantity

$$C=c\partial A_k^\dagger/\partial x^k+\rho \quad (9)$$

vanish identically, i.e., be equal to the $c$ number 0. But as is well known this cannot be true in quantum theory since $C$ fails to commute with certain other variables, e.g., $A_k$, $U_k$. But $C$ commutes with $H$ and with all gauge-invariant quantities;[4] therefore eigenstates of the system may be characterized by definite eigenvalues $C'$ of $C$. $C'$ depends parametrically on $x$, $y$, $z$ but is constant in time even if the system interacts with other systems, so long as the interaction is gauge-invariant. We can therefore replace the fourth Maxwell equation by the statement that only those states of the system occur in nature for which $C$ has the eigenvalue

$$C'(xyz)\equiv 0.$$

[4] See Heisenberg and Pauli, Zeits. f. Physik **56**, 1, **59**, 168 (1929). More generally $C$ commutes with all variables invariant under those restricted gauge transformations which leave the scalar potential unchanged. $H$ is of this type.

It is seen that our Hamiltonian gives the equations of motion in a gauge for which the scalar potential $A_4$ vanishes. Heisenberg and Pauli[4] show how to make the theory relativistically invariant by adding to the Hamiltonian a term (involving $A_4$) which vanishes in this gauge but not necessarily in others. We shall not require such a term in our calculations. The time-components of the vector $U$ and the tensor $G$ are defined by

$$U_4=-4\pi c\{\partial/\partial x^k-(ie/\hbar c)A_k\}U_k^{*\dagger},$$
$$G_{4k}=-G_{k4}=4\pi\kappa cU_k^{*\dagger}. \quad (10)$$

Using (10), we see that the equations of motion (5)–(8) agree with those of references 1–3. It is convenient to write the current-charge-density vector $S^\nu$ in terms of (10), writing contravariant suffixes as superscripts and covariant ones as subscripts;

$$S^\nu=(ie/4\pi\hbar\kappa c)(U_\mu G^{\nu\mu*}-U_\mu^*G^{\nu\mu}). \quad (11)$$

## II. The Method of Approximation

This method, similar to one used by Weisskopf,[5] considers the above Hamiltonian as an operator on the Schrödinger functional $\Psi(U_k,U_k^*,A_k,t)$,[6] and considers the dependence of this operator on the parameter $e$ (electronic charge). The operator $U_k$ results merely in multiplying $\Psi$ by the argument $U_k$, the operator $U_k^\dagger$ is $(\hbar/i)$ times the functional derivative of $\Psi$ with respect to $U_k$, etc.[4] Therefore the operator $H$ depends on $e$ only as explicitly shown in (1) and the abbreviations (2), (3). This dependence we will denote by

$$H=H(e).$$

If $e$ is increased by $de$, the Hamiltonian acquires the additional term $H'(e)de$ and by perturbation theory the energy of a given stationary state $s$ increases by an amount

$$dW(s,e)=(s,e\,|\,H'(e)\,|\,s,e)de.$$

So if $e$ is increased from zero to $e_0$ the total increase of energy is

$$W(s,e_0)=\int_0^{e_0}(s,e\,|\,H'(e)\,|\,s,e)de. \quad (12)$$

As indicated, the matrix element of $H'(e)$ is to

[5] V. F. Weisskopf, Phys. Rev. **56**, 72 (1939).

[6] $U_k$, $U_k^*$, $A_k$ are the coordinates, and $t$ the time.

be calculated from the exact wave-functional representing the state $s$ when the electronic charge has the value $e$. If this could be done, Eq. (12) would of course give the self-energy exactly. To approximate we set

$$(s,e|H'(e)|s,e)=a_0+a_1e+a_2e^2+\cdots \quad (13)$$

and then

$$W(s,e)=a_0e+\tfrac{1}{2}a_1e^2+\cdots. \quad (14)$$

As is well known, the self-energy can contain only even powers of $e$, and therefore $a_0=0$. Then approximately,

$$W(s,e)\approx\tfrac{1}{2}a_1e^2\approx\tfrac{1}{2}(s,e|eH'(e)|s,e). \quad (15)$$

$eH'(e)$ can be calculated from (1), and we find

$$\tfrac{1}{2}eH'(e)=-\tfrac{1}{2}\int S^kA_k\,dV, \quad (16)$$

where $S^k$ is given by (11). We require the diagonal matrix element (or time average) of this quantity for state $s$. It is therefore convenient to regard the quantities in the last term of (16) as matrices. The matrix $A_k$ will depend on $e$ (since the wave functions from which it is calculated depend on $e$) and so we write

$$A_k=A_k^0+A_k', \quad (17)$$

where the matrix $A_k^0$ is the value of $A_k$ for $e=0$, and $A_k'$ is the rest. Similar remarks hold for the field strengths $\boldsymbol{B}$, $\boldsymbol{E}$, and they can be separated into $\boldsymbol{B}^0$, $\boldsymbol{E}^0$, $\boldsymbol{B}'$, $\boldsymbol{E}'$. $A_k^0$ represents the zero point field (solution of the homogeneous Maxwell's equations) and the part depending on $e$ can be obtained from

$$A_\mu'(x,t)=\int\frac{S_\mu(x',\,t-|x-x'|/c)}{|x-x'|}dV' \quad (18)$$

by a gauge transformation which reduces $A_4$ to zero. The primed field-strengths are related to the density $S^k$ by Maxwell's equations and using these equations we partially eliminate $S^k$ from (16). We also do partial integrations with respect to the space coordinates and with respect to time (the latter being allowed since the diagonal matrix element is the time average). $W$ is then the time average of

$$(1/8\pi)\int(\boldsymbol{E}'^2-\boldsymbol{B}'^2)dV-(1/2)\int S^kA_k^0\,dV.$$

We separate the electric field into longitudinal and transverse parts. The divergence of the former part is given by (9) and so

$$\boldsymbol{E}'_{\text{long}}(x,t)=-\nabla\int\frac{\rho(x',t)-C(x')}{|x-x'|}dV'.$$

Since neither $\rho$ nor $C$ has any matrix elements connecting different eigenvalues $C'$ it is seen that for purposes of calculating the time average of $(E'_{\text{long}})^2$ in a state with eigenvalue $C'\equiv0$, the operator $C$ in the above equation can be ignored completely. Consequently $W$ is the time average of

$$\frac{1}{2}\int\int\frac{\rho(x)\rho(x')}{|x-x'|}dV\,dV'+\frac{1}{8\pi}\int(\boldsymbol{E}'_{\text{transverse}})^2dV \quad (19)$$
$$-(1/8\pi)\int(\boldsymbol{B}')^2dV-\frac{1}{2}\int S^kA_k^0\,dV$$

or

$$W=W_{\text{st}}+U_{\text{el}}-U_{\text{mag}}+W_{\text{fluct}}$$

in the notation of Weisskopf.[5]

## III. Calculations

Following Yukawa[1] except for a slight change, we resolve $U_\nu$ in plane waves as follows:

Let $k_\mu$ or simply $k$ represent any one of a set of four-vectors whose components are

$$k_x=2\pi n_x/L,\quad n_x=0,\ \pm1,\ \pm2,\ \cdots,$$
etc.
$$k_4=\pm(k_x^2+k_y^2+k_z^2+\kappa^2)^{\frac{1}{2}}. \quad (20)$$

For any $k$ let $e_{1k}, e_{2k}, e_{3k}$, be 3 mutually orthogonal unit four-vectors, i.e., $(e_{1k})_x^2+(e_{1k})_y^2+(e_{1k})_z^2-(e_{1k})_4^2=1$ etc. Further, to agree as closely as possible with the notation of Yukawa we suppose that the space-part of $e_{1k}$ is parallel to the space-part of $k$. Then the field can be written as

$$U_\nu=\sum_k\sum_{j=1}^{3}u_{jk}(e_{jk})_\nu e^{ik_\mu x_\mu}. \quad (21)$$

For free mesotrons the $u_{jk}$ are constants and the number of particles in state $jk$ is given by the dynamical variable

$$N_{jk}=\begin{cases}\dfrac{|k_4|\,\Omega}{2\pi\hbar\kappa^2c}u_{jk}^*u_{jk} & \text{if } k^4>0\\[2ex] \dfrac{|k_4|\,\Omega}{2\pi\hbar\kappa^2c}u_{jk}u_{jk}^* & \text{if } k^4<0.\end{cases} \quad (22)$$

The particle's charge is + or − according as $k^4>0$ or $<0$.

We calculate $W$ approximately by deriving the $\rho$ and primed field strengths from these free-mesotron wave functions for a state $S$ in which

$$\begin{aligned} N_{jk}&=1 \quad \text{for } jk=j_0k_0 \\ N_{jk}&=0 \quad \text{otherwise,} \end{aligned} \tag{23}$$

and we take the space part of $k_0=0$ (mesotron at rest). This means simply substituting (21) into (2) into (11) into (18) into (19) and carrying out the indicated mathematical operations, retaining only those terms diagonal in the occupation numbers (23).

We express the result in terms of a "cut-off momentum" $P$, which is the highest value we allow for the space part of $\hbar k$ in our summation. We call $\mathfrak{W}=W-W(\text{vac.})$ where $W(\text{vac.})$ is calculated for all $N$'s$=0$. The results are

$$\mathfrak{W}_{\text{st}}=\frac{e^2\kappa}{12\pi}\lim_{P\to\infty}\left[3\left(\frac{P}{mc}\right)^2+9\ln\frac{P}{mc}\right] +\text{finite terms},$$

$$\mathfrak{U}_{\text{el}}=\frac{e^2\kappa}{12\pi}\lim_{P\to\infty}\left[\frac{1}{2}\left(\frac{P}{mc}\right)^4-\frac{1}{2}\left(\frac{P}{mc}\right)^2+\frac{3}{4}\ln\frac{P}{mc}\right]+\text{f.t.}, \tag{24}$$

$$\mathfrak{U}_{\text{mag}}=\frac{e^2\kappa}{12\pi}\lim_{P\to\infty}\left[\frac{1}{2}\left(\frac{P}{mc}\right)^4+\frac{3}{2}\left(\frac{P}{mc}\right)^2-\frac{5}{4}\ln\frac{P}{mc}\right]+\text{f.t.}$$

$W_{\text{fluct}}$ requires special consideration. If we write $S^k=S^{k(0)}+S^{k'}$ where $S^{k(0)}$ is calculated for free mesotrons and $S^{k'}$ is the correction obtained by first-order perturbation theory, it can be seen that $\int S^{k(0)}A_k{}^0dV$ has no diagonal elements at all. $S^{k'}$ is a rather complicated quantity, but after dropping parts which contribute nothing to the final answer either because they are irrotational (and because $\nabla\cdot A^0=0$) or because they yield no diagonal elements, the only part of the current $S^{k'}$ remaining is

$$-e^2A^{k(0)}/mc^2L^3$$

as in the cases discussed by Weisskopf, so that we can adopt his result

$$W_{\text{fluct}}=\frac{e^2\kappa}{12\pi}\lim_{P\to\infty}12\left(\frac{P}{mc}\right)^2.$$

By way of check we have also calculated $\mathfrak{U}_{\text{el}}-\mathfrak{U}_{\text{mag}}+\mathfrak{W}_{\text{fluct}}$ directly by a second-order perturbation calculation and the result agrees with the expressions given above.

## IV. Discussion

The most strongly divergent terms arise from the spin, but there the electric and magnetic contributions cancel as far as terms in $1/a^4$ are concerned, so that $W$ diverges as $1/a^2$ in our approximation. $a=\hbar/P$ may be considered the "radius" of the mesotron. According to Weisskopf,[4] $W$ also diverges as $1/a^2$ for particles of spin 0, where there are of course no spin terms. For particles with spin $\frac{1}{2}$ in the hole theory, Weisskopf finds that the spin terms do not cancel each other, being of order $1/a^2$ and both negative but that they together cancel the quadratic contribution of $W_{\text{fluct}}$, with the result that $W$ diverges only logarithmically in this case.

The author wishes to express thanks to Professor V. Weisskopf for suggesting this calculation and to him and Professor F. Bloch for many discussions during its progress.

# The Variation of the Adiabatic and Isothermal Elastic Moduli and Coefficient of Thermal Expansion with Temperature through the λ-Point Transition in Ammonium Chloride*

ANDREW W. LAWSON†
*Pupin Physics Laboratories, Columbia University, New York, New York*
(Received December 29, 1939)

Measurements of the temperature variation of the adiabatic and isothermal Young's and rigidity moduli and of the coefficient of thermal expansion of pressed specimens of ammonium chloride in the neighborhood of the λ-point transition at 242.8°K are reported. It is found that a large difference exists between the adiabatic and isothermal compressibilities below the critical temperature, and hence a large difference between the specific heat at constant pressure and the specific heat at constant volume. The data, in conjunction with the known temperature variation of the specific heat at constant pressure, permit the evaluation of the temperature variation of the specific heat at constant volume, and from this it is concluded that the transition is not to be associated, as previously suggested by Pauling, with the occurrence of almost free rotation of the ammonium radicals in the crystal lattice.

## INTRODUCTION

THE crystalline structure of ammonium chloride is cubic.[1] The chlorine atoms lie at the vertices of the elementary cubes and the nitrogen atoms at the centers. Four hydrogen atoms form a tetrahedral array about each nitrogen atom and, at low temperatures at least, there appears to be a common preferred orientation for all the tetrahedra in the crystal, *viz.* one in which a symmetry axis of the tetrahedron lies parallel to a diagonal axis of the cube.[2]

Many physical properties of ammonium chloride vary sharply but continuously with temperature in the neighborhood of 242.8°K. Thus, as the temperature is raised through an interval of only a few degrees, the specific heat at constant pressure[3] and coefficient of thermal expansion[4] increase many times in value and then decrease; the substance ceases to be piezoelectric;[5] the dielectric constant and dielectric absorption increase;[2] there is a shift in the characteristic infra-red absorption frequencies;[6] and a change in the Raman spectrum.[2]

Now x-ray analysis reveals no change in the lattice structure in this critical temperature interval,[7] hence the foregoing phenomena must be associated in some manner with the behavior of the hydrogen tetrahedra: for the light hydrogen atoms alone leave no trace of their presence on the x-ray record. The object of the present research is to obtain further data upon which to base a study of this behavior. In particular, it is desired to know the way in which the specific heat at constant volume varies with temperature during the transition.

The specific heats at constant pressure and constant volume are related by the formula

$$c_p - c_v = Tv\alpha^2/\kappa_t, \qquad (1)$$

in which $c_p$ and $c_v$ denote, respectively, the two molal specific heats, $T$ the absolute temperature, $v$ the molal volume, $\alpha$ the volume coefficient of thermal expansion, and $\kappa_t$ the isothermal compressibility. It is proposed to calculate $c_v$ by inserting measured values of the remaining quantities in this formula, but it must be remarked that, in virtue of its origin, Eq. (1) is directly applicable only to *reversible* processes,

* Publication assisted by the Ernest Kempton Adams Fund for Physical Research of Columbia University.
† University Fellow, Columbia University.
[1] G. Bartlett and I. Langmuir, J. Am. Chem. Soc. **43**, 84 (1921); R. Wyckoff, Am. J. Sci. **3**, 177 (1922); **4**, 193 (1922).
[2] A. C. Menzies and H. R. Mills, Proc. Roy. Soc. **A148**, 407 (1935).
[3] Simon, von Simson and Ruheman, Zeits. f. physik. Chemie **A129**, 339 (1927).
[4] F. Simon and R. Bergman, Zeits. f. physik. Chemie **B8**, 255 (1930); A. Smits and G. H. MacGillavry, Zeits. f. physik. Chemie **A166**, 97 (1933); H. Adenstedt, Ann. d. Physik **26**, 69 (1936).
[5] S. Bahrs and J. Engl, Zeits. f. Physik **105**, 470 (1937).
[6] A. Hettner and F. Simon, Zeits. f. physik. Chemie **B1**, 293 (1928); A. G. Pohlmann, Zeits. f. Physik **79**, 394 (1932).
[7] F. Simon and C. von Simpson, Naturwiss. **14**, 880 (1926); J. A. Ketelaar, Nature **134**, 250 (1934).

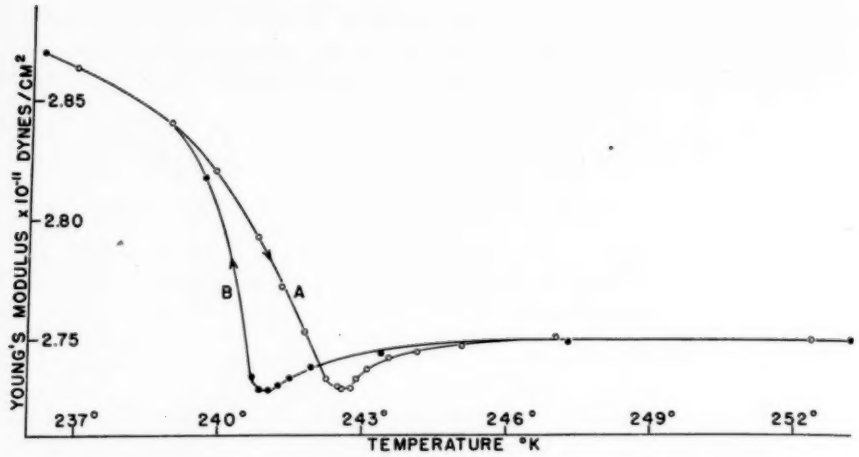


FIG. 1. The way in which the adiabatic Young's modulus varies with temperature near the transition when the material is (A) heated, and (B) cooled.

that is, to processes during which the state of the system, as determined by specific values of the thermodynamic coordinates, does not depend upon the previous history of the system. In this sense the processes here under review are not reversible, for it is known that the values of $\alpha$ and $\kappa$ at a given temperature in the transition region depend upon whether the material has been brought to that temperature by heating it or by cooling it. The nature of this phenomenon is illustrated by the curves of Fig. 1, in which the quantity dealt with is the adiabatic Young's modulus. Accordingly, the validity of Eq. (1) is subject to question when $T$ lies in the transition interval. It is proposed to resolve this question in the following manner:

The isothermal and adiabatic compressibilities of a substance are related by the formula

$$\kappa_t - \kappa_s = Tv\alpha^2/c_p, \tag{2}$$

in which $\kappa_s$ denotes the adiabatic compressibility, and this equation is subject in the same manner to the same condition concerning reversibility as is Eq. (1), for both follow from the two fundamental thermodynamic formulae known[8] as the "$T\,dS$ equations." If, therefore, the validity of Eq. (2) over the transition interval can be established experimentally, then that of Eq. (1) may be accepted without demur.

The compressibility of an isotropic material is related to the Young's and rigidity moduli by the formula

$$\kappa = (9/E) - (3/\mu), \tag{3}$$

where $E$ and $\mu$ denote, respectively, the Young's modulus and the rigidity modulus. The adiabatic and isothermal values of the latter are identical, since pure torsion involves no change in volume. Hence, for the purpose of the preceding argument, Eq. (2) may be replaced by the equation

$$(9/E_t) - (9/E_s) = Tv\alpha^2/c_p. \tag{4}$$

The experimental verification of this formula requires the measurement of the variations of $E_t$, $E_s$, $\alpha$ and $c_p$ with temperature on a homogeneous, isotropic specimen. The variation of $c_p$ with temperature through the transition has been measured by Simon, von Simson and Ruheman,[3] and their data are used in the calculations which follow. The experiments here reported are concerned with $E_t$, $E_s$, $\mu$ and $\alpha$.

## EXPERIMENTAL METHODS

### The adiabatic moduli

A complete description of the dynamical method employed for measuring the adiabatic Young's and rigidity moduli has appeared in previous issues of this journal.[9] Accordingly it will suffice here briefly to review its essential features. The specimen is in the form of a right circular cylinder 4.7 cm in diameter and a few

[8] See, for example, M. Zemansky, *Heat and Thermodynamics* (McGraw-Hill, 1937), p. 225.

[9] L. Balamuth, Phys. Rev. **45**, 715 (1934); M. E. Rose, Phys. Rev. **49**, 50 (1936); M. A. Durand, Phys. Rev. **50**, 449 (1936).

centimeters long. The required data are deduced from the observed behavior of a separately excited composite piezoelectric oscillator constructed by cementing to one end of the specimen a suitably cut cylinder of crystalline quartz of identical cross section. Silver electrodes are deposited in proper position on the quartz, and the oscillator is suspended vertically by delicate supports attached at the middle of the quartz cylinder. The fundamental frequency of free longitudinal or torsional vibration of this system is measured by observing the variation of the electrical impedance of the composite oscillator with the frequency of the applied voltage, and from this the frequency, $f$, of free longitudinal or torsional vibration of the specimen cylinder alone is calculated. The latter quantities are related, respectively, to $E_s$ and $\mu$ by the formula

$$2fL=(M/\rho)^{\frac{1}{2}}, \qquad (5)$$

where $L$ is the length of the specimen cylinder, $\rho$ the density, and $M$ the elastic modulus.

**Thermal expansion**

The coefficient of thermal expansion is obtained by graphical differentiation of a linear thermal expansion curve plotted from data taken with the simple form of dilatometer described by Siegel and Quimby.[10] The change in length of a specimen 4 cm long can be measured with an accuracy of 0.001 mm, and the consequent uncertainty in the normal value of $\alpha$ is 1 percent.

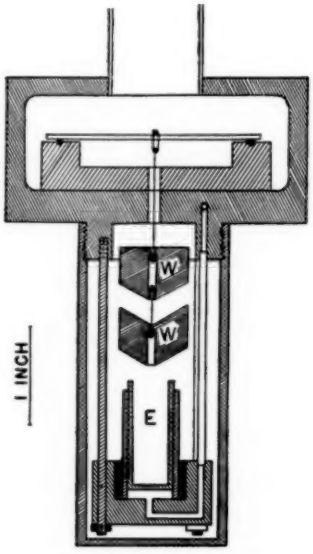


FIG. 2a. Cross-sectional diagram of the apparatus for measuring the temperature variation of the isothermal Young's modulus, showing the mounted specimen, weights and hydraulic elevator.

**Isothermal moduli**

The adiabatic and isothermal values of Young's modulus differ by less than 2 percent at temperatures removed from the transition region. Furthermore, the adiabatic modulus can be measured, by the method outlined above, with far greater accuracy than can the isothermal modulus. Thus, *at any temperature removed from the transition*, a better value of $E_i$ can be obtained from the corresponding value of $E_s$ with the aid of Eq. (4), than can be obtained by direct measurement. Accordingly, the apparatus about to be described is designed only to measure the *ratio* of the value of $E_i$ at a fixed temperature to that at any other temperature.

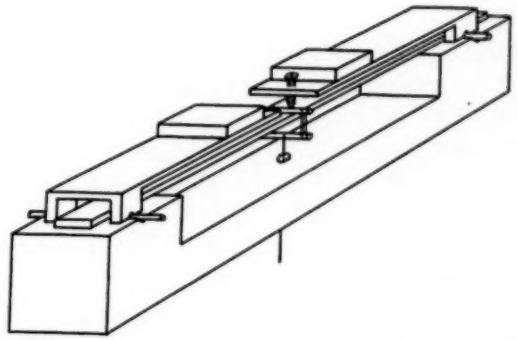

FIG. 2b. Detailed diagram of specimen mount, showing lever and mirror system.

Figure 2 is a schematic diagram of the apparatus. The specimen, in the form of a rectangular beam 6 cm long by 4 mm wide by 1.5 mm thick, rests horizontally on two smooth fused quartz rods 1 mm in diameter and 5 cm apart. The specimen is bent by two Duralumin weights hung from a centrally located stirrup, and applied singly by lowering a hydraulic elevator constructed from parts of a glass hypodermic syringe. The elevator liquid is methanol, and the operation is effected by manipulation of a duplicate syringe in fluid connection with the first. The amount of bending of the specimen is measured by observing the relative angular

[10] S. Siegel and S. L. Quimby, Phys. Rev. **54**, 76 (1938).

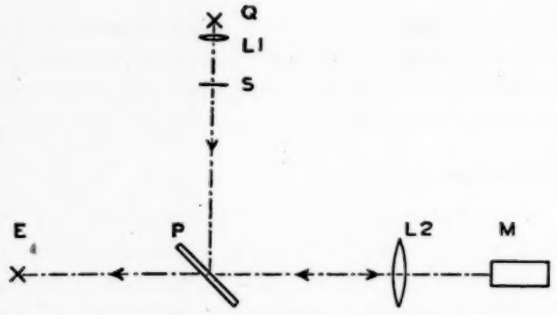


FIG. 3. The optical system for measuring the amount of bending of the specimen.

deflection of two light beams reflected one from each of two small horizontal mirrors attached to two levers. One end of each lever rests on the specimen at a point near its center, and the other end pivots on one of the quartz rods which support the specimen.

The specimen and the associated lever system are mounted in a stout, sealed copper box, which is supported, through a one-inch copper to glass seal, by a vertical glass tube. The incident and emerging light beams pass through this tube. The entire apparatus is immersed in the cryostatic bath described below.

Figure 3 is a plan diagram of the remainder of the optical system employed to measure the beam deflection. Light from a strip filament lamp, $Q$, is focused on a horizontal slit, $S$, which is a focal length distant from a lens, $L_2$. Light emerging from the slit is, in part, reflected through $L_2$ by a plate glass mirror, $P$, is rendered parallel by $L_2$, and reflected downward onto the lever mirrors by a silvered mirror, $M$. The returning beams of parallel light are reflected back by the mirror $M$ through the lens $L_2$, which forms two images of the slit in the focal plane of a filar micrometer eyepiece, $E$. When the specimen beam is bent, these two images separate, and the amount of this separation, as measured by the filar micrometer, is proportional to the downward displacement of the center of the beam.

The focal length of the lens $L_1$ is 4 cm, and that of $L_2$ is 115 cm. The minimum observable displacement of the beam center is $10^{-5}$ cm. Proportionality between stress and strain in the material is verified at each temperature by comparison of the displacements produced, respectively, by one and both of the weights.

### Internal friction

The experimental method, described above, for measuring the adiabatic elastic moduli yields at the same time values of the coefficients of internal friction of the substance.[11] These quantities are associated with the types of normal vibration of a body, and are defined, one for each type, as the coefficient of the vibrational stress amplitude squared in the expression for the energy dissipated per unit volume per cycle of vibration.[12] They thus resemble the elastic moduli in that their definition requires the specification of a stress. The types of stress here dealt with are the stretch and twist associated, respectively, with the longitudinal and torsional vibration of a slender bar.

### Temperature control

Observations of $E_s$, $E_t$, $\mu$ and $\alpha$ are made with the specimen, enclosed in the appropriate envelope, immersed in a well-stirred methanol bath contained in a large Dewar vessel. This liquid is cooled by a continuous circulation of cold methanol through a pair of copper coils, one of which is immersed in the bath and the other in a solution of carbon dioxide snow and methanol. The circulation is maintained by a centrifugal pump, which is itself immersed in the solution. The temperature of the bath is kept constant to 0.01°K by adjusting the flow of the cooling liquid, and also the power dissipated in a quick acting electric immersion heater located in the bath.

The temperature is measured with a platinum resistance thermometer, used in connection with a Mueller bridge. The thermometer calibration is certified by the National Bureau of Standards, and is checked at the melting point of ice and the boiling point of a quantity of oxygen which has stood in a Dewar vessel for a week.

## RESULTS

### Specimen material

The ideal specimen material for an investigation of the lattice properties of a solid is, of course, a single crystal. Natural crystals of ammonium chloride occur in lava deposits, but

[11] S. Siegel and S. L. Quimby, Phys. Rev. **49**, 663 (1936).
[12] W. T. Cooke, Phys. Rev. **50**, 1158 (1936).

are small and very impure. Unsuccessful attempts were made to grow single crystals by slow cooling from the molten material,[13] and by slow crystallization from a saturated solution containing pectic acid.[14] Crystals formed by the first method were shattered by the large change in volume which accompanies the crystallographic transformation at 186°C, and the second method failed to produce crystals of adequate size or structural perfection. It will be noted, however, that to obtain the data here sought, namely the temperature variations of $c_v$, $\alpha$ and $\kappa$, it is not necessary to use a single crystal, and the foregoing difficulties discouraged further attempts to secure one.

Polycrystalline specimens are cut from a block of material prepared by compressing dry granulated ammonium chloride[15] to 50,000 lb./in.$^2$ in a steel cylinder at room temperature. The result is a coherent array of microcrystals whose average linear dimension, as revealed by photomicrographs, is $5\times10^{-3}$ cm. Experiments made on specimen cylinders cut along different directions in the block reveal no trace of anisotropy. The densities of different blocks at 24°C vary slightly about the value 1.520 g/cm$^3$, which is slightly less than the density of crystalline ammonium chloride as measured by Wulf and Cameron,[16] namely 1.527 g/cm$^3$.

TABLE I. *The variation of the thermal expansion of polycrystalline ammonium chloride with temperature.*

| $T$ °K | $\Delta L/L$ ×100 | $\alpha$ ×10$^4$ | $T$ °K | $\Delta L/L$ ×100 | $\alpha$ ×10$^4$ |
|---|---|---|---|---|---|
| 224.0 | 0.593 | 1.70 | 242.5 | 0.325 | 23.3 |
| 228.0 | .562 | 2.64 | 242.6 | .313 | 29.4 |
| 232.0 | .523 | 3.28 | 242.7 | .294 | 51.0 |
| 235.0 | .487 | 3.85 | 242.8 | .261 | 183. |
| 237.0 | .461 | 4.17 | 242.9 | .218 | 103. |
| 238.0 | .446 | 4.65 | 243.0 | .184 | 38.8 |
| 239.0 | .430 | 5.12 | 243.1 | .178 | 14.3 |
| 240.0 | .411 | 6.42 | 243.2 | .174 | 7.40 |
| 241.0 | .388 | 8.00 | 243.5 | .168 | 3.56 |
| 241.6 | .370 | 10.4 | 244.5 | .161 | 2.00 |
| 241.9 | .359 | 12.1 | 246.0 | .152 | 1.89 |
| 242.1 | .351 | 14.3 | 249.0 | .133 | 1.86 |
| 242.2 | .346 | 16.0 | 255.0 | .095 | 1.83 |
| 242.3 | .340 | 18.1 | 263.0 | .049 | 1.67 |
| 242.4 | .333 | 20.5 | 273.2 | .000 | 1.23 |

[13] H. Rassow, Zeits. f. anorg. allgem. Chemie **114**, 117 (1920).
[14] F. Ehrlich, Zeits. f. angew. allgem. Chemie **203**, 26 (1931).
[15] Eimer and Amend Company, New York, Tested Purity Reagent.
[16] P. Wulff and H. K. Cameron, Zeits. f. physik. Chemie **B10**, 347 (1930).

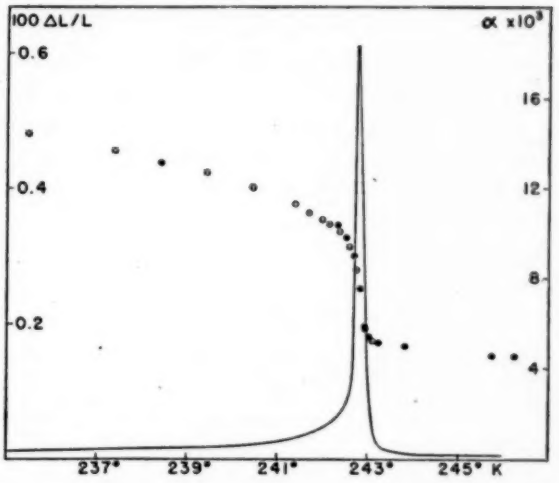


FIG. 4. The thermal contraction curve and the variation of the volume coefficient of thermal expansion with temperature near the transition.

Except as otherwise specified, the measurements which follow were all made on specimens whose density is 1.520 g/cm$^3$, and all were made as the temperature of the specimen was progressively *raised*.

### Thermal expansion

The observed linear thermal expansion of two specimens of ammonium chloride between 236°K and 247°K is plotted in Fig. 4. The curve in this figure shows the variation of the volume coefficient of thermal expansion with temperature, the ordinates being three times the slope of a smooth curve drawn through the plotted $\Delta L/L$ data. The maximum value of $\alpha$ occurs at the temperature 242.8°K. Corresponding data over the temperature range 224°K to 273°K are given in Table I.

The thermal expansion of a pressed specimen whose density is 1.512 g/cm$^3$ is indistinguishable by the present experimental method from that of a specimen whose density is 1.520 g/cm$^3$.

### Adiabatic elastic moduli

The variations of the adiabatic Young's modulus, rigidity modulus, compressibility, and Poisson's ratio with temperature over the transition interval are shown in Figs. 5 and 6. The compressibility, $\kappa_s$, is calculated from the observed $E_s$ and $\mu$ with Eq. (3), and Poisson's ratio, $\sigma_s$, with the formula

$$\sigma_s=(E_s/2\mu)-1. \qquad (6)$$

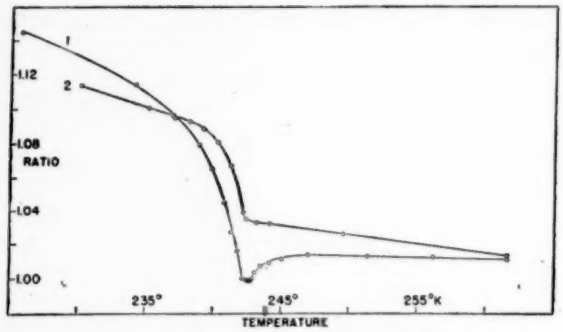


FIG. 5. The variation of the adiabatic Young's modulus (curve 1) and rigidity modulus (curve 2) with temperature near the transition point. The ordinates are the ratios of the values at the given temperature to the values at 273.2°K.

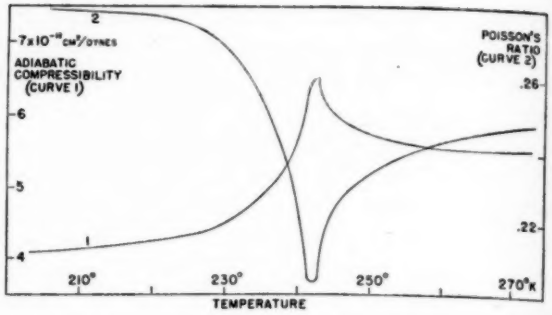


FIG. 6. The variation of the adiabatic compressibility (curve 1) and Poisson's ratio (curve 2) with temperature.

Complete data over the temperature interval 205°K to 273°K are presented in Table II. The second column of this table contains values of $E_s$ measured at the temperatures given in the first column. The corresponding values of $\mu$, which appear in the third column, are obtained from the measured values of this quantity by graphical interpolation. The remaining columns are calculated with Eqs. (3) and (6). It will be noted that the maximum value of the compressibility and the minimum values of Young's modulus and Poisson's ratio occur at the temperature 242.8°K.

The isothermal compressibility of the present specimens of ammonium chloride, computed from the data of Tables I and II with the aid of Eq. (2), is $5.64\times10^{-12}$ cm²/dyne at 0°C. The only other measurement of this quantity of which the writer is aware is that of Bridgman,[17] who worked with polycrystalline specimens pressed at about 310,000 lb./in.². The density of these specimens is not reported. Bridgman's experiments lead to the value $5.60\times10^{-12}$ cm²/dyne.[18] It must not, however, be assumed that either of these values is characteristic of the crystal lattice. Indeed, it is found that the compressibility of a pressed specimen depends to a marked degree upon its density. Thus the isothermal compressibility of a specimen whose density is 1.512 g/cm³ is 6.7 percent greater than that of a specimen whose density is 1.520 g/cm³. A cognate example of the discordance between observations made on single and polycrystalline specimens is found in magnesium oxide, for which the observed compressibility of a single crystal is $0.59\times10^{-6}$ cm²/kg, while that of a pressed specimen is $0.99\times10^{-6}$ cm²/kg.[19]

It is further found, however, that small changes in density are very nearly without effect on the *temperature variations* of the elastic moduli, expressed in percent change per degree. For example, the ratios of the values of the compressibilities at 220°K to those at 273°K for the two specimens cited above differ by only 1.2 percent, the less dense specimen having the larger ratio.

**Isothermal elastic moduli**

The variation of the isothermal Young's modulus with temperature through the transition interval is given in Table III. The second column of this table contains values of the ratios $E_t^0/E_t$, where $E_t^0$ denotes the value of the modulus at 235.73°K and $E_t$ that at the temperature indicated in the first column. This ratio is related to the observed ratio of the corresponding beam displacements, $y^0/y$, by the formula

$$E_t^0/E_t=(y/y^0)(1+4\delta_L), \qquad (7)$$

where $\delta_L$ denotes the change in length per unit length of the specimen material between 235.73°K and the temperature of observation. The correction term in this formula represents the effect of lateral thermal expansion on the stiffness of the beam.

The value of $E_t^0$ used in computing the data given in the third column of Table III is calculated, as before mentioned, from the observed value of $E_s$ at 235.73°K with Eq. (4).

It is found that ammonium chloride is plastic over a temperature interval of about 0.3°K at the

[17] P. W. Bridgman, Phys. Rev. **38**, 182 (1931).
[18] A. May, Phys. Rev. **52**, 339 (1937).
[19] P. W. Bridgman, Proc. Am. Acad. Sci. **67**, 345 (1932).

transition, and it is therefore impossible to measure $E_t$ at temperatures which lie in this range. The beam displacement increases steadily with time after the load is applied, at such a rate that the increase in 5 minutes is about half the initial displacement. This plasticity disappears immediately above and immediately below the transition temperature. Copper-gold alloys[20] and quartz[21] have been shown to behave in a similar manner at their transition temperatures.

It will be recalled that the object of the isothermal measurements is to establish the validity of Eq. (4) in the transition interval. The affirmative nature of the result is indicated in Fig. 7. The points plotted in this figure indicate the *observed* values of the ratio $E_t^0/E_t$, and the smooth curve values *calculated* with Eq. (4) from the data given in Tables I and II, together with those on $c_p$ obtained by Simon, von Simson and Ruheman.[3] The hiatus left in this curve signifies the uncertainty, admitted by the last named investigators, in their values of $c_p$ immediately at and immediately above the transition temperature.

TABLE II. *The variation of the adiabatic elastic moduli of polycrystalline ammonium chloride with temperature.*

| $T$ °K | $E_s\times10^{-11}$ DYNES/CM² | $\mu\times10^{-11}$ DYNES/CM² | $\kappa_s\times10^{11}$ CM²/DYNES | $\sigma_s$ |
|---|---|---|---|---|
| 205.42 | 3.2372 | 1.2633 | 0.406 | 0.281 |
| 216.27 | 3.1832 | 1.2445 | .417 | .279 |
| 225.72 | 3.1286 | 1.2280 | .434 | .274 |
| 234.18 | 3.0462 | 1.2119 | .479 | .258 |
| 236.92 | 2.9975 | 1.2034 | .510 | .245 |
| 238.94 | 2.9492 | 1.1948 | .541 | .234 |
| 239.87 | 2.9134 | 1.1886 | .565 | .226 |
| 240.81 | 2.8567 | 1.1770 | .602 | .214 |
| 241.32 | 2.8220 | 1.1656 | .615 | .211 |
| 241.79 | 2.7777 | 1.1502 | .632 | .207 |
| 242.25 | 2.7378 | 1.1375 | .650 | .203 |
| 242.50 | 2.7319 | 1.1343 | .650 | .204 |
| 242.59 | 2.7300 | 1.1337 | .651 | .204 |
| 242.75 | 2.7299 | 1.1331 | .649 | .204 |
| 242.87 | 2.7377 | 1.1329 | .649 | .208 |
| 243.10 | 2.7461 | 1.1327 | .629 | .212 |
| 243.52 | 2.7546 | 1.1322 | .618 | .216 |
| 244.15 | 2.7610 | 1.1314 | .608 | .220 |
| 245.08 | 2.7668 | 1.1301 | .598 | .224 |
| 247.04 | 2.7721 | 1.1274 | .586 | .229 |
| 251.38 | 2.7696 | 1.1223 | .577 | .234 |
| 256.21 | 2.7684 | 1.1165 | .564 | .240 |
| 261.61 | 2.7635 | 1.1100 | .554 | .245 |
| 273.18 | 2.7316 | 1.0953 | .556 | .247 |

[20] W. S. Gorsky, Physik. Zeits. Sowjetunion **8**, 562 (1935).
[21] A. Perrier and R. de Mandrot, Mem. Soc. Vaud. **1**, 333 (1924).

## Internal friction

The way in which the internal friction associated with longitudinal vibration of the specimen cylinders varies with temperature is shown in Fig. 8. The torsional internal friction behaves in a similar manner.[22] Little of a quantitative nature can be written concerning this phenomenon at the present state of development of the theory. The high internal friction at the transition is, of course, associated with the observed plasticity of the material at this temperature. Again, the thermoelastic theory of Zener[23] indicates that the total internal friction contains a part proportional to $c_p-c_v$, and it will be seen that the value of the latter quantity becomes very large at the transition temperature.

TABLE III. *The variation of the isothermal Young's modulus of polycrystalline ammonium chloride with temperature.*

| $T$ °K | $E_t^0/E_t$ | $E_t\times10^{-11}$ DYNES/CM² | $T$ °K | $E_t^0/E_t$ | $E_t\times10^{-11}$ DYNES/CM² |
|---|---|---|---|---|---|
| 228.71 | 0.956 | 3.034 | 241.97 | 1.284 | 2.259 |
| 235.73 | 1.000 | 2.901 | 242.24 | 1.410 | 2.057 |
| 237.58 | 1.034 | 2.830 | 242.39 | 1.589 | 1.826 |
| 238.90 | 1.035 | 2.763 | 242.48 | 1.788 | 1.622 |
| 239.53 | 1.085 | 2.706 | 243.08 | 1.113 | 2.606 |
| 240.51 | 1.098 | 2.625 | 243.33 | 1.095 | 2.649 |
| 240.81 | 1.112 | 2.583 | 243.82 | 1.084 | 2.676 |
| 241.47 | 1.185 | 2.452 | 244.31 | 1.078 | 2.691 |
| 241.87 | 1.235 | 2.338 | 245.28 | 1.066 | 2.721 |

## Specific heat at constant volume

The difference $c_p-c_v$ is evaluated with Eqs. (1) and (2), from the observed values of $\alpha$, $\kappa_s$ and $c_p$ by eliminating $\kappa_t$ between the two equations, and the value of $c_v$ then follows. The result is shown in Fig. 9, in which the circles are a plot of Simon, von Simson and Ruheman's data and the dots are the calculated values of $c_v$. The latter quantities appear in the last column of Table IV. The estimated uncertainty in the quantity $c_p-c_v$ increases from 0.2 cal./mol-deg. at 236°K to 2 cal./mol-deg. at 242.4°K.

Two questions arise in connection with the foregoing procedure, since this requires the combination of data obtained by different observers working with different specimens. The first is concerned with the value of $c_p$, but the writer can

[22] The internal friction of $\beta$-brass likewise is large at the transition; see Koster, Zeits. f. Electrochem. **45**, 30 (1939).
[23] C. Zener, Phys. Rev. **53**, 90 (1938).

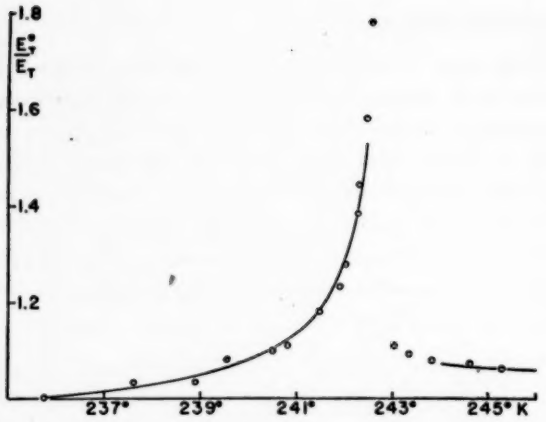


FIG. 7. Comparison of the observed ratios of the values of the isothermal Young's modulus at different temperatures (the circles), with those computed from the corresponding values of the adiabatic modulus with Eq. (4) (the curve).

adduce no reason why this quantity should depend upon the nature of the specimen. It appears that the value of $c_p$ must be the same, whether measured on a pressed specimen, a powder, or a single crystal, provided only that large internal stresses do not exist. The absence of such stresses is indicated by the reproducibility of measurements made on successive traversals of the transition temperature, at which the material is plastic. The second is concerned with the identity of the two temperature scales employed. The fact that Simon and his co-workers found the maximum values of $c_p$ and $\alpha$ at the same temperature, 242.8°K, as that here found for the occurrence of the maximum values of $\kappa_s$, $\alpha$ and the coefficient of internal friction, and the minimum value of $E_s$, indicates that the two temperature scales coincide with a somewhat surprising precision.

Still a third question is concerned with the meaning of $c_v$ in connection with a pressed specimen whose density is less than that of a single crystal. The result of the isothermal measurements proves that there is, associated with a pressed specimen, a quantity which plays the role of $c_v$ in the (correct) description of the behavior of the specimen offered by Eq. (1). The question is, how much will the value of this quantity differ from that which would be obtained from measurements made on a single crystal? An answer is suggested by comparison of the preceding data with the result of a duplicate set of measurements made on a pressed specimen whose density, 1.512 g/cm³, differs from that of the first specimen, 1.520 g/cm³, by about the same amount that the latter differs from that of a single crystal. The values of $c_p - c_v$ obtained from both specimens are presented for comparison in Table IV. It will be noticed that the indicated difference between corresponding values of $c_v$ is not more than 1 cal./mol-deg., and is in the direction which would be expected, i.e.,

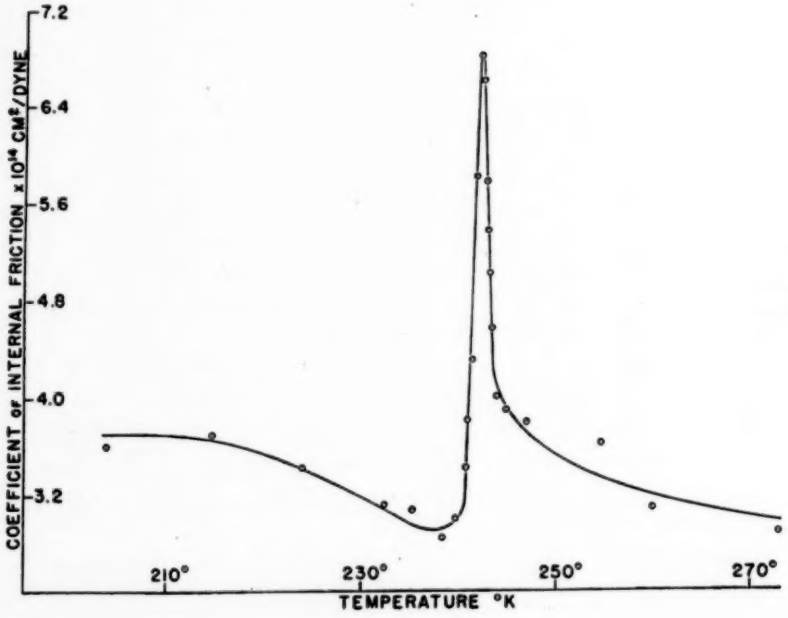


FIG. 8. Variation of the longitudinal internal friction with temperature in polycrystalline ammonium chloride.

$c_v$ is larger for the less dense specimen. It is therefore concluded that the maximum value of $c_v$ yielded by the denser specimen is, perhaps, one or two cal./mol-deg. larger than that which would be obtained from measurements made on a single crystal.

The uncertainty, mentioned above, in the values of $c_p$ immediately at and immediately above the transition temperature discourages an attempt to calculate $c_v$ in this interval. Indeed, unpublished data kindly supplied the writer by Dr. Ziegler of Johns Hopkins University[24] indicate that the values of $c_p$ plotted on the dotted portion of the curve of Fig. 9 may be appreciably too high. It may be remarked that experiments designed to resolve this uncertainty are now in progress in this laboratory.

Two significant observations are suggested by a scrutiny of Fig. 9. The first is the large difference between $c_p$ and $c_v$ near the transition. This requires that any theory, such as that of Fowler,[25] which offers a description of the temperature variation of $c_v$ through the transition must be compared with the observed variation of *this* quantity, and not, as has been done, with that of $c_p$.

The second concerns the value of $c_v$ just above the transition, which is 18 cal./mol-deg. Of this amount, 12 cal./mol-deg. represents energy associated with the normal vibrations of the ammonium chloride lattice, and the remaining

TABLE IV. *Values of $c_p - c_v$ obtained from measurements made on pressed specimens of different density; and the variation of $c_v$ with temperature through the transition in ammonium chloride.*

| T °K | $c_p - c_v$ CAL./MOL-DEG. $\rho = 1.512$ G/CM³ | $\rho = 1.520$ G/CM³ | $c_v$ CAL./MOL-DEG. $\rho = 1.520$ G/CM³ |
|---|---|---|---|
| 236.0 | 4.7 | 5.0 | 19.8 |
| 237.0 | 5.0 | 5.4 | 20.0 |
| 238.0 | 5.9 | 6.2 | 20.1 |
| 239.0 | 6.8 | 7.2 | 21.1 |
| 240.0 | 9.3 | 9.8 | 21.3 |
| 241.0 | 13.0 | 13.2 | 21.9 |
| 241.5 | 16.5 | 17.1 | 21.2 |
| 242.0 | 23.8 | 24.8 | 21.2 |
| 242.2 | 31.0 | 31.1 | 21.4 |
| 242.4 | 42.5 | 43.5 | 21.5 |
| 245.0 | 1.7 | 1.8 | 20.2 |
| 246.0 | 1.1 | 1.2 | 19.2 |

[24] These results were reported at the Boston meeting of the American Chemical Society, in September 1939.
[25] R. H. Fowler, Proc. Roy. Soc. **A149**, 1 (1935); T. S. Chang, Proc. Camb. Phil. Soc. **33**, 524 (1937).

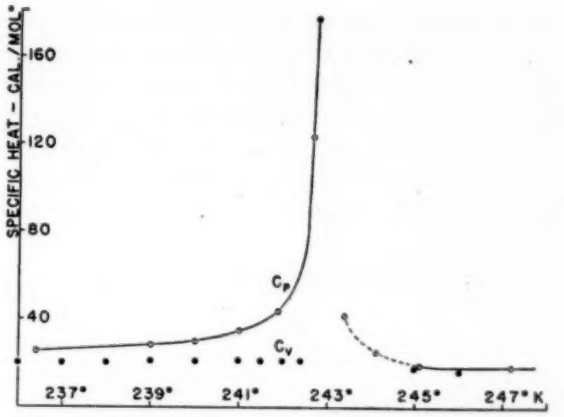


FIG. 9. The variation of $c_p$ and $c_v$ with temperature through the transition in polycrystalline ammonium chloride. The circles represent the data of Simon, von Simson and Ruheman.

6 cal./mol-deg. energy associated with the tetrahedral arrays of hydrogen atoms described at the beginning of this article. In accordance with classical statistical mechanics, the latter quantity is to be reckoned at the rate of 1 cal./mol-deg. for each quadratic term in the Lagrangian function of a tetrahedron, considered as a unit.[26] Now the theory of Fowler, cited in the preceding paragraph, is based upon the hypothesis, due to Pauling,[27] that at temperatures above the transition point the hydrogen tetrahedra rotate freely in the lattice, and that the inception of this free rotation is responsible for the phenomena here under review. This hypothesis, however, now seems untenable, since it implies a contribution, on the part of the tetrahedra, of three cal./mol-deg. to the specific heat instead of six.

Frenkel,[28] on the other hand, argues against the inception of free rotation at the transition on the ground that there is no supporting evidence for the implied concurrent weakening of the interatomic binding force. Frenkel's view is that the tetrahedra execute rotational *oscillations* both below and above the transition temperature; that below it there exists an order in the orientations of the axes about which the oscillations occur; that at the transition temperature this order is destroyed, so that above it the

[26] The energy associated with the internal degrees of freedom of the ammonium ion is inappreciable at the temperatures here contemplated.
[27] L. Pauling, Phys. Rev. **36**, 430 (1930).
[28] J. Frenkel, Acta Physicochemica **3**, 23 (1935).

orientations are irregularly distributed throughout the lattice and, furthermore, may change discontinuously from time to time. This model yields the correct contribution to $c_v$ above the transition and, in virtue of the cooperative nature of the phenomenon, accounts qualitatively for the higher value of $c_v$, *viz.* 22 cal./mol-deg., below it.

In conclusion the writer desires to acknowledge his indebtedness to Professor Krefeld and Mr. Kenyon, of the Department of Civil Engineering at Columbia University, for their cooperation and assistance in preparing the specimens; to Mr. Richard Scheib, for his constant aid in the construction and manipulation of the apparatus; and to Dr. S. L. Quimby, who followed the progress of the research with helpful counsel and encouragement.

---

MARCH 1, 1940 PHYSICAL REVIEW VOLUME 57

# Paramagnetic Relaxation Times for Titanium and Chrome Alum

J. H. VAN VLECK
*Harvard University, Cambridge, Massachusetts*

(Received December 26, 1939)

The relaxation times for spin-lattice coupling in titanium and chrome alum are computed on the basis of a specific model obtained by combining the thermodynamic theory of Casimir and du Pré with the writer's previous treatment of the normal modes of a cluster of the form $X \cdot 6H_2O$, where X contains an incomplete shell. The calculation includes both the first-order or direct processes important at low temperatures, and the second-order or "Raman" type of term predominant in the liquid-air region. There is no difficulty in understanding the observed absence of dispersion in titanium alum at liquid-air temperatures, but, barring crystal imperfections, it is hard to understand this absence at helium temperatures unless the nearest excited states are unreasonably deep. The agreement between the orders of magnitude of the calculated and experimental relaxation times is adequate in chromium both at high and low temperatures. The calculations predict, in agreement with experiments, that at liquid-air temperatures the relaxation time should increase when a constant field $H_0$ is applied and should be independent of the direction of $H_0$. The computed increase, however, is apparently not great enough. At helium temperatures, $\tau$ is theoretically not quite isotropic, and $d\tau/dH_0$ has the wrong sign, unless one abandons the usual formula $\rho_\omega \sim \omega^2$ for the density of lattice oscillators. The calculations on chromium should also apply qualitatively to iron alum, discussed at the very end.

## I. INTRODUCTION

A NOTEWORTHY series of experiments on magnetic absorption and dispersion in paramagnetic media at radio and lower frequencies have been performed within the last few years by Gorter and other Dutch physicists.[1] In solid bodies the spin and orbit are largely decoupled, and the magnetism results almost entirely from spin. At first sight, it may seem that, owing to this decoupling, the spin moment is a constant of the motion, and so does not undergo any of the oscillations prerequisite to absorption or dispersion. The constancy is, however, spoiled by "spin-spin coupling," i.e., interaction between the spins of different paramagnetic atoms, and also by a slight potential energy of alignment of spin relative to the crystal lattice which arises because the spin is never perfectly decoupled from the orbit, and so indirectly feels the influence of the crystalline Stark effect acting on the orbit. The measurements on absorption and dispersion are particularly instructive because of the light which they shed on (*a*) the relaxation time $\tau_s$ involved in spin-spin interaction and (*b*) that $\tau$ characteristic of the coupling between spin and lattice. The present paper is devoted to $\tau$ rather than $\tau_s$. Ordinarily $\tau_s$ is small compared to $\tau$ and is unimportant at the frequencies employed experimentally. The most elegant way of determining $\tau$ is furnished by the thermodynamic treatment of Casimir and du Pré,[2]

[1] See *Physica*, from 1936 on, or the dissertations of Brons and of Teunissen (Groningen, 1939).

[2] H. B. G. Casimir and F. K. du Pré, Physica **5**, 507; also especially Casimir, Physica **6**, 156 (1939).

the essence of which is as follows: If the impressed frequency $\omega$ is small compared with $1/\tau_s$, the spins are in thermodynamic equilibrium with each other so that it makes sense to talk of a "spin temperature" $T_s$. The latter, however, will not be the same as the lattice temperature if $\omega$ is comparable with, or larger than $1/\tau$. Obviously the magnetic susceptibility will be of the isothermal variety in the region $\omega \ll 1/\tau$, where spin and lattice are in equilibrium, but becomes adiabatic when $\omega \gg 1/\tau$. The critical transition region $\omega \sim 1/\tau$ is characterized by dispersion (cf. our later Eq. (27)) and by determining this region, $\tau$ can be evaluated experimentally.

The theoretical calculation of $\tau$ was begun by Waller.[3] He assumed that the lattice vibrations influence the spin only by modulating the spin-spin interaction, and as a result obtained relaxation times entirely too large to agree with experiment. Actually the modulations of the crystalline Stark effect are more important. Even so, however, the attempts of Heitler, Teller,[4] and Fierz[5] to include schematically the latter type of modulation still lead to estimates too large by a factor about $10^2$ to $10^4$.

There are two types of relaxation effects which affect $1/\tau$, and the results of previous calculations on both these contributions to $1/\tau$ have always been too small, even when fairly liberal allowance has been made for possible ambiguities in uncertain factors. One type, the only variety important at low temperatures, is that in which the spin system absorbs a quantum of energy from the lattice vibrations, or else imparts a quantum to the latter. This we shall call the "direct process," as it is the analog of simple absorption or emission in radiation theory. The second type, predominant at high temperatures, is that where the spin absorbs a quantum of one frequency, and scatters that of another. This we shall allude to as the Raman process, for it is similar to incoherent scattering in optics.

A further puzzle has been the fact that titanium alum empirically exhibits much shorter relaxation times than the usual (i.e., ferric or chrome) alums. In fact, the relaxation time $\tau$ for

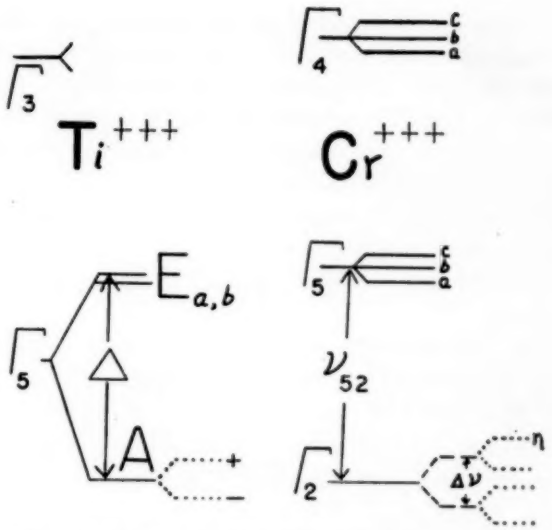


FIG. 1. Solid lines refer to orbital energy levels. States associated with the same $\Gamma$ index coincide in a strictly cubic field. The dashed lines show the incomplete decomposition of the spin structure of the basic orbital level by a trigonal crystalline field, and the dotted lines illustrate the complete resolution by an applied magnetic field. The diagram is obviously not to scale, for the trigonal splitting $\Delta$ is small compared with a cubic interval such as $\nu_{52}$, and the spin separations are very small compared with the orbital ones.

the titanium alum is so short that no dispersion at all can be detected in the frequency range so far employed experimentally, so that one can say that $\tau \leqq 10^{-3}$ sec. and $\tau \leqq 10^{-7}$ sec. at helium and liquid-air temperatures, respectively. The corresponding value for the ordinary alums are of the order $10^{-2}$ and $10^{-6}$. Now the ground level of titanium alum is only doubly degenerate, and so, in virtue of a well-known theorem of Kramers, cannot split in a crystalline field. Hence one might expect, at first sight, the lattice vibrations to be unable to modulate the crystalline Stark effect, and so not to influence the spin system except via the spin-spin interaction, which is too small. Thus one would anticipate that titanium should exhibit a very much longer, rather than shorter, relaxation time than the other alums.

However, as Kronig[6] has already pointed out, and as we have also found independently, the idea that titanium cannot interact with the lattice via the Stark effect is based on a misconception. Matrix elements due to this interaction do appear. They have the property of being proportional to the frequency $\omega$ of the energy

[3] I. Waller, Zeits. f. Physik **79**, 370 (1932).
[4] W. Heitler and E. Teller, Proc. Roy. Soc. **155**, 629 (1936).
[5] M. Fierz, Physica **5**, 433 (1938).
[6] R. de L. Kronig, Physica **6**, 33 (1939).

quantum exchanged between the spin and the lattice in the direct effect, and to the product of the incident and scattered frequencies in the Raman case. These elements are of the nonadiabatic nature, i.e., disappear in the limit $\omega=0$, and so there is no contradiction of Kramers' theorem. On the other hand, our calculations in Sections VI and VII show that the most important terms in chromium or iron are of the adiabatic variety.

In the present paper we shall give explicit calculations of the paramagnetic relaxation times of titanium and chrome alum as typical of ions in which the important effects are, respectively, nonadiabatic and adiabatic. Generally speaking, the nonadiabatic terms are insignificant, but they are abnormally strong in $Ti^{+++}$ because small frequency denominators are encountered in the perturbation calculation, because of the existence of low-lying excited levels. The latter are separated from the ground state in $Ti^{+++}$ only in virtue of the small, noncubic portion of the crystalline field, rather than by a large cubic splitting as in $Cr^{+++}$ (cf. Fig. 1).

The model which we use can be described as a combination of the thermodynamic theory of Casimir,[2] and the analysis which we made in a previous paper,[7] henceforth called l.c., of the Jahn-Teller effect in clusters of the form $X\cdot 6H_2O$. In the alums, the most important part of the crystalline potential exerted on the paramagnetic ion is doubtless that arising from the surrounding water molecules of coordination. So we are led to study the interaction between the magnetic moment of the paramagnetic ion and the normal vibrational coordinates (Fig. 2) of a complex $X\cdot 6H_2O$, as was done in the calculations of l.c. The latter were ostensibly in connection with the static paramagnetic susceptibility, but can be extended in a natural way to paramagnetic relaxation by expanding the normal coordinates in terms of the Debye elastic waves, as we shall do in Section II. As explained in l.c., the theory of the normal modes of vibration is quite different from the usual, standard classical variety when the complex contains a degenerate atom, as is the case with our paramagnetic ions with an odd number of electrons. Namely, a fundamental theorem of Jahn and Teller informs us that unless the degeneracy is lifted, the normal coordinates appear linearly rather than quadratically. It is only because of this linearity that the relaxation times are short enough to be important.

The calculations with a detailed model are of necessity somewhat long and involved, and cannot claim a high degree of accuracy, but still they do appear rather essential because purely schematic estimates, such as those of Heitler, Teller, Fierz, and Kronig are not at all reliable. Thus it proves that when the computations are made for chromium with an explicit model (Sections VI and VII) the calculated relaxation times are no longer larger than the observed values. On the other hand, the relaxation times yielded by our calculation for titanium at low temperatures (direct process, Section III) are larger by a factor $10^2$, for a given separation $\Delta$ in Fig. 1, than the provisional estimate of Kronig. At liquid-air temperatures (Raman process, Section IV) our computed relaxation times are a great deal smaller than Kronig's for the same $\Delta$, because his Raman matrix elements vanish in the limit $H=0$, whereas ours do not. This difference arises because his model was too simplified to exhibit the most general type of term. We find that there is no difficulty in understanding the absence of observed disperion in titanium alum at liquid-air temperatures, even if $\Delta$ is as large as $10^3$ cm$^{-1}$. Quite irrespective of the question of orders of magnitude, the calculations are of interest because they lead to certain general conclusions (Section VIII) regarding the dependence on the magnitude and direction of the applied magnetic field $H_0$ which do not depend on numerical values of the constants, and which furnish a rather interesting test of the thermodynamic model and the usual theory of lattice vibrations. Previous schematic estimates of the transition probability did not use the properties of the thermodynamic model explicitly enough to reveal the necessary relationships.

[7] J. H. Van Vleck, J. Chem. Phys. **7**, 72 (1939); referred to henceforth as l.c. The following typographical errata in this paper may be noted: Eq. (24) read $-C_1(d^3\,{}^4F)$ and $-C_2(d^3\,{}^4F)$ in place of $-C_1(d^2\,{}^4F)$ and $-C_2(d^3\,{}^2F)$, respectively; Table II, read $Q_4'$ in place of $Q_3$; Eq. (8), p. 64 of the article immediately preceding l.c., read $\cos 3(\beta_i-\beta_0)$ for $\cos(\beta_i-\beta_0)$.

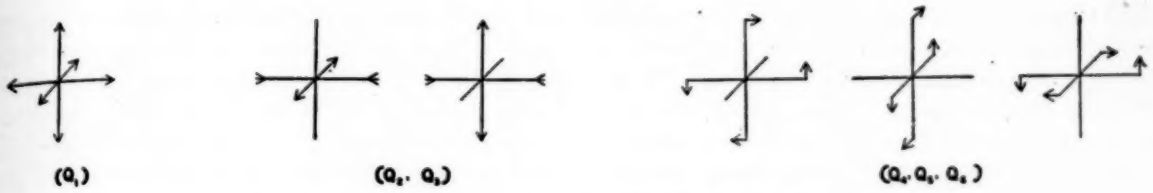


FIG. 2. Even modes of vibration of the complex $Ti \cdot 6H_2O$ or $Cr \cdot 6H_2O$.

## II. THE HAMILTONIAN FUNCTION FOR TITANIUM

Apart from modulations due to thermal vibrations, the crystalline field acting on a paramagnetic ion in the alums is of trigonal, but nearly cubic symmetry.[8] In titanium, unlike chromium, the calculation may be made by considering only those states which belong to the same orbital cubic representation $\Gamma_5$ as the ground level. Namely, nonvanishing elements of spin-orbit coupling are obtained by considering transitions merely internal to $\Gamma_5$, and so in comparison the effect of matrix elements nondiagonal in the cubic representation, which involve much higher frequencies, is unimportant. Thus only three orbital levels need to be considered, *viz.*, the nondegenerate ground state $\Gamma_5 A$, and the two components $a,b$ of the doubly degenerate excited state $\Gamma_5 E$, as shown in Fig. 1. We henceforth omit the index $\Gamma_5$, since it is common to all states under consideration. Superposed there are two possibilities for spin orientation denoted by subscripts $+$ and $-$ when they need to be distinguished. The Hamiltonian function may be written

$$\mathcal{H}=\mathcal{H}_O+\mathcal{H}_L+\mathcal{H}_Z+\mathcal{H}_{SO}+\mathcal{H}_{OL}+\mathcal{H}_{SS}. \tag{1}$$

Here $\mathcal{H}_O$ is the "Stark" energy of the orbit, regarded as completely decoupled from the spin. It arises from the crystalline potential exerted by the surrounding atoms at their equilibrium positions. $\mathcal{H}_L$ is the "lattice" energy, due to thermal motions of the atoms, or in other words the Debye waves. These oscillations may, to a sufficient approximation for our purposes, be regarded as simple harmonic. In our system of representation, both $\mathcal{H}_O$ and $\mathcal{H}_L$ are diagonal. Their characteristic values are, with the most convenient choice of origin (zero energy for $A$), respectively,

$$\mathcal{H}_O(A)=0, \quad \mathcal{H}_O(E_a)=\mathcal{H}_O(E_b)=h\Delta, \quad \mathcal{H}_L=\textstyle\sum_i k\omega_i(n_i+\frac{1}{2}), \tag{2}$$

where $n_i$ is the number of quanta associated with the $i$th mode of vibration, of frequency $\omega_i$.

The Zeeman energy $\mathcal{H}_Z$ plays a role in our calculations primarily in lifting the Kramers degeneracy. Without removal of the latter, there would be no energy to be exchanged with the lattice when the spin "turns over." We shall use a system of representation in which the spin is space quantized relative to the axis of the field $H$, which does not in general coincide with the trigonal axis. Then the part of $\mathcal{H}_Z$ due to spin is diagonal, and has the characteristic values

$$\mathcal{H}_Z(A_+)=\mathcal{H}_Z(E_+)=\beta H, \quad \mathcal{H}_Z(A_-)=\mathcal{H}_Z(E_-)=-\beta H. \quad (\beta=he/4\pi mc). \tag{3}$$

If there is no appreciable applied magnetic field, the Kramers degeneracy is lifted primarily by the spin-spin interaction

$$\mathcal{H}_{SS}=\textstyle\sum_i V_{ij}, \quad \text{with} \quad V_{ij}=4\beta^2\sum_i[\mathbf{S}_i\cdot\mathbf{S}_j-3r_{ij}^{-2}(\mathbf{S}_i\cdot\mathbf{r}_{ij})(\mathbf{S}_j\cdot\mathbf{r}_{ij})]r_{ij}^{-3}. \tag{4}$$

We shall neglect the modulation of the spin-spin energy by lattice vibrations. Although this modulation represents the type of spin-lattice coupling originally considered by Waller, it is now well recognized to be too small to be significant, and is much weaker than the spin-lattice interaction which we will obtain via the Stark effect. However, $\mathcal{H}_{SS}$ can still be of importance in lifting the Kramers degeneracy. For our purposes, as we will show more fully in Section VIII in connection with

[8] See x-ray data by H. C. Lipson and C. A. Beevers, Proc. Roy. Soc. **148**, 664 (1935).

the Temperley effect, it is adequate to use Kronig and Bouwkamp's[9] approximation of regarding the spin-spin interaction as equivalent to a random magnetic field whose intensity is distributed according to the Gaussian law. We therefore henceforth drop $\mathcal{H}_{SS}$ from the Hamiltonian function, and interpret $H$ in the Zeeman energy, not as merely the external magnetic field, but rather as the vector resultant of the applied field $H_0$, and the internal field due to spin-spin interaction. The applied static field $H_0$ is not to be confused with the much weaker, radiofrequency field which is used to measure the alternating susceptibility or dispersion.

The term $\mathcal{H}_{SO}$ in the Hamiltonian function is the spin-orbit energy $\zeta L\cdot S$. Its matrix elements are

$$\begin{gathered}\mathcal{H}_{SO}(E_{a\pm};E_{b\pm})=\pm\tfrac{1}{2}i\zeta l_{xx'},\quad \mathcal{H}_{SO}(A_{\pm};E_{a\pm})=\pm\tfrac{1}{2}i\zeta l_{yx'},\quad \mathcal{H}_{SO}(A_{\pm};E_{b\pm})=\pm\tfrac{1}{2}i\zeta l_{zx'},\\ \mathcal{H}_{SO}(E_{a\pm};E_{b\mp})=\tfrac{1}{2}i\zeta(l_{zx'}\pm il_{xy'}),\quad \mathcal{H}_{SO}(A_{\pm};E_{a\mp})=\tfrac{1}{2}i\zeta(l_{yx'}\pm il_{yy'}),\\ \mathcal{H}_{SO}(A_{\pm};E_{b\mp})=\tfrac{1}{2}i\zeta(l_{zx'}\pm il_{xy'}).\end{gathered}\tag{5}$$

Here the $l$'s are the direction cosines connecting two sets of axes $x,y,z$ and $x',y',z'$ such that the trigonal axis is along $z$ and $H$ is along the $z'$ axis. Only nonvanishing elements are written out. Elements in which all the initial and final indices are interchanged can be obtained from the Hermitian property. The result (5) can be obtained by noting that matrix elements of spin angular momentum are of the usual Pauli type referred to the $x',y',z'$ axes, while those of the orbital angular momentum $L$ can be obtained by using wave functions as given in Eqs. (20) and (21) of l.c. With proper orientation of the $x,y$ axes one has $L_z(E_a;E_b)=L_y(A;E_a)=L_x(A;E_b)=i$. Corresponding to these matrix elements, there are also off-diagonal elements of the Zeeman energy which arise entirely from the orbital moment, and which have the values

$$\mathcal{H}_z(E_{a\pm};E_{b\pm})=i\beta Hl_{zx'},\quad \mathcal{H}_z(A_{\pm};E_{a\pm})=i\beta Hl_{yx'},\quad \mathcal{H}_z(A_{\pm};E_{b\pm})=i\beta Hl_{zx'}.\tag{6}$$

The portion $\mathcal{H}_{OL}$ of (1) is that which gives the orbit-lattice coupling, and arises from modulation of the crystalline Stark effect by the elastic waves. The great bulk of the Stark splitting comes from the fields due to the nearby water molecules of coordination. The thermal vibrations cause these molecules to be instantaneously nearer or more remote from the paramagnetic cation than at their equilibrium positions, and so cause oscillations in the Stark pattern. Now the vibrations of a complex of the form $\mathbf{X}\cdot 6\mathrm{H_2O}$ are conveniently specified by a set of normal coordinates $Q_1$, $Q_2$, $Q_3$, $Q_4$, $Q_5$, $Q_6$ or $Q_1$, $Q_2$, $Q_3$, $Q_4'$, $Q_5'$, $Q_6'$ described in detail in l.c. so that their definitions need not be repeated here. The quantities $Q_4',Q_5',Q_6'$ are linear combinations of the vibrations $Q_4,Q_5,Q_6$ shown in Fig. 2. There are also other coordinates $Q_7,\cdots,Q_{21}$ but they appear only quadratically and so do not concern us. Because of the Jahn-Teller effect there are matrix elements of the crystalline potential linear in $Q_2,\cdots,Q_6$. These elements are found in Eq. (25) of l.c. to be

$$\begin{gathered}\mathcal{H}_{OL}(A_{\pm};E_{a\pm})=\sqrt{6}aQ_3+\tfrac{1}{3}\sqrt{3}bQ_6',\quad \mathcal{H}_{OL}(A_{\pm};E_{b\pm})=-\sqrt{6}aQ_2+\tfrac{1}{3}\sqrt{3}bQ_5',\\ \mathcal{H}_{OL}(E_{a\pm};E_{b\pm})=\sqrt{3}aQ_2+\sqrt{\tfrac{2}{3}}bQ_5',\quad \mathcal{H}_{OL}(E_{a\pm};E_{a\pm})=\sqrt{3}aQ_3-\sqrt{\tfrac{2}{3}}bQ_6'-\sqrt{\tfrac{1}{3}}bQ_4',\\ \mathcal{H}_{OL}(E_{b\pm};E_{b\pm})=-\sqrt{3}aQ_3+\sqrt{\tfrac{2}{3}}bQ_6'-\sqrt{\tfrac{1}{3}}bQ_4',\quad H_{OL}(A_{\pm};A_{\pm})=2\sqrt{\tfrac{1}{3}}bQ_4'\end{gathered}\tag{7}$$

with $$a=3\rho_1{}^0/7-25\rho_2{}^0/63,\quad b=-6\rho_1{}^0/7+10\rho_2{}^0/21,\quad \rho_1{}^0=-4e\mu\overline{r_0{}^2}R^{-5},\quad \rho_2{}^0=-6e\mu\overline{r_0{}^4}R^{-7}.\tag{8}$$

Here the bars over $r^2$ and $r^4$ denote, respectively, the mean square and mean fourth power radius of the electron orbit, and $R$ denotes the equilibrium distance from the cation to any one of the six water molecules. The latter, in our model, each have a dipole moment $\mu$ which we suppose radially directed and which we regard as responsible for the crystalline field. The results of our calculation would not be significantly modified if a point charge instead of dipole field were used.

The $Q$'s will continually oscillate due to the thermal motions of the lattice. They are thus in turn

[9] R. de L. Kronig and C. J. Bouwkamp, Physica **5**, 521 (1938).

to be regarded as linear functions of the normal coordinates $q_i$ associated with the lattice heat waves so that

$$Q_k=\sum_i a_{ki}q_i. \tag{9}$$

It is clearly to be understood that there are $3N$ coordinates $q_i$, where $N$ is the number of atoms in the entire crystal, whereas there are only a small number of $Q$'s, since the $Q$'s are coordinates merely for the cluster $Ti\cdot 6H_2O$.

If the $x_k$, $y_k$, $z_k$ be the Cartesian coordinates of a water molecule, with equilibrium values $x_k^0$, $y_k^0$, $z_k^0$ then $x_k$, for instance, depends on any given thermal mode $i$ of vibration in the form

$$x_k-x_k^0=q_i\Phi_{xi}\cos(\gamma_{ki}-\delta_i),\quad \gamma_{ki}=2\pi\omega(\lambda_{xi}x_k^0+\lambda_{yi}y_k^0+\lambda_{zi}z_k^0)/v_i. \tag{10}$$

Here $q_i$ and $\Phi_{xi}$, $\Phi_{yi}$, $\Phi_{zi}$ are the direction cosines of the amplitude of the wave $q_i$ while $v_i$ and $\lambda_{xi}$, $\lambda_{yi}$, $\lambda_{zi}$ are its velocity, and the cosines specifying its direction of polarization. We shall suppose that the wave-length of the lattice vibration is large compared with the cluster's cross section $2R$ so that we can take

$$\cos(\gamma_{ki}-\delta_i)=\cos\delta_i+\gamma_{ki}\sin\delta_i. \tag{11}$$

This approximation is amply warranted in the calculations at helium temperatures, where the "direct process" is important. On the other hand, it must be kept in mind that at higher (i.e., liquid air) temperatures, where the Raman mechanism comes in, the most important frequencies are those near the high frequency "cut-off," of the Debye spectrum. These have wave-lengths of the order $10^{-7}$ cm, so that $\gamma_{ki}$ is of the order unity ($2\pi R$ is about $1.2\times10^{-7}$ cm). Using (10) (11), and the formulas of l.c. expressing the normal coordinates $Q_k$ in terms of the $x,y,z$, we find that the coefficients $a_{ki}$ in (9) have the following values

$$\begin{aligned}
a_{2i}&=U(\lambda_{xi}\Phi_{xi}-\lambda_{yi}\Phi_{yi}),\quad a_{3i}=U(\lambda_{xi}\Phi_{xi}+\lambda_{yi}\Phi_{yi}-2\lambda_{zi}\Phi_{zi})/\sqrt{3},\\
a_{4i}'&=U(\lambda_{xi}\Phi_{yi}+\lambda_{yi}\Phi_{xi}+\lambda_{xi}\Phi_{xi}+\lambda_{xi}\Phi_{zi}+\lambda_{yi}\Phi_{zi}+\lambda_{zi}\Phi_{yi})/\sqrt{3},\\
a_{5i}'&=U(\lambda_{xi}\Phi_{zi}+\lambda_{zi}\Phi_{xi}-\lambda_{yi}\Phi_{zi}-\lambda_{zi}\Phi_{yi})/\sqrt{2},\\
a_{6i}'&=U(\lambda_{xi}\Phi_{zi}+\lambda_{zi}\Phi_{xi}+\lambda_{yi}\Phi_{zi}+\lambda_{zi}\Phi_{yi}-2\lambda_{yi}\Phi_{xi}-2\lambda_{xi}\Phi_{yi})/\sqrt{6},
\end{aligned} \tag{12}$$

with

$$U=(2\pi R\omega_i/v_i)\sin\delta_i. \tag{13}$$

The matrix elements of the lattice coordinates $q_i$ are given by the harmonic oscillator expression

$$q_i(n_i;n_i+1)=q_i(n_i+1;n_i)=[h(n_i+1)/4\pi^2M\omega_i]^{\frac{1}{2}}, \tag{14}$$

where $M$ is the total mass of the crystal, due, of course, largely to atoms other than titanium. This formula contains a factor 4 rather than the customary 8 in the denominator, because not all the atoms of the crystal are located at antinodes, and so do not share in the full amplitude of vibration.

It must be cautioned that (14) is not a particularly good approximation, perhaps the weakest link in our whole calculation. It assumes that the amplitude of vibration is the same for all varieties of atoms in the crystal, regardless of their mass, whereas actually the heavy atoms have smaller, the lighter larger, motions than average.

## III. Calculation of Direct Processes for Titanium

We now make a perturbation calculation, regarding the crystalline Stark potential, the lattice vibrations, and the spin part of the Zeeman energy as incorporated in the original Hamiltonian function, and the spin-orbit and orbit-lattice couplings as together constituting the perturbation. When the calculation is carried out to the second order, it turns out that the new or transformed Hamiltonian function will contain elements of the desired type $\mathcal{H}(A_{\pm}n_i;A_{\mp}n_i+1)$ in which the spin

"turns over" and the lattice vibration simultaneously changes by one quantum unit. The appropriate perturbation formula[10] is

$$\mathcal{H}_{\text{new}}(ii') = \sum_k [\mathcal{H}(ik)\mathcal{H}(ki')/h\nu(ik)]. \tag{15}$$

The frequency denominators in (15), represent, as usual, the change in the diagonal part of the energy, which is the sum of (1), (2), and (3). The conservation of energy, requires that $W(i) = W(i')$. One of the $\mathcal{H}$ factors in the right side of (15) is to be taken as coming from $\mathcal{H}_{OL}$, and the other from $\mathcal{H}_{SO}$, since clearly it is only by superposition of spin-orbit and orbit-lattice coupling that we will obtain the desired final spin-lattice coupling. There are two types of terms, in which $\mathcal{H}_{OL}$ and $\mathcal{H}_{SO}$ are, respectively, the first and second $\mathcal{H}$ factors, and vice versa. These two types of terms very nearly cancel because by (5) and the Hermitian property any element of $\mathcal{H}_{SO}$ changes sign when one makes the interchange of initial and final indices involved in reversing the order of $\mathcal{H}_{SO}$ and $\mathcal{H}_{OL}$. A corresponding sign change does not occur in $\mathcal{H}_{OL}$. The compensation of terms due to the two possible orderings would be complete were it not that the Zeeman energy makes the energy of the appropriate intermediate state slightly different in the two cases. Obviously Kramers' theorem requires complete compensation unless $H \neq 0$. Thus

$$\begin{aligned}\mathcal{H}_{\text{new}}(A_+n_i;A_-n_i+1) &= \sum_{\alpha=\alpha,b}\left\{\frac{\mathcal{H}_{SO}(A_+;E_\alpha-)\mathcal{H}_{OL}(E_\alpha n_i;An_i+1)}{-h(\Delta-2H\beta)}+\frac{\mathcal{H}_{OL}(An_i;E_\alpha n_i+1)\mathcal{H}_{SO}(E_{\alpha+};A_-)}{-h(\Delta+2H\beta)}\right\}\\ &= -4\beta H h^{-1}\Delta^{-1}\sum_{\alpha=\alpha,\beta}\mathcal{H}_{SO}(A_+;E_\alpha-)\mathcal{H}_{OL}(E_\alpha n_i;An_i+1).\end{aligned} \tag{16}$$

Here we have made use of the fact that $2\beta H$ can be regarded as very small compared with the Stark splitting $\Delta$, and that the conservation of energy demands that the change $h\omega$ in lattice energy just counterbalance that $2\beta H$ in Zeeman energy.

Equations (15) and (16), as we have used them, do not allow for the effect of the orbital Zeeman energy (6). Actually, the latter leads to terms coordinate in importance with (16). These terms are to be computed by adding to (15) the expression

$$\mathcal{H}_{\text{new}}(ii') = \sum_{j,k}[\mathcal{H}(ij)\mathcal{H}(jk)\mathcal{H}(ki')/h\nu(ij)h\nu(ik)], \tag{17}$$

where one $\mathcal{H}$ factor is to be taken from the spin-orbit energy (5), another from the orbit-lattice coupling (7), and the remaining factor from the interaction energy (6) of the orbital moment with the magnetic field $H$. Formula (17) can give results coordinate in order of magnitude with (15) because in (17) nonvanishing contributions can be obtained without considering the modulation of the frequency denominators by the magnetic field or the lattice vibrations.

By standard perturbation theory, the probability that an atom in the state $A_+$ reverse its spin and pass to $A_-$, exciting a quantum of vibration to the lattice is

$$A_{+\to-} = (4\pi^2/h^2)\langle \rho_\omega \,|\, \mathcal{H}_{\text{new}}(A_+n_i;A_-n_i+1)\,|^2\rangle_{\text{Av}}. \tag{18}$$

Here the average is over all directions of propagation and polarization of the oscillators, as well as over all values of the quantum number $n_i$. The expression $\rho_\omega$ is the oscillator density relative to frequency, and is to be evaluated at $\omega = 2\beta H$. By a well-known formula, the values of $\rho_\omega$ for longitudinal and transverse waves are, respectively,

$$\rho_{\omega l} = 4\pi\omega^2 V/v_l^3, \quad \rho_{\omega t} = 8\pi\omega^2 V/v_t^3, \tag{19}$$

where $v_l$ and $v_t$ are, respectively, the velocities for longitudinal and transverse waves, while $V$ is the volume of the crystal. We have now to compute the explicit value of (16) by means of (5–14),

[10] Cf., for instance, W. Heitler, *The Quantum Theory of Radiation*, p. 90, Eq. (43b).

and perform the averaging in (18). In connection with the latter, we utilize the fact that

$$\langle n_i\rangle_{Av}=1/(1-e^{-h\omega/kT}), \tag{20}$$

$$\langle\lambda_{qi}{}^2\Phi_{qi}{}^2\rangle_{Av}=1/5,\quad \langle\lambda_{qi}{}^2\Phi_{pi}{}^2\rangle_{Av}=\langle\lambda_{qi}\Phi_{qi}\lambda_{pi}\Phi_{pi}\rangle_{Av}=1/15 \text{ (longitudinal waves)}$$
$$\langle\lambda_{qi}{}^2\Phi_{qi}{}^2\rangle_{Av}=1/15,\quad \langle\lambda_{qi}\Phi_{qi}\lambda_{pi}\Phi_{pi}\rangle_{Av}=-1/30,\quad \langle\lambda_{qi}{}^2\Phi_{pi}{}^2\rangle_{Av}=2/15 \text{ (transverse)}(p,q=x,y,z;p\neq q). \tag{21}$$

Averages of products analogous to the above, but involving three different subscripts, are zero. The work of averaging is considerably shortened by noting that the average of cross product terms in the normal coordinates, such as $Q_2Q_3$, is zero; this follows from the orthogonality of our normal coordinates, as well as from explicit computation by (12). Hence the relaxations due to the different normal modes of vibration of the surrounding water cluster can be regarded as taking place independently. For every given wave there is also another wave which stands in a reciprocal relation as regards the position of nodes and antinodes. Thus, the effective mean value of $\sin^2\delta_l$ is $\frac{1}{2}$. In consequence of this fact and of (21), one finds that the average squares of the coefficients (12) are

$$\langle a_{2i}{}^2\rangle_{Av}=\cdots=\langle a_{6i}{}'^2\rangle_{Av}=(8\pi^2R^2\omega_i{}^2/15v_l{}^2)\text{(longitudinal)},\quad =(6\pi^2R^2\omega_i{}^2/15v_l{}^2)\text{(transverse)}. \tag{22}$$

It is also necessary to average over the four possible directions for the trigonal axis, related to each other as are the four body-diagonals of a cube, for in the alums there are these four different types of surroundings for a paramagnetic ion, so that all told there is cubic macroscopic symmetry.[8] Because of the latter, we may equate to $\frac{1}{3}$ the square of any direction cosine, while cross-products such as $\lambda_{xi}\lambda_{yi}$ etc. drop out. Were only the spin portion (3) of the Zeeman energy retained, only these easily averaged quadratic forms would be encountered, but when the orbital part (6) is included, the expression for the transition probability involves biquadratic expressions in the direction cosines, for which the averaging is somewhat more complicated. We finally find

$$A_{+\rightarrow-}=(1+\epsilon_1+5\epsilon_2 w)\beta H^5Be^{h\omega/kT}/(e^{h\omega/kT}-1),\quad (\omega=2\beta H) \tag{23}$$

with
$$B=\frac{2}{3}\left(\frac{16\pi^3V}{hM}\right)\frac{R^2\zeta^2}{h^4\Delta^4}\left[\frac{8}{5}a^2+\frac{4}{45}b^2\right]2^5h^{-3}\beta^4\left[\frac{1}{v_l{}^5}+\frac{3}{2v_l{}^5}\right], \tag{24}$$

$$w=m_1{}^2m_2{}^2+m_1{}^2m_3{}^2+m_2{}^2m_3{}^2,\quad \epsilon_1=(144a^2+56b^2)/(864a^2+48b^2),$$
$$5\epsilon_2=(252a^2-10b^2)/(864a^2+48b^2). \tag{25}$$

Here $m_1,m_2,m_3$ denote the direction cosines of the magnetic field relative to the principal cubic axes of the alum, and consequently the $\epsilon_2$ term gives a dependence of the relaxation on the direction of the applied field. If the orbital Zeeman energy (6) were omitted, the expressions $\epsilon_1,\epsilon_2$ would be zero.

It is customary to say that $A_{+\rightarrow-}$ is of the order of the relaxation time due to transfer of energy between spin and lattice. However, the very beautiful thermodynamic treatment of Casimir and du Pré[2] gives us a more exact view of things. They assume that the spin system has a temperature $T_S$ which is not the same as that $T$ of the lattice. The specific heat $C_H$ of the spin portion at constant applied field $H_0$, is of the form[2]

$$C_H=[b'+C'H_0{}^2]/T_S{}^2\quad\text{with}\quad C'=4N\beta^2\cdot\tfrac{1}{3}S(S+1). \tag{26}$$

It is supposed that the spin specific heat is very small compared with that of the container, an assumption warranted at helium temperatures only if the specimen is in contact with a constant temperature bath, for the specific heat of the lattice proper is very small at low temperatures because of the Debye $T^3$ law. Fortunately such contact appears to be present in the usual experiments. The heat flow from spin to lattice is taken to be $\alpha(T_S-T)$, in other words proportional to the difference between the spin and lattice temperatures. Casimir and du Pré[2] show that the relation between the

static susceptibility $\chi_0$ and that $\chi_\nu$ appropriate to a frequency $\nu$ is

$$\chi_\nu=\chi_0(1-F)+[\chi_0 F/(1+4\pi^2\tau^2\nu^2)], \quad \text{with} \quad \tau=C_H/\alpha, \quad F=C'H_0^2/(b'+C'H_0^2). \tag{27}$$

The relaxation time $\tau$ is thus the ratio of the spin specific heat $C_H$ to the conductivity constant $\alpha$ governing the heat flow between spin and lattice.

The rate of transfer of heat from the spin to the lattice is

$$dQ/dt=2\beta H[N_1A_{+\to-}-N_{-1}A_{-\to+}], \tag{28}$$

where $N_{M_S}$ is the number of atoms with spatial spin quantum number $M_S$. The relation connecting $N_{M_S}$ with the spin temperature $T_S$ is

$$N_{M_S}=Ne^{-2\beta HM_S/kT_S}/[e^{2\beta HS/kT_S}+\cdots+e^{-2\beta HS/kT_S}]\sim Ne^{-2\beta HM_S/kT_S}/(2S+1), \tag{29}$$

where for present purposes we can put $S=\frac{1}{2}$, but we give (29) in a general form so that it can later be used in chromium.

The expression for $A_{-\to+}$ is identical with that (23) for $A_{+\to-}$, except that the factor $e^{h\omega/kT}$ is missing from the numerator, to allow for the fact that the Boltzmann factor is different for an upper than for a lower state of a lattice oscillator. Since $\beta H/kT=\frac{1}{2}h\omega/kT$ is small, we may replace the denominator of (20) by $2\beta H/kT$, and we see that

$$\alpha=\lim_{T_S\to T}[(T_S-T)^{-1}dQ/dt]=(1+\epsilon_1+5\epsilon_2 w)BNH^6\beta^2/T. \tag{30}$$

The final expression must be averaged with respect to the field $H$, which is the resultant of the applied field $H_0$ and the apparent field due to spin-spin interaction. The latter we suppose distributed according to the Gaussian law, so that the probability for instance, that the $x$ component of $H$ falls in the interval $H$, $H+dH$ is $(6/\pi K^2)^{\frac{1}{2}}\exp[-3(H_x-H_{0x})^2/2K^2]dH$. Here $K$ denotes the mean square resultant spin-spin field, inclusive of $x$,$y$, and $z$ components. By appropriate adaptation of the formulas of Kronig and Bouwkamp,[9] one finds that[11]

$$K^2=2g^2\beta^2S(S+1)\textstyle\sum_j r_{ij}^{-6}=[4\beta^2S(S+1)][28.8/r_0^6], \tag{31}$$

where $r_0=2^{1/6}N^{-1/3}$ is the distance between titanium atoms which are nearest neighbors. The same expression can also be obtained in somewhat more quantum-mechanical fashion by using matrix algebra, along lines given by Waller.[3] The numerical value of $K$ given by (31) for titanium alum is 130 gauss.

The term $b'$ in the specific heat (26) is in the case of titanium due entirely to the spin-spin interaction, and can be computed accurately.[12] Its value is $b'=\frac{1}{2}NK^2\beta^2$. As we might conjecture, the resulting formula for $C_H$ is the same as that which would be obtained by setting $b'=0$, and replacing $H_0^2$ by $H_0^2+\frac{1}{2}K^2$ in (26), i.e., by taking the effective square of the field as the sum of the true square of the applied field $H_0$ and half the mean square spin-spin field. The factor $\frac{1}{2}$ arises in connection with the latter because spin-spin interaction represents mutual energy.

When one utilizes (26) and (30), and performs the Gaussian averaging explained above, one finds that the formula for the relaxation time $\tau=C_H/\alpha$ becomes[13]

$$\tau=\frac{H_0^2+\frac{1}{2}K^2}{kTB[(1+\epsilon_1+5\epsilon_2 w_0)H_0^6+\frac{1}{3}(21+21\epsilon_1+10\epsilon_2+55\epsilon_2 w_0)H_0^4K^2+(35/3)(1+\epsilon_1+\epsilon_2)H_0^2K^4+(35/9)(1+\epsilon_1+\epsilon_2)K^6]} \tag{32}$$

[11] Our value of $K^2$ is, however, larger by a factor $3(S+1)/S$ than the corresponding mean square field of Kronig and Bouwkamp, reference 9, since one should use the quantal rather than classical square of the moment, and since we are dealing with the sum of the squares of the $x$, $y$, and $z$ components.

[12] I. Waller, Zeits. f. Physik **104**, 132 (1936); J. H. Van Vleck, J. Chem. Physics **5**, 320 (1937); M. H. Hebb and E. M. Purcell, *ibid.* **5**, 338 (1937).

[13] If $K=0$, one can show that the expression $\tau$ given by (32), (or later by Eq. (43) for the Raman process) satisfies the relation $1/\tau=2\langle A_{+\to-}\rangle_{Av}$ proposed by Gorter and Kronig (Physica **3**, 1009 (1936)). With $K\neq0$, however, the proportionality factor ceases to be 2. This fact is not surprising, as with $K\neq0$, the spins interact with each other, and their postulate that equilibrium is secured solely by contact with a thermostat (lattice) no longer applies.

where $w_0$ is similar to the expression $w$ defined in (25) except that the direction cosines now relate to the applied field $H_0$ rather than to the total effective field $H$. Usually measurements are made on a powder, and then $w_0$ can obviously be replaced by its mean value $\frac{1}{3}$. The values of $\epsilon_1,\epsilon_2$ are, respectively, 0.66 and 0.01, so that the correction for the orbital Zeeman effect, represented by the $\epsilon_1,\epsilon_2$ terms makes $\tau$ about three-fifths as large as it would be otherwise. Since $\epsilon_2$ is so small, the anisotropy coming from the $w_0$ terms is negligible even for a single crystal, amounting to only about one percent and with existing experimental accuracy $\tau$ should be independent of direction.

To evaluate (8), (24), and (32) numerically we use the following values of the constants

$$\begin{gathered} R=2\times10^{-8}\ \text{cm}^{-1},\quad \rho_1{}^0R=14{,}400\ \text{cm}^{-1},\quad \rho_2{}^0R=10{,}800\ \text{cm}^{-1},\\ M/V=2.0,\quad \Delta=1000\ \text{cm}^{-1},\quad \zeta=154\ \text{cm}^{-1},\quad v_l=v_t=2.3\times10^5\ \text{cm/sec}. \end{gathered} \tag{33}$$

The values of $R$ and $M/V$ (the density) are furnished directly by the crystalline dimensions, while $\zeta$ is known from spectroscopy. The above determinations of $\rho_1{}^0$, $\rho_2{}^0$ and $\Delta$, based partly on empirical Stark splittings and partly on an explicit model treating the field from the water molecules as of dipole character, are fully explained in l.c.[7] or elsewhere.[14] Our calculations are not so refined that it is worth while to try and distinguish between the longitudinal and transverse velocities of sound. Instead we shall use an affective common velocity $v=2.3\times10^5$ cm/sec., which is that given by specific heat data[15] when the effect of the two types of waves is not resolved. Actually the longitudinal velocity may be almost double the transverse one, but the error is not as serious as it would seem, since both in specific heats and in our relaxation calculations by far the greater weight is attached to the transverse waves, so that the effective common velocity is nearly the same as $v_t$. This is true not merely because the transverse vibrations are twice as numerous as the longitudinal, but also because the transverse velocity is lower and weighted according to a fairly high inverse power. Namely the specific heat formulas involve the inverse cube of $v$, while our expression (23–4) for the transition probability contains the inverse fifth power. (The inverse tenth occurs in our corresponding later formula (38) for Raman processes.) The lumping together of the two varieties of sound velocities would not be an adequate approximation if the longitudinal vibrations were appreciably more effective in modulating the Stark effect than are transverse disturbances of the same velocity and amplitude. Our explicit calculations indicate that fortunately this is not the case; contrary to Heitler and Teller's conjecture[4] that only the longitudinal waves would be important.

The values of $\tau$ computed from (32) with the aid of (33) are, $5\times10^4$, $1.7\times10^2$, and $1.8\times10^{-2}$ sec., respectively, for applied fields $H_0$ of intensity 0, $10^3$, and $10^4$ gauss at a temperature $T$ of 1.2 degrees. The agreement with experiment is miserable. The absence of any observed dispersion in the Leiden experiments[16] on titanium alum at helium temperatures shows that $\tau$ cannot possibly exceed $10^{-3}$ sec. for a range of field strengths about 100 to 2000 gauss. Our estimate of the relaxation time in fields of 1000 gauss is greater than Kronig's by a factor $10^4$. Out of the $10^4$, about $10^2$ is due to his use of an interval $\Delta$ one-third of ours, while the remaining $10^2$ is due to his estimating the matrix elements of $\mathfrak{IC}$ by rough considerations of orders of magnitude rather than with a model.

It appears impossible to eliminate the tremendous discrepancy between our results and the experimental data unless (*a*) the frequency distribution law (19) for the lattice waves is grossly in

[14] The value of $\Delta$ was calculated, in a paper immediately preceding l.c. (J. Chem. Phys. **7**, 61 (1939)) and was found to be 1450 cm$^{-1}$. This preceding article was unfortunately marred by an error, because its Eq. (14) did not include the contribution of the off-diagonal elements (47) of the present article to the splitting $\Delta\nu$ of the basic state of chromium. Further modification results from the fact that according to the recent measurements of Bleaney, reference 18, the splitting $\Delta\nu$ has the value 0.17 cm$^{-1}$ in place of the primitive estimate 0.12 of Hebb and Purcell previously employed. When both corrections are taken into account, it is found that the amount of distortion of the water octohedron necessary to explain the observed $\Delta\nu$ is about a quarter as great as previously calculated and the calculated splittings for vanadium and titanium become, respectively, 545 and 1075 cm$^{-1}$. At best only qualitative significance should be attached to this calculation, so we use the round value $\Delta=1000$ cm$^{-1}$. The revised estimate for vanadium raises difficulties, as it is questionable whether the trigonal symmetry of the deepest state of the cluster $V\cdot6H_2O$ is sufficiently stabilized.

[15] Casimir, de Haas and de Klerk, Physica **6**, 241 (1939).

[16] W. J. de Haas and F. K. du Pré, Physica **5**, 969 (1938).

error or, (*b*) the Stark splitting is considerably smaller than the value $10^3$ cm$^{-1}$ assumed in (33). The possibility of (*a*) will be discussed in Section VIII. As regards (*b*), since $\Delta$ enters in the inverse fourth power in (24), our estimates of $\tau$ would be lowered by a factor $10^{-4}$ if the assumed value of $\Delta$ were reduced by a factor 10 to 100 cm$^{-1}$. Such a drastic change in $\Delta$ presents difficulties. Some calculations by the writer[14] indicate that it is very difficult to find a reasonable crystalline potential which will reconcile a $\Delta$ of only 100 or 200 cm$^{-1}$ in titanium with the splitting of 700 cm$^{-1}$ in vanadium alum demanded by Siegert's theory of the magnetic behavior of $V^{+++}$, or with the behavior of the energy levels of $Cr^{+++}$ indicated by adiabatic demagnetization data.

It should be mentioned that the reliability of the existing Leiden data, for titanium alum, is perhaps not beyond question, since, I am told, the crystals may have lost some of their water of hydration. The dehydration is doubtless insufficient to lower the density anything like enough to make exchange forces important, but, as mentioned to the writer by Dr. van den Handel, might warp the crystal so that it no longer has the ideal structure assumed in our calculation. The distortion could scarcely materially lower the interval $\Delta$ for all atoms, but fluctuations in the field due to the imperfection might cause an appreciable number of atoms to have values of $\Delta$ nearly zero, and so a large coupling to the lattice, as well as deviations from Curie's law could be obtained. This explanation seems rather fantastic, but further experimental work will be awaited with interest, especially since at present different specimens yield somewhat divergent results.

If the interval $\Delta$ is reduced to 100 cm$^{-1}$, or so, as appears necessary if the existing relaxation measurements are correct and the discrepancy is to be blamed on $\Delta$, then the Raman terms become more important than the direct processes even at helium temperatures. We therefore proceed to examine the Raman mechanism. We shall see that it accounts nicely for the experimental results at liquid-air temperatures even if $\Delta$ is not reduced below $10^3$ cm$^{-1}$.

## IV. Calculation of Raman Processes for Titanium

In order to obtain transitions in which one lattice quantum is absorbed, and another emitted, we must compute the new Hamiltonian function by means of (17), taking two of the $\mathcal{H}$ factors in (17) to represent orbit-lattice coupling (7), and the other of the spin-orbit type (5). The frequency denominators $\nu$ are to be considered as representing the combined change in the orbital Stark energy levels and in the lattice vibrational energy. In the present computation, unlike that for the direct processes, the spin-spin and Zeeman contributions to the frequency $\nu$ may be disregarded. Consequently the absorbed and emitted vibrational quanta, which are in general very much larger than these contributions, may be taken to have a common value $h\omega$. In this respect our calculations differ materially from Kronig's. The appropriate elements of his transformed Hamiltonian function $\mathcal{H}_{new}$ vanish in the limit $H=0$. As a result, his calculated Raman transition probabilities turn out several orders smaller than ours, instead of larger as for the the direct processes. Written out explicitly, (17) becomes, in the present case,

$$\mathcal{H}_{new}(A_+n_in_j;A_-n_i-1n_j+1)=\left[\frac{f_{ij}^+-f_{ji}^-}{(-\Delta)(-\Delta+\omega)}+\frac{f_{ji}^--f_{ij}^+}{(-\Delta)(-\Delta-\omega)}+\frac{2g_{ij}^+-2g_{ji}^-}{-\Delta\omega}\right]$$
$$+\left[\frac{-g_{ij}^++g_{ji}^-}{(-\Delta+\omega)(+\omega)}+\frac{-g_{ji}^-+g_{ij}^+}{(-\Delta-\omega)(-\omega)}+\frac{h_{ij}^+}{(-\Delta+\omega)^2}+\frac{h_{ji}^-}{(-\Delta-\omega)^2}\right], \quad (34)$$

with

$$f_{ij}^{\pm}=h^{-2}\sum_{a,\,a'-a,\,b}\mathcal{H}_{SO}(A_+;E_{a-})\mathcal{H}_{OL}(E_an_i;E_{a'}n_i\mp1)\mathcal{H}_{OL}(E_{a'}n_j;An_j\pm1),$$
$$g_{ij}^{\pm}=h^{-2}\sum_{a-a,\,b}\mathcal{H}_{SO}(A_+;E_{a-})\mathcal{H}_{OL}(E_an_i;An_i\mp1)\mathcal{H}_{OL}(An_j;An_j\pm1), \quad (35)$$
$$h_{ij}^+=-h_{ji}^-=h^{-2}\sum_{a,\,a'-a,\,b}\mathcal{H}_{OL}(An_i;E_an_i\mp1)\mathcal{H}_{SO}(E_{a+};E_{a'-})\mathcal{H}_{OL}(E_{a'}n_j;An_j+1).$$

The various terms on the right side of (34) represent the different possible orders of the three $\mathcal{H}$

factors on the right side of (17). The first bracket of (34) represents the contribution of terms in which $\mathcal{H}_{SO}$ is the first or last factor, while the second bracket comes from the terms in which $\mathcal{H}_{SO}$ is the middle factor. In writing (35), we have made use of the fact that by (6) or (13) the matrix elements of $\mathcal{H}_{OL}$ are invariant under interchange of the initial and final orbital indices, or of the initial and final vibrational indices (i.e., $\mathcal{H}_{OL}(An_i;En_i')=\mathcal{H}(En_i;An_i')=\mathcal{H}(An_i';En_i)$), while by (5) and the Hermetian property, the elements of $\mathcal{H}_{SO}$ alter their sign when the initial and final orbital indices are permuted. The various terms of (34) do not quite destroy each other when $\omega\neq 0$. We may suppose $\omega$ small compared with $\Delta$, and so (34) becomes

$$\mathcal{H}_{\text{new}}(A_+n_in_j;A_-n_i-1n_j+1)=\omega\Delta^{-2}[2f_{ij}^{+}-2f_{ji}^{-}+2g_{ij}^{+}-2g_{ji}^{-}+4h_{ij}^{+}]. \tag{36}$$

The transition probability $A_{+\to-}$ that an atom reverse the sign of its spin is

$$A_{+\to-}=(4\pi^2/h^2)\int_0^{\theta k/h}\langle[\,|\mathcal{H}_{\text{new}}(A_+n_in_j;A_-n_i-1n_j+1)\,|^2\rho_{\omega i}\rho_{\omega j}\rangle_{\text{Av}}d\omega_i. \tag{37}$$

Here $\theta$ is the usual Debye characteristic temperature, and $\omega_i=\omega_j$, but we cannot set $\rho_{\omega i}=\rho_{\omega j}$ because $i$ may be a transverse wave, and $j$ a transverse one, or vice versa, so that different oscillator densities (19) may be relevant. As compared with (18) there is the difference that we must integrate over all oscillator frequencies, since the conservation of energy is secured by the equality of the absorbed and emitted quanta, and so the available oscillators are no longer restricted to those of very low frequency in the Zeeman range.

The average in (37) is, of course, over all amounts of excitation and of directions of propagation and of polarization for the two oscillators now involved. The spatial averaging for them may be done independently. The requisite formulas are the same as those given in (20) and (22) and discussed thereafter. On computing the explicit value of (37) by means of (5–11), and on performing the requisite averaging, it is finally found, after considerable straight forward calculation, that

$$A_{+\to-}=64(256V^2\zeta^2R^4\pi^4h^2/75\Delta^6M^2)(v_l^{-5}+\tfrac{3}{2}v_i^{-5})^2[a^4+(11/18)a^2b^2+(11/648)b^4]I_8, \tag{38}$$

where

$$I_n=\int_0^{\theta k/h}[\omega^n e^{+h\omega/kT}/(e^{h\omega/kT}-1)^2]d\omega \tag{39}$$

with $n=8$ for present purposes. The integral $I_8$ represents the appropriate statistical factor for the two oscillators participating in our Raman process, one of which is excited and the other de-excited. The expression (19) for the oscillator density would suggest that $\omega$ should occur to only the fourth power; however, the eighth power enters when one allows for the appearance of $\omega$ in (13), (14), (36), etc. At low temperatures, where $T/\theta\ll 1$, as in the helium range, one can legitimately make the approximation

$$I_n=\int_0^{\infty}\omega^n e^{-h\omega/kT}d\omega=n!(kT/h)^{n+1}. \tag{40}$$

At higher temperatures, where $T\sim\theta$, as in the liquid-air region, the great bulk of the integral (39) comes from the vicinity of the cut-off frequency $\omega_0=h\theta/k$, so that without great error, we can expand the exponential factors in (39) as a Taylor's series about $\omega_0$, and keep only the constant, and perhaps also the linear term. Then (39) becomes

$$I_n=\left(\frac{k\theta}{h}\right)^{n+1}\left[\frac{e^{\theta/T}}{(n+1)(e^{\theta/T}-1)^2}+\frac{\theta}{(n+1)(n+2)T}\frac{(e^{\theta/T}+1)e^{\theta/T}}{(e^{\theta/T}-1)^2}-\cdots\right]. \tag{41}$$

When $n=8$, the limiting value of (39) appropriate to the case $\theta/T\ll 1$ is clearly $k^9h^{-9}\theta^7T^2/7$. A cor-

responding limiting formula is also yielded by (41), except that the denominator becomes 9 instead of 7 if only the first term of (41) is utilized, and $7\frac{1}{2}$ if both members of (41) are included. The expression (41) is an adequate approximation for our purposes unless $\theta/T$ is large, but the experiments are never conducted at such high temperatures that it is allowable to use the limiting values proportional to $T^2$ characteristic of $\theta/T \ll 1$. Formula (41) tends to underestimate the value of $I_n$ but this is proably a good thing, as it tends to counterbalance the error latent at higher temperatures in the approximation (11), wherein the wave-length was taken to be large compared with the interatomic distance.

To compute the relaxation time by the thermodynamic method, we note that the expression for the rate of transfer of energy to the lattice is still given by (28) with $N_{\frac{1}{2}}$, $N_{-\frac{1}{2}}$, as in (29). The transition probability $A_{-\to+}$ differs from $A_{+\to-}$ by a factor $e^{-2\beta H/kT}$, nearly, but not quite equal to unity. Up till now we regarded the absorbed and emitted quanta as equal, but this is not strictly true—otherwise no energy exchange would be possible. Instead the two quanta will differ by an amount $2\beta H$, where $H$ is the resultant of the applied and spin-spin fields. In place of (30) and (32) we now have

$$\alpha = 2\beta^2 N(A_{+\to-}/kT^2)\langle H^2\rangle_{Av} = 2\beta^2 N(A_{+\to-}/kT^2)(H_0^2+K^2) \tag{42}$$

and

$$\tau = C_H/\alpha = \tfrac{1}{2}[(H_0^2+\tfrac{1}{2}K^2)/A_{+\to-}(H_0^2+K^2)]. \tag{43}$$

To evaluate $\tau$ at liquid-air temperatures, we need to know $\theta$. We shall take $\theta = 90°$, as this is the magnitude yielded by the conventional formula $\theta = (vh/k)(3N/4\pi V)^{\frac{1}{3}}$, with $v = 2.3\times10^5$ cm/sec. With the values (33) of the other constants, one finds from (38), (41) and (43) that $\tau = 0.13\times10^{-8}$ sec. at 77°K if $H_0 \gg K$, and $\tau = 0.07\times10^{-8}$ if $H_0 \ll K$. Thus even if the interval $\Delta$ is kept as high as $10^3$ cm$^{-1}$, the theory is adequate to explain the unusually short relaxation times characteristic of titanium alum at liquid-air temperatures. Namely, all that is known experimentally[17] is that from the absence of any observed dispersion over the frequency interval employed, $\tau$ must be less than $4\times10^{-8}$ sec. at 77°K.

At helium temperatures, on the other hand, a relaxation time sufficiently small to agree with experiment can be obtained only if $\Delta$ is of the order 100 cm$^{-1}$, or if drastic changes be made instead in some of the other constants. Namely, if we use the constants (33) as they stand, and if $H_0 \gg K$, then by (38), (40), and (43), the value of $\tau$ at low temperatures is $1.0\times10^3/T^9$, at least 100,000 times too large. It is, however, possible to bring $\tau$ down to within the necessary limit $\tau < 10^{-3}$ sec., if we take $\Delta = 10^2$ cm$^{-1}$, as then $\tau$ becomes $0.2\times10^{-3}$ at 1.2°K and $0.5\times10^{-4}$ at 1.4°K.

If $\Delta$ is reduced sufficiently to bring agreement with experiment in the helium region, then the Raman mechanism is likely to be more important than the direct process even here. Namely, in fields of 1000 gauss, the value of $\tau$ for the direct process was found to be $1.7\times10^{-2}$ sec. at 1.2°K with $\Delta = 10^2$ cm. This is about ten times as large a value of $\tau$ as our Raman estimate given above. At fields of the order $10^4$ gauss or so, the direct process does, however, yield much the greater transition probability or smaller $\tau$, because the direct interaction varies as the fourth power of $H$.

In the preceding paragraph we compared the Raman and direct processes on the assumption that agreement with experiment is to be obtained by altering $\Delta$. If, on the other hand, the discrepancy is to be removed by altering other constants, i.e., increasing $aR$ or $bB$, or assuming that the effective mass to be used in (14) is less than that of an average molecule, then it can be shown that the margin of superiority in favor of the Raman terms becomes even greater. However, if the distribution law (19) for the lattice oscillators is badly in error at low frequencies, a possibility which we discuss near the end of the paper, the direct process might be adequate to explain the absence of observed dispersion at helium temperatures. Another possibility is that some other mechanism than the lattice vibrations serves as the thermostat.

It would obviously be of interest if critical experiments could be performed which would decide between the direct and Raman mechanisms for temperatures in the helium range. Further evidence

[17] Gorter, Teunissen and Dijkstra, Physica **5**, 1013 (1938).

could be secured by studying the effect of diluting titanium with nonmagnetic ingredients in weak applied fields. (Some field is necessary, as $F$ in Eq. (27) vanishes if $H_0=0$.) Dilution decreases the effective spin-spin field $K$, which enters quite differently in (43) and (32). With the Raman process, the relaxation time is slightly increased by dilution, but with the direct type it is materially lengthened so that ultimately a measurable dispersion should set in even without extending the measured frequencies to higher values than those employed in the existing Leiden experiments. It appears probable that in any case the beginning of the dispersion is not very far on the high frequency side of the present limit. Once the dispersion can be detected, an enormous difference between the two types of mechanisms will appear, for with Raman transitions, $\tau$ is tremendously temperature sensitive ($\sim T^{-9}$ if $T\ll\theta$) and increases slightly when a field is applied, whereas with the direct transfers $\tau$ varies but slightly with temperature, and is greatly diminished by introducing a field $H_0$.

Owing to the $T^9$ factor in the Raman mechanism, the equilibrium at the very low temperatures ($\sim$0.01 to 0.1°K) obtained by adiabatic demagnetization is undoubtedly achieved by the direct type of process. Despite the rather large values of the direct $\tau$ which we compute, Casimir[2] shows that the equilibrium takes place practically instantaneously in demagnetization experiments because of the fact that the lattice is no longer in a constant temperature bath, as in relaxation measurements such as we are discussing. Instead it is isolated from external contacts and hence has a very low heat capacity, proportional to $T^3$.

## V. The Hamiltonian Function for Chromium

We now proceed to the corresponding calculations of the direct and Raman processes for chromium. As compared with titanium, there is the big difference (cf. Fig. 1) that the excited states belong to a different cubic representation than the ground level, so that it is necessary to consider matrix elements of the spin-orbit and orbit-lattice interaction which are nondiagonal in the cubic index $\Gamma$, and to specify the orbital states by their cubic representation. By extending somewhat the calculations of l.c., one finds the matrix elements of the spin-orbit interaction are

$$\mathcal{H}_{SO}(\Gamma_i\sigma_1;\Gamma_j\sigma_2)=\zeta\sum_{q=x,y,z}L_q(\Gamma_i;\Gamma_j)S_q(\sigma_1;\sigma_2), \tag{44}$$

with

$$\begin{aligned}
&L_x(\Gamma_2;\Gamma_{5a})=L_x(\Gamma_2;\Gamma_{5b})=L_y(\Gamma_2;\Gamma_{5c})=+2i;\\
&-L_y(\Gamma_{4a};\Gamma_{4b})=L_x(\Gamma_{4a};\Gamma_{4c})=-L_x(\Gamma_{4b};\Gamma_{4c})=-\tfrac{3}{2}i;\\
&L_y(\Gamma_{5a};\Gamma_{5b})=-L_x(\Gamma_{5a};\Gamma_{5c})=+L_x(\Gamma_{5b};\Gamma_{5c})=-\tfrac{1}{2}i;\\
&-L_y(\Gamma_{4a};\Gamma_{5b})=-L_x(\Gamma_{4a};\Gamma_{5c})=-L_x(\Gamma_{4b};\Gamma_{5c})=L_y(\Gamma_{5a};\Gamma_{4b})=L_x(\Gamma_{5a};\Gamma_{4c})=L_x(\Gamma_{5b};\Gamma_{4c})=-\tfrac{1}{2}\sqrt{15}i,
\end{aligned} \tag{45}$$

$$S_z(\sigma;\sigma)=\sigma,\quad (S_x+iS_y)(\sigma;\sigma-1)=[S(S+1)-\sigma(\sigma-1)]^{\frac{1}{2}},\quad (S=\tfrac{3}{2}). \tag{46}$$

The matrix elements of $L$ are Hermitian, i.e., change sign on permutation of initial and final indices. The $S$ matrices are also Hermitian and are, of course, the usual angular momentum matrices. Elements not written down (or obtained by mere interchange of initial and final indices) are all zero. The index $\sigma$ gives the component of spin parallel to the $z$ axis, which we choose as the axis of spin quantization. The $x,y,z$ axes are taken as the principal cubic axes. We thus use a different choice of axes and of spin quantization than in the preceding section. It is not necessary to use a trigonal index ($A$ or $E$) in connection with designating the orbital states, as the trigonal splitting of the upper state has no appreciable repercussion on the relaxation behavior of the ground state, since the latter is separated from excited states by a large interval due to the cubic part of the field. The three sub-states $a,b,c$ of $\Gamma_4$ or $\Gamma_5$ are the same as the system of representation used in Eq. (21) of l.c. and are not eigenstates of the trigonal field.

The nonvanishing matrix elements of orbit-lattice coupling connecting the ground state $\Gamma_2$ with excited levels are

$$\mathcal{H}_{OL}(\Gamma_2 n_i;\Gamma_{4x}n_i\pm1)=+Q_{4,6,5}(n_i;n_i\pm1)[44\rho_1-5\rho_2]/11\sqrt{15},\quad (x=a,b,c) \tag{47}$$

where the subscripts 4,6,5 apply, respectively, to the cases $a,b,c$ and where $\rho_1=-3\rho_1^0/7$, $\rho_2=+11\rho_2^0/7$, with $\rho_1^0$, $\rho_2^0$ defined as in (8). The only other matrix elements of $\mathcal{3C}_{OL}$ needed in connection with the calculation of the direct process are those internal to $\Gamma_5$ i.e., of the form $\mathcal{3C}_{OL}(\Gamma_{5x}n_3;\Gamma_{5y}n_3\pm1)$. These are given in Eqs. (21) and (22d) of l.c.,[7] with $a,b,c$ referring to the rows or columns of (21), and need not be repeated here. There are no matrix elements of $\mathcal{3C}_{OL}$ connecting $\Gamma_2$ and $\Gamma_5$, or of the type $Q_2$, $Q_3$ joining $\Gamma_2$ and $\Gamma_4$. (This statement is easily proved from group theory, since the representations corresponding to $Q_2$, $Q_3$ and to $Q_4$, $Q_5$, $Q_6$ are, respectively, $\Gamma_3$ and $\Gamma_5$, and the appropriate direct products are $\Gamma_2\times\Gamma_5=\Gamma_4$, $\Gamma_2\times\Gamma_3=\Gamma_1+\Gamma_2+\Gamma_3$.) On the other hand, the orbital angular momentum involved in the spin-orbit coupling has the transformation properties of $\Gamma_4$, and so this interaction does not join $\Gamma_2$ and $\Gamma_4$. Such vanishing of the matrix elements materially simplifies the calculations.

## VI. Calculation of Direct Processes for Chromium

To compute the elements of the new or transformed Hamiltonian function to be used in (18), we employ the third-order expression (17), taking two of the $\mathcal{3C}$ factors as due to the spin-orbit interaction, and one as due to orbit-lattice. The frequency denominators in (17) can be taken as the Stark splitting due to the cubic field alone, without the necessity of including the modulations due to either the lattice oscillations or the magnetic field. In this respect the present calculations differ materially from those on titanium. The reason is that we are now dealing with an atom whose basic state is a quartet. Its initial degeneracy is fourfold rather than twofold and so can be partially lifted without introducing magnetic fields even when the lattice vibrations are treated in an adiabatic fashion. Hence it is not necessary to allow for the modulation of the frequency denominators, which is a nonadiabatic effect. It is, however, essential to include two powers of the spin-orbit interaction rather than one as in the case of titanium, since the second-order expression (15) vanishes if we take one $\mathcal{3C}$ factor as the spin-orbit, and the other as the orbit-lattice interaction. This vanishing of (15) is caused by the compensation of terms representing different orders of the factors, and would be spoiled if we allowed for modulation of the frequency denominators. In fact, such modulation was the cause of the direct relaxation effect in titanium. However, the corresponding effect in the present case of chromium is negligible. Namely, it is reduced in the ratio $\Delta^4/\nu_{52}{}^4$ as compared with titanium, inasmuch as the normal states is separated from excited levels by a large cubic splitting $\nu_{52}$ rather than by a comparatively small trigonal separation $\Delta$.

Proceeding as above, we find that the matrix internal to $\Gamma_2$ in the new Hamiltonian function is

$$\mathcal{3C}_{new}=\epsilon_1[Q_3(2S_z^2-S_x^2-S_y^2)+\sqrt{3}Q_2(S_y^2-S_x^2)]+\epsilon_2[Q_4(S_xS_y+S_yS_x)+Q_5(S_xS_z+S_zS_x)+Q_6(S_yS_z+S_zS_y)]=\sum_{k=2,\cdots,6}H_{new}^{(k)}Q_k \quad (48)$$

with

$$\epsilon_1=4\zeta^2[175\rho_2/396][h\nu_{52}]^{-2}\sqrt{3},$$
$$\epsilon_2=4\zeta^2[\rho_1+(5\rho_2/33)][h\nu_{52}]^{-2}+8\zeta^2[\rho_1-(5\rho_2/44)][h\nu_{52}h\nu_{42}]^{-1}. \quad (49)$$

Here and elsewhere we use the abbreviation $h\nu_{52}=W(\Gamma_5)-W(\Gamma_2)$, etc. In (48), the $S$'s are to be construed as matrices, whose elements are given by (46).

We can assume that the cubic potential is of fourth-order character $D'[x^4+y^4+z^4]$. This supposition involves no loss of generality since we are dealing with $d$ electrons (cf. reference 14). Then the frequency denominators involved in (49) are

$$h\nu_{52}=10Dq, \quad h\nu_{42}=18Dq \quad \text{with} \quad Dq=2D'\overline{r^4}/105. \quad (50)$$

Here $Dq$ is the constant of Schlapp and Penney, which we shall take as having the value 1500 cm$^{-1}$ (cf. p. 81 of l.c.[7]).

Let us imagine the matrix elements of the spin in (49) computed not in the system of representation (46), but rather in one which diagonalizes the combined energy, apart from fluctuations caused by lattice oscillations, of the spin in the magnetic field $H$, and in the electric field due to surrounding ions, which indirectly affects the spin via the spin-orbit coupling. Let the eigenstates of the energy, shown by dotted lines in Fig. 1, be denoted by $W_{\eta'}$, $W_{\eta''}$, $\cdots$. Then by obvious generalization of (25), (26) to systems with more than two spin components, the rate of transfer from spin to lattice, is

$$dQ/dt=\sum_{\eta',\eta''}N_{\eta'}A_{\eta'\to\eta''}(W_{\eta'}-W_{\eta''}). \tag{51}$$

The transition probabilities $A_{\eta'\to\eta''}$ are connected with the matrix elements in the $\eta$ system of representation by relations analogous to (18), and the matrix elements of the $Q$'s are, of course, still given by (9), (12), (14). One now has, however, $h\omega=W_{\eta''}-W_{\eta'}$ instead of $h\omega=2\beta H$, and $N_\eta=\frac{1}{4}Ne^{-W_\eta/kT_S}$ in place of (29). Since $A_{\eta'\to\eta''}=e^{h\omega/kT}A_{\eta''\to\eta'}$, and since we still have $h\omega/kT\ll 1$, $T_S-T\ll T$ we can write

$$N_{\eta'}A_{\eta'\to\eta''}(W_{\eta'}-W_{\eta''})+N_{\eta''}A_{\eta''\to\eta'}(W_{\eta''}-W_{\eta'})=\tfrac{1}{8}N[A_{\eta'\to\eta''}+A_{\eta''\to\eta'}](W_{\eta'}-W_{\eta''})^2(T_S-T)/kT^2. \tag{52}$$

When average values are computed by means of (20) and (22), which reduces to $\langle n_i\rangle_{h\omega}=kT/h\omega$, it is found that $dQ/dt=\alpha(T_S-T)$ with

$$\alpha=NC\sum_{k=2\cdots 6}\sum_{\eta',\eta''}|H^{(k)}(\eta';\eta'')|^2|W_{\eta'}-W_{\eta''}|^4,\quad C=R^2(4v_l^{-5}+6v_t^{-5})\pi^3V/15TMh^4. \tag{53}$$

Eq. (53) can also be written as

$$\alpha=NC\sum_{k=2,\cdots,6}\text{spur}\,[V_kW-WV_k]^2,\quad V_k=WH^{(k)}-H^{(k)}W, \tag{54}$$

where $W$ is the matrix (internal to $\Gamma_2$) associated with the Hamiltonian function whose proper values are the $W_\eta$. The great advantage of writing (54) as a spur is that (54) is valid in any system of representation, and so it is not necessary to actually find the system which diagonalizes $W$. In chrome alum the matrix $W$ has the structure

$$W=2\beta[H_xS_x+H_yS_y+H_zS_z]+\tfrac{1}{6}h\Delta\nu[S_x+S_y+S_z]^2. \tag{55}$$

The first member of (55) is clearly the Zeeman energy in the field $H$. The second is the energy of the crystalline electric field. The latter has trigonal rather than perfect cubic symmetry and so splits the quartet ${}^4\Gamma_2$ into two doublets, whose separation is denoted by $h\Delta\nu$, and which correspond, respectively, to $S_{z'}=\pm\frac{3}{2}$, and $S_{z'}=\pm\frac{1}{2}$, where the $z'$ direction is parallel to the trigonal axis. The Hamiltonian function associated with the crystalline Stark effect may thus, apart from an additive constant, trivial for our purposes, be written as $S_{z'}{}^2h\Delta\nu/[(\frac{3}{2})^2-(\frac{1}{2})^2]$. The form employed in (55) follows from the fact that the trigonal axis is a body diagonal $x=y=z$ of our $x,y,z$ system, so that $S_{z'}=[S_x+S_y+S_z]/\sqrt{3}$. The explicit value of the expression (54) for $\alpha$ can now be computed with the aid of (48) and (55), and the conventional commutation relations for angular momentum matrices. After some calculation, one finds that

$$\alpha=72C(2\beta)^4[(8\epsilon_1{}^2+3\epsilon_2{}^2)(H_x{}^4+H_y{}^4+H_z{}^4)+(10\epsilon_1{}^2+8\epsilon_2{}^2)(H_x{}^2H_y{}^2+H_y{}^2H_z{}^2+H_z{}^2H_x{}^2)]$$
$$+C\beta^2h^2\Delta\nu^2(H_x{}^2+H_y{}^2+H_z{}^2)(3072\epsilon_1{}^2+1280\epsilon_2{}^2)+12Ch^4\Delta\nu^4(6\epsilon_1{}^2+2\epsilon_2{}^2). \tag{56}$$

As in the calculations on titanium, we consider the magnetic field $H$ to arise in part from an applied field $H_0$, and in part from an effective field $H_s$ representing spin-spin interaction. As previously, we regard $H_s$ to be oriented at random, and distributed in Gaussian fashion, with a root mean square value $K$. With these assumptions, and the corresponding averaging over $H_s$, Eq. (56) becomes

$$\alpha=\alpha'+72C(2\beta)^4[(8\epsilon_1{}^2+3\epsilon_2{}^2)(2H_0{}^2K^2+K^4)+(10\epsilon_1{}^2+8\epsilon_2{}^2)(\tfrac{2}{3}H_0{}^2K^2+\tfrac{1}{3}K^4)]$$
$$+C\beta^2h^2\Delta\nu^2[3072\epsilon_1{}^2+1280\epsilon_2{}^2]K^2, \tag{57}$$

where $\alpha'$ denotes the expression (56) with $H$ everywhere replaced by $H_0$. On calculating the explicit value of the specific heat (26), for the present case of chromium, it is found that the relaxation time $\tau$ appearing in (27) becomes

$$\tau = C_H/\alpha = [\tfrac{1}{4}(h^2\Delta\nu^2) + 5(H_0^2 + \tfrac{1}{2}K^2)\beta^2]/\alpha T^2. \tag{58}$$

To compute numerical values, we recall that by definition $\rho_1 = -3\rho_1^0/7$, $\rho_2 = 11\rho_1^0/7$ and take $\rho_1^0$, $\rho_2^0$, $v$ as in (33), but $K$ and $\zeta$ are now, respectively, 290 gauss and 88 cm$^{-1}$. The density $M/V$ is now 1.7 instead of 2.0, as we are dealing with $KCr(SO_4)_2 \cdot 12H_2O$ rather than $CsTi(SO_4)_2 \cdot 12H_2O$. The appropriate values of $\nu_{ij}$ are cited in connection with (50). The splitting $\Delta\nu$ we consider to be 0.17 cm$^{-1}$, as this is the value indicated by recent experiments on adiabatic demagnetization.[18] The computed values of $\tau$ at 1.4°K are then 0.011, 0.0090, 0.0067 and 0.0030 second, respectively, for $H_0 = 0$, 500, 1000, and 3000 gauss. Most of the energy transfer when $H_0 = 0$ results in virtue of the Stark splitting $\Delta\nu$ rather than the spin-spin coupling $K$, for if we take $K = 0$, the value of $\tau$ at $H_0 = 0$ is raised merely to 0.014 second.

The agreement with experiment as to order of magnitude is adequate. The only available experimental measurements are those made at Leiden, not yet in final form. A preliminary analysis of them, kindly communicated to the writer by Professor Casimir, yields relaxation times $\tau$ equal to 0.018 and 0.007 second at temperatures of 2° and 3.5°K, respectively, both at a field strength of 1350 gauss. The corresponding values yielded for these conditions by our calculations are 0.0035 and 0.0020 second. The experimental accuracy is estimated as only 20 percent, but the error in our calculations is doubtless even greater. It is gratifying that the calculated relaxation times actually turn out smaller than the observed values, inasmuch as in previous work there has been a pronounced discrepancy in the opposite direction.

However, the predicted dependence on field strength is entirely wrong, for theoretically the relaxation time should decrease when the field is increased, whereas experimentally the reverse is true. (The empirical increase of $\tau$ with $H_0$ is rather small, and conceivably the data might be consistent with a $\tau$ independent of $\nu$, but even so the theoretical prediction $d\tau/dH_0 < 0$ is contradicted.) Possible explanations of this discrepancy will be sought for in Section VIII. The dependence on temperature is also incorrect. Theoretically $\tau$ should be proportional to $1/T$, whereas comparison of the data at 2° and 3.5°K indicates that more nearly $\tau \sim T^{-1}$ or $T^{-2}$.

## VII. Calculation of Raman Processes for Chromium

We now proceed to the calculation of second-order processes for chromium. The mechanism for these is different than in the case of titanium. There are contributions from two main types of terms, I and II which prove to be approximately coordinate in importance and which are as follows:

I. Those which are obtained by using a fourth-order perturbation formula, analogous, except for order, to (15) or (17). Two of the $\mathcal{H}$ factors in the numerator are to be taken as due to spin-orbit interaction (44), and two due to orbit-lattice coupling.

II. Terms which are obtained by employing the third-order perturbation formula (17), but expanding the crystalline potential to the second rather than first order in the normal coordinates $Q_1, Q_2, \cdots$. The orbit-lattice coupling energy such as (47), or Eq. (21) of l.c., is then replaced by an expression of the second order in the $Q$'s. In (17), one of the $\mathcal{H}$ factors is due to this extension of the orbit-lattice interaction, while the two others are contributed by the spin-orbit energy (44).

Besides I and II, there are two other types of contribution III, IV, as follows, which require examination, but which prove to be of minor importance.

III. Terms which result from the third-order formula (17), taking two of the $\mathcal{H}$ factors as due to the orbit-lattice energy (47), linear in the $Q$'s, and one factor only as due to the spin-orbit energy, but allowing for the modulation of the frequency denominators by the energy changes in the lattice oscillators. In I and II, these denominators can be

[18] B. Bleaney, in press.

regarded as arising from the cubic crystalline potential alone, but without the modulation, the structure III would make no contribution to the relaxation.

IV. Terms obtained by using the second-order formula (15), but expanding the orbit-lattice energy to the second order in the $Q$'s as in II, and simultaneously allowing for the modulation of the frequency denominators as in III. One of the $\mathfrak{IC}$ factors is due to the second-order extension of the orbit-lattice interaction, and the other to the spin-orbit energy.

Effects I and II may be characterized as obtained by an adiabatic, and III–IV by a nonadiabatic perturbation calculation; since the modulation of the frequency denominators is essentially an allowance for the fact that the oscillations in the crystalline potential do not take place infinitely slowly. In making the calculation, one must be careful to notice that I and II contribute additively only to the transformed Hamiltonian function $\mathfrak{IC}_{\text{new}}$ and not to the transition probability, or to the heat transfer constant $\alpha$, as either of the latter is proportional to $\mathfrak{IC}_{\text{new}}^2$. Similar remarks apply to III, IV. On the other hand, the contributions of I+II to $\alpha$ can be proved to be additive with respect to those of III+IV. Detailed calculation, of which we omit the details, shows that the transition probabilities due to III and IV are only of the order of magnitude $10^{-3}$ compared with those due to I and II. Hence we can safely disregard III and IV, as we do henceforth. In titanium, on the other hand, III was the main effect, and I and II were nonexistent, while IV was negligible in comparison with III, and so was neglected entirely. The reason that this was permissible is that in Ti, the important excited levels were separated from the ground state only in virtue of the splitting $\Delta$ due to the noncubic portion of the crystalline potential. Consequently the extra frequency denominator contained in III as compared with IV was $\Delta$ rather than the cubic splitting $\nu_{52}$(or $\nu_{42}$). So in Ti, the effect of III, instead of being comparable with IV as in Cr, was enhanced relative to IV by a factor $\nu_{52}/\Delta$ in $\mathfrak{IC}_{\text{new}}$ or $(\nu_{52}/\Delta)^2$ in $\alpha$.

We shall compute only the parts of I and II due to vibrations of the type $Q_2$, $Q_3$. This restriction suffices to fix approximately the order of magnitude of the relaxation time, and very materially simplifies the calculation because $Q_2$, $Q_3$ do not give rise to any matrix elements joining $\Gamma_2$ with $\Gamma_4$ or $\Gamma_5$. A more complete calculation, where all types of vibration are fully considered, would be quite laborious, and does not seem warranted at the present time.

In order to compute the result of the mechanism I, with the above simplifications, it is necessary to have besides the matrix elements of the orbit-lattice energy internal to $\Gamma_5$ given in (21) and (22d) of l.c., also those of type $Q_2$, $Q_3$ joining $\Gamma_4$ and $\Gamma_5$. The latter can be shown to be

$$\mathfrak{IC}_{OL}(\Gamma_{4a};\Gamma_{5a})=-2pQ_2,\quad \mathfrak{IC}_{OL}(\Gamma_{4b};\Gamma_{5b})=p(Q_2-\sqrt{3}Q_3),\quad \mathfrak{IC}_{OL}(\Gamma_{4c};\Gamma_{5c})=p(Q_2+\sqrt{3}Q_3),$$

with $p=[-3\rho_1+(25/44)\rho_2]/\sqrt{15}$.

To calculate the influence of II, one makes use of the fact that expansion of the crystalline potential given in (9) of l.c. to the second order has the effect of replacing $\rho_2Q_2$, $\rho_2Q_3$, respectively, by

$$\rho_2Q_2-7\rho_2R^{-1}Q_2Q_3/2\sqrt{3},\quad \rho_2Q_3-7\rho_2R^{-1}(Q_2^2-Q_3^2)/4\sqrt{3},$$

in (21) of l. c., providing we neglect all terms involving other coordinates than $Q_2$, $Q_3$.

In essentially the same way that we obtained (48), except that the perturbation theory is carried one order higher, we find for the transformed Hamiltonian function involving the effect of I and II

$$\mathfrak{IC}_{\text{new}}=E\{[Q_3^2-Q_2^2][2S_z^2-S_x^2-S_y^2]+2\sqrt{3}Q_2Q_3[S_x^2-S_y^2]\},\tag{59}$$

with

$$E=-\left[\frac{4\zeta^2}{h^3\nu_{52}^3}\right]\left[3\left(\frac{175}{396}\rho_2\right)^2-\frac{7}{4}\frac{h\nu_{52}}{R}\left(\frac{175}{396}\right)\rho_2-\frac{1}{15}\frac{h\nu_{52}}{h\nu_{42}}\left(-3\rho_1+\frac{25}{44}\rho_2\right)^2\right].$$

The calculation now proceeds in more or less the same fashion as in connection with the Raman terms for Ti, but with the difference that there is a splitting of the basic multiplet due to the crystalline potential as well as the applied field. However, solution of the secular problem can be avoided, as in the case of the direct processes for Cr, by expressing the results in the form of an invariant diagonal sum. Eqs. (51) and (52) are still applicable and it is finally found that the formula for the energy transfer constant is

$$\alpha=GNI_6k^{-1}T^{-2}R^4(16\pi^2EV/15M)^2(v_l^{-5}+\tfrac{3}{2}v_t^{-5})^2,\tag{60}$$

TABLE I. *Relaxation time for chrome alum due to Raman process.*

| | $H_0=0$ | 800 | 1600 | 2400 | 3200 | ∞ GAUSS |
|---|---|---|---|---|---|---|
| $T_{calc}\times10^6$ (90°K) | 0.14 | 0.18 | 0.22 | 0.24 | 0.26 | 0.28 |
| $T_{obs}\times10^6$ (90°K) | | 0.06 | 0.12 | 0.16 | 0.19 | |
| $T_{calc}\times10^6$ (64.4°K) | 0.43 | 0.56 | 0.70 | 0.77 | 0.80 | 0.86 |
| $T_{obs}\times10^6$ (64.4°K) | | 0.53 | 0.76 | 0.92 | 1.02 | |

where $I_6$ is defined as in (39), and

$$G=\text{spur}\,[(2S_z^2-S_x^2-S_y^2)W-W(2S_z^2-S_x^2-S_y^2)]^2+3\,\text{spur}\,[(S_x^2-S_y^2)W-W(S_x^2-S_y^2)]^2. \quad (61)$$

Here, $W$ is the matrix (55) of the Hamiltonian function representing the combined energy due to the Zeeman effect and the crystalline potential. Explicit computation of $G$ gives

$$G=72h^2\Delta\nu^2[1+8(H\beta/h\Delta\nu)^2]. \quad (62)$$

We can now calculate the relaxation times with the aid of (58), (60), (62) and numerical values of the constants as stated after (58). We shall multiply all estimates of $\tau$ thus obtained by a factor 1/10, as we have considered only the vibrations of the type $Q_2$, $Q_3$, and a rough calculation[19] shows that the transition probability will be increased by a factor of the order 10 when allowance is made for vibrations of the form $Q_4,Q_5,Q_6$, and for the interplay between $Q_2,Q_3$, and $Q_4,Q_5,Q_6$, etc. With this modification, the relaxation times which we calculate from our formulas at 90° and 64.4° are shown in Table I for various applied fields, along with recent experimental determinations made by Gorter and collaborators.[20] The agreement between the calculated and observed orders of magnitude of the relaxation time must be regarded as adequate in view of the approximate character of the theoretical model. The predicted dependence on temperature is obviously not rapid enough. The calculated ratios of the relaxation times at two different temperatures has theoretically a particularly simple origin, as it arises solely in virtue of the factor $I_6$ in (60), defined by (39). The disagreement is doubtless due mainly to the fact that the actual frequency spectrum for the lattice does not conform to the $\omega^2$ law at high frequencies, and need not cause concern, since it is well known that the law fails badly in the vicinity of the cut-off frequency $k\theta/h$. Also in this region the assumption (11) that the wavelength is long compared with the radius $R$ of the cluster $Cr\cdot6H_2O$ is not warranted and the resulting error will change the temperature dependence somewhat. The discrepancies in the dependence of $\tau$ on the magnetic field appear to be more fundamental, as we shall see in Section VIII.

## VIII. Dependence of $\tau$ on the Applied Magnetic Field $H_0$

The calculated orders of magnitude of the relaxation time naturally depend on the numerical values selected for the various constants, such as (33). On the other hand, the predictions regarding the variation of $\tau$ with the applied field $H_0$ are of a very general character not contingent on how these constants are selected, or upon the approximation (11).

At liquid-air temperatures, where only the Raman processes are important, the relaxation time $\tau$ should theoretically depend on $H_0$ in the fashion

$$\tau=(1+d^2H_0^2)\tau_0/(1+c^2H_0^2) \quad (63)$$

as can be seen from Eqs. (58), (60), and (62). In (63), $\tau_0$ is the relaxation time for zero field strength and $d$ and $c$ are constants. With our choice (33) of constants, $d$ and $c$ have, respectively, the values $1.2\times10^{-3}$ and $0.85\times10^{-3}$

[19] In this connection it should be mentioned that uneven vibrations of the type $Q_7$, $\cdots$, $Q_{18}$, defined in l.c., can contribute to the transition probability through the terms of the structure II described at the beginning of Section VII. This is true because the Taylor's expansion of the potential does not involve solely the even modes of vibration when quadratic terms are included. Also $Q_1$ can be involved in II, since proper choice of origin only eliminates the linear term in $Q_1$.

[20] I am much indebted to Professor Gorter for communicating these results in advance of publication.

gauss. As $d$ is larger than $c$, the relaxation time should increase with field strength. The critical frequency region in which $\tau$ is most sensitive to $H_0$ is predicted correctly, but the calculated variation is not rapid enough (cf. Table I, Section VII). The latter discrepancy is not to be dismissed lightly, as theoretically the ratio $d^2/c^2=\tau_\infty/\tau_0$ has a value 2 quite irrespective[21] of the choice of values assigned the cubic splittings, the decomposition $\Delta\nu$ of the basic quartet, the vibrational amplitude, etc., whereas at 90° experimentally $\tau$ varies by a factor 3 when $H_0$ is increased from 800 to 3200 gauss. Possibly there may be some uncertainty in the empirical relaxation times, since the experimental points are fitted so as to make $\chi_\nu$ in (27) extrapolate to the theoretical value $\chi_0(1-F)$ when $\nu=\infty$. Small departures of $\chi_\infty$ from the ideal value $\chi_0(1-F)$ are to be expected if the assumption of a spin temperature fails at the highest field strength at liquid-air temperatures, and this fact might alter slightly the variation with $H_0$ to be assigned to $\tau$.

[21] Strictly speaking, the statement that $\tau_\infty/\tau_0$ can only have the value 2.0 is not true. Were we to consider Raman terms arising from $Q_4$, $Q_5$, $Q_6$ as well as merely from $Q_2$, $Q_3$, we would find that the transformed Hamiltonian function contained spin matrices of the type $S_xS_y$, $S_yS_z$, $S_xS_z$, like those associated with $\epsilon_2$ in (48), whereas the function (59) which we use involves only those of the type connected with $\epsilon_1$ in (48). (In the language of group theory, the $\epsilon_1$, $\epsilon_2$ structures appear according as the symmetrical direct product of the $Q$'s corresponding to our Raman process has the transformation properties of the representation $\Gamma_3$ or $\Gamma_5$.) With the $\epsilon_2$ type, $\alpha$ is proportional to $1+12(H\beta/h\Delta\nu)^2$ instead of (62). The $\Gamma_3$ and $\Gamma_5$ forms thus give upper and lower limits 2.5 and 1.7 for $d^2/c^2$ in (63). In constructing Table I and giving a numerical value for $d$ in (63) we have assumed that the two structures contribute equally to $\alpha$, so that $\alpha$ is proportional to $1+10(H\beta/h\Delta\nu)^2$. It may be that the lattice vibrations important for the $\epsilon_1$ and $\epsilon_2$ forms have a different frequency spectrum, and so a different temperature dependence. If so, $d^2/c^2$ can be a function of temperature, rather than a constant independent of $T$, as we have treated it to be. Actually $d^2/c^2$ does vary with $T$, but it is doubtful whether sufficient variation is given by our theory, for even under the most extreme assumptions the calculated variation would be only between 1.7 and 2.5. (In iron, the corresponding values are 1.7 and 4.5, so that there is more leeway.)

If the nonadiabatic terms were effective, $\mathfrak{IC}_{\text{new}}$ would be linear in the spin matrices, rather than quadratic, as in (48) or (59), and one can show that then in the Raman case in chromium we have $d^2/c^2=3.0$ in somewhat better agreement with experiment. However, as already mentioned, the nonadiabatic terms appear to be considerably smaller than the adiabatic ones. Kronig's study of the relation between transition probability and relaxation time (Physica 5, 65 (1938)), which is a generalization to $S>\frac{1}{2}$ of the Kronig and Gorter article mentioned in note 13, assumed essentially a linear $\mathfrak{IC}_{\text{new}}$, so that his discussion applies to the nonadiabatic terms only.

At helium temperatures, where the direct rather than Raman processes are important, the predicted dependence on field strength is entirely wrong. The values of $d$ and $c$ in (63) become, respectively, $1.2\times10^{-3}$ and $1.6\times10^{-3}$ gauss$^{-1}$, as one finds from (57) and (58) if one disregards the part of $\alpha'$ of the fourth order in $H_0$. As $d$ is now considerably less than $c$, the relaxation time should decrease with field strength, in marked contradiction with the experimental data. To make matters worse, if the field strength is large ($\sim10^3$ gauss) we must, by (56), add to the denominator of (63) a term of the structure

$$e_1^4[H_{0x}^4+H_{0y}^4+H_{0z}^4]+e_2^4[H_{0x}^2H_{0y}^2+H_{0y}^2H_{0z}^2+H_{0z}^2H_{0x}^2] \quad (64)$$

with $e_1=0.78\times10^{-3}$, $e_2=0.88\times10^{-3}$ gauss$^{-1}$. These extra terms accentuate still further the theoretical decrease of relaxation time with increasing field strength.

**The effect of Temperley**

In an interesting paper, Temperley[22] has suggested that the difficulties regarding dependence on field strength, and of the incorrect orders of magnitude of the relaxation times calculated in previous investigation and still present for titanium at helium temperatures can be avoided by taking account of the fact that several atoms may reverse their spins simultaneously. Supposedly the heat transfer between the spin and lattice is thus enhanced, and if the applied field inhibits concerted action, an explanation is obtained of why the relaxation time increases with field strength. Unfortunately, we do not believe that the effect of Temperley exists to an appreciable extent *if the spins are really in thermal equilibrium with each other*. In our opinion his estimates of numerical orders of magnitudes are misleading because they do not take cognizance of the possibility of writing the answers as invariant diagonal sums not materially influenced by cluster formation. If his effect were important it would imply that the assumption that spin-spin interaction can be represented by a Gaussian distribution of internal magnetic fields, is grossly incorrect. It is possible to extend our calculations so as to incorporate the spin-spin interaction exactly, rather than by means of the hypothesis of an internal field, and hence to examine whether Temperley's mechanism really gives an essential modification of the results. We may for simplicity suppose that the phase of the Debye waves is the same for all the atoms of the crystal, for this assumption is the most favorable to the existence of the constructive interference between atoms presupposed by Temperley. We can regard the whole crystal as a structural unit. Then the new Hamiltonian function involves summation over all the

[22] C. N. V. Temperley, Proc. Camb. Phil. Soc. **35**, 256 (1939).

paramagnetic atoms of the crystal instead of applying to a single atom. Thus the transfer constant is given by (53) or (60), but with the factor $N$ deleted, and with the matrices $S_x^2$, $S_xS_y$ etc. in the definitions (48) and (61) of $H^{(k)}$ and $G$ replaced, respectively, by $\Sigma_i S_{xi}^2$, $\Sigma_i S_{xi}S_{yi}\cdots$, where the subscript $i$ means that the spin in question relates to atom $i$. Also the quantity $W$ is no longer defined as in (55), and is instead

$$W=\Sigma_i 2\beta \boldsymbol{H}_0\cdot\boldsymbol{S}_i+\Sigma V_i+\Sigma_{j>i}V_{ij}, \tag{65}$$

where $V_{ij}$ is the spin-spin coupling (4) and $V_i$ is the crystalline potential

$$V_i=\tfrac{1}{6}h\Delta\nu(S_{xi}+S_{yi}+S_{zi})^2.$$

Because of the fact that $V_{ij}$ commutes with $S_k$ unless $i=k$ or $j=k$ and because of the fact that

$$\text{Spur }[S_{xi}^2V_{ij}-V_{ij}S_{xi}^2][S_{xk}^2V_{kl}-V_{kl}S_{xk}^2], \text{ etc.}$$

vanishes unless $i=k$, $j=l$ or $i=l$, $j=k$, one sees that interference between only two atoms at a time can be involved in (61), where $W$ occurs quadratically. Since $(x+y)^2 \leqq 2x^2+2y^2$, this means that the interference effects can only double the calculated transition probability. Similarly, in (53), where $W$ occurs biquadrically, one can show that only four atoms at a time will interfere, so that at most the amplification due to the Temperley effect is by a factor 4. Temperley, on the other hand, needed a cooperative effect inside a cluster containing about 300 atoms. Our estimates of the amount of interference in the spin-spin terms are only upper limits, and furthermore the main part of (65), results not from the dipolar coupling $V_{ij}$, but from the crystalline potential $V_i$ whose contribution to the relaxation is purely additive from the various atoms. In consequence of the partial interference, the value of $C$ in (63) is slightly changed, but we find that even on taking the extreme limits derived above, the alteration is nothing like sufficient to make $d/c>1$ for the direct process for chromium, as is required if the relaxation time is to increase with field strength at helium temperatures.

In the preceding discussion we have tacitly given the impression that our use of a Gaussian distribution of internal magnetic fields to represent the dipole-dipole coupling would be rigorous if we neglected the possibility of two or more spins reversing simultaneously. This is not really so in the calculation of the direct processes. Here the fourth power of the internal field or dipole-dipole interaction is involved, and the Gaussian law does not necessarily give the correct dispersion, i.e., it may not give the proper mean fourth power although it is adjusted to work on the square. Examination of an explicit calculation which the writer[23] has made of the mean fourth power in the somewhat related case of exchange coupling indicates that the resulting error is not serious. There is also a correction because of the fact that in computing the direct process for atom $i$ the dipole interaction joining atoms $i$ and $j$ does not commute with the crystalline potentials $V_j$ of atom $j$. Consequently atom $i$ feels the crystalline potential of other atoms via the dipole-dipole coupling. The resulting modifications can be computed, but prove to be of minor importance, as well as in the wrong direction.

*Possible explanations of the difficulty.*—Since, in our opinion, the Temperley effect does not enter appreciably with the thermodynamic model, one looks for other reasons why our calculated dependence of $\tau$ on field strength is wrong at low temperatures. The most obvious suggestion is that the assumption of a spin temperature is not warranted, but any explanation of this character seems to be pretty well refuted by the usual conformity of the dispersion curves to formula (27), and especially by the fact that the empirical and theoretical values of the constant $F$ in (27) agree so well. The incorrect dependence on field strength is due to the factor $\omega^2$ in the frequency spectrum (19) of the lattice oscillators. This factor makes the energy transfer constant $\alpha$ for the direct processes proportional to the fourth power of the energy quantum $\Delta W$ exchanged between spin and lattice, whereas only the square occurs in the case of the Raman mechanism (cf. Eqs. (53) and (61)). The applied field modulates $(\Delta W)^4$ to a greater extent than it does $(\Delta W)^2$, (e.g. the coefficient of $H^2$ is six times as large in an expression of the form $(1+xH_0)^4$ as for $(1+xH_0)^2$). So in the direct process the increase of $\alpha$ $(=\alpha_0[1+d^2H_0^2])$ with $H_0$ is so great as to more than offset the corresponding increase of the specific heat $C_H$ $(=C_0[1+c^2H^2])$, whereas with the Raman mechanism this is not true. Since $\tau=C_H/\alpha$, the sign of $d\tau/dH_0$ is thus different in the two cases. The troublesome $\omega^2$ factor would be removed if at low temperatures the spins owed their heat contacts to conduction electrons rather than lattice oscillators, but apparently the apparatus actually does not have important metallic connections.

Another interesting but highly conjectural possibility is that the use of the conventional distribution law $\rho_\omega\sim\omega^2$ for lattice oscillators is not warranted at exceedingly low frequencies. Undoubtedly this law would be accurate for infinitely small vibrations of small $\omega$, but the zero-point energy requires finite amplitudes, which are particularly large for the vibrations of lowest frequency (cf. Eq. (14)). Hence the anharmonic corrections may make the distribu-

[23] J. H. Van Vleck, Phys. Rev. **55**, 927 (1939).

tion materially different from the usual idealized form. Similar remarks apply to the effect of disturbances caused by contact of the oscillators with the "walls" (e.g. helium bath). If the interruptions are sufficiently rapid, $\omega$ loses meaning and the frequency distribution is blurred out, diminishing the apparent dependence of $\rho_\omega$ on $\omega$. Conceivably the oscillations most active in modulating the cluster $Cr \cdot 6H_2O$ are not typical of the crystal as a whole and have a different distribution law. If $\rho_\omega$ could for our purposes be treated as independent of $\omega$ for low values of $\omega$, then the dependence of $\tau$ on $H_0$ would be the same for the direct as for the Raman processes and we would have in either case $d\tau/dH_0>0$, as desired.

*Dependence on direction of applied field.*— Experiments on the dependence of $\tau$ on the direction of the applied field at helium temperatures are not yet available but would be particularly desirable because of the light which they would throw on the preceding considerations. According to our calculations of the relaxation due to the direct processes with the usual frequency distribution law (19), $\tau$ should exhibit some anisotropy at helium temperatures at high field strengths, because of the addition of (64) to the denominator of (63). The resulting anisotropy is small, amounting to about 10 percent in fields of 3000 gauss or greater, but is not beyond detection in refined experiments (unlike the negligible anisotropy calculated in Section III for the direct processes in titanium). On the other hand, if the $\omega^2$ factor due to the frequency distribution law (19) is removed, as we suggested in the preceding paragraph, then $\tau$ becomes isotropic even for the direct processes.

The calculation of Section VII (or of Section III for titanium) show that the relaxation times due to the Raman mechanism do not depend on the direction of the applied field. This prediction is in accord with experiments made by Teunissen and Gorter at liquid-air temperatures.[24]

## IX. Iron Alum

There are more extensive experimental data on paramagnetic dispersion for iron than for chrome alum, but the theory of the Stark decomposition for the basic state of the $Fe^{+++}$ ion is somewhat ambiguous. For this reason we have made our detailed calculations on $Cr^{+++}$. Still there is a certain parallelism between the two ions. The temperature dependence is governed by similar factors, and in particular our conclusions in Section VIII regarding the dependence on field strength should also apply to $Fe^{+++}$. There is still the difficulty that $d\tau/dH_0$ has the wrong sign at helium temperatures. In the Raman processes characteristic of the liquid-air region, the calculated values of the ratio $d^2/c^2$ connected with (63) range from 1.7 to 4.5, depending on the assumption one makes concerning the nature of the crystalline field and the type of vibration effective.[25] The most likely value is in the neighborhood of 2.5. The computed ratios are thus somewhat larger than for chromium and so give somewhat better agreement with the experimental dependence on field strength than that shown in Table I for chromium.

As regards orders of magnitude, one should expect the Raman $\tau$ to be roughly of the same size in iron as for chromium. This prediction agrees with observation. On the other hand, the direct processes occur in iron only if one includes matrix elements nondiagonal in the principal quantum number, or else retains higher powers of the spin-orbit interaction than in chromium.[26] So it is hard to understand why $\tau$ at helium temperatures is not experimentally markedly larger for iron than for chromium.

[24] Teunissen and Gorter, Physica **5**, 855 (1938); (measurements on iron alum, but our prediction of isotropy still applies).

[25] It is uncertain whether the splitting of the spin components of the basic state of the iron ion is due primarily to the cubic or axial (trigonal) members of the crystalline potential. There is no similar ambiguity in chromium, since a cubic field cannot decompose the basic state of $Cr^{+++}$. For a cubic field in iron alum the value of $d^2/c^2 = \tau_\infty/\tau_0$ characteristic of the $\epsilon_1$ and $\epsilon_2$ structures cited in note 21 are, respectively, 1.7 and 4.5. For a second-order axial field of type $x^2+y^2-2z^2$ the corresponding values are 2.7 and 2.2. If, as in Section VIII, it is assumed that the $\epsilon_1$ and $\epsilon_2$ forms contribute equally to $\alpha_0$, then the appropriate mean values for the cubic and axial cases are, respectively, 2.5 and 2.4. These estimates are inclusive of the effect of the contributions of the spin-spin field $K$ to $\alpha_0$ and $C_H$, which are very much more important than in chromium. (If we could set $K=0$, the maximum value of $\tau_\infty/\tau_0$ would be 6.25 rather than 4.5). Teunissen's data, reference 1, give some evidence that $\tau_\infty/\tau_0$ is lower experimentally for iron nitrate than for the alums, as is perhaps reasonable since the nitrates have rhombic rather than cubic symmetry.

[26] See C. J. Kynch, Trans. Faraday Soc. **33**, 1402 (1937), also J. H. Van Vleck and W. G. Penney, Phil. Mag. **17**, 961 (1934) concerning vanishing of matrix elements in half-completed shells.

# Variable Structures and Continuous Scattering of X-Rays from Layer Silicate Lattices

STERLING B. HENDRICKS
*Bureau of Agricultural Chemistry and Engineering, Washington, D. C.*

(Received September 22, 1939)

Crystals of some micas and related compounds having "layer" lattices show pronounced continuous scattering of x-rays together with normal interference maxima. Continuous scattering is explained as arising from destruction of the lattice periodicity normal to the perfect cleavage of these types of substances. This is a result of translation of some layers along the $b$ axis and parallel to the cleavage by $nb_0/3$, where $b_0$ is the unique lattice periodicity and $n$ is an integer. Various crystals differ in their degree of randomness and four general types are recognized; (1) no irregularity, (2) most elements of the crystal mosaic have a few irregular layers, (3) some elements have a regular sequence of layers while others have many irregular layers, (4) all elements have many irregular layers which leads to a small pseudo unit of structure. The phenomenon is illustrated by reproductions of photographs.

MANY crystals give x-ray interference maxima that cannot be accounted for as reflections from normal lattices. Friedrich[1] as early as 1913 observed streaks running through the normal reflections on Laue photographs of NaCl and KCl. Crystals that are naturally in a strained condition or that have been subjected to distortion show "asterism" of Laue spots which can often be removed by annealing. Barrett[2] considered that the anomalous reflections appearing from an iron crystal subjected to compression resulted from increased displacements of elements in the usual crystal mosaic. A similar explanation had earlier been advanced by Dickinson[3] to account for anomalous reflections from potassium iodide and other alkali halide crystals. A somewhat similar explanation was given for radial streaks on Laue photographs made with the x-ray beam approximately normal to the basal cleavage of mica that had been heated or bent.[4] These explanations treat the various "anomalous" reflections as properties of crystal aggregates.

In studying "anomalous" reflections from NaCl, MgO, and Duralumin, Preston[5] has shown that intensities of such reflections are strongly dependent upon temperature. He, moreover, has demonstrated that they result from degradation of the crystal mosaic by lattice vibrations. The reflections are normal interference maxima from small groups of atoms having the arrangement typical of the particular lattice. Diffuse reflections of an apparently different type have been observed to accompany age-hardening of some aluminum-copper alloys of the Duralumin class. Guinier[6] and Preston[7] have shown that the effects are due to segregation of copper atoms in particular lattice planes, but not in a sufficiently regular manner to give a superlattice. In one element of the crystal mosaic copper atoms tend to segregate in (010) in other elements in (100) or (001). Systematic approach to regularity among the segregating atoms can result in an asymmetric distribution of intensity in an "anomalous" reflection (Preston).

The following work deals with diffuse reflection of x-rays from several silicate minerals having "layer lattices" of which mica perhaps is the best known. Such reflections were mentioned by Mauguin[8] and he suggested that they result from random arrangement of heavy ions in the oxygen frameworks of the structures. An understanding of the cause for the diffuse reflections leads to considerable information about the nature of the mosaic structure in these particular crystals.

## EXPERIMENTAL

X-ray diffraction photographs of some mica crystals made with radiation from a tube with a copper anticathode operated at 40 kv peak and on an x-ray goniometer of the type first described by Weissenberg are reproduced in Fig. 1. An x-ray goniometer is a device in which re-

[1] Friedrich, Physik. Zeits. **14**, 1079 (1913).
[2] C. S. Barrett, Phys. Rev. **53**, 1021 (1938).
[3] R. G. Dickinson, Phys. Rev. **22**, 199 (1923).
[4] W. L. Bragg, Nature **124**, 125 (1929). S. B. Hendricks, Zeits. f. Krist. **71**, 269 (1929).
[5] G. D. Preston, Proc. Roy. Soc. (London) **A172**, 116 (1939).
[6] A. Guinier, Comptes rendus **206**, 1641, 1972 (1938); Nature **142**, 570 (1938).
[7] G. D. Preston, Proc. Roy. Soc. (London) **A167**, 526 (1938); Nature **142**, 570 (1938); Phil. Mag. **26**, 855 (1938).
[8] C. Mauguin, Comptes rendus **187**, 303 (1928).

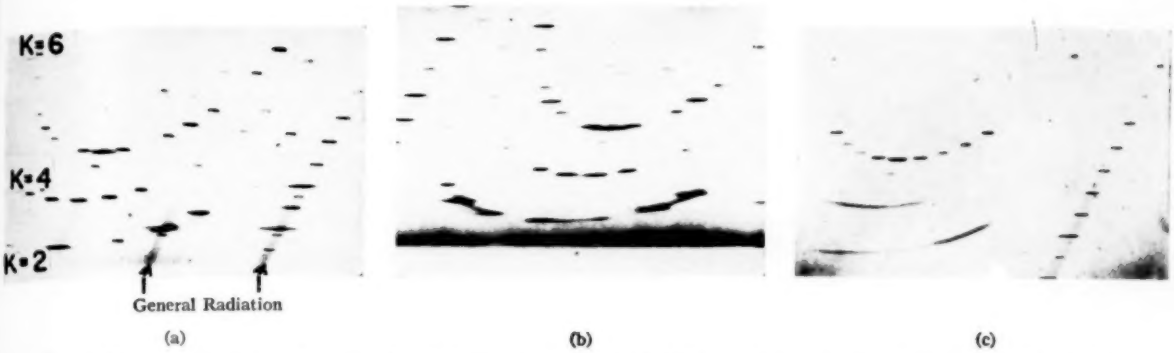


FIG. 1. X-ray goniometer photographs of three mica crystals showing various degrees of continuous scattering.

flections (spots) given by a crystal rotating about a fixed axis are recorded on a film synchronously translated behind a slit. Photographs reproduced in Figs. 1 and 3 were made on a cylindrical film coaxial with the axis of rotation of the crystal which was taken as the crystallographic $a$ direction. They were restricted to the equatorial zone or to the first layer line by the slit before the film and thus show reflections only from planes having the $h$ index zero, $(0kl)$, or one, $(1kl)$, respectively.

Indices of planes, reflections for which appear on Fig. 1a, are indicated on the sketch in Fig. 3d. In Fig. 1b it can perhaps be seen that curves along which $k$ is constant show continuous scattering, particularly near some of the more intense reflections. This phenomenon which can be detected on the original of Fig. 1a is very prominent in Fig. 1c. It can further be seen from these photographs that while scattering along the $k=2$ and $k=4$ curves might either be sharp or diffuse, normal spots are present along curves having $k=0$ and $k=6$. Qualitative examination indicates that the continuous scattering has a symmetrical intensity distribution about the normal reflection in many cases.

Photographs of the first layer line of one biotite mica (United States National Museum C3675) showed pronounced continuous scattering along the $k=1$ and $k=5$ curves and very weak continuous scattering along $k=3$ curves. None was observed along $k=n\times3$ with $n$ odd, curves on photographs of several other micas showing pronounced continuous scattering along other $k$ constant curves. Further experiments on crystals from one hundred different mica specimens show that continuous scattering is present, with the one exception mentioned, only along curves having the $l$ index variable with $h$ and $k$ indices constant and the $k$ index not divisible by three, i.e., $(h_ak_al)$, $k_a\neq n\times3$. Eighty of the specimens were similar in structure to biotite or black mica and gave the effect with but few exceptions. None of the twenty crystals examined having the muscovite or white mica structure showed observable continuous scattering.

Curves of continuous scattering appear as

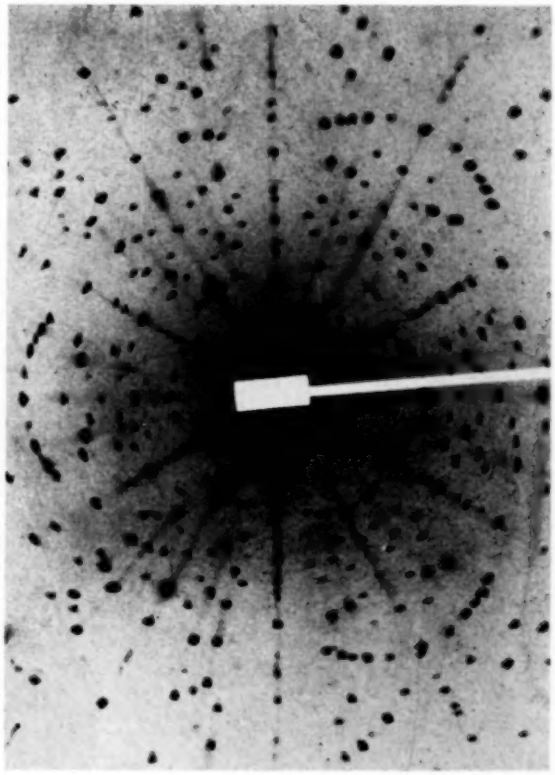

FIG. 2. Laue photograph showing radial streaks resulting from random structure.

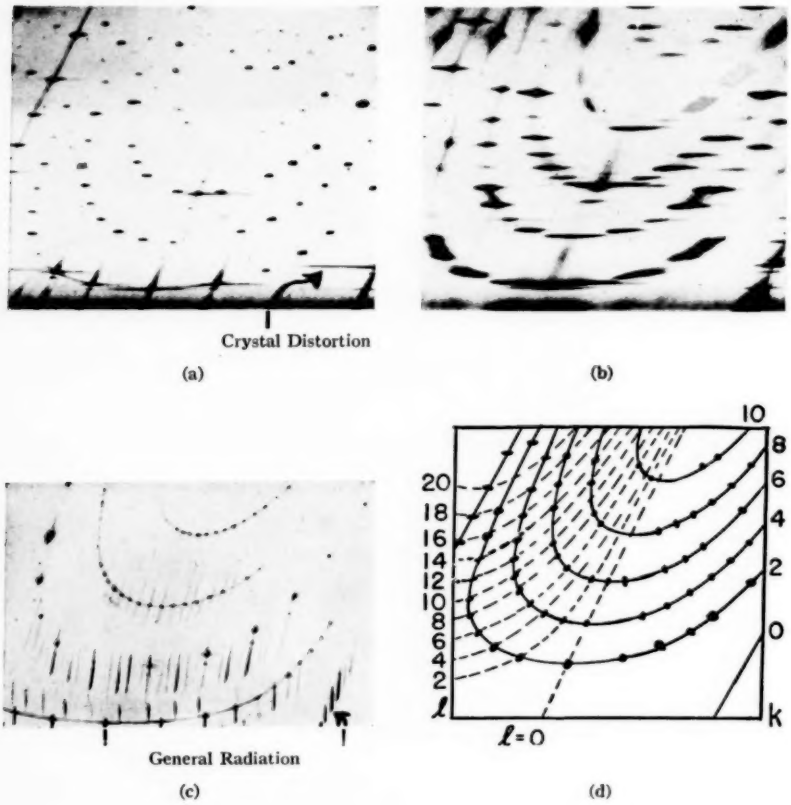


FIG. 3. X-ray goniometer photographs of (a) talc, (b) pyrophyllite, and (c) cronstedite. Indices of reflecting planes appearing on the talc photograph are indicated on the sketch in (d).

radial streaks on Laue photographs made with the x-ray beam normal to the perfect cleavage of mica, (001), and to the photographic plate. A photograph showing moderate development of streaks is reproduced in Fig. 2. Such streaks can be confused with those mentioned in the introduction as arising from crystal distortion. However, they do not show the necessary absorption limits of the photographic plate required by distortion and they are absent for some of the more intense reflections. Rotating crystal photographs from the appropriate mica specimen rotated about the $a$ axis show continuous scattering as a continuous background along the layer lines where it cannot be confused with the trace of the general radiation. Monochromatic radiation must be used to demonstrate continuous scattering along the equatorial zone of such photographs.

Photographs made from the silicate layer minerals, pyrophyllite, talc, and cronstedite are reproduced in Fig. 3. Indices of reflecting planes for pyrophyllite and talc are shown on the accompanying sketch, Fig. 3d. The talc photograph shows features similar to those generally found for biotite micas and this was true for another talc specimen. On the pyrophyllite photograph, however, continuous scattering is present not only along $k=2$ and $k=4$ curves but also, although considerably fainter, along the $k=6$ curve. Further, continuous scattering is largely restricted to regions between two normal reflections with a probable maximum value intermediate between them. Both talc and pyrophyllite crystals are very easily deformed since they are not elastic like mica. For this reason the photographs show more prominent traces due to distortion of crystals during their reduction to adequate size for use. Natural scarcity of specimens containing large crystals further limited the observations to a few samples.

The cronstedite photograph is of the first layer line with rotation about the $a$ axis and accordingly shows reflections only from planes having $k$ odd, $(1kl)$. It was made with radiation from an iron anticathode. Here again continuous scattering is present only along curves $(h_a k_a l)$, $k_a \neq n \times 3$. Traces due to general radiation from

the source are perhaps confusing since prolonged exposures were necessary to bring out traces of continuous scattering along curves having $k$ constant. The intensity of the continuous scattering is very weak compared with that of strong normal reflections appearing at scattering angles near 45°. Normal reflections appear along $(h_ak_al)$, $k_a \neq n\times 3$ curves but they too are very weak as compared with $(h_ak_al)$, $k_a = n\times 3$ reflections, although they are stronger than the continuous scattering. Three specimens of cronstedite were examined.

### Structures of Compounds Showing Continuous Scattering

Before advancing an explanation for the phenomenon described in the previous section, it is necessary to discuss the structures of some of the various minerals for which it has been observed; namely biotite and brittle micas, talc, pyrophyllite, vermiculites, chlorites, stilpnomelanes, and cronstedite.

Pauling[9] showed that a number of silicates having micaceous cleavage possess the common structural element of tetrahedral $SiO_4$ groups, joined by the sharing of oxygen ions, at tetrahedral corners, into an extended net. These layers are combined with octahedral groupings of oxygen ions, common to $SiO_4$ groups, and hydroxyl ions about $Fe^{+++}$, $Fe^{++}$, $Mg^{++}$, $Al^{+++}$, $Li^{+}$, etc. to form multiple layers. Pauling found the structures of the close knit multiple layers but he did not determine the manner in which layers are superimposed parallel to the cleavage. Later studies have been directed to this end and in them is found the explanation for the continuous scattering.

The manner in which layers are stacked is largely determined by the spatial relationship of adjacent atoms in contiguous layers. This relationship of the top of one layer to the bottom of another is fixed in every case by certain principles of structure, four different ones being involved. In brucite, $Mg(OH)_2$, where hydroxyl groups are in both surfaces the superposition is determined by their close packing as spheres. All the other compounds under discussion have oxygen atoms of a silicate sheet in at least one surface and micas, talc, and pyrophyllite have both surfaces of this type. In talc and pyrophyllite each oxygen ion in a surface is placed so that it has as many neighboring oxygen ions as possible in the adjacent surface which cannot be an arrangement of close packed spheres because of the oxygen positions in a surface. The superposition of silicate layers in micas is determined by the twelve-fold coordination of potassium between the layers with respect to oxygen ions in the surfaces. Vermiculites, cronstedite, and kaolin minerals have a hydroxyl group or water molecule in one layer surface so placed as to approach closely to one oxygen ion of the neighboring layer, an arrangement brought about by interaction through the hydrogen atom of the hydroxyl group.

The top layer in a sequence of biotite mica layers can have any of three orientations, differing by 60° in rotation about the layer normal, without affecting the relationship of neighboring oxygen ions in the last adjacent surface since they are arranged in an hexagonal array. Each of the three orientations, however, results in a different placing of a succeeding layer relative to the sequence and thus would produce a new lattice if repeated. Actually six different crystal structures corresponding to various regular sequences of layers have been observed among the biotite micas.[10] All except one of these modifications showed continuous scattering of x-rays along the $(h_ak_al)$, $k_a \neq n\times 3$ curves.

Muscovite, the ordinary white mica, in contrast to biotite, the black mica, is invariant in structure among twenty specimens examined. The most striking difference in their diffraction patterns is the presence of $(06l)$, $l$ odd, reflections for muscovite. This indicates that the silicate layer in muscovite is distorted from the ideal structure described by Pauling. The distortion could be a result of incomplete filling of positions with octohedral coordination, only two-thirds of which are filled with aluminum ions, accompanied by substitution of $Al^{+++}$ for $Si^{+4}$ in tetrahedral coordination. Irrespective of the explanation the silicate layer seems to be suffi-

[9] L. Pauling, Proc. Nat. Acad. Sci. **16**, 123, 578 (1930). Note W. L. Bragg, *Atomic Structure of Minerals* (Cornell Univ. Press, 1937), p. 203 f for a discussion of structures of the micas, etc., and for drawings illustrating the structures.

[10] S. B. Hendricks, Nature **143**, 800 (1939). Am. Mineral **24**, 729 (1939).

ciently distorted to make different orientations nonequivalent and thus lead to a unique structure. This might appear contrary to first expectations, but it is equivalent to stating that regular blocks (biotites) can be stacked in many more ways to fill space than can irregular ones (muscovite). Muscovite crystals, it will be recalled, show no observable continuous scattering under experimental conditions giving very pronounced effects with biotite.

Adjacent surfaces of layers in talc and pyrophyllite can have either of two relationships,[11] both of these further can possibly have the various orientations mentioned for biotite. Silicate layers in pyrophyllite more closely resemble those of muscovite than those of biotite micas, in that only a part of the octahedral coordination positions are filled. Pyrophyllite, however, as well as talc shows continuous scattering along the constant $k$ curves.

Successions of kaolin layers too are determined by their orientations. Polymorphic modifications of kaolin, namely the minerals kaolinite, dickite, and nacrite, are analogous in structure to various forms of biotite mica.[12] Only dickite and nacrite form crystals sufficiently large for use on an x-ray goniometer and those of dickite are very small. Continuous scattering was not observed for either mineral. Silicate layers in the mineral cronstedite are similar to those of kaolin. In them, however, half of the $Si^{+4}$ ions having tetrahedral coordination are replaced by $Fe^{+++}$ ions and positions having octahedral coordination are filled by $Fe^{+++}$ and $Fe^{++}$ ions. Cronstedite, however, shows very pronounced continuous scattering in contrast with the other kaolin minerals; in fact it affords one of the best illustrations of the phenomenon.

## Explanation for Continuous Scattering. Nature of the Crystal Mosaic

Since some orders of reflection from a particular plane are normal and others are diffuse, the phenomenon must be a lattice property rather than a property of a crystal aggregate. Thus in Fig. 1c the second and fourth orders of reflection from (010) are diffuse while the more intense sixth order (060) is normal. Alternative orientations of a symmetrical layer are equivalent to translations along the $b$ axis of the lower silicate net by $nb_0/3$ with respect to the upper. Such translations do not alter the lattice periodicities along the $a$ axis and accordingly are without effect on the Laue conditions for interference in that direction. They determine the periodicity along the $b$ and $c$ axes, however, and thus determine the Laue condition in those directions. If the translations are random values of $nb_0/3$ in any crystal mosaic the $c$ direction will have an indefinite periodicity and the reflections will be greatly broadened along the $(h_a k_a l)$ curves. The translations are without apparent effect on the $b$ periodicity if the $k$ index is a multiple of three and these planes will have normal reflections with a $c$ periodicity corresponding to one layer.

Before considering application of this explanation to the various lattices mentioned in the preceding section it is necessary to recall some features of a crystal mosaic. The concept of a mosaic crystal was introduced by Darwin in his work on diffraction of x-rays by crystals[13] and it is not to be confused with the term as used by some later workers. Darwin demonstrated that the observed intensities of x-ray reflections require crystals to consist of many small elements of volume deviating slightly from perfect alignment. The total reflection is the summation of x-rays scattered from the various elements, which act independently of one another except for secondary extinction. While line width, line shape, and intensities are affected, the phenomenon has not been very susceptible of study and the distribution of sizes of the mosaic volumes are unknown.

If a layer in a mosaic element of a silicate mineral of the type described is translated by $b_0/3$ or $2b_0/3$ from its position in a regular lattice, the whole sequence of layers is altered and there is a resulting shift in phase of scattered radiation unless the $k$ index is a multiple of three. The intensity of the reflection will depend upon which element or elements of the mosaic are translated. The breadth of the reflection will be a function of the number of translated elements and the intensity distribution across it

[11] S. B. Hendricks, Zeits. f. Krist. **A99**, 264 (1938).
[12] S. B. Hendricks, Am. Mineral. **23**, 295 (1938). Zeits. f. Krist. **100**, 509 (1939).
[13] C. G. Darwin, Phil. Mag. (6) **27**, 325 (1914).

will be determined by their distribution. A limiting condition will be where all approach to regularity along the $c$ axis is destroyed. Accordingly there should be continuous scattering along the $(h_a k_a l)$, $k_a \neq n \times 3$, curves without normal reflections. In a less extreme case the continuous scattering will be restricted to the neighborhood of the normal reflections.

Analyses of the crystal structures of the micas[10] show that relative intensities of normal $(hkl)$, $k \neq n \times 3$, reflections can be calculated by the usual methods. They decrease in absolute intensity, however, as continuous scattering increases. Some elements of the crystal mosaics therefore have regular structures while others are highly irregular after the manner described above. The number of elements in which only a few layers are translated, moreover, must be small compared with the number giving the extreme conditions. This character of the crystal mosaic of the micas is further shown by the presence of two or more different regular structures in some biotite crystals. One biotite mica sample[10] had a periodicity of 240A along the $c$ axis, which requires regular superposition of twenty-four layers within the unit of structure. All reflections are normal and continuous scattering is not present. In order to establish the periodicity and give the observed narrow reflections the crystal mosaic must be at least ten lattice periods in thickness, 2400A. A crystal could readily be cleaved having this thickness and in fact it should be possible to obtain one less than a lattice period in thickness. Crystals actually used were considerably larger than this, being of the order of 0.05 mm in thickness. Absence of continuous scattering in these crystals suggests that the structure is of the nature of a large regular lattice, a superlattice, and that other irregular lattices are ones having a tendency to form a superlattice from a simple array.

One modification of kaolin, nacrite, apparently has a regular lattice in most elements of the crystal mosaic since continuous scattering is not present and it is possible to calculate intensities of all reflections.[12] It too shows reflections equivalent to $(06l)$, $l$ odd, reflections of muscovite, white mica, which indicates some distortion of the symmetrical layer that results in unique stacking of layers. In the case of dickite, a second modification of kaolin, continuous scattering is not observed. Intensities of $(hkl)$, $k = n \times 3$ reflections can be calculated satisfactorily but $(hkl)$, $k \neq n \times 3$, intensities cannot be explained by a regular structure. It follows therefore that most of the elements in the crystal mosaic have one or several layers displaced from the regular sequence. Reflections from $(06l)$, $l$ odd, are absent for dickite.

The mineral cronstedite affords an extreme example in that it shows practically continuous scattering along the $(h_a k_a l)$, $k_a \neq n \times 3$ curves. Intensities of $(hkl)$, $k = n \times 3$, reflections can be satisfactorily calculated on the basis of a pseudo-rhombohedral unit of structure formed by averaging the three orientations with equal weight.[14] This pseudo-unit apparently contains fractional atoms, its contents being in various equivalent sets of points, (a) $\frac{1}{3}\,Si^{++++} + \frac{1}{3}\,Fe^{+++}$, (b) $1\,Fe^{++}$, $Fe^{+++}$, (c) $\frac{1}{3}\,O^{--} + \frac{2}{3}\,OH^{-}$, (d) $OH^{-}$, (e) $\frac{1}{6}\,O^{--}$, (f) $\frac{1}{6}\,O^{--}$. It therefore follows that every element in the crystal mosaic must have a very irregular lattice.

Lattice irregularities similar to those of cronstedite have earlier been observed in the simpler compounds $NiBr_2$ and $CdBr_2$.[15] In these compounds the $Br^{-}$ ions form cubic close packed arrays. If $NiBr_2$ is crystallized from alcohol the nickel ions are in definite positions having octahedral coordination as required by the cadmium chloride type of structure. Formation of crystals by sudden condensation from the vapor results in a structure having random shifting of layers while preserving close packing of ions in contiguous layers, i.e., a mixing of cubic and hexagonal close packing. Since observations have been restricted to x-ray powder diffraction photographs, possible continuous scattering has not been observed. The mineral brucite, $Mg(OH)_2$, might be expected to behave in a similar way but it has not been subjected to detailed study.

Both pyrophyllite and talc show continuous scattering and in both cases intensities of $(hkl)$, $k = n \times 3$, reflections can readily be calculated while intensities of reflection from $(hkl)$,

[14] S. B. Hendricks, Am. Mineral. **24**, 529 (1939).

[15] J. A. A. Ketelaar, Zeits. f. Krist. **88**, 26 (1934). J. M. Bijvoet and W. Nieuwenkamp, Zeits. f. Krist. **86**, 466 (1933).

$k \neq n \times 3$, cannot be explained by a regular lattice. In both cases the continuous scattering is weak. It follows therefore that most elements of the crystal mosaic have one or more translated layers and that some elements have many displaced layers. This is intermediate between dickite and cronstedite.

Pyrophyllite and one biotite mica sample differed from the other substances examined in showing some continuous scattering along $(h_a k_a l)$, $k_a = n \times 3$, curves. In both cases this was very weak compared with that observed along $(h_a k_a l)$, $k_a \neq n \times 3$ curves, on the same photographs. Continuous scattering on the pyrophyllite photographs further has a tendency to be restricted to the region between two normal reflections with a maximum of intensity midway between them. The intensity maximum is evidence of a tendency for the crystals to form a definite superlattice. No entirely satisfactory explanation has been found for the continuous scattering along $(h_a k_a l)$, $k_a = n \times 3$, curves for pyrophyllite, but the following might possibly hold. The parameter along the $b$ axis ($y$) defining the relative positions of the layers might differ slightly from $nb_0/12$. Irregular sequence of layers in an element of the crystal mosaic thus would have some effect on the $(hkl)$, $k = n \times 3$ reflections. An alternative explanation would be that the layers in pyrophyllite are somewhat distorted in a manner similar to that of muscovite but not sufficiently to prevent random orientations. Reflections from $(hkl)$, $k = n \times 3$ and $l$ odd, would normally appear though weak for a regular structure and would be broadened to the point of not being observable as irregularity was introduced. The actual photographs might be an intermediate stage in this process. Composition of the specimen examined eliminates any possibility that the phenomenon was caused by the nonhomogeneous distribution of some component.

MARCH 1, 1940 PHYSICAL REVIEW VOLUME 57

# Excited States of the $O^{16}$ Nucleus

DAVID M. DENNISON
*University of Michigan, Ann Arbor, Michigan, and University of California, Berkeley, California*
(Received January 18, 1940)

IN a recent Letter to the Editor, Oppenheimer and Schwinger[1] have discussed the excited states of the nucleus $O^{16}$ which are formed subsequent to the bombardment of fluorine by protons. Fowler and Lauritsen[2] have shown that this bombardment gives rise, in addition to short and long range groups of $\alpha$-particles, to monochromatic $\gamma$-rays of energy $6.3 \pm 0.1$ Mev and to the production of pairs with the energy of $5.9 \pm 0.3$ Mev. According to the interpretation of Oppenheimer and Schwinger, the pairs are produced by internal conversion from an excited state of $O^{16}$ which has zero angular momentum and even parity to the ground state which is likewise a $0^+$ state. The $\gamma$-rays, on the other hand, result from a transition from an excited $1^+$ or possibly $2^-$ state to the ground state. It is rather essential for this explanation that there exist no intermediate excited levels of such a character that transitions to them from the upper states will be of sufficient intensity to compete actively with the pair production or with the 6.3-Mev $\gamma$-ray transitions. The object of the present note is to examine the levels of $O^{16}$ as predicted by the $\alpha$-particle model and to see to what extent they may satisfy the requirements postulated by Oppenheimer and Schwinger. It is clear that the independent particle model will not readily predict a low excited $0^+$ state since the first steps of excitation will probably consist in raising a particle from a $P$ state to a $2S$ state, thus producing levels of the type $2^-$, $1^-$ and $0^-$.

The $O^{16}$ nucleus will be thought of as a close packed grouping of four $\alpha$-particles whose equilibrium configuration is that of a regular

[1] J. R. Oppenheimer and J. S. Schwinger, Phys. Rev. **56**, 1066 (1939).
[2] W. A. Fowler and C. C. Lauritsen, Phys. Rev. **56**, 840 (1939).

tetrahedron. An estimate of the vibration amplitudes indicates that the $\alpha$-particle model should have some validity as a means of describing $O^{16}$ and that in first approximation the energies and wave functions may be separated into vibrational and rotational parts. As has been pointed out by Wheeler[3] and by Hafstad and Teller,[4] the requirement that the $\alpha$-particles must satisfy Bose statistics greatly reduces the number of allowed states. The energy of a rotating vibrating tetrahedral model may be written in the following form:

$$W=(j^2+j)\hbar^2/2A+\omega_1\hbar(n_1+\tfrac{1}{2})+\omega_2\hbar(n_2+1)+\omega_3\hbar(n_3+\tfrac{3}{2})+I_{n_3 j}\pm\epsilon_i.$$

$A$ is here the moment of inertia, and $\omega_1$, $\omega_2$ and $\omega_3$ are three normal frequencies expressed in circular units ($\omega_i=2\pi\nu_i$). As is well known, these frequencies are single, double and triple, respectively. $I_{n_3 j}$ represents an interaction between vibration and rotation which arises from the fact that the motion associated with the frequency $\omega_3$ possesses an internal angular momentum $\zeta\hbar$. The final term $\pm\epsilon_i$ denotes the two energy states associated with the tunneling process by which a tetrahedron expressed in a right-hand coordinate system passes over into a tetrahedron in a left-hand system.

The states whose wave functions are invariant under an interchange of any two $\alpha$-particles (Bose statistics) and which correspond to low vibrational and rotational quantum numbers are listed in Table I. The first four columns give the quantum numbers, the fifth column the parity, and the last column the energy above the normal state. The term $9\hbar^2/8A$ in the last column represents the interaction energy, which for this state is $-(j+1)\zeta\hbar^2/A+\zeta^2\hbar^2/2A$. It may be shown that $\zeta=-\frac{1}{2}$ when $n_3=1$.

The normal frequencies $\omega_1$, $\omega_2$ and $\omega_3$ may be found by the usual methods of normal coordinates. There are six internal coordinates, and these will be chosen as the six displacements $q_1\cdots q_6$ along the edges of the tetrahedron. Let $q_1$, $q_2$; $q_3$, $q_4$; and $q_5$, $q_6$ represent displacements along opposite edges. The potential energy is a function of the $q_s$ and can be developed in a power series. Retaining no powers beyond the second, we have

$$V=\tfrac{1}{2}[a(q_1^2+q_2^2+q_3^2+q_4^2+q_5^2+q_6^2)+2b(q_1q_3+q_1q_4+q_1q_5+q_1q_6+q_2q_3+q_2q_4+q_2q_5+q_2q_6+q_3q_5+q_3q_6+q_4q_5+q_4q_6)+2c(q_1q_2+q_3q_4+q_5q_6)].$$

The three frequencies are readily found as a function of the three constants $a$, $b$ and $c$ together with $M$, the mass of an $\alpha$-particle.

$$\omega_1^2=(4a+16b+4c)/M$$
$$\omega_2^2=(a-2b+c)/M \qquad \omega_3^2=(2a-2c)/M.$$

Although it appears that the three normal frequencies may be arbitrarily assigned, the nature of the nuclear forces would lead us to believe that the constant $a$ must be large compared with either $b$ or $c$ and we would reject as physically unlikely any solution for which this condition is not satisfied. The quantity $\epsilon_i$ may be estimated from the theory of the two-minima problem and is given in terms of the frequency $\omega_3$ through whose motion the tunneling may be effected. For a reasonable form of potential function we may estimate $2\epsilon_0/\omega_3\hbar \geqq 3\times10^{-3}$ and $\epsilon_1 \geqq 25\epsilon_0$.

It is clear that the $\alpha$-particle model, in contrast to the independent particle model, predicts in a natural fashion that one of the low excited states of $O^{16}$ is a $0^+$ state which therefore upon transition to the ground state may give rise to the production of pairs. The 6.3-Mev $\gamma$-rays, according to Oppenheimer and Schwinger, result from a transition from an excited state with a different parity-angular momentum. From the observed high intensity of the $\gamma$-rays one would expect that the captured proton is in an $S$ state and produces a $1^+$ excited state of $Ne^{20}$ which subsequently emits an $S$ $\alpha$-particle to form a $1^+$ level of $O^{16}$. Unfortunately the $\alpha$-particle model

TABLE I. *States whose wave functions are invariant under an interchange of any two $\alpha$-particles.*

| $n_1$ | $n_2$ | $n_3$ | $j$ | $p$ | $W$ |
|---|---|---|---|---|---|
| 0 | 0 | 0 | 0 | + | 0 |
| 0 | 0 | 0 | 3 | − | $6\hbar^2/A$ |
| 0 | 0 | 0 | 4 | + | $10\hbar^2/A$ |
| 1 | 0 | 0 | 0 | + | $\omega_1\hbar$ |
| 0 | 1 | 0 | 2 | + | $3\hbar^2/A+\omega_2\hbar$ |
| 0 | 1 | 0 | 2 | − | $3\hbar^2/A+\omega_2\hbar+2\epsilon_0$ |
| 0 | 0 | 1 | 1 | − | $\hbar^2/A+\omega_3\hbar+9\hbar^2/8A-\epsilon_1+\epsilon_0$ |

[3] J. A. Wheeler, Phys. Rev. **52**, 1083 (1937).
[4] L. R. Hafstad and E. Teller, Phys. Rev. **54**, 681 (1938).

furnishes no low excited $1^+$ state. One explanation which may be made is that the emitted $\alpha$-particle is in a $P$ state and thus produces a $0^-$ or $2^-$ level of $O^{16}$. This process while less probable than the emission of an $S$ state $\alpha$-particle may still be sufficiently intense to explain the strength of the $\gamma$-rays. Our model, as has been seen, predicts the existence of an excited $2^-$ level.

A more serious difficulty is the position of the rotational level $3^-$ which depends inversely upon the square of the nuclear radius. We are here concerned with a mass distribution radius and it appears more logical to adopt the estimate of the nuclear dimensions based upon the Coulomb energy differences[5] between such nuclei as $N^{13}-C^{13}$ and $F^{17}-O^{17}$, namely, $R \geqq 3.1\times10^{-13}$ cm rather than the radius $3.7\times10^{-13}$ which is derived from the $\alpha$-particle penetrability of the natural radioactive nuclei. This leads to an energy value for the $3^-$ level of 4.1 Mev. The existence of a level at this position presents certain difficulties which however are perhaps not insurmountable. In the first place transitions might occur to it from the excited $0^+$ level. Since these transitions take place by means of electric octopole radiation and since the energy difference is only 1.8 Mev, their probability would be small and hence would probably not complete actively with the pair production. On the other hand, transitions from the excited $2^-$ level to this $3^-$ level might occur with the same order of intensity as the main 6.3-Mev transitions to the ground $0^+$ state since the former consist of magnetic dipole and electric quadrupole radiation and the latter of magnetic quadrupole radiation only. Thus the fact that no $\gamma$-rays of 4.1 Mev have been observed argues against this choice for the position of the $3^-$ level.

These difficulties would be almost completely obviated if the $3^-$ level lay somewhat higher, say at 5.1 Mev since in this case the energy differences between it and the $2^-$ and the excited $0^+$ levels would be small enough to preclude frequent $\gamma$-ray transitions. Such a value for the $3^-$ level leads to a mass distribution radius for $O^{16}$ of $2.8\times10^{-13}$ cm which is lower than we should expect.

The remainder of the calculation follows naturally. If the $2^-$ level lies at 6.3 Mev and the $0^+$ level at 5.9 Mev, we have a condition upon the potential constants which is satisfied by letting $b=-a/14$ and $c=0$. The following values for the excited levels are then readily obtained, $3^-=5.1$, $0^+=5.9$, $2^+=6.29$, $2^-=6.3$, $1^-=6.6$ and $4^+=8.5$ Mev. There should also be two excited levels $0^+$ lying at about 7.5 and 9.9 Mev due to the first overtones of $\omega_2$ and $\omega_3$, respectively. These are more uncertain however since the $\alpha$-particle model will be less valid for the overtones of normal frequencies because these imply larger vibrational amplitudes. The numerical values which we have just calculated would not be greatly altered if the $3^-$ level were considered to lie at 4.1 rather than at 5.1 Mev.

If the $3^-$ rotational state of $O^{16}$ possesses the energy 5.1 Mev, we may estimate the lowest rotational levels of $C^{12}$ and $Be^8$. We shall employ the arguments of Wheeler[3] concerning the appropriate relative mass distributions of these nuclei although these cannot be regarded as very certain. The lowest level of $C^{12}$ would be a $2^+$ state and would lie at 4.3 Mev. Experimentally the lowest level lies at 4.3 Mev. In the case of $Be^8$ the lowest level, also a $2^+$ state, would be predicted from the $O^{16}$ datum to be a 6.5 Mev. Actually it is observed to lie at 2.9 Mev. This circumstance would argue for a much looser grouping of the $\alpha$-particles in $Be^8$ than in $O^{16}$ and might be brought in harmony with the fact that the binding energy of the $\alpha$-particles is practically zero for this nucleus.*

I would like to extend my most sincere thanks to Professor J. R. Oppenheimer and to Dr. L. I. Schiff for their encouragement and helpful criticism which have made this note possible.

[5] The Coulomb energy for this series is given by $0.6z(z-1)/A^{1/3}$ Mev. For a surface distribution of charge, $A=16$, this gives $R=3\times10^{-13}$; for a uniform volume distribution, which is surely the better approximation, $R=3.6\times10^{-13}$. Even taking into account the somewhat tighter binding in $O^{16}$, $R=3.1\times10^{-13}$ seems to us a *minimum* permissible value.

* *Note added in proof.*—The assumption of the separability of the rotational and the vibrational energies is considerably less well satisfied for the $\alpha$-particle model than for molecular models. An estimate of the vibration-rotation interaction terms for the low-lying states of $O^{16}$ shows that they are of the order of 0.5 to 1 Mev; some contributions being positive and some negative and depending upon the details of the potential function. This means that the numerical values which we have obtained must not be taken too literally. In particular, the $3^-$ level may lie as high as 5.1 Mev without the nuclear radius being as small as $2.8\times10^{-13}$ cm.

# LETTERS TO THE EDITOR

*Prompt publication of brief reports of important discoveries in physics may be secured by addressing them to this department. Closing dates for this department are, for the first issue of the month, the eighteenth of the preceding month, for the second issue, the third of the month. Because of the late closing dates for the section no proof can be shown to authors. The Board of Editors does not hold itself responsible for the opinions expressed by the correspondents.*

**Communications should not in general exceed 600 words in length.**

## Radioactive Standards*

A series of radioactive standards is being prepared under the direction of the Committee on Standards of Radioactivity of the National Research Council. These standards will be deposited at the National Bureau of Standards in Washington, D. C. to be issued as working standards to investigators who may desire them.

The standards under preparation at present are:

(1) *Radium standards.*—(a) 100-cc solutions sealed in 200-cc Pyrex flasks containing $10^{-9}$ and $10^{-11}$ gram of radium to be used as emanation standards either directly or by subdilution. (b) 5-cc solutions sealed in Pyrex ampoules containing 0.1. 0.2, 0.5, 1.0, 2.0, 5.0, 10, 20, 50 and 100 micrograms of radium to be used as gamma-ray standards. If desired, these may be obtained in sets of 13 with two each of the 0.2, 2, and 20-microgram standards.

(2) *Thorium standards.*—Sealed ampoules containing sublimed $ThCl_4$. These may be used in preparing standard thorium solutions. Directions for use will be furnished with the standards.

(3) *Standard rock samples.*—The following rocks, ground to pass 40-mesh screen and be retained on 100-mesh screen are available in 100-gram samples: Quartzite (Virginia), Triassic diabase (Virginia), Milford granite (Massachusetts), Chelmsford granite (Massachusetts), Gabbro-diorite (Massachusetts), Columbia River basalt (Idaho), Berea sandstone (Ohio), Dunite (North Carolina), Carthage granite (Missouri), Carthage limestone (Missouri), Deccan trap (India), Kimberlite (South Africa).

These samples of rock will be analyzed for radium and thorium content and are intended for use as working standards to check methods used in extraction of radon and thoron from rock samples. They may be used for direct fusion in the electric furnace or for carbonate fusion.

All of the above samples will be analyzed at a number of laboratories equipped to make such measurements and ultimately certificates will be issued by the National Bureau of Standards. This work is in progress but will require considerable time for its completion so that final figures are available only for a part of the samples at the present time.

Accurate knowledge of the radioactive content of the materials of the earth's crust is of primary importance in many phases of geology, geophysics and cosmology. Reliable radioactive standards are also essential in studies of radium and thorium poisoning and in biological and medical investigations using the technique of radioactive indicators, or internal artificial radioactivity therapy. For the latter purposes calibrated standard sources of $\beta$-rays will be made available.

It is hoped that the standards which have been prepared by the Committee will provide all workers in these fields with a common basis for comparison of measurements and also improve the accuracy of all measurements of this type. It is likely that they will have other applications and the Committee would appreciate hearing from interested persons who may desire similar standards for their work. The Committee is also glad to cooperate as far as possible in aiding investigators to use these standards to the best advantage and welcomes specific inquiries regarding their use. It is urged that any suggestions regarding other desirable radioactive standards, not at present available, be submitted promptly to the Committee. In particular, it will facilitate the work of the Committee if those laboratories and individuals which can make use of these standards advise the Committee of their probable requirements.

Communications may be addressed to the Chairman, Professor Robley D. Evans, Department of Physics, Massachusetts Institute of Technology, Cambridge, Massachusetts.

L. F. CURTISS
CLARK GOODMAN
ALOIS F. KOVARIK
S. C. LIND
C. S. PIGGOT
ROBLEY D. EVANS

Massachusetts Institute of Technology,
Cambridge, Massachusetts,
February 7, 1940.

* This work is being supported in part by a generous grant from the American Philosophical Society to the Massachusetts Institute of Technology.

## On Bose-Einstein Fluids. A Correction

(Phys. Rev. **57**, 241 (1940))

Through an editorial oversight in proofreading, the authorship of the Letter to the Editor carrying the above title in the issue of February 1 was ascribed to J. C. Findlay, A. Pitt, H. Grayson Smith and Louis Goldstein. Louis Goldstein is the sole author of that letter. The other names should be deleted from the signature but added to reference 3. This reference should read:

[3] E. F. Burton, Nature **141**, 970 (1938); J. C. Findlay, A. Pitt, H. Grayson Smith and J. O. Wilhelm, Phys. Rev. **54**, 506 (1938).

The Editor extends his apologies to all concerned.

THE EDITOR

## Deviation from the Coulomb Law for a Proton*

In a recent paper,[1] Fröhlich, Heitler and Kahn were led to believe that the interaction between an electron and a proton might become repulsive at small distances on the basis of a second[2]-order perturbation calculation made with one of the mesotron theories now current. My criticism[3] of this paper attempted to show that the appearance of a repulsion in the electron-proton force with these theories meant only that the perturbation theory was not convergent, and that, for example, if convergence factors were introduced so that it was made convergent, the repulsion would not be obtained. FHK[4] have more recently challenged the validity of some of my arguments, but as I will indicate below, I am unable to agree with them. My discussion always has application only to calculations made with theories similar to the present mesotron theories in which perturbation theory to second (or possibly finite higher) order is used, and in which the inherent divergences are avoided by means of a convergence factor. No other kind of *calculation* is possible at the present time; anything else would be even more of a guess.

The charge density about a proton may be written in the form

$$\rho(\mathbf{r})=e(1-\int\rho_1(\mathbf{r})d\mathbf{r})\delta(\mathbf{r})+e\rho_1(\mathbf{r}), \qquad (1)$$

where the first term gives the contribution of the point charge at the heavy particle, and the last term represents the charge density due to the mesotrons. The cogency of my criticism depends on the following three properties of $\rho(\mathbf{r})$. (*a*) The charge density $\rho(\mathbf{r})$ about a proton was assumed to be spherically symmetrical. This follows merely from symmetry arguments for a system of angular momentum $\hbar/2$, such as a proton or neutron. (*b*) It was assumed that $\rho_1(\mathbf{r})$ was everywhere positive. As is obvious in the calculation of (1) in second order, $\rho_1(\mathbf{r})$ has always the form[5]

$$\rho_1(\mathbf{r})=\left(\frac{g^2}{2}\right)\sum_{jk}\{c_k^*c_j\}\left[\left(\frac{\epsilon_k}{\epsilon_j}\right)^{\frac{1}{2}}+\left(\frac{\epsilon_j}{\epsilon_k}\right)^{\frac{1}{2}}\right]\exp i(\mathbf{p}_j-\mathbf{p}_k)\cdot\mathbf{r}, \qquad (2)$$

where the coefficients $c_j$ depend on the form of the mesotron theory used, and $\epsilon_j$, $\hbar\mathbf{p}_j$ are the energy and momentum of a positive mesotron in the state $j$. It was pointed out by FHK,[4] in effect, that the $c_j$ might, in principle, be chosen so as to make $\rho_1(\mathbf{r})$ negative in certain small regions of space, contrary to my use of it. The point here, however, as I was careful to make clear before,[6] is that in the forms of the mesotron theory that are now in use, $\rho_1(\mathbf{r})$ is in fact actually positive everywhere. Furthermore, even if the $c_j$ are chosen so that $\rho_1(\mathbf{r})$ is negative for $r\to 0$, one may easily see that the proton-electron force will be attractive for $r\to 0$, provided only that

$$\alpha=\int\rho_1(\mathbf{r})d\mathbf{r}=g^2\sum_j|c_j|^2$$

is less than unity. Thus repulsive domains could be possible, if at all, only for intermediate distances, but not for the smallest distances, as would be necessary for the explanation of the supposed anomalies in the fine structure[7] of the $H\alpha$ lines.

(*c*) The third point was that a value of $\alpha$ larger than unity corresponded to a physically inadmissible nonconvergence of the perturbation theory, since it meant that the proton was more than 100 percent of the time transformed into a neutron: in other words, I used $\alpha$ as the "dissociation time" of the proton. This was challenged by FHK, since $\alpha$ can be defined in terms of $\rho_1(\mathbf{r})$, and this is not simply related to mesotron particle density or the probability that a mesotron be found at $\mathbf{r}$. Hence they concluded that $\alpha$ is not the total probability of finding a mesotron at a finite distance from the heavy particle,[8] and thus were led to believe that $\alpha$ is not the dissociation time of the proton. However, I reassert that it is just that, and that this may be seen in the following way: The total *charge* at the origin is $e(1-\alpha)$, because $e\alpha$ is the total *charge* in the mesotron cloud, and the total charge of the proton system must be conserved. But since the heavy particles (unlike the mesotrons) are treated nonrelativistically, their *charge* density is just their *particle* density, apart from a constant factor $e$. One has then a right to ask, "What are the probabilities of finding a proton or a neutron at a certain point $\mathbf{r}$?" These are given by[9]

$$(1-\alpha)\delta(\mathbf{r}) \quad \text{and} \quad \alpha\delta(\mathbf{r}),$$

respectively, so that the total probabilities of finding the heavy particles at all are $(1-\alpha)$ and $\alpha$, respectively. These values are, of course, also the results of a direct calculation to second order of the expectation values of the quantized wave operators $\mathbf{P}^*(\mathbf{r})\mathbf{P}(\mathbf{r})$ and $\mathbf{N}^*(\mathbf{r})\mathbf{N}(\mathbf{r})$ of the proton and neutron *particle* densities. Thus we see that $\alpha$ does in fact have the physical meaning ascribed to it above. However, even apart from this, a value of $\alpha>1$ indicates a breakdown of perturbation theory, since the condition that the wave function of the system should be little changed is just that

$$\alpha=g^2\sum_j|c_j|^2\ll 1.$$

For the present, at least, it seems that one may draw qualitative conclusions from a divergent field theory, if at all, only if it is found that one's results are not seriously affected by the introduction of a reasonable converging device. This criterion, for example, would indicate that the neutron-proton forces given by the theory might have some qualitative significance.

W. E. Lamb, Jr.

Department of Physics,
Columbia University,
New York, New York,
January 29, 1940.

* Publication assisted by the Ernest Kempton Adams Fund for Physical Research of Columbia University.

[1] H. Fröhlich, W. Heitler, B. Kahn, Proc. Roy. Soc. **A171**, 269 (1939).

[2] Their calculations were actually to third order, but only to second order in the interaction between mesotrons and heavy particles.

[3] W. E. Lamb, Jr., Phys. Rev. **56**, 384 (1939).

[4] H. Fröhlich, W. Heitler, B. Kahn, Phys. Rev. **56**, 961 (1939). Referred to as FHK. I am indebted to Professor Heitler for sending me a resumé of this letter before publication, and other interesting correspondence.

[5] The two "pair" terms cancel one another, which means that the $W^{ii}+W^{iii}$ of references 1 and 4 cancel instead of adding.

[6] Reference 3, line below Eq. (3).

[7] More recent experimental evidence seems to indicate that much of the supposed anomaly can be ascribed to the presence of molecular hydrogen lines.

[8] This is quite correct, since mesotron pairs would be created in a measurement. This would, however, not affect the total charge.

[9] The recoil of the heavy particle when it emits a mesotron has been neglected here, as in references 1 and 4.

### Possible Production of Radioactive Isotopes of Element 85

We have previously reported[1] the production of artificial alpha-particle emitters from the bombardment of bismuth with 32 Mev alpha-particles. We wish to make a preliminary report at this time on our attempts to establish the chemical identity of this substance.

Two ranges of alpha-particles are emitted, one of approximately 6.1 cm and the other of approximately 4.2 cm. Both groups decay with the same half-life, 7.5 hours. About 60 percent of the total number of alpha-particles is in the long range group and about 40 percent is in the short range group. We have been unable to find a genetic relationship between these groups. Associated with the alpha-particle activity is a beta-ray activity and an x-ray or gamma-ray activity both of 7.5 hours half-life. The x-ray or gamma-ray has an energy of roughly 90 kev, as determined by absorption measurements.

In attempting to identify the alpha-emitter chemically we have succeeded in eliminating thallium, lead, bismuth and polonium by the experiments which are listed below. In all cases the bombarded bismuth was dissolved in nitric acid and brought to a 0.25 normal concentration in nitric acid. We precipitated lead and thallium as chlorides with hydrochloric acid and found no activity in the precipitates. We tested for bismuth in several ways. We precipitated bismuth with stannous chloride in alkaline solution and found no activity. We also made a fractional precipitation of bismuth with hydrogen sulphide in an acid solution. Starting with 6 normal hydrochloric acid concentration and diluting progressively we found a higher specific activity in the first fractions. We also made a fractional hydrolysis of bismuth again finding a decreasing specific activity in the last samples.

The chemical properties of the unknown substance are very close to those of polonium. However, we have established that it is not polonium by using polonium as a tracer. We prepared the tracer polonium by bombarding bismuth with deuterons. The bismuth containing the polonium (radium F) was dissolved in the same way as the bismuth containing the unknown activity. We then mixed a known amount of the standard polonium solution with each sample of the unknown. The experiments which eliminate polonium are as follows: In a 0.25 normal nitric acid solution the polonium deposited on a piece of metallic bismuth placed in the solution, but the unknown activity did not. In the fractional sulphide precipitates mentioned above the ratio of unknown activity to polonium activity was different in each sample. The same was true of the fractional hydrolysis. We then took a sample of the nitric acid solution containing both the unknown activity and the polonium, added potassium iodide and extracted the iodine with carbon tetrachloride. The iodine was reduced with sulphite and precipitated with silver nitrate. The precipitate contained only the 7.5-hour activity—the polonium having been left behind. The extraction of the unknown activity was not complete, however. We also added potassium iodide to a sample and distilled off the iodine. In this case some of the unknown activity followed the iodine, while all the polonium stayed behind. However, we have not yet found the condition for reproducing the distillation quantitatively, though the polonium never distills over.

Thus it seems definite that the unknown alpha-emitter is not thallium, lead, bismuth, polonium or any of the known elements up to uranium. So if it is an element in this region of the periodic table it must be element 85 (eka-iodine). However, its chemical properties are much closer to those of polonium than they are to those of iodine: it precipitates as a sulphide and it is precipitated by zinc in sulphuric acid solution, both reactions being characteristic of a metal and not of iodine; it precipitates incompletely with silver nitrate under conditions in which halogens precipitate quantitatively.

The possibility of fission is not eliminated since we have not ruled out all the elements below thallium. Fission seems unlikely, however, since no alpha-emitters are found in the known fission products. Furthermore the complex decay periods characteristic of fission products are missing.

At the suggestion of Dr. J. G. Hamilton and with his aid we have injected known amounts of the supposed eka-iodine into two hyperthyroid guinea pigs, on the chance that it might behave like iodine and be concentrated in the thyroid. The guinea pigs were killed about 4.5 hours after administration of the radioactive material and various portions of the bodies were examined for activity. In one animal the thyroid contained roughly 100 times as much activity as equal masses of other portions of the body. The concentration was somewhat less in the case of the second animal. This experiment has not been performed with polonium, however.

We wish to thank Professor Lawrence for his interest in this work. This research has been aided by grants to the laboratory by the Rockefeller Foundation and by the Research Corporation.

D. R. Corson
K. R. MacKenzie
E. Segrè

Radiation Laboratory,
Department of Physics,
University of California,
Berkeley, California,
February 16, 1940.

[1] D. R. Corson and K. R. MacKenzie, Phys. Rev. **57**, 250 (1940).

---

### Energy Losses of Fast Mesotrons and Electrons in Condensed Materials

Cross sections for energy losses by collision of fast charged particles are according to Fermi[1] not independent of the physical state of the material traversed but are larger in gases than in condensed materials. This effect was calculated as arising from the induced electromagnetic field and found to be characterized by the dielectric properties of the material. The result obtained from the model of a single type of dispersion electrons, was reported to be essentially independent of special assumptions as to the dielectric properties of the substance.

On learning about these deliberations we did not feel satisfied as to the relationship of this effect to the dielectric properties of the material. We have therefore carried out

a more detailed investigation of this essentially classical phenomenon and also studied more general models for the dispersing system including the case of conductors.

We confirm the existence of a density-dependence of the collision cross section; but this interesting effect cannot in our opinion be in general related to the dielectric constant of the material for relevant velocities.

The effect can best be described by discussing certain limiting cases for a model containing two dispersion frequencies:

(*a*) Velocities so near the velocity of light that

$$1-(v^2/c^2)\ll(ne^2/\pi m\nu_2^2),$$

where $n$ is number of electrons per unit volume and $\nu_2$ the *larger* frequency in the atoms of the absorber. In this case the reduction in loss is found to be

$$\frac{2\pi ne^4}{mv^2}\left[\log\frac{ne^2/\pi m\nu_m^2}{1-v^2/c^2}-1\right], \tag{1}$$

where $\nu_m$ is the *geometric mean* of the atomic frequencies[2]

$$(\nu_m=13.5Z \text{ ev}=3.5Z10^{15} \text{ sec.}^{-1})$$

(*b*) $1-(v^2/c^2)\ll(ne^2/\pi m\nu_1^2)$; $\quad 1-(v^2/c^2)\gg(ne^2/\pi m\nu_2^2)$.

Reduction in loss:

$$\frac{2\pi ne^4}{mv^2}\left[\log\frac{\alpha}{\nu_1[2(1-v^2/c^2)]^{\frac{1}{2}}}-\frac{1}{2}\right], \tag{2}$$

where

$$\alpha^2=ne^2/\pi m.$$

Expressions (1) and (2) have been extended to cover more general dispersion- and conduction-models.

In applying these results to the passage of mesotrons we find that they afford no possibility of explaining away the surmised radioactivity. In particular, evaluation of the data given by Rossi, Hilberry, and Hoag[3] seems to show that the correction due to (1) would probably affect the value for the lifetime not much more than the inherent inaccuracy due to lack of precise knowledge of the mesotron velocities.

The observations of Pomerantz and Johnson[4] on the relative stopping power for mesotrons in water and lead agree well with our formulae for a reasonable choice of the frequencies involved.

The experiment of Crane, Oleson, and Chao[5] on the energy loss of 10 Mev electrons in carbon give according to the authors the following values:

| | |
|---|---|
| Observed | 1.86 Mev |
| Correction for radiative loss | 0.13 |
| Theoretical (Bloch-Bethe) | 1.93 |
| Theoretical Fermi | 1.40 |
| Theoretical (our formula (1)) | 1.72. |

The details of the calculations and the comparisons with experiments will be given in a subsequent paper.

OTTO HALPERN

New York University,
University Heights,
New York, New York.

HARVEY HALL

College of the City of New York,
New York, New York,
February 9, 1940.

[1] E. Fermi, Phys. Rev. **56**, 1242 (1939).
[2] W. Heitler, *Theory of Radiation* (Oxford, 1936), p. 218.
[3] Rossi, Hilberry and Hoag, Phys. Rev. **56**, 837 (1939).
[4] M. A. Pomerantz and T. H. Johnson, Bull. Am. Phys. Soc., New York Meeting, Feb. 1940, No. 4.
[5] Crane, Oleson and Chao, Bull. Am. Phys. Soc., New York Meeting, Feb. 1940, No. 3.